IRON SULPHIDE FILMS ON STEEL SURFACES

by

Andrew William BATCHELOR

A thesis submitted for the degree of

DOCTOR OF PHILOSOPHY

of the University of London

and also for the

DIPLOMA OF MEMBERSHIP

of the IMPERIAL COLLEGE

September 1982

Lubrication Laboratory,
Department of Mechanical Engineering,
Imperial College of Science & Technology,
London, SW7 2BX.

If riches have importance then human life does not.

From 'Caligula' by Albert Camus

ABSTRACT

A test rig has been developed and used to test the hypothesis that Extreme-Pressure action functions by the rapid formation of sacrificial sulphide films. The rig consists of a scraping tool which removes a thin layer from a fast moving steel strip. The newly exposed metal surface is then covered with model lubricant and after a short reaction period is rinsed so as to stop the reaction. Strip speeds of up to 10 m/sec enabled reaction times as short as 4 m/sec to be investigated. Temperatures up to 185^{o}C have been reached.

The amount of reacted sulphur on the surface has been measured by using Energy Dispersive X-ray analysis in a quantitative manner. Infra-Red Spectroscopy has also been used in an attempt to characterise the chemistry of the reaction problem

Two model lubricants, elemental sulphur in hexadecane and dibenzyl disulphide in hexadecane have been investigated. The results for elemental sulphur have been subjected to multiple regression analysis. Thus trivial variables have been eliminated leaving reaction time and temperature as controlling variables. It has also been shown that much more data is needed for precise knowledge of film formation rates. It is found that elemental sulphur is very reactive, forming films of about 100 Å thickness within a few hundredths of a second. Asperity collision analysis suggests that this fast growth is the basis of Extreme Pressure action by elemental Sulphur. Dibenzyl disulphide is not nearly so reactive, so a different mechanism is proposed based on subsequent oxidation and improved adsorption of surfactants. Some theoretical work is presented

to suggest that the diffusivity of oxygen in oil may play a significant role in scuffing. Negligible diffusivity of solutes in organic solvents at high pressures is suggested as the reason for the importance of the Out-of-Contact period in Extreme Pressure Lubrication.

ACKNOWLEDGEMENTS

I would like to thank Professor A. Cameron and Dr. H.A. Spikes for their kind and helpful supervision of this work. The support of both the Science Research and Engineering Research Council and the Esso Petroleum Co.Ltd. (who were the CASE sponsors) is gratefully acknowledged. The advice and assistance given by Mr. E. Kendrick and Dr. R. Hall (both of Esso Petroleum Co.) made a great difference to the success of the work.

Reg Dobson and Tony Wymark deserve my thanks for making the Lubrication Laboratory a pleasant place to experiment in. I should thank also Mrs. E. Noel for her typing of the manuscript.

The support and encouragement given by my mother and father should also be mentioned here.

I am particularly grateful to Dr. Gwidon Stachowiak both as a friend and for his invaluable help with the work.

Finally thanks are due to all members of the Lubrication Laboratory, who have been such cheerful and helpful companions.

LIST OF CONTENTS

LIST OF FIGURES

Chapter 3

Chapter 5

5.1, 5.2, 5.3, 5.4. Three dimension graphs of data and regression surfaces, sulphur 'signal' versus reaction time and temperature

5.1 Linear regression, 4 independent variables

5.2 Linear regression, 2 independent variables

5.3 Exponential regression 4 independent variables

5.4 Exponential regression, 2 independent variables

5.5 Graph of time-compensated 'signal' versus temperature, 'm' = 1

5.6 Graph of time-compensated 'signal' versus temperature, 'm' = 2

5.7 Graph of time-compensated 'signal' versus temperature, 'm' = 4

5.8 Graph of time-compensated 'signal' versus temperature, 'm' = 10

5.9 Graph of time-compensated 'signal' versus temperature, 'm' = 12

5.10 Graph of time-compensated 'signal' versus temperature, 'm' = 1000

5.11 Illustration of narrow section approach to analysis of reaction time dependence in data

5.12 Graph of average signal versus reaction time at 110°C

5.13 Graph of average signal versus reaction time at 118°C

5.14 Graph of average signal versus reaction time at 135-137°C

5.15 Graph of average signal versus reaction time at 139-140°C

5.16 Graph of average signal versus reaction time at 147-150°C

5.17 Graph of average signal versus reaction time at 150-154°C

5.18 Graph of average signal versus reaction time at 154-156°C

Appendix 1

A.1.1 Illustration of temperature measurement at low scraping speeds

A.1.2 Illustration of temperature measurement at high scraping speeds

Appendix 2

A.2.1 Illustration of manner of sharpening the scraping tool

A.2.2 Illustration of intended disposition of the wick

A.2.3 Illustration of means of adjusting the cross alignment of the scraping tool

A.2.4 Illustration of mode of mounting the rinse barrier

A.2.5 Illustration of rinse fluid supply system

Appendix 3

A.3.1 Illustration of method of temperature measurement of speciment material

A.3.2 Graph of measured temperature profiles of specimen material

A.3.3 Graph of 'plateau temperature' versus square of voltage setting

A.3.4, A.3.5, A.3.6, A.3.7
Graphs of specimen material temperature profiles at 'plateau temperatures' of 140, 155, 170, 185^{o}C respectively.

LIST OF TABLES

Glossary of Symbols and Abbreviations used

E.P. 'Extreme Pressure'

Chapter 1			Equation where first appeared
ω	=	wear volume	1.1
K_1	=	Archard wear probability factor	1.1
a	=	real area of contact	1.1
D	=	sliding distance	1.1
W	=	load	1.2
Pm	=	yield (flow) pressure of metal	1.2
τ	=	duration of a 'wearing contact'	1.3
V	=	sliding velocity	1.3
t	=	time, i.e. duration of wear or film formation	1.4
Δm^{11}	=	mass per unit area of oxide at a critical thickness	1.6
$\bar{k}$	=	Wagner constant	1.6
ρ	=	density of oxide film	1.7
ξ	=	critical thickness of oxide film	1.7
f	=	ratio of weight of oxygen uptake to weight of ocide created	1.9
A_o	=	pre exponential constant to Arrhenius equation	1.11
E	=	activation energy	1.11
R	=	gas constant	1.11
T	=	absolute temperature	1.11
N	=	number of asperity contacts occurring on a wearing pin	
Q	=	fraction of surface covered by oxide islands	1.15
n_{m-m}	=	number of metal to metal contacts	

n_{o-o}	=	number of oxide-island to oxide-island contacts	1.15
n_{m-o}	=	number of metal to oxide-island contacts	1.17
a_{m-m}	=	contact area of an individual metal to metal asperity contact	1.18
f_{m-m}	=	frictional force resulting from one metal-metal asperity contacts	1.19
Sm	=	metal to metal asperity shear strength	1.19
α_m	=	metal to metal ductility factor	1.19
F_{m-m}	=	total of frcition forces for all metal metal asperity contacts	1.20
F_{m-o}	=	total of friction forces for all metal to oxide island asperity contacts	1.22
α_{m-o}	=	ductility factor for metal to oxide asperity interactions	1.22
F_{o-o}	=	total frictional force for all oxide island to oxide island asperity interactions	1.23
S_o	=	shear strength of oxide island to oxide island asperity contact	1.23
α_o	=	ductility factor for oxide island to oxide island asperity interactions	1.23
Po	=	flow pressure of oxide as present in the oxide island	1.23
F	=	total frictional force of all asperity contacts	1.24
μ	=	coefficient of friction	1.25
i	=	ratio of asperity interface shear strengths, oxide island to oxide island compared to metal to metal	1.25
k	=	ratio of flow pressures (on the same basis as i)	1.27
S.A.E.	=	Society of Automotive Engineers	
Fe	=	iron, the chemical element	
S	=	sulphur, the chemical element	
V_1	=	forward reaction velocity, sulphid-adtion of iron	1.7.1

K_{10}	=	constant relating to law of Mass Action	1.7.2
V_2	=	forward reaction velocity, removal of iron sulphide	1.7.3.
K_{20}	=	Mass Action constant relating to V_2	1.7.4
'L'	=	abbreviation for S which is a constant in the context used	
m	=	constant relating to the surface concentration of unreacted iron over the whole reaction area	
'C'	=	FeS	
C_∞	=	value of C at $t = \infty$	

Chapter 2

L	=	thickness of iron oxide or iron sulphide film	
R_o	=	constant of proportionality between flux of ferrous, oxide or sulphide ions across the film and resultant film growth rate	2.3
J_o	=	total flux of mobile ferrous oxide or sulphide ions	2.3
J_D	=	flux of mobile ferrous, oxide or sulphide ions by Fickian diffusion	
J_E	=	diffusivity coefficient of ions in the oxide or sulphide film	2.4
x	=	thickness ordinate of film, direction perpendicular to plane of film, origin at interface between metal and oxide	2.4
E	=	flux of mobile ions due to electric field across the oxide or sulphide film	
μ	=	ionic mobility coefficient	
C	=	concentration of mobile ions at any given point in the oxide or sulphide film, defined as a function of 'x'	2.5
F	=	electric field within the oxide film	2.17
N	=	number of mobile ions per unit volume in the oxide	
a	=	'jump distance' or distance which each mobile ion moves on transferring from one vacant site to another in the crystal lattice of the oxide film	2.17

ν	=	'jump frequency'; i.e. frequency at which 'jumps' of length a occur for each mobile ion	2.17
E_o	=	true value of activation energy of diffusion	2.19
E_A	=	apparent or effective value of diffusion activation energy for the particular conditions of film growth	2.19
a_o	=	lattice parameter	2.21
K	=	film growth rate constant	2.23
K_{de}	=	value of film growth rate where decomposition of the oxidant compound is the limiting step	2.24
K_{sat}	=	value of film growth rate where the oxidant compound saturates the outer surface of the oxide (or sulphide) film and the rate of film growth is limited by the flux of ions across the film	2.24
$\left(\frac{dL}{dt}\right)_{sat}$	$\equiv$	K_{sat} since $K \equiv \frac{dL}{dt}$	2.26
Pc	=	probability of collision between one asperity and another in a partial E.H.L. contact	2.28
L_c	=	distance from inlet to outlet of the E.H.L. contact	2.28
$\bar{r}$	=	average radius of individual asperity collision area	2.28
σ	=	ratio of asperity contact area to E.H.L. contact area	2.28
t_r	=	time for one revolution of the rotating disc	2.29
t_c	=	average time between collision for any one asperity	2.29
n	=	fraction of asperity peaks which are 'virtually clean'	2.30
t_{ox}	=	time for the worn surface to oxidise and so cease to be 'virtually clean'	2.31
Ra	=	ratio defining the likelihood of propagation of nascent surface	2.31

'$conc_s$' = abbreviation for concentration of sulphur as a solute in a carrier fluid or gas

Chapter 3

E.D.A.X. Energy Dispersive Analysis by X-ray (discussed in Chapter 4)

X.P.S. X-ray photoelectron spectroscopy as used for example by Wheeler (22)

S.E.M. Secondary Electron Microscope

'Scraper' Structure to mount scraping tool

'Signal' Normalised value of sulphur signal from surface analysis by E.D.A.X.

Chapter 4

C_{214}, C_{2300}, C_{2460} = Channel counts for E.D.A.X. at 2140, 2300, 2460 electron volts of X-ray energy respectively

Chapter 5

Y = dependent variable or sulphur 'signal' by E.D.A.X.

$Y_1, Y_2, Y_3, Y_4, \bar{Y}$ = 1st, 2nd, 3rd, 4th and average of signals for a particular sample analysed by E.D.A.X.

X_1, X_2, X_3, X_4 = independent variables

X_1 = distance scraped at location of test sample in mm

X_2 = time of scraping to location of sample in ms

X_3 = reaction temperature of sample in degrees Kelvin

X_4 = reaction time of sample in ms

C_o, C_1, C_2, C_3, C_4 = regression coefficients

α = level of significance in regression analysis

Chapter 6

Symbols used in this chapter correspond to those of Chapter 2.

Additional symbols

t_{sulp} = time for a film of iron sulphide to be formed on a steel surface with thickness sufficient to change the surface from 'virtually clean' to 'sulphidised' 6.1

$R_{oxygen\ only}$ = value of R_a where only oxygen is the effective E.P. agent 6.2

$R_{sulphur\ present}$ = value of R_a where there is also sulphur to act as an E.P. agent 6.2

R_{II} = value of R_a associated with Type II collisions; Type I, II, III collisions described in 2.4.1.2

R_I = value of R_a associated with Type I collisions

V_1 = velocity of reaction $Fe + S \rightarrow FeS$ 6.3

V_2 = velocity of reaction $FeS + 2O_2 \rightarrow FeSO_4$ 6.4

SYNOPSIS

The value of blending different substances to produce the best possible lubricant for any particular situation has been known for a long time. Practical experience in the 19th Century showed that small amounts of certain substances could cause valuable reductions in friction and wear. A good example of this is the addition of sulphur to oil; direct sulphurization of the oil was often used to tame troublesome bearings (1). As late as 1859 the use of Flowers of Sulphur was considered patentable knowledge (2). There was little theoretical understanding of this effect until the 1920's when the development of the hypoid gear gave the necessary impetus for systematic study. The hypoid gear permitted a lower centre of gravity for the vehicle, but the increased levels of load and sliding (compared to previous gearings) made scuffing a serious problem. Substances, henceforth known as Extreme-Pressure additives were developed to solve the problem. Organo-sulphurs were usually the critical ingredients. Dowson (1) states that as their use spread to other mechanical devices a general uprating in the acceptable level of compressive stress and sliding speed was achieved.

A full understanding of E.P. action and the avoidance of scuffing still eludes us, Dyson (3) wrote in 1975 that much work remained to be done. Thus this sector of tribology has been chosen as the object of this thesis.

Sulphur and chlorine based additives are generally assumed to lubricate by forming a layer of reaction product. This layer acts as a buffer film to prevent damaging metal-metal

contact in partial E.H.L. There is evidence (Chapter 1) that the film requires a significant amount of time to be formed and that it must function in a sacrificial manner (4). Thus the Out-of-Contact time is an important parameter. The nature of the surface is a further complication. On unworn surfaces the oxide film is always present, under E.P. conditions it may be absent due to mechanical removal of the oxide. If the oxide film is absent then the steel surface is much more reactive. Rates of film formation measured for oxide-covered surfaces will not apply to 'nascent' surfaces.

The following chapters describe an investigation into the reactivity of a nascent (unoxidised) surface with sulphur and sulphur-compounds in an oil-like carrier fluid. Short periods of time (msecs) and moderately high temperatures are involved. From the data, conclusions about the chemistry of nascent steel-sulphur systems have been arrived at and an attempt made to use the data as a test of the link between E.P. lubrication and the fast growth of sulphide films.

CHAPTER 1

LITERATURE SURVEY

1.1 Introduction

The literature survey reviews some of the theoretical and experimental work in E.P. lubrication and related subjects. By this means it is intended to provide a context for a mechanistic approach to E.P. lubrication. As mentioned in the Synopsis the project centres on the Out-of-Contact theory; the substance and theme of the survey also centres on this theory. The survey starts with an illustration of the need for some kind of lubrication for metal-metal contact and then goes on to discuss the significance of Boundary Lubrication. Sacrificial film mechanisms for E.P. conditions and mild wear are then described. The factors affecting E.P. lubrication are next discussed and the survey finishes with an outline of related theoretical work and the conclusions.

1.2 Function of a Lubricant

The adhesivity of metals necessitates the avoidance of true contact between metallic sliding surfaces since actual atom to atom contact between metals results in excessive friction (5).

Where true metal-metal contact is present to a large extent as it is in the interface between a cutting tool and chip then sliding in the strict sense is impossible: no discontinuity in sliding velocity can exist (6). Figure 1.1 illustrates the velocity discontinuity inherent in sliding.

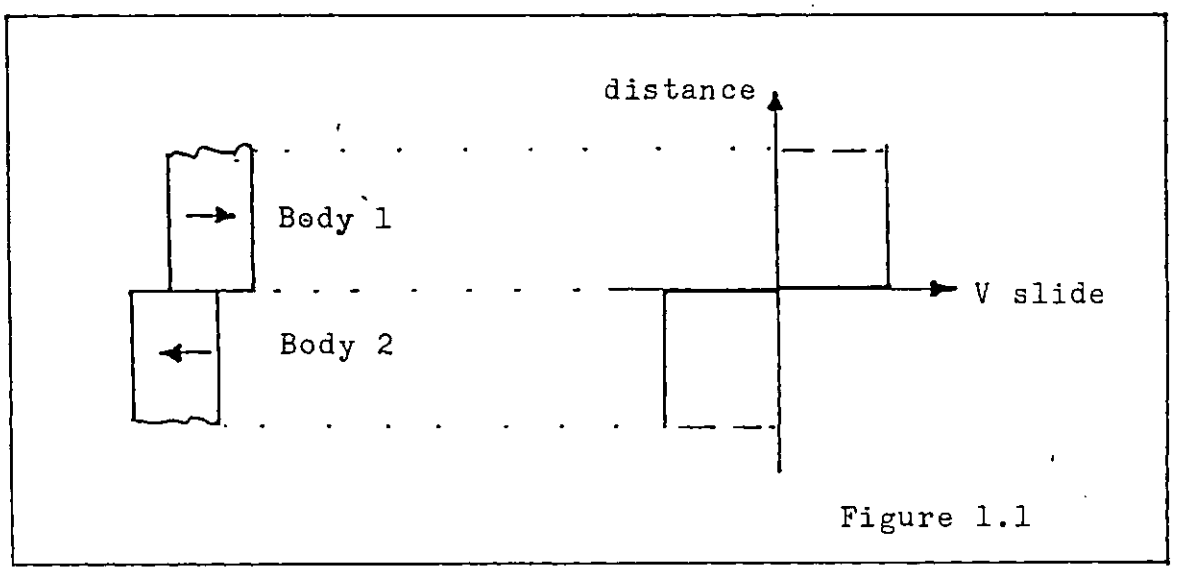

Figure 1.1

The weaker of the two metals flows past the other and a no-slip or seized condition prevails similar to that found in a fluid.

Load and sliding speed are effective agents for promoting true contact with the attendant consequences of friction and

surface destruction (wear). Thus the purpose of a lubricant is to alter the nature of the contact so as to lower the friction and wear rates for a given load and sliding speed.

1.3 Lubrication Regimes and Differences Between Them

The literature delineates three broad categories of lubrication, hydrodynamic, elasto-hydrodynamic (EHL) and boundary. Our recognition of these regimes is generally attributed to Reynolds (7), Ertel and Grubin (8) and Hardy (9) respectively.

Cameron (10) describes three types of lubrication in detail and a full discussion of the first two regimes is not attempted here. In these first two mechanisms the contacting surfaces are separated by a considerable distance, 25 to 0.1 microns, whilst boundary lubrication functions on a molecular scale, 0.1 μ to 10^{-4} μ (1 Å). Hydro-dynamics and EHL require the lubricant to operate as a fluid and separate the surfaces by hydrostatic pressure; boundary lubrication depends on the integrity of the molecular film.

There are certain fundamental differences between boundary lubrication and the other two mechanisms. The principle differences are listed below:

(a) Hydrodynamics and EHL are precise idealized mechanisms based on a rigorous theory, thus they can only partly explain the behaviour of most tribological phenomena. Usually some form of 'boundary lubrication' must be

present to allow for exceptional roughness or entrapped particles.

(b) Since the term 'boundary lubrication' refers to an empirical classification no-one has a precise idea of what it is. This has weakened the theoretical development of the subject (Hardy's work was the pioneering step) and has also obscured the fact that boundary lubrication consists of several different mechanisms.

Three of the most important contributions are:

(a) Solid Lubricants (11) such as graphite, molybdenum disulphide and PTFE. These are used neat or incorporated into a formulation e.g. MoS_2 strengthened grease.

(b) Polar base oils. Some base oils such as esters and fats have a significant boundary lubricating effect.

(c) Organic additives in base oils.

Many organic compounds can be added to a base oil to provide boundary lubrication e.g.

(i) Fatty acids, stearic acid for example.

(ii) Halogenated hydrocarbons, e.g. hexachloroethane.

(iii) Organo-sulphur, e.g. dibenzyl disulphide.

(iv) Organo-phosphorous additives, the metal is usually zinc, e.g. zinc dialkyl diphosphate.

Each formulation has its own particular use; or discussion of which is beyond the scope of the work presented. Campbell (12) has written an excellent review about the uses of various boundary lubricants. Of interest here is that organo-sulphur compounds are a popular souce of additives for solving problems caused by extremes of contact pressure.

Ever present atmospheric oxygen and water should not be forgotten either as they can influence E.P. lubrication.

1.4 Mechanisms of Boundary Lubrication by Air and Sulphur Containing Lubricants

In this section a comparison of boundary lubrication mechanisms involving atmospheric oxygen with and without sulphur containing lubricants is presented. From the literature a division of the mechanisms into four categories seemed appropriate. They are:

1. Unlubricated Mild Wear (air only).
2. Lubricated Mild Wear (air plus sulphur containing lubricant).
3. Lubrication under E.P. conditions.
4. Severe wear and seizure.

The discussion to come follows this ordering, thus unlubricated mild wear is the first topic to be presented.

The dichotomy of mild wear - severe wear was first described by Archard and Hirst (13) who discovered that it depended on the presence or absence of an oxide film. After more than a decade of intensive research some promising theories have been developed. From the accessible literature two theories are to be noted.

1.4.1 High temperature theory of unlubricated mild wear

This theory was largely developed by Quinn (14,15) and is applicable to situations where the flash temperature is of the order of several hundreds of degrees Celsius and rapid oxide growth is possible. The mechanisms is illustrated by a series of diagrams contained in Figure (1.2).

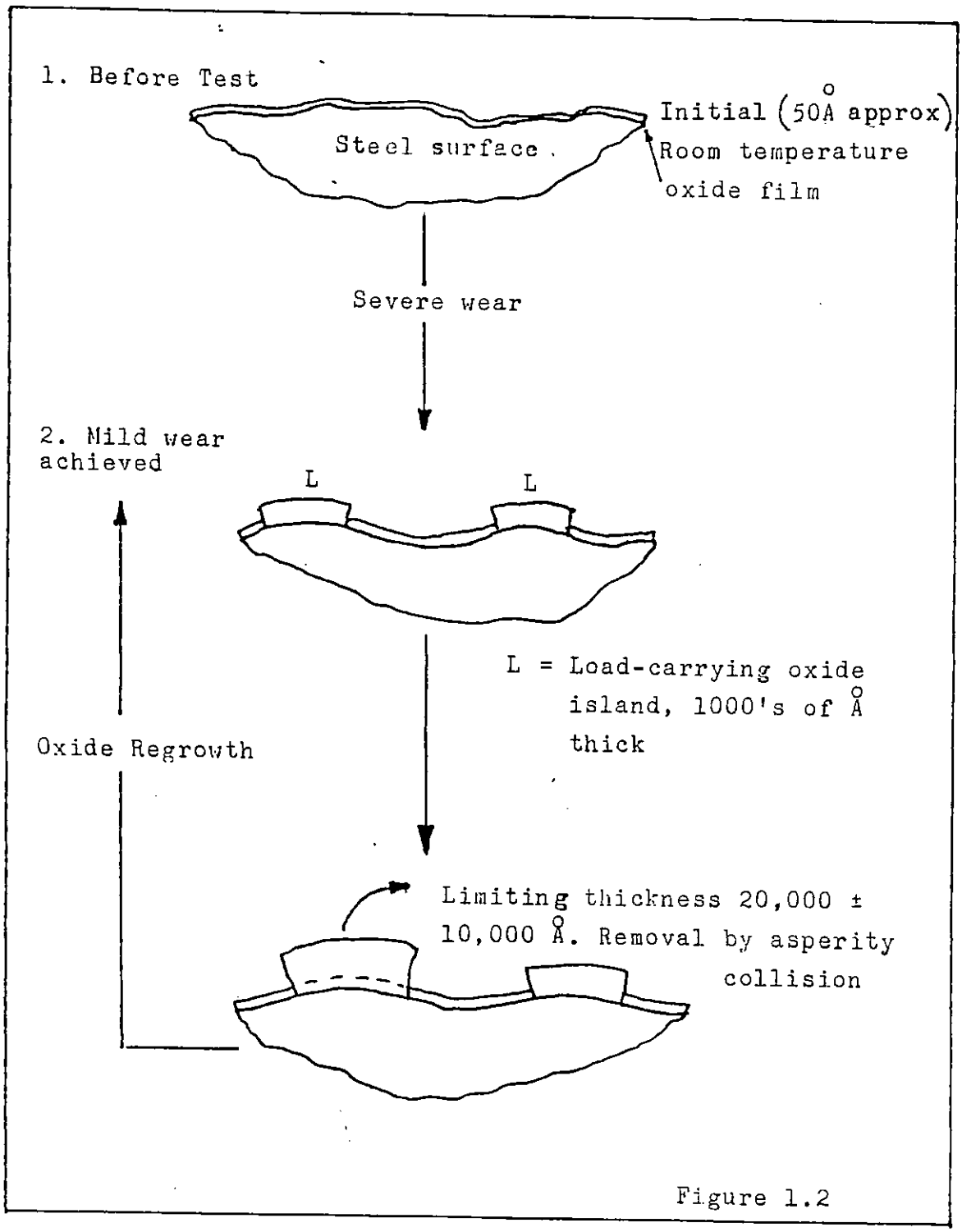
1. Before Test
Steel surface
Initial (50Å approx)
Room temperature
oxide film
Severe wear
2. Mild wear
achieved
L
L
L = Load-carrying oxide
island, 1000's of Å
thick
Oxide Regrowth
Limiting thickness 20,000 ±
10,000 Å. Removal by asperity
collision

Figure 1.2

It is easily demonstrated that if appropriate load and speed conditions exist then initial severe wear soon changes to mild wear. Quinn's theory relates to these latter conditions and does not attempt to explain initial severe wear.

Because the observed wear is 'mild', the load must be borne by an oxide film rather than metal. High temperature is essential for the thick oxide 'islands' observed in practice (16). Two assumptions are made:

1. Thick oxide is confined to the real area of contact i.e. asperity peaks.
2. Oxidation only occurs during moments of high surface temperature, i.e. during asperity collision.

Quinn developed his theory around the pin and disc system. The pin is believed to wear more than the disc since the oxide islands reach their critical thickness much faster than the oxide on the disc. The derivation starts with a consideration of the Archard equation for wear (3.1).

$$\text{Wear volume of pin} = \omega = K_1 a D \qquad (1.1)$$

where K_1 = Archard wear probability factor

a = real area of contact

D = sliding distance

Also from Archard

$$a = W/Pm \qquad (1.2)$$

where W = load

Pm = yield (flow) pressure of metal

Quinn reasoned that since the wear debris is mostly oxide (from his own work) then the wear probability factor must directly relate to the probability of removing an oxide island. In other words, $1/k_1$ must be the average number of passes needed to remove an oxide film of critical thickness.

If τ is the duration of a 'wearing contact' then

$$\tau = d/V \qquad (1.3)$$

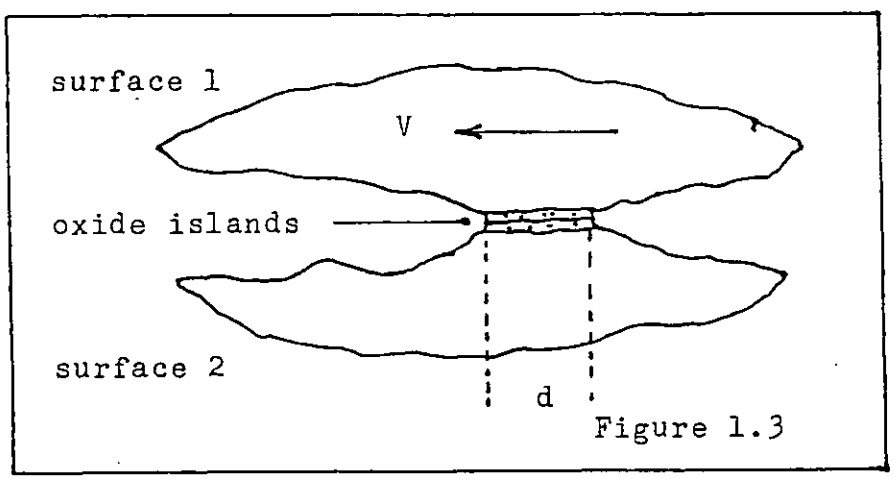

Figure 1.3

Where d is the distance over which the wearing contact is made (Fig.1.3), defined as equal to the average diameter of the asperity contact patch. V = sliding velocity. Hence 't' the time for rapid (i.e. significant) oxidation is given by the expression

$$t = \tau/K_1 \qquad (1.4)$$

Substituting for τ,

$$t = d/VK_1 \qquad (1.5)$$

Assuming a square wave oxidation rate profile (as shown in Figure 1.4).

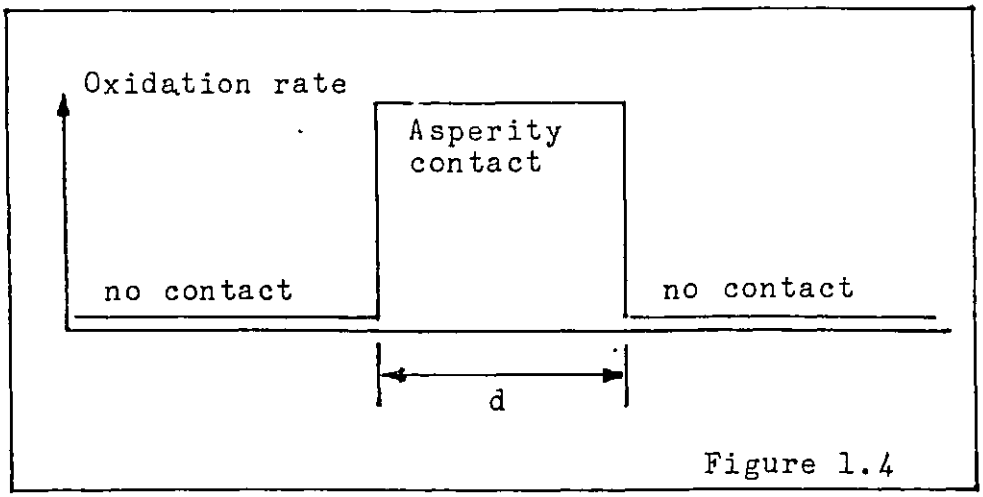

Figure 1.4

And assuming that steel oxidizes according to the Wagner equation (discussed in Chapter 2) then

$$\Delta m'' = \bar{k}t \qquad (1.6)$$

where $\Delta m''$ = mass per unit area of oxide at the critical thickness

$\bar{k}$ = Wagner constant

Mass per unit area = density x thickness

$$\rho\xi = \Delta m'' \qquad (1.7)$$

and $$\xi^2 = \bar{k}t/\rho^2 \qquad (1.8)$$

In his later work Quinn (15) introduces a factor f to allow for the difference between oxygen uptake and oxide creation.

Thus

$$\Delta m''_{\text{uptake}} = f\ \rho\ \xi \qquad (1.9)$$

Since most corrosion data give values of oxygen uptake not oxide weight. However 'f' can be allowed for in the constant '$\bar{k}$' of the Wagner equation, therefore no further mention of it is made here.

Substituting for 't' again re: Equ.(1.5)

$$\xi^2 = \bar{k}\, d/VK_1\, \rho^2 \qquad (1.10)$$

Wagner parabolic oxidation equation obeys the Arrhennius law which is in the form

$$\bar{k} = A_o \exp(-E/RT) \qquad (1.11)$$

where A_o = pre-exponential constant

E = activation energy

R = gas constant

T = temperature, absolute.

hence $$\xi^2 = d\, A_o \exp(-E/RT)/VK\rho^2 \qquad (1.12)$$

The oxidation temperature is considered identical to the flash temperature and in his early work of Quinn, used Archard's equation (17) to deduce the flash temperature which is

$$T \approx (0.2\, W^{\frac{1}{2}} V\mu + 273) \text{ Kelvine} \qquad (1.13)$$

Later work allowed for the partition of heat between pin and disc (15) and this is used as a test of fit between theory and experiment (as shown below).

The wear factor K_1 is eliminated by applying Equ.(1.1)

Equ.(1.1) $w = K_1\, a\, D$

to transform Equ.(1.12)

$$K_1 = d\, A_o \exp(-E/RT)/V\rho^2\xi^2$$
$$= w/aD$$

Thus

$$w/D = d\, a\, A_o \exp(-E/RT)/V\xi^2\rho^2 \qquad (1.14)$$

where w/D, the wear per unit distance, is a measurable experimental parameter

Estimation of variables

A computer search method was used by Quinn, Coy et al to find the 'best' values for the variables of Equ.(1.14). The procedure has been described in a recent publication (15).

Quinn and Coy's Computer Program

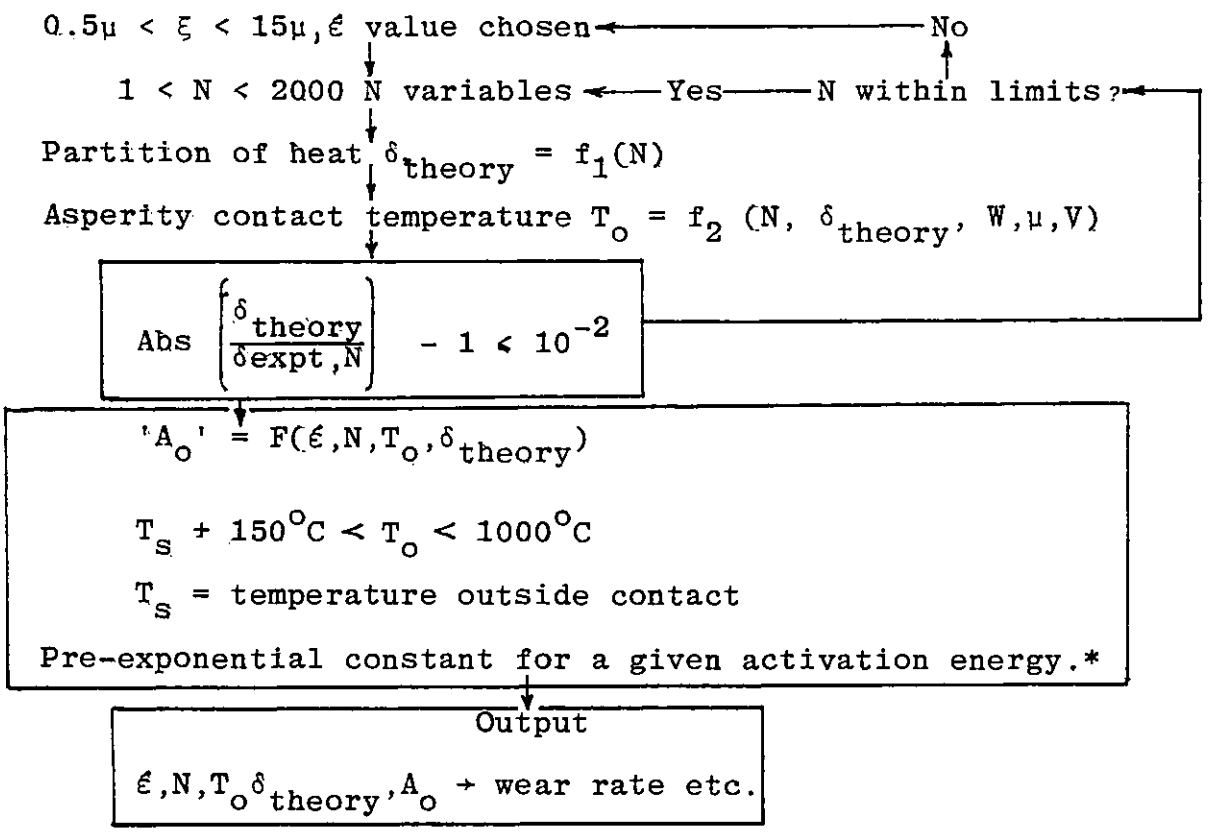

A reasonable agreement between experiment and theory has been found provided one accepts a fairly erratic variation in the values of A_o, N and ε. Since one cannot observe the wear process in detail it is very difficult to judge the acceptability of this variation.

This model of oxidative wear appears most applicable to situations like a pin on disc with an apparent contact stress of a few MPa and a flash temperature of at least 200-250°C. Below 200°C, the Wagner law is unlikely to apply (as discussed in Chapter 2).

---

*Iron oxidises in a complex manner, three activation energies must be considered, depending on the temperature. The change in activation energy corresponds with the change in oxide i.e. Fe_2O_3 - Fe_2O_4 - FeO (as mentioned Chapter 2).

1.4.1.2 Low temperature theory of unlubricated mild wear

Wilson, Stott and Wood (18) have gone to the other extreme with flash temperature, it is deliberately minimized by setting a very slow sliding speed of a few mm/sec. Consequently a radically different mechanism is deduced. As with the high temperature case, the theory applies to a situation where initial severe wear is followed by mild wear as shown in Figure (1,5),

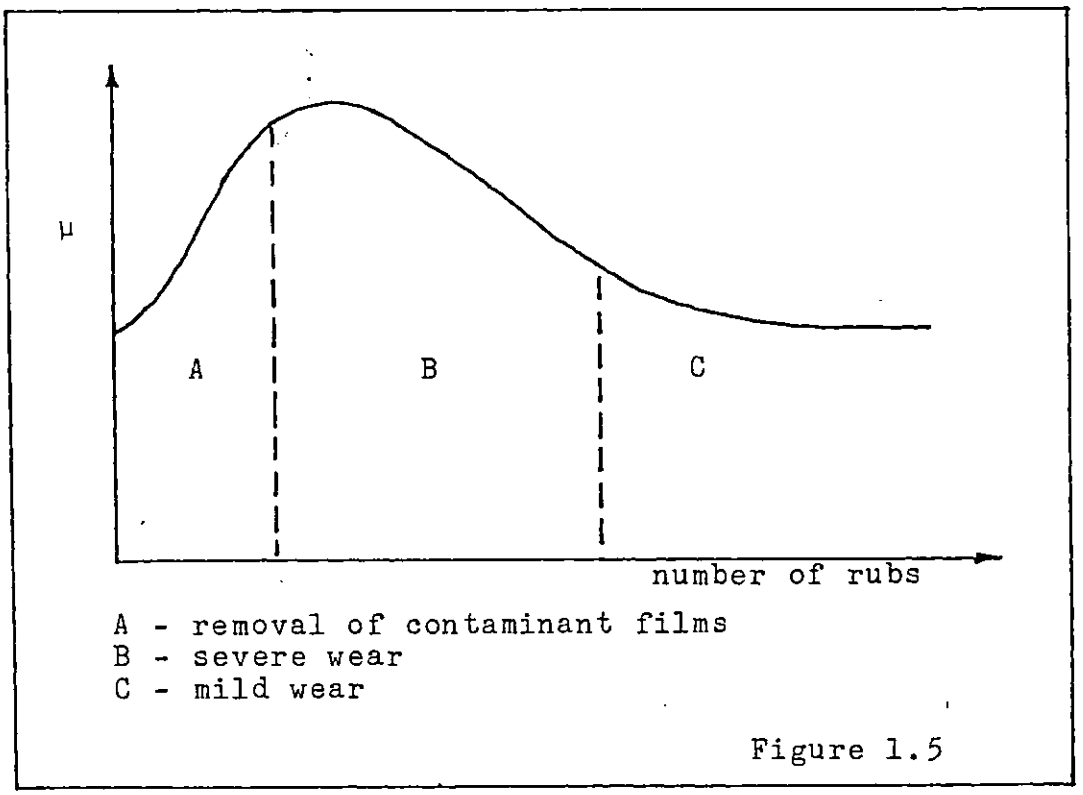

Figure 1.5

Wilson et al's mechanism for low flash temperature mild wear is illustrated in Figure (1.6).

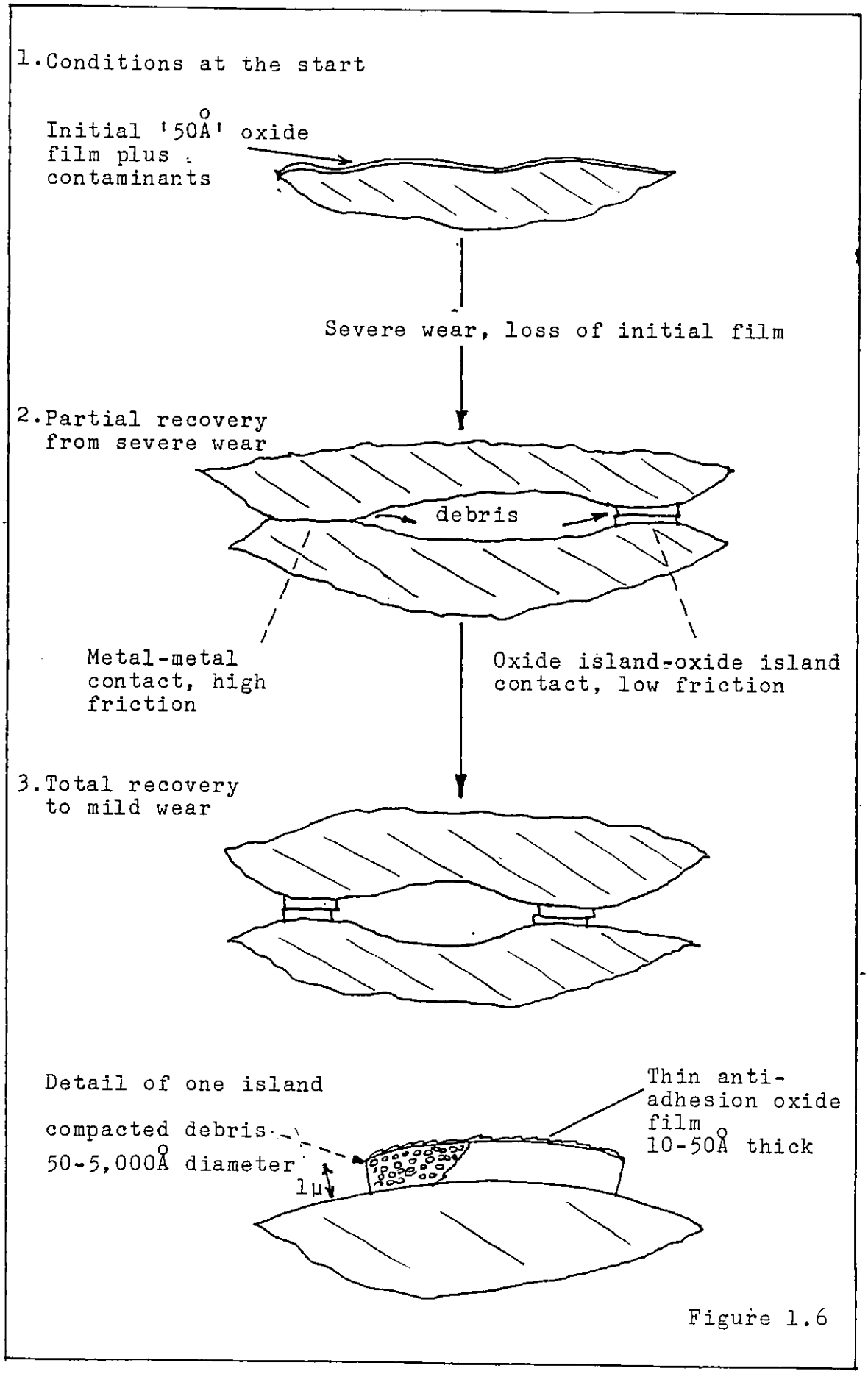
1.Conditions at the start
Initial '50Å' oxide film plus contaminants
Severe wear, loss of initial film
2.Partial recovery from severe wear
debris
Metal-metal contact, high friction
Oxide island-oxide island contact, low friction
3.Total recovery to mild wear
Detail of one island
compacted debris 50-5,000Å diameter
1μ
Thin anti-adhesion oxide film 10-50Å thick

Figure 1.6

Wilson, Stott and Wood's mathematical model

Wilson et al (18) divided the surface into two categories:

(a) metal surface, clean or only covered with a very thin film i.e. ≤ 25 Å thickness,

(b) oxide-debris covered surface - 'islands'.

If Q is the fraction of surface covered by islands, A is the true area of contact and N the number of contacts then:

$$n_{m-m} = (1 - Q)^2 N \quad (1.15)$$

$$n_{o-o} = Q^2 N \quad (1.16)$$

$$n_{m-o} = 2Q(1 - Q)N \quad (1.17)$$

where n is the sub-total of contacts for each category; i.e. m-m or metal-metal, o-o or oxide to oxide, m-o metal to oxide.

Friction force equations are developed on the basis of a shear stress x asperity area x ductility factor formula. All asperities are assumed to bear the same load.

Thus

$$a_{m-m} = W/NP_m \quad (1.18)$$

$$f_{m-m} = s_m \alpha_m a_{m-m} \quad (1.19)$$

where a_{m-m} = metal asperity area, f_{m-m} is the frictional force on just one asperity, s_m is metal-metal asperity shear strength, α_{m-m} = metal ductility factor.

Thus

$$F_{m-m} = n_{m-m} f_{m-m} = s_m \alpha_m n_{m-m} \frac{W}{NP_m} \quad (1.20)$$

$$= \frac{sm}{P_m} \alpha_m (1 - Q)^2 W \quad (1.21)$$

Iron-Oxide is harder than iron so the contact area a_{m-o} is controlled by metal deformation. The oxide-substrate metal

interface is assumed to be strong so the shear occurs in the opposing metal asperity.

Hence

$$F_{m-o} = \frac{Sm}{Pm} \alpha_{m-o} 2Q(1 - Q)W \qquad (1.22)$$

where α_{m-o} ductility factor for metal to oxide interactions.

Oxide-oxide interactions: deformation of oxide controls the contact area in this case so:

$$F_{o-o} = \frac{So}{Po} \alpha_o Q^2 W \qquad (1.23)$$

α_o = ductility factor for oxide-oxide interactions

Po = flow pressure of thick oxide.

Summing up all the friction forces:

$$\Sigma F = F_{m-m} + F_{m-o} + F_{o-o}$$

$$= W \left[\frac{Sm}{Pm} \alpha_m (1 - Q_r)^2 + \frac{Sm}{Pm} \alpha_{m-o} (2Q - 2Q^2) + \frac{So}{Po} \alpha_o Q^2 \right] \qquad (1.24)$$

The definition of friction is

$$\frac{\Sigma F}{W} = \mu \qquad (1.25)$$

Define

$$i = \frac{So}{Sm} \text{ and } k = \frac{Po}{Pm} \qquad (1.26, 1.27)$$

then:

$$\mu \frac{\Sigma F}{W} = \frac{Sm}{Pm} \left[\alpha_m (1 - Q)^2 + \alpha_{m-o} (2Q - 2Q^2) + \alpha_o \frac{i}{k} Q^2 \right] \qquad (1.28)$$

The long term friction value is assumed to correspond to pure 'island to island' contact. Thus Q = 1 is deduced and only the last term is Equ.(1.28) remains. Since typically μ = 0.6 and on the basis of literature evidence [18] Sm/Pm = 0.2, then α_o i/k = 3. From previous

experimental work by Wilson et al. $\alpha_m = 9$. The remaining unknown is α_{m-o}. As long as its value is less than 2.0 Wilson et al consider its precise value to be not critical. To complete the derivation one must consider the change in Q with rubbing, $\frac{dQ}{dD}$ or more precisely $\frac{dQ}{dt}$. Oxide and oxide covered debris to form the islands comes from metal to metal asperity contacts. At atmospheric pressure the metal surfaces will have reached the saturation thickness 20-25 Å (see Chapter 2) of very thin oxide film in a fraction of the time for each pass of the slider.

The debris resulting from a metal-metal contact will also be of a 'saturation' value. Thus the growth of the islands is proportional to the surface not covered by islands multiplied by the number of passes. For a constant amplitude the number of passes is equivalent to the sliding distance.

i.e. $$\frac{dQ}{dD} \propto (1 - Q) \qquad (1.29)$$

$$Q = 1 - \exp(-BD) \text{ , where } B = \text{constant} \qquad (1.30)$$

Given that the relation for μ is usually similar to this example of equations quoted by Wilson et al.

$$\mu = 1.8 - 2.8Q + 1.5\,Q^2 \qquad (1.31)$$

It is evident that μ also tends towards a limiting lower value as wear progresses.

This theory is more recent (publ. 1980) than Quinn's and probably will undergo the same process of qualification. One fundamental result to note is the dependence of the mechanism on operational conditions such as load and speed.

1.4.2 Lubricated mild wear

The difference between lubricated mild wear and E.P. conditions has been recognised since the early work of Davey and Edwards (19). There is as yet no developed model for lubricated wear comparable to that for dry mild wear. With sulphur compounds present it appears that the film under mild or Anti-Wear conditions is very thin thus surface analysis meets severe difficulties. Allum and Forbes (20) postulated a thin mercaptide layer on the surface of EN31 steel lubricated by a low sulphur base oil containing Di-n-dodecyl, diphenyl, di-tert-butyl and di-allyl disulphides. Coy and Quinn (21) using the same steel lubricated by dibenzyl, di-tert-butyl and di-phenul disulphides found a thin Fe-So-O film. Wheeler (22) recently investigating 3040 stainless steel lubricated by D.B.D.S. (18-20% Chromium, 8-12% Nickel, less than 0.081%carbon) found that during mild wear only a oxide film 50% to 100% thicker than the unworn film was found. To give an idea of film thickness, unworn films have thicknesses of 30-50Å, so the worn film would be 45-100 Å thick. Wheeler found that iron sulphide films are only formed during severe wear which is in direct contrast to Coy, Quinn, Allum and Forbes. It could be however, that different steels form different films.

Wheeler also concluded that there was a possibility that DBDS worked by adsorption during mild wear since his technique was not sensitive enough to detect a monolayer of adsorbed species. Spikes and Cameron (23) agree with this finding.

Bird and Galvin (24) however remarked on the inhomogeneity of a frictional film compared to a corrosion film. Godfrey (25) also stated that part of the film (e.g. between asperities) may be non-functional. Realising that the active areas of surface (i.e. asperity collision areas) are only of micron size then the use of large area analysis to deduce a mechanism is a difficult task. This point is discussed further in Chapter 2.

1.4.3 Lubrication under E.P. conditions

The chemical basis for E.P. action is illustrated below in Figure

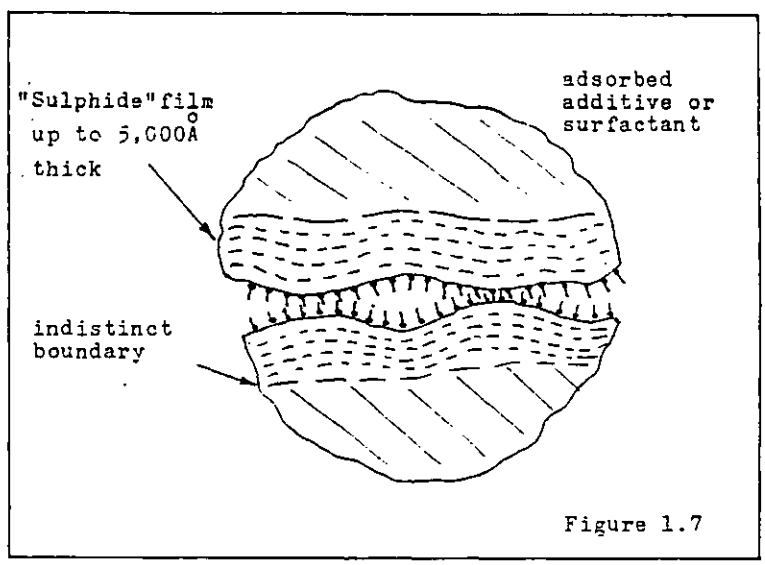

Figure 1.7

The coincidence of sulphur rich areas and regions of E.P. loading has been noted by many workers e.g. Loeser, Wiquist and Twist (26), Borsoff and Wagner (27) and Campbell (28). The deposition of iron sulphide as opposed to 'entrained sulphur' was detected by Allum and Forbes (20) using an electron-micro-probe analyzer. Prutton (29) was the first to suggest that iron sulphide formed the E.P. layer, most

other workers agree that this is broadly true though the actual film is more complex than that.

The current understanding of the E.P. mechanism appears to be as follows.

Under extreme conditions of sliding speed and load, high frictional temperatures are generated in the contact zone. These enable a thick film to be formed by fairly rapid corrosion of the metal. Allum and Forbes (20) cited evidence to show that it acts in a sacrificial manner despite its thickness. There is only indirect evidence of film 'sacrificiality' i.e. the load bearing film is rubbed off on each asperity collision. Baldwin (30) found that pre-formed sulphide films do not last very long in the Falcex test which implies that any sulphide film will soon be worn away by rubbing. Spikes and Cameron (23) found that E.P. activity declines quickly in a ball on triplane test when the operating temperature is lowered to below the reaction start temperature of the E.P. additive. Baiely and Cameron (4) also deduced 'sacrificiality' by comparing the friction results for inert pin on reactive ball with reactive pin on inert ball in a triplane rig. This film consists of a mixture of sulphides and oxides with sulphur additives, depending on lubricant and conditions (20,32). Because of its thickness, and apparent independence of adsorption of surfactants e.g. stearic acid, it is capable of lubricating under very extreme conditions. The question of adsorption on E.P. films is still unresolved. Sakurai et al (33) originally postulated that the iron sulphide adsorbs fatty acids very strongly and presented apparently valid data to prove it.

However Date (34) in some recent work showed that slightly oxidized iron sulphide i.e. $FeSO_4$ are the species with strong adsorption properties. Summarizing, it appears that the presence of surfactants keeps the coefficient of friction low at 0.1. The coefficient of friction will otherwise rise to 0.3 as Greenhill (35), Mills and Cameron (36) found.

More recently, Spikes and Cameron (23) and McCarroll Mould, Silver and Sims (37) have presented evidence against the thick film theory, instead of thousands of Å a few hundred Å film thickness appears crucial which would make the assumption of 'sacrificiality' more reasonable. Thus the picture of E.P. action is still not certain in the details despite the large amount of effort spent in research.

1.4.4 Severe wear and seizure

Severe wear is generally regarded as the breakdown of any mild wear or E.P. lubrication mechanisms leading to excessive friction and surface damage. The details of the mechanism of severe wear are not of great interest to this work and thus no detailed discussion follows.

1.4.5 Other methods of avoding severe wear

Because of the corrosivity of E.P. additives, there is considerable interest in other means of avoiding scuffing. Nitriding, cyaniding and 'Sulzurf' (38) are some of the principal options. The philosophy behind these measures is to reduce 'adhesivity' by surface hardening and lessening metal content; e.g. substitution by sulphides, carbides and nitrides. A broad review of surface coating has been compiled by Gregory (39).

1.5 Variables and Factors Determining E.P. Lubrication

The influencing variables are numerous and to facilitate an understanding of their roles, they are sorted into 5 groups. These are:-

1) Operating variables; load, speed etc.
2) Lubricant, physical and chemical characteristics.
3) Material factors, metallurgy, surface and bulk chemistry, topography and surface science.
4) Environmental: ambient conditions, oxygen and water.
5) Dependent variables; friction wear rate etc.

In Figure 1.8 a tetra-hedron is used to illustrate the relationship between all the families of variables i.e. each group interacts with all the others to a certain extent.

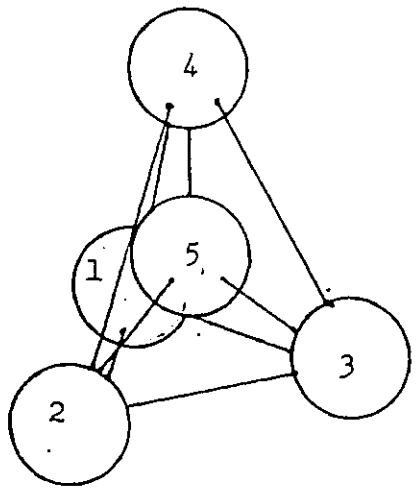

Figure 1.8

1.5.1 Operating variables

The operating variables of greatest interest to this work are: sliding and rolling speed, load, contact geometry, residual surface stress and surface roughness.

Operating variables tend to combine to cause an effect, thus the discussion is largely arranged in terms of the effect 'A' of operating variables, effect 'B' etc.

1.5.1.1 Effect of operating variables on contact temperature

The prime influence of operational variables is on the temperatures within the contact. In any sliding contact, temperature may be divided into 3 components. These are: bulk, conjunction and transient temperature components, Figure 1.9 illustrates their role.

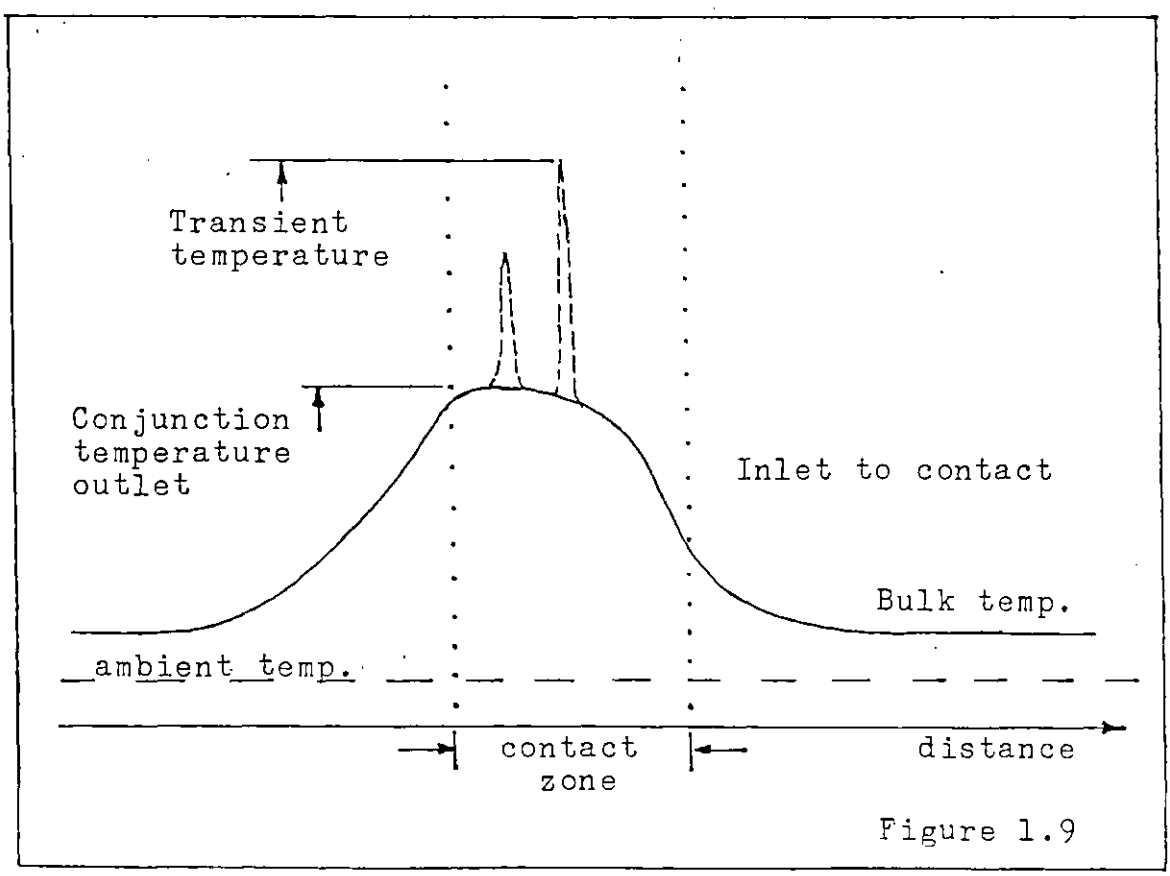

Figure 1.9

Bulk temperature is a steady state temperature caused by the cumulative effect of a large number of contact temperature cycles. It is strongly influenced by the geometry of contact and may raise or lower the conjunction temperature (10) accordingly Conjunction temperatures, first postulated by Blok (40) are thought to determine the desorption of adsorbed additives thus leading to scuffing (41). This 'conjunction theory' is of great practical interest and as such has been the focus of much work. Workers such as Archard (17) and Francis (42) have refined the theory. Transient temperatures as demonstrated by Furey (43) are very high but of very short duration, their tribological importance is uncertain. The Conjunction Theory does not allow for the cooling effect of lubricant which often has a marked cooling effect (44). On the other hand there is evidence that the theory may under-estimate conjunction temperature in certain situations. Hsu and Klaus (45) found a mismatch between temperature values derived from the Arrhenius law and those derived from conjunction theory. However they did not consider 'mechanical activation' (mentioned below) and maybe the answer lies there. Conjunction temperature is still one of the great uncertainties in lubrication. Consequently the development of any theory of lubrication involving chemical kinetics is severely hindered.

1.5.1.2 The effect of operating variables on the out-of-contact time and the influence of rolling and sliding speed on E.P. action and scuffing

Out-of-contact time as advocated by Bailey and Cameron may be important. The thick sulphide films of 1000 + Å investigated by Campbell (28) and Barcroft et al (46) must

require a considerable amount of time to form judging by Sakurai's data(47). Thus if the film is sacrificial in nature, then the contact frequency must be important. Hence contact geometry and rotational speed should affect E.P. action insofar as they determine contact frequency.

The effect of rolling and sliding speeds. Bell, Dyson and Hadley (48) have shown the importance of rolling speed on scuffing independent of its influence on flash temperature: an increase in rolling speed may reduce the likelihood of scuffing and the nature of scuffing varies with rolling speed. Scuffing can be slow or fast to develop for small or large rolling speed respectively. This suggests a minimum number of scuff contacts. Carper, Ku and Anderson (49) reached similar conclusions, their view being that at constant sliding velocity increasing the scum speed of the two discs would raise the flash temperature. As yet the reasons for this trend are unclear, it appears to contradict the Out-of-Contact theory in its current form (this theory would apply to oxygen as well as to sulphur). An explanation may lie in the Borsoff effect (50). Spikes (51) and Rowe (52) have shown that lubricity agents need a finite time to desorb. A shortening of the contact time raises the flash temperature needed to cause desorption.

Bollani (53) has shown that high sliding speed reduces the amount by which sulphur additives raise the scuff load compared to lower speeds. Bell et al (48), Bell and Dyson (54) and Carper et al (49) have also observed that sliding speed lowers the flash temperature, however no convincing explanations have been given.

1.5.1.3 Influence of residual stress and initial roughness on E.P. action and scuffing

Residual stress has been shown to affect E.P. activity (55), some additives are improved by tensile stress, others are hindered by it, DBDS is scarcely affected.

It appears likely that surface roughness will have an effect on E.P. action there is little evidence in the literature on this. Uya (56) in a literature review cited work showing the effect of roughness on scuffing in plain oils. It is theorized that an appreciable roughness is beneficial otherwise opposing surfaces can touch without significant asperity deformation. Asperity deformation leads to accelerated oxidation by mechanical activation. Rabinowicz (59) suggested that the ratio of wear particle size to roughness may be important. There is however considerable evidence of an optimum roughness for lubricity agents (57,58).

1.5.1.4 Influence of load on scuffing and E.P. action

Though load itself is an operating variable most investigators consider 'scuffing load'. Thus there are not so many works on the influence of load on scuffing and E.P. action. Salomon (60) however describes the effect of load on scuffing on E.P. action.

Figure 1.14 is based on Salomon's illustration of the load effect.

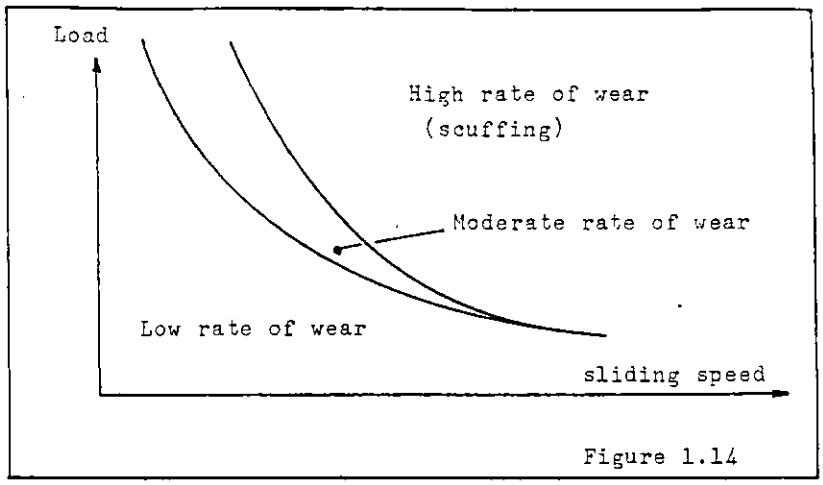

Figure 1.14

1.5.2 Lubricant characteristics

A lubricant can generally be regarded as having two components, a carrier fluid and an additive package.

(a) Carrier fluid

This is often envisaged as chemically inert and thus merely determinesthe hydro-dynamics of the contact. In practice it can exert a considerable effect on Boundary Lubrication. The carrier fluid will dissolve oxygen in accordance with Henry's law to a degree largely dependent on its atomic weight (61). Vinogradov (62) has hinted at the importance of diffusion in 4-ball tests where anti-seizure lubricant is oxygen. Begelinger (68) considers that aromatics in the base stock were beneficial since they are 'transfer' agents for oxygen. Even if the oxygen does not affect the lubrication process directly, it may react with the carrier fluid to produce polar impurities which can have an adverse affect on lubrication (64,65). It is also very difficult to eliminate impurities. The lubrication of many devices have been shown to rely on impurities, a good example is aircraft fuel pumps (66,67). Thus E.P. action exhibited by real lubricants may not directly

correspond to that of laboratory formulations using pure substances.

(b) Additives

I. Organo-sulphur E.P. additives. Under E.P. conditions the critical parameter appears to be chemical reactivity (68) or lability as McCarroll et al stated (37). An unreactive additive has little or no E.P. properties (68). The ability of the additive to react with the steel to form a sulphide layer has been recognized by many workers (29,26)) as crucial to E.P. lubrication. Allum and Forbes found a correlation between sulphur content in a wear scar and E.P. performance in a 4-ball wear test (20). Sakurai et al showed a proportionality between log-sulphide film formation rate and log mean Herzt load (69). For mild wear however the ranking of sulphur additives is on a different basis (20).

II. Other additives. Substances, not necessarily connected with E.P. lubrication may influence or block E.P. action. Spikes and Cameron (23) have shown for example how high temperature detergents may obstruct E.P. additives by preferential adsorption on the reaction surface.

1.5.3 Material factors

Of relevance to E.P. lubrication and scuffing are the bulk physical and metallurgican properties of the material and the surface metallurgical, chemical and physical properties of the friction interface. These topics are discussed in this order.

1.5.3.1 Bulk physical and metallurgical properties

High thermal conductivity is valuable in removing heat, Housz (70) showed that nylon to steel was preferable to nylon-nylon in gears because of the lack of conductivity in either of the mating surfaces.

The different phases of steel, ferrite, pearlite, martensite, austenite and carbide all have different strengths and hardness which should affect scuff propensity. It is believed that adhesivity varies with solid state parameters, and a major factor (71) is crystal structure. Whatever the causes, there is direct evidence for different E.P. behaviour with the various steels. Grew and Cameron (72) have suggested that austenite is the least reactive and therefore should be avoided. Rounds (73) stated the contrary and recently Jahanmir (74) showed that ferrite-pearlite steels produce different surface films than martensite steels. The information available is not yet sufficient for a definite answer to this question,

1.5.3.2 Surface metallurgy

Often the metallurgy of the surface is not the same as that of the bulk material (75). The average crystal orientation of the surface may change so as to minimize adhesion (76). In very severe conditions of friction and wear, 'white layers' are formed (77). Coy and Quinn (21) showed that 'white layers' coincide with poor E.P. performance, whether these are a cause or a consequence of E.P. failure is unknown. White layers are very hard, Baxter (78) suggested that they could be deliberately promoted in order to improve a surface. As with texturing (76), as mentioned above the philosophy is

to minimize adhesivity rather than directly increase E.P. activity. The alloy content of a rubbed surface is known to be different from the bulk. Godfrey (32) has argued that the E.P. conditions of corrosion and surface heating favour alloy migration to the surface. Migration of silicon to the surface is particularly marked in steels. Ferrante and Buckley have shown a similar effect with rubbed copper alloys.(80) Moreover, oxide may become incorporated into the surface layers as has been shown for copper rubbed by steel (81). Thus it can be seen that there is considerable feedback between the causes and the effects in a wearing contact. In this case, friction and wear influence surface metallurgy which in turn affects friction and wear.

1.5.3.3 Surface physics

According to the standards of surface physics (82) the surfaces encountered in a frictional contact are complex and particular. One of the most popular models of the surface is the Terrace-Ledge-Kink model (88). The model stems from the realization that crystal planes are usually neither perpendicular nor parallel to the surface. Thus a surface consists of a series of terraces and ledges, as illustrated in Figure (1.10).

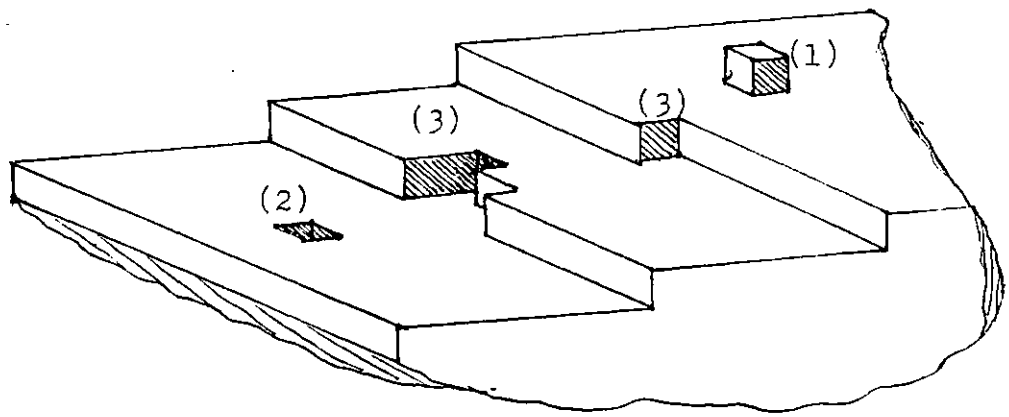

Figure 1.10

There are also various secondary features such as adatoms (1) (shown in Figure 1.10) vacancies (2), gaps and deviations in the terracing (3). There are also present screw dislocations and edge dislocations. These topographical features are not stationary but have a mobility proportional to temperature. At half the absolute melting point, mobility is quite marked. Atomic topography should affect adhesion, presumably the 'mismatch' it creates reduces the adhesive bond. Chowdhbury and Pollock (84) showed that a critical load is needed before adhesion occurs between clean titanium surfaces. The value of load corresponds to that required to deform the nano-meter size 'mini' asperities. Landheer, Dackus and Klostermann (101) have devised a model of asperity adhesion where micro roughness limits (atomic roughness) true atom-to-atom contact to areas of dimensions $(10^{-8}m)^2$. Figure 1.11 shows the form of asperity contact envisaged by Landheer et al.

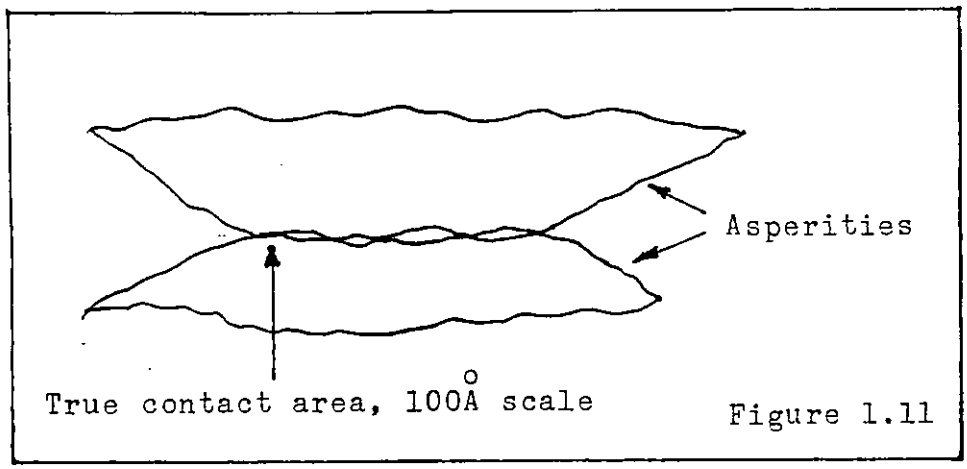

Figure 1.11

Dislocation density is limited to $10^{10}/m^2$ so that plastic flow within a 100 Å x 100 Å area is not easy. Thus effective adhesion is limited by the lack of true contact.

A satisfactory answer to the question of adhesion between opposing asperities with all the implications for E.P. action and scuffing must await the future efforts of workers in this field.

Another aspect of surface physics which has received more attention in lubrication is surface atomic density. Buckley (85) has discussed the relevance of this parameter. Surface atomic density is known to affect surface energy (86) Rabinowicz (87,88) has advocated the fundamental importance of surface energy for B.L., since this must determine the adhesion in a contact. However Buckley has remarked on the difficulty of measuring surface energy (87), different methods of measurement give grossly diverging values. Thus it would not appear that the concept of surface energy of solids can be not easily applied to the solution of tribological problems.

It is evident that the term 'nascent surface' is but a name for a complex and variable object, and that

results derived by one method of producing a nascent surface may not have a general validity.

1.5.3.4 Surface chemistry

Gulbransen (90) emphasised some two decades ago, the importance of surface defects in accelerating corrosion, in his view it was a valid question as to whether a surface devoid of all known imperfections would react at all.

Muetterties (91) uses the Terrace-Ledge-Kink model to explain surface chemistry of metal plus hydrocarbon systems. The various types of surface feature e.g. a 'ledge' provide favourable bonding sites for different adsorbed molecules. Decomposition reactions may occur at these sites or more significantly, film formation reactions may be nucleated. Thus the nature of the surface has a strong influence on the kinetics of film formation.

Another important topic is mechanical activation by plastic deformation. Heidermeyer (92) has provided examples of the strong effect mechanical activation has on kinetics and equilibria. The 'start temperature' of a surface reaction can be lowered significantly by mechanical activation. Meyer et al as discussed in Chapter 2 and (93) showed that this effect, 'start temperature lowering' occurs on reaction of activated steel powder with organosulphur compounds. Groszek (94) has also shown that mechanical activation also increases the heat of adsorption of surfactants on oxide surfaces.

1.5.4 Environmental conditions

The environment supplies two substances and determines on variable which significantly affect E.P. action. These are oxygen, water and ambient temperature respectively.

1.5.4.1 Ambient temperature

Ambient temperature is the lowest temperature at which the lubricant must function. Thus it determines the type of lubricant most applicable, e.g. oils at 150°C, solid lubricants at 400°C. A sudden decline in ambient temperature, e.g. hypoid rear axle of truck involved in a short period of cold weather, has been the cause of E.P. failures. However these are rare cases and for most purposes ambient temperature may be regarded as a constant. It is not therefore of prime interest concerning means to extend E.P. activity.

1.5.4.2 The influence of oxygen

Oxygen influences E.P. action in several ways:

(i) dissolves in oil to act as an E.P. agent;

(ii) produces polar agents by oxidation of the oil;

(iii) inhibits other E.P. agents;

(iv) when present with other E.P. agents it provides a component of the reaction film.

(i) As referred to previously, oxygen is essential to the mechanism of mild wear (13). Bjerk (95) showed that refined oils containing no additives can successfully lubricate under quite severe conditions provided an oxygen atmosphere is present. Removal of oxygen from the oil by flushing with

nitrogen renders scuffing inevitable for quite small loads.

(ii) Oxidation of the oil is generally considered undesirable, but it can produce useful boundary agents (96). These oxidation products (their structure is usually unknown) can act in a similar manner to fatty acids by providing lubricity (97).

(iii) Buckley has shown that diatomic oxygen will displace adsorbed H_2S in a vacuum wear test (98). Tomaru et al (99) having noted Buckley's result performed hot-wire corrosion tests on steel by sulphur solutions, (Barcroft's hot-wire device (100)) in various concentrations of oxygen. Accelerated corrosion of high carbon steel was observed when oxygen was displaced from the oil by argon. Irrespective of oxygen concentration, the corrosion film contained mostly sulphide. The oxygen could only have exerted an inhibitory effect. The film's appearance under a scanning electron microscope was also different, though the relevance of this is not exactly obvious. Toyaguchi and Tokai (140) also reached a similar conclusion. They stated that E.P. action was improved by oxygen and corrosion reduced.

(iv) Oxides and sulphides occur in varying concentrations on E.P. film. Severity of conditions appear to decide the balance between oxides and sulphides. Most workers e.g. those quoted previously (20,32), found that in a 4-ball test of E.P. behaviour, iron sulphide (FeS) predominates. Allum and Forbes (20), Baldwin (30), Coy and Quinn (21) have advocated the use of sulphur surface concentration as an index of E.P. activity. The shared view of these workers is that a virtually

pure sulphide film is an essential component of the E.P. mechanism. But the work of Bjerk (95) contradicts this; namely that with a twin-disc rig, only scuffed areas have high concentrations of sulphur. Successfully lubricated discs, or parts of in a partially scuffed disc, have films of mainly oxide. Godfrey (32) has shown that for many well lubricated surfaces (SAE E.P. tests and hypoid gear tests) the wear debris is mostly Fe_3O_4 or γ-Fe_2O_3. Fein (discussion to 32) corroborated Godfrey's findings with some results of his own. By studying wear debris Fein concluded that moderately scuffed regions were covered by oxides of iron with some amorphous silicon dioxide whilst severely scuffed regions were covered by FeS. Though Godfrey's and Fein's work rests on the assumption that wear debris has the same composition as the E.P. film, its correlation with Bjerk's work gives support to the recent view that the concept of a 'sulphide film' is an oversimplification. Tomaru et al (99) showed that the dramatic increase in corrosion by DBDS and sulphur when oxygen was excluded from the oil was not matched by a significant rise in E.P. performance.

One topic that seems to be absent from the literature is the concept of the inhomogeneous friction surface. As with mild wear true contact is limited to a small part of the apparent contact area. Deduction of mechanism by large area analysis is not easy since it involves looking at a very small part of the apparent contact area.

A note on oxide films

Oxide films have been known for more than a century. Farraday is generally believed to be the first to postulate

their existence (102). They exhibit a wide range of properties and significantly modify the behaviour of metal or non-metal e.g. silicon. They are also very sensitive to environment. Farnsworth (103) stated that transition metal oxides are the most sensitive surfaces known for detecting contaminants. High vacuum and bake-out is needed to clean the surfaces. In a typically dirty engineering situation it can be assumed that the properties of the surface are largely a function of immediate conditions.

1.5.4.3 The influence of water

Water is also important in E.P. lubrication though its role is not yet clearly understood. In lightly loaded systems the combination of water and oxygen can cause excessive corrosive wear (104), but in lubricity experiments involving fatty acids the combination is essential for low friction and wear (105). It can have a harmful effect in E.P. situations (106).

1.5.5 Dependent variables: friction and wear

As mentioned in the discussion on surface metallurgy, there is a significant feedback between wear and friction, 'the dependent parameters' and the independent parameters such as load and speed. Usually the feedback is beneficial e.g. texturing (76), surface hardening (78) and stimulated oxidation (107).

When a system is transmitting a lot of energy which largely depends on load and speed, small changes in friction can be important. In a slow speed Bowden-Leben machine, a change in the coefficient of friction from 0.1 to 0.5 will

be merely of experimental interest. By contrast, in a large gear box, a change in the coefficient of friction from 0.1 to 0.2 can precipitate a disastrous rise in contact temperature. Dyson (3) has reviewed some theories relating to energy instabilities in high speed contacts. Padmore and Rushton (108) found evidence of temperatures as high as 500°C in scuffed gear surfaces. So for systems with large intensities of transmitted and dissipated energy generated by contact load and speed, wear rates and contact temperatures could change too rapidly for protective mechanisms to come into effect.

1.6 Subsurface E.P. Effect

Bancroft and Daniel (46) showed that in very heavily loaded gears, sulphur penetrated to 5,000 nm depth. It is not known whether this is a cause or effect of E.P. action. The sulfinız process however gives some E.P. protection on the basis of subsurface sulphur, so presumably the E.P. mechanism is not entirely determined by the surface film.

1.7 A Discussion of Various Theories Relating to E.P. Lubrication

As is well known, the present state of knowledge of E.P. action does not suffice to form an exact theory. Considerable advances though have been made in areas of tribology relating to E.P. action. A short description of the major contributions is presented below.

Rabinowicz has theorised on the size of a wear particle as a function of material properties and on the thermodynamics of boundary lubrication (87,88,109). Blok

developed the transition theory of scuffing (41) and Bowden and Tabor pioneered the theory of adhesive wear and friction (68). The theories of these latter three workers constitute necessary background reasoning to E.P. lubrication since it is the characteristics of adhesive wear and the adsorption of surfactants that create the need for E.P. lubrication. Rowe (51,110) and Spikes (52) have provided theories to explain the effect of speed on friction transition temperatures. Cameron (111) has applied the Laws of Thermodynamics to friction transition temperatures. Quinn (15) and Wilson et al (18) have produced theories on dry mild wear as described previously. Finkin (112) considered the tangential and normal stresses when a sulphide film is loaded by a spherical asperity and thus deduced the variation of coefficient of friction with film thickness. Stolarski (113) has devised a computer program to predict adhesive wear rates by combining the theories of many workers. Landheer et al (101) have applied a theory of adhesion between asperities on the atomic scale. Finally, Sakurai et al (114) deduced a formula for the slow wear rate of steel during lubrication by organo-sulphur compounds.

Thus it is evident that though there are a lot of theories relating to phenomena connected with E.P. lubrication there is nothing that really tackles this subject.

The last mentioned work by Sakurai et al is discussed in detail below as it represents virtually the only quantitative theory on sulphide film formation in a wearing contact.

For a ball-on-disc wear experiment Sakurai et al considered the rate of formation of iron sulphide on the rubbed area of the disc.

$$Fe + S \xrightarrow{V_1} FeS \qquad (1.7.1)$$

By the law of mass action, the forward reaction velocity is proportional to the products of the concentrations of the iron and sulphur.

$$V_1 = k_{10} [F_e][S]$$

where k_{10} = constant

[Fe] , [S] = concentrations of iron and sulphur

(1.7.2)

The thickness of the iron sulphide film is assumed to be negligible and implicitly the temperature is constant. The next step is to consider the rate of removal of iron-sulphide debris.

$$FeS \xrightarrow{V_2} \text{Friction debris} \qquad (1.7.3)$$

where

$$V_2 = k_{20} [FeS] \qquad (1.7.4)$$

and where [FeS]is the interfacial concentration of iron sulphides.

Metallic iron is also present in the wear debris but in their work the prime consideration is the fate of the iron sulphide. The net gain in iron sulphide is the balance of creation and loss thus:

$$\frac{d[FeS]}{dt} = k_1 [Fe] [S] - k_2 [FeS] \qquad (1.7.5)$$

Sulphur is assumed to be in adsorption equilibrium with the friction surface thus (1.7.5) can be replaced by a constant 'c'. Also the area of free iron is the portion of the friction area not covered by FeS. Presumably Sakurai et al visualised the surface as a finely sub-divided 'mosaic' of free iron surface and iron sulphide covered surface (Figure 1.12).

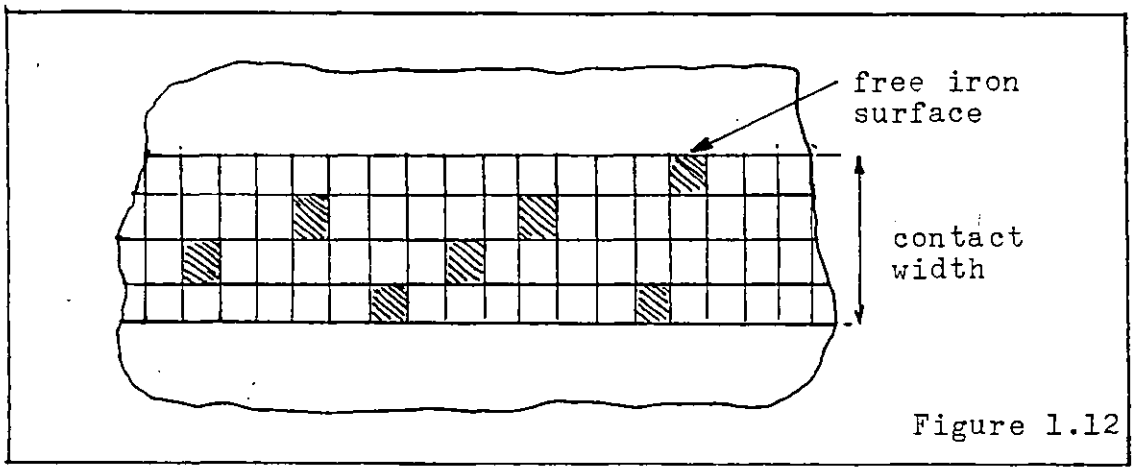

Figure 1.12

Thus $[Fe] = m - [FeS]$ (1.7.6)

where m is a constant relating to the overall reaction area. $[FeS]$ is represented by the variable 'C' then the revised form of the growth equation (1.7.5) becomes:

$$\frac{dC}{dt} = k_{10}L\,(m - C) - k_2C \qquad (1.7.7)$$

Solving the equation:

$$C = C_\infty\,(1 - \exp((-\,(k_{10}L + k_{20})t) \qquad (1.7.8)$$

where

C_∞ = long term concentration

$$= \left(\frac{k_{10}\,Lm}{k_{10}L + k_{20}}\right) \qquad (1.7.9)$$

This gives an assymptotic growth law for the friction iron sulphide as shown in Figure (1.13).

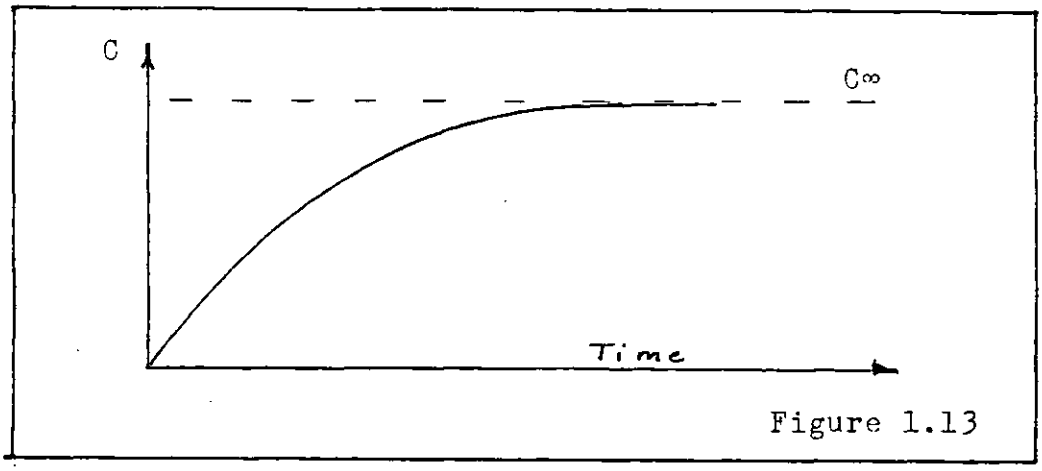

Figure 1.13

A reasonable agreement between theory and experimental results from a ball-on-disc rig was achieved. The emphasis of the work however, was on finding wear rates over thousands of contact cycles and not on finding criteria for deciding whether rapid seizure is likely (

1.8 Conclusions

A lot of investigations into E.P. action have been carried out and a useful understanding of what kind of factors will influence E.P. action has been achieved. But a good picture of the mechanism with some useful formulae has not yet been discovered. Scuffing is still an unpredictable phenomenon, Ku (discussion to (48)) considers that current knowledge is inadequate from both a practical and a theoretical point of view.

The Out-of-Contact theory seems to be the only theory with a reasonable chance of explaining the physico-chemical aspects of the mechanism of E.P. lubricants. The theory though is still in a rudimentary stage. Phenomenological approaches to E.P. lubrication have not found the answer thus

it was decided that a mechanistic approach to the problem be pursued. The rest of the thesis conforms to this aim.

CHAPTER 2

DEVELOPMENT OF A THEORETICAL BASIS FOR E.P. LUBRICATION

2.1 Introduction

Some attempts at developing a firm basis for Bailie and Cameron's 'Out-of-Contact' (as mentioned in Chapter 1) theory are presented in this chapter. This theory explains the mechanism of E.P. lubrication by the rapid formation and destruction of load-carrying sulphide films. Thus E.P. lubrication has been considered from the stand-point of a film kinetic problem. To this end, film kinetics literature as well as tribological works have been studied and are thus discussed in this chapter. The physics of thin oxide-film growth and investigations into the corrosion of steel by sulphur have been the primary sources of literature material and so this chapter mainly relates to these two subjects.

The corrosion of steel by sulphur is a less complex and more empirical subject than thin oxide film physics. Consequently the former is discussed first and suggested implications for E.P. mechanism presented before moving on to the latter subject. The discussion of thin oxide-film physics is started with a literature review which is intended as an introduction to the theoretical work to follows. Developments of the Out-of-Contact theory for E.P. action by sulphur and oxygen are then presented to complete the chapter.

2.2 Corrosin Science - A Comparison of Published Data

Sulphur and sulphur compounds can corrode steel to form iron sulphide films. Since E.P. additives are believed to form by reaction with steel to form iron sulphide, E.P. lubrication may be regarded as a manifestation of sulphur corrosion. Thus E.P. film growth rates should be comparable to corrosion rates by sulphur.

It has been found that the corrosion of steel to form an iron sulphide layer is generally governed by the Wagner law (also discussed in 2.3.6); which is:

$$L^2 = t\ A_o \exp\ (-\ E/RT) \qquad (2.1)$$

where

L = thickness of sulphide film

A_o = constant

t = time

E = apparent activation energy

R = universal gas constant

T = absolute temperature

The Wagner law is used as a means of collating and comparing corrosion data since this can be done by plotting $\ln(L^2/t)$ versus $1/T$. Ideally one might obtain a universal value of constants in the Wagner equation for any chosen corroding agent. This is attempted below for the corrosion of steel by sulphur.

From the literature, four works dealing with the corrosion of iron and steel by elemental sulphur were chosen for evaluation according to the method described above. These works were chosen because the data presented was

easily usable and because only pure iron or mild steel with elemental sulphur alone was investigated. Complications such as the presence of other substances e.g. oxygen or chlorine and steel alloying elements were avoided since these can affect corrosion rates markedly.

The four authors are:

1. Foroulis (115). Iron with sulphur vapour, 250° to 500°C. Microns of sulphide film.
2. Dravnieks (116). Mild steel (0.08-0.06% C) with liquid sulphur, approx. 200°C to 6.p. sulphur 445°C. Microns of sulphide film.
3. Sakurai (117). Carbon steel surrounded by vapour of sulphur compounds, sulphur and hydrocarbons (hot-wire experiments). 0.1 to 0.5 microns sulphide film.
4. Llopis et al (118). Iron with a hexadecane solution of sulphur. 100 to 200°C. 0 to $\approx$ 0.05 micron sulphide. For lack of suitable precautions the surfaces may be assumed to be oxide-covered.

The authors' data is plotted on a gaph of log (L^2/t) versus 1/T (Figure 2.1). The units of L^2/t are $Å^2$/second and 1/T is expressed in Kelvins^{-1}. Initial letters of the authors are used to identify plots, e.g. F for Foroulis. Time to form a 1,000 Å film is also given on the ordinate.

From the graph it is evident that all the results conform to the same broad trend with respect to temperature but also that significant differences exist between the various authors' work. For instance Dravniek's and Foroulis' data do not show a common change in activation energy (slope

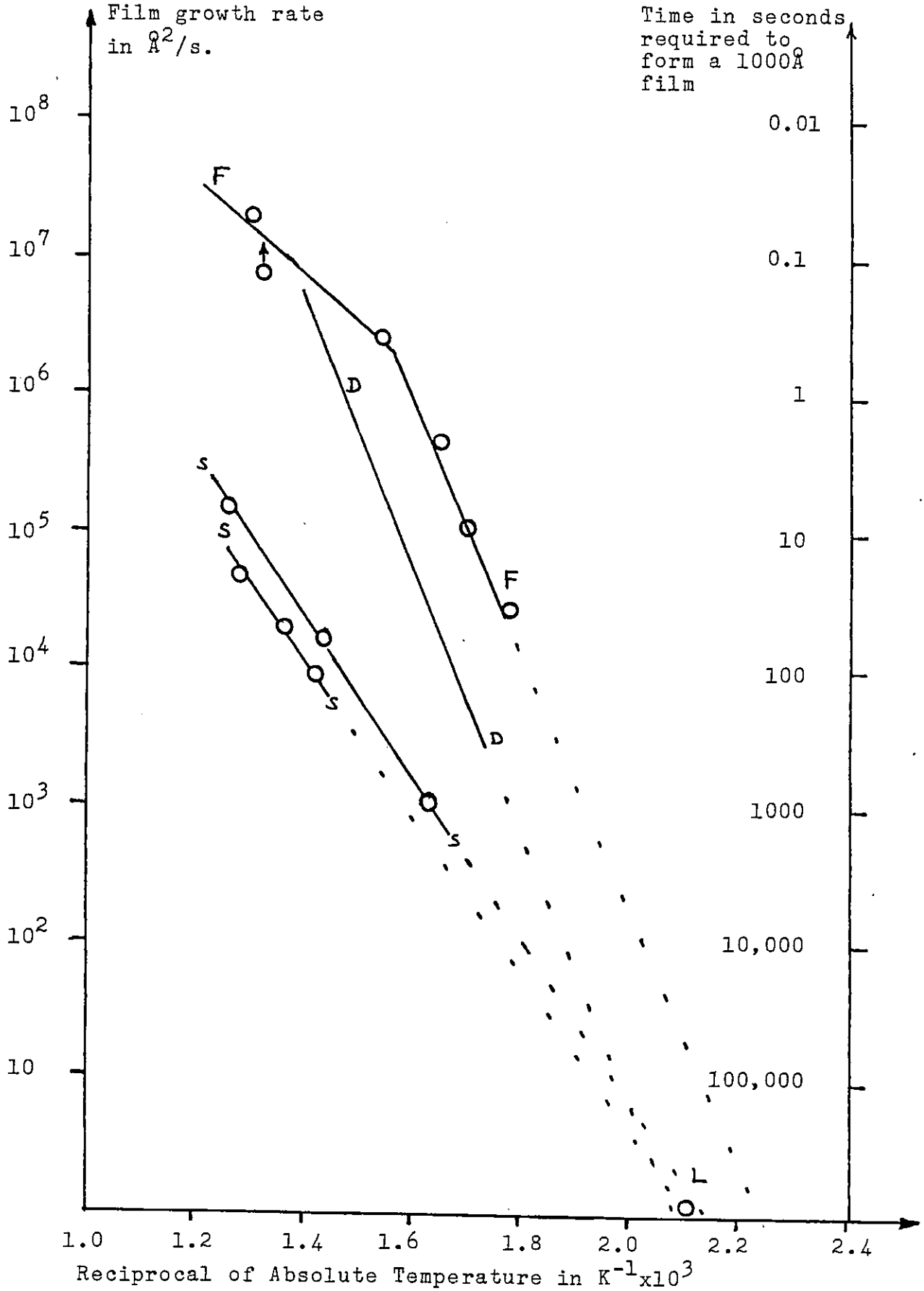

Figure 2.1 Graph of published data on rate of sulphidation of iron versus temperature

of plot). So it may be concluded that a universal growth rate law for an iron sulphide film cannot as yet be derived even for a surface originally covered with oxide.

The approximate correspondence between all the data allows one to make however an inexact estimate of growth rates at any temperature. In particular at around 200°C, a high operating temperature for a gear-box oil, the growth rate of a sulphide film is about a few Å^2/sec. By applying the parabolic relationship i.e. $L^2 \propto t$, one can also find the time to form a film with thickness typical of E.P. conditions Choosing 5,000 Å as the thickness value one has:

$$(5{,}000\ \text{Å})^2 = 2.5 \times 10^7\ \text{Å}^2$$

$$10^7\ \text{Å}^2/(1\ \text{Å}^2/\text{sec}) = 10^7 \text{ seconds}$$

This is a long period of time, thus as observed by Bayles (141) rapid formation of E.P. films on oxide-covered surfaces does not occur.

The next question considered was what are corrosion rates for nascent-surfaces? Now, while one would expect very rapid corrosion up to a few hundred Å (this is discussed further in 2.3), rates beyond a 500-1,000 Å would most probably be similar to oxide covered surface. Given that in a high speed contact, a sacrificial E.P. film would have to be formed within say 0.1 seconds then it appears very unlikely that thick sacrificial E.P. films could exist.

Thus a different picture of E.P. mechanism, from that commonly envisaged, has to be devised in order to sustain the Out-of-Contact theory. This is illustrated below in Figure (2.2)

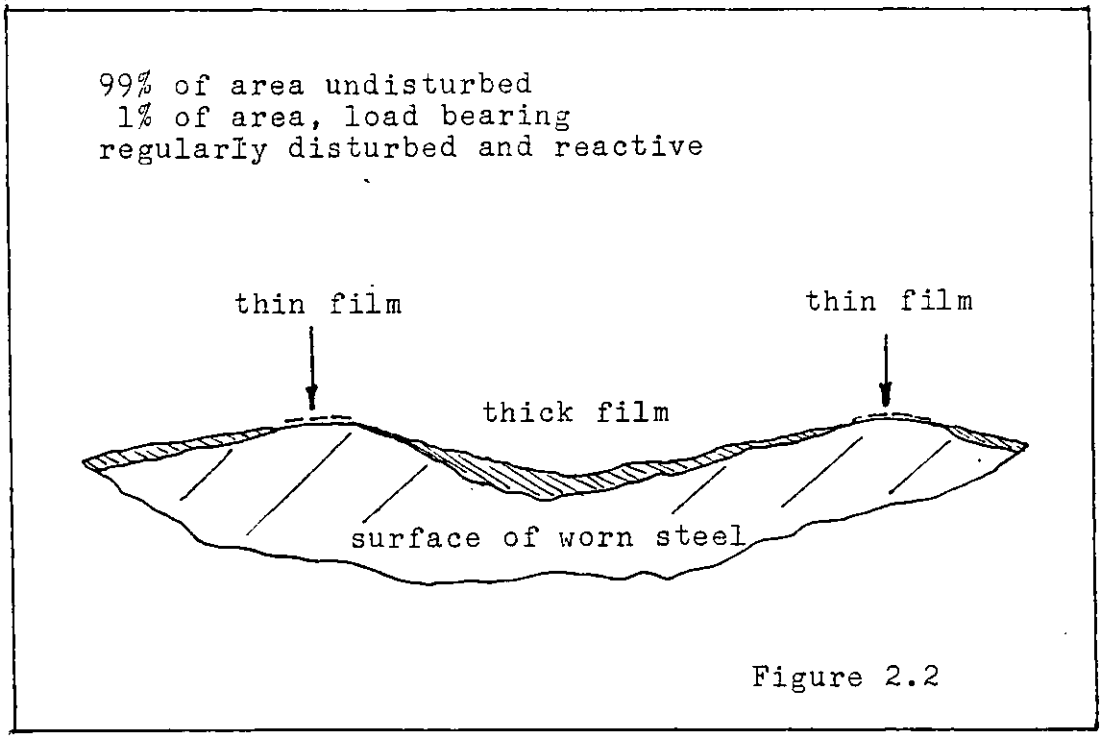

Figure 2.2

Usually about 99% of the surface is not subjected to regular asperity contact and so corrodes in a relatively undisturbed manner (save for conditions in a 4-ball test). Thick films (5,000 Å) can be accumulated on the wearing surface over several hours of running time e.g. in a hypoid reat axle. Normally about 1% of the surface is load carrying; its film is probably thin, a few hundred Å perhaps, and it is regularly removed to expose nascent surface. The film kinetics of this area is different from the larger undisturbed area. The small areas are virtually impossible to detect, since they only give a weak sulphur signal in a surface analysis and thus do not stand out from the bulk area.

Greenhill (35) has shown for example that thick sulphide films of several thousand Å do have lubricating properties, but corrosion kinetics must preclude a key role for these films in E.P. lubrication.

Date's work (34) showed that thick films last about 10 wearing contacts. Therefore as wear progresses and a once quiescent area becomes regularly rubbed, then the thick film originally present will last a few wearing contacts and thereafter a thin film will be formed.

2.3 The Physics of Oxide and Sulphide Film Formation

2.3.1 Introduction

Atmospheric oxygen forms oxide films by chemical reaction on almost every metal known to man. These oxide films range in thickness from 2μ to 20 Å and the oxide may be amorphous, polycrystalline and monocrystalline (rare). In the case of iron, chemical composition of the oxide will vary with time, temperature and position within the film. Sulphide films are not so common, they are formed only when oxygen is in short supply. They show however the same complexities as oxide films and have similar characteristics.

In the past 25 years much theoretical work on the physics of oxide film formation has been carried out. The theories developed by Wagner (119), Cabrera and Mott (120) and Fromhold (119) are able to predict oxide growth with remarkable accuracy. Though the emphasis is on oxide films, Fromhold (119) has stated that sulphide films could be explained by the same means.

The physics of thin film oxidation should therefore contain vital clues to the E.P. mechanism.

In this section; 2.3; the mechanisms, theories and limitations to theories relating to thin-film oxidation and sulphidation are discussed. In addition to constituting a

review of thin film physics this section is intended as an introduction to Section 2.4 "Applications of thin film physics to E.P. phenomena".

2.3.2 Empirical growth laws

Two main types of film growth are generally recognised: parabolic-law growth and non-parabolic-law growth. (Fig.2.3)

Parabolic law growth is a high temperature process and is a consequence of the fast 'random-walk' diffusion of ions shown in Section 2.3.6.1.

Non-parabolic law growth depends on more complicated processes such as electron tunnelling and forced movement of ions by electric fields. Below 300°C-200°C, iron oxidizes very rapidly to 20 Å and then follows the logarithmic law (122,123), above 300°C the parabolic law applies Sulphidization of iron follows a similar course but with certain differences. Iron sulphide is a non-stoichiometric defective compound, and ion diffusion is easier, thus the threshold for parabolic growth appears to be lower at about 200°C (118).

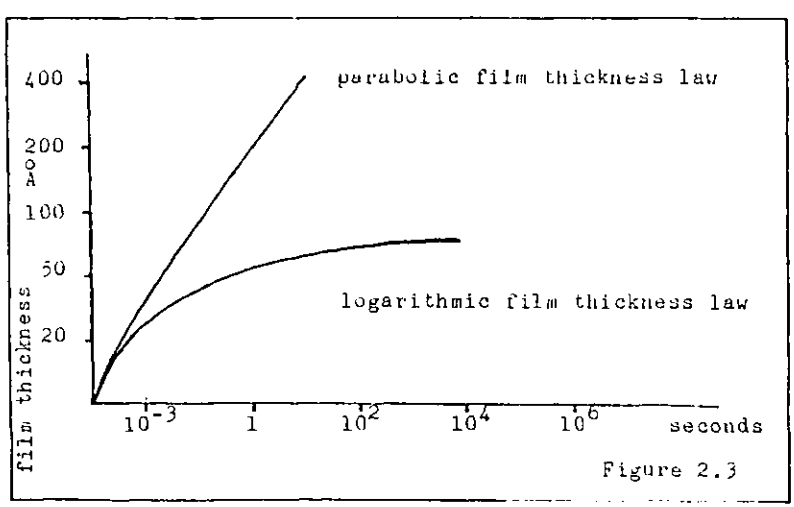

Figure 2.3

2.3.3 Chemical composition of the oxides and sulphides formed

Several different types of oxides and sulphides are formed when iron is corroded by oxygen or sulphur. The variety of reaction product makes the oxidation and sulphidation of iron much more complex than e.g. Nickel.

Four forms of iron oxide are commonly found (102), Ferrous oxide (Wüstite, FeO), Ferrosoferric oxide (magnetite, Fe_3O_4), γ-Fe_2O_3 and α-Fe_2O_3 (hematite). At temperatures less than 200°C (102), γ-Fe_2O_3 or Fe_3O_4 is formed, beyond 200°C only α-Fe_2O_3 is formed. At a temperature between 250 and 275°C the remaining γ-Fe_2O_3 is converted to α-Fe_2O_3. Beyond 575°C Wüstite is formed with thin layers of Fe_3O_4 and α-Fe_2O_3 superimposed. The sequence of oxides is then iron-FeO-Fe_3O_4-α-Fe_2O_3-air.

For sulphides, defective pyrrhotite ($Fe_{1-\delta}S$) is the usual product (122). Foroulis(115) stated hoever that below 370°C a thin gas-side layer of pyrites (FeS_2) is formed. This is partly confirmed by Dravnieks (116) who found that for temperatures below the boiling point of sulphur (445°C), three reaction products were formed. Dravniek's result is illustrated in Figure (2.4).

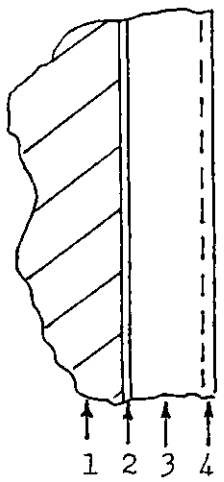

(after Dravnieks (116))

1. Iron
2. Pyrrhotite (FeS) non magnetic
3. Pyrrhotite, magnetic
4. Pyrite (FeS_2), magnetic

Figure 2.4

Both Foroulis and Dravnieks investigated very thick films of several microns thickness. With thin 0.1 μm films sulphide structure may be different. Sakurai (117) found FeS, Fe_2O_3 as the sole products of reaction between iron and sulphur at 490°C, however at 500°C with dibenzyldisulphide instead of sulphur some FeS_2 was found. Sakurai's film thicknesses ranged from 0.1 to 0.5 μm. From the literature available it is evident that much more research needs to be done on the sulphidation process before its mechanism is fully understood.

The composition of the oxide or sulphide film can have a strong influence on the film growth rate and thus must be known before any calculations of growth rate can be performed.

2.3.4 Mechanisms of oxide formation on iron and steel

According to the work of Cabrera, Mott and Fehlner (124) the process of film formation may be conveniently divided into three stages:-

(a) impingement of the first few oxygen molecules to initiate oxidation on the nascent surface;

(b) rapid oxidation by the 'place exchange' process to a very thin 20 Å quasi-oxide layer;

(c) formation of true oxide, further growth proceeds relatively slowly e.g. log.law growth.

The mechanism of oxide formation is illustrated below.

(a) Unoxidized nascent surface

Before any reaction can occur, oxygen molecules must impinge on the surface and be adsorbed. Iron (and steel) is a reactive metal so virtually all the oxygen molecules impinging before a monolayer is formed are adsorbed and bonded to iron as shown in Figure (2.5)

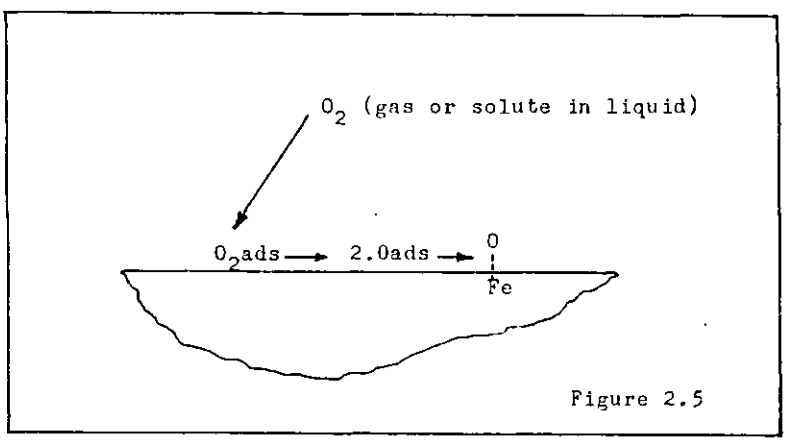

Figure 2.5

A half-monolayer structure of O^{--} ions is formed (Figure 2.6)

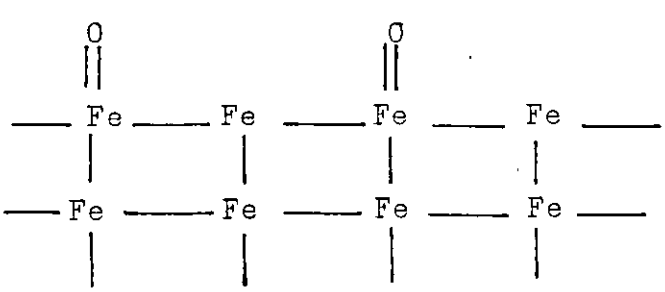

Figure 2.6

(b) Rapid oxidation by the place-exchange process

Further oxidation occurs by the Ely and Wilkinson (127) exchange mechanism. This is illustrated in Figures 2.7 and 2.8 and also described below.

An oxygen molecule is adsorbed in one of the alternate vacant sites. The adjacent bonded oxygen and iron ions exchange places. The shifted iron atoms bonds with the oxygen atom furthest from the metal, the other oxygen atom bonds with the iron on the alternate site. This process repeats itself till perhaps 5 atom layers of oxide are created. Steel oxidizes by the same process according to Tennyson Smith and Crane (126).

(c) Growth of an oxide-film

Growth proceeds by the movement of irons. With α-Fe_2O_3 the O^{--} anion is the more mobile ion, with Fe_3O_4 the Ferrous ion is more mobile (122). The process is illustrated in Figure (2.9) and described below.

Numbers indicate sequence of events

* Place exchange; co-ordinated movement

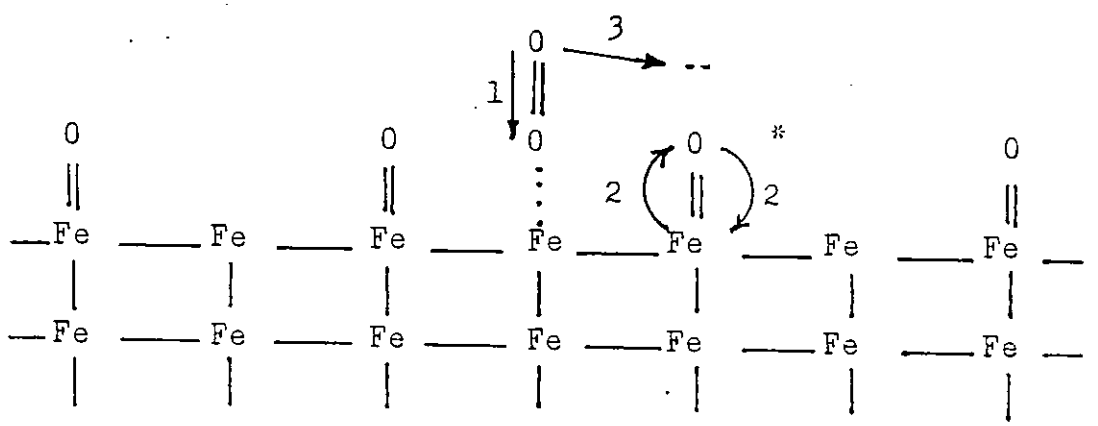

Figure 2.7

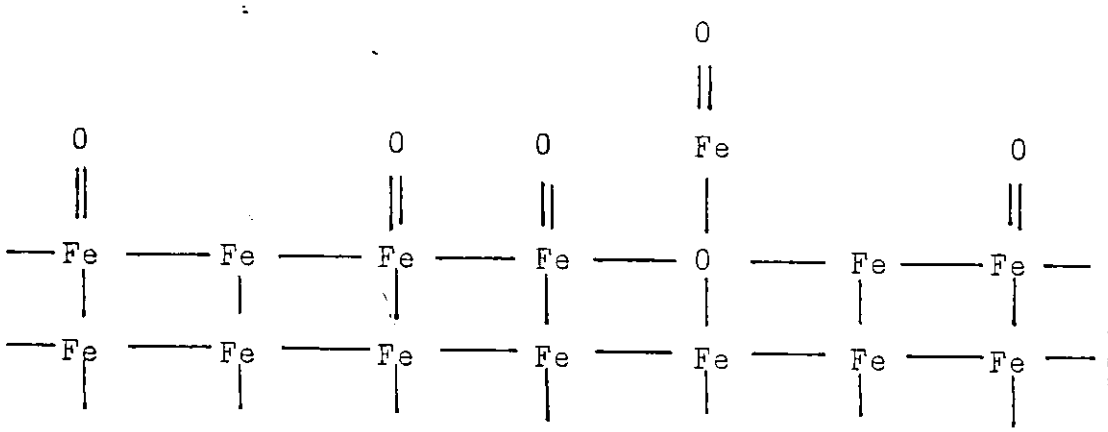

Figure 2.8

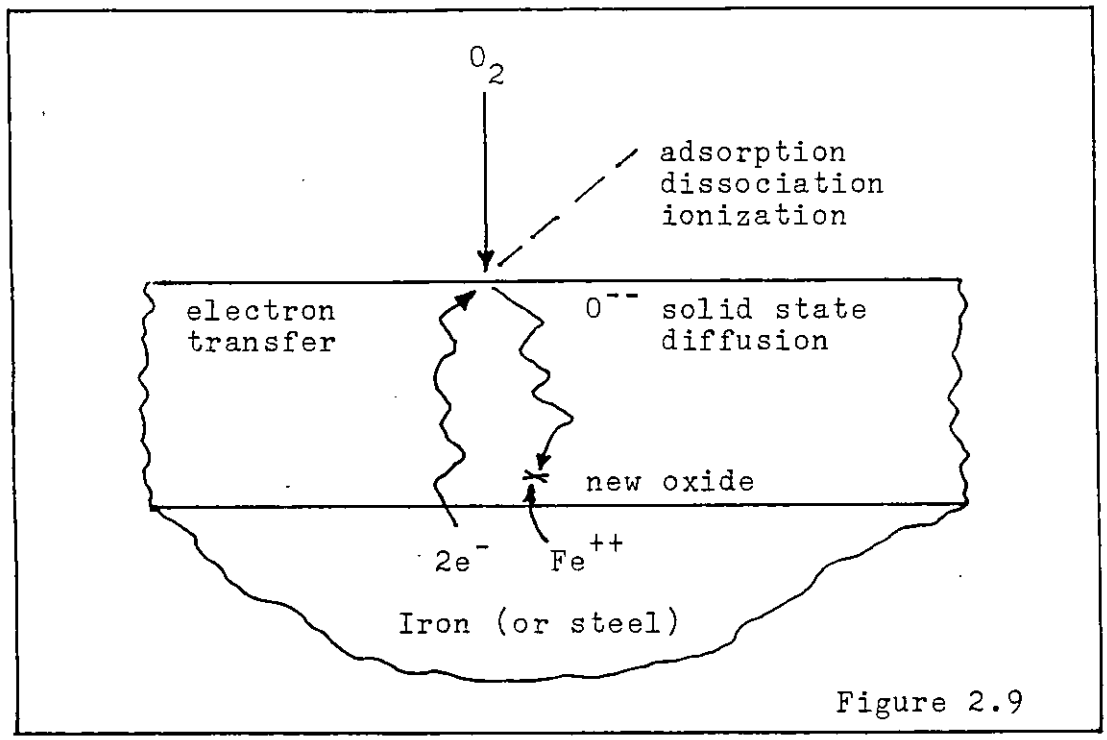

Figure 2.9

Oxygen ions on the surface diffuse through the film to the waiting ferrous ions. New oxide is formed close to the iron-oxide interface. Electrons released by the ionization of iron ($Fe_{metal} \rightarrow Fe^{++}_{oxide}$) balance the flow of charge.

The solid state diffusion of ions through the film is often the rate controlling process. Fick's law is then applicable i.e. ion diffusion is proportional to concentration gradient of ions multiplied by diffusivity coefficient. The concentration gradient is not nearly so sensitive to temperature as the diffusivity which obeys the Arrhenius law:

$$D = A_o \exp(-E/RT)$$

where D = diffusivity coefficient

A_o = pre-exponential constant

E = activation energy of diffusion

R = universal gas constant

T = absolute temperature

The activation energy can have quite a high value e.g. 80 kJ/Mole. Thus at low temperatures, processes other than Fick's law diffusion such as field driven diffusion are necessary for appreciable film growth.

2.3.5 Mechanism of sulphidation

Like oxygen sulphur is quickly adsorbed by a nascent iron surface. 'Fast' sulphidation however, is limited to one-half monolayer and place-exchange does not occur (126). The large size of the sulphide anion (126) is generally believed to be the cause of half-monolayer saturation. Figure 2.10 illustrates the adsorption mechanism for sulphur.

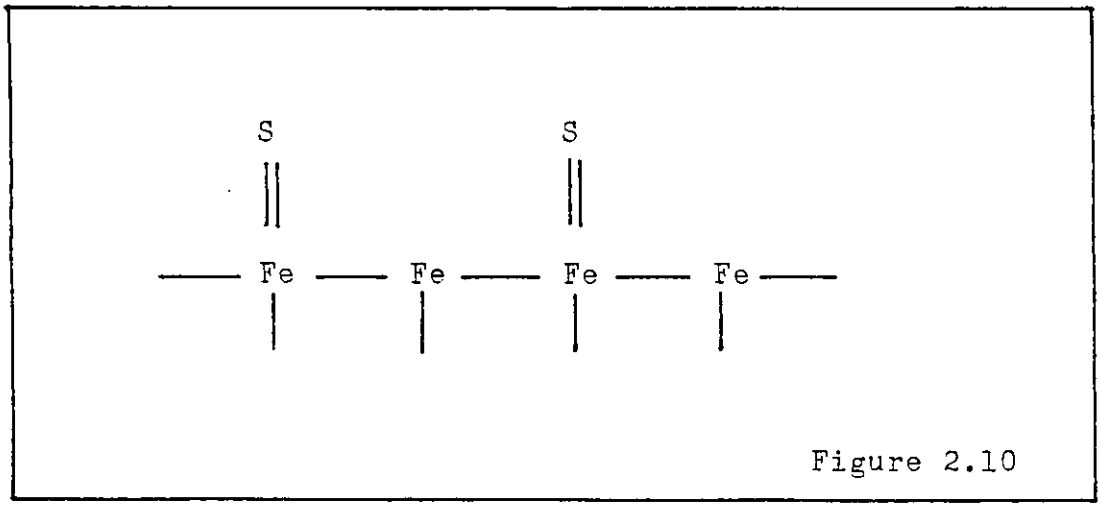

Figure 2.10

What happens immediately after a half monolayer is formed has not been investigated thoroughly.

2.3.6 Equations defining the various stages of oxidation and sulphidation

The first two stages, initial adsorption and subsequent fast growth can proceed very quickly(120). The limiting factors are probably transport to the iron suface and decomposition of the oxygen or sulphur compound. The defining equation is usually linear: $c = kt$, where c is the amount of oxygen or sulphur reacted per unit area, k is a constant (determined by transport of decomposition) and t is time. Oxide film formation by oxygen dissolved in oil appears to be a good example of diffusion limited transport, it is further discussed in the work presented.

The third stage - growth by ion and electron transport, is much more complicated and consists of several sub-stages.

Essentially, ions and electrons move by diffusion except between 5 and 20 Å where tunnelling is important for electrons. Diffusion is driven by concentration differences and by electric fields arising in the growing oxide or sulphide film. The electric field is a result of the electron affinity of oxygen, or sulphur. There are also the complicating factors of space charge and the transfer of cations and electrons across the metal-oxide interface. The term 'space charge' refers to the effect on ion movement by the concentration gradients of charged vacancies and ions within the film.

Fromhold (119) has summarised the ranges of various modes of film growth which is shown in Figure (2.10).

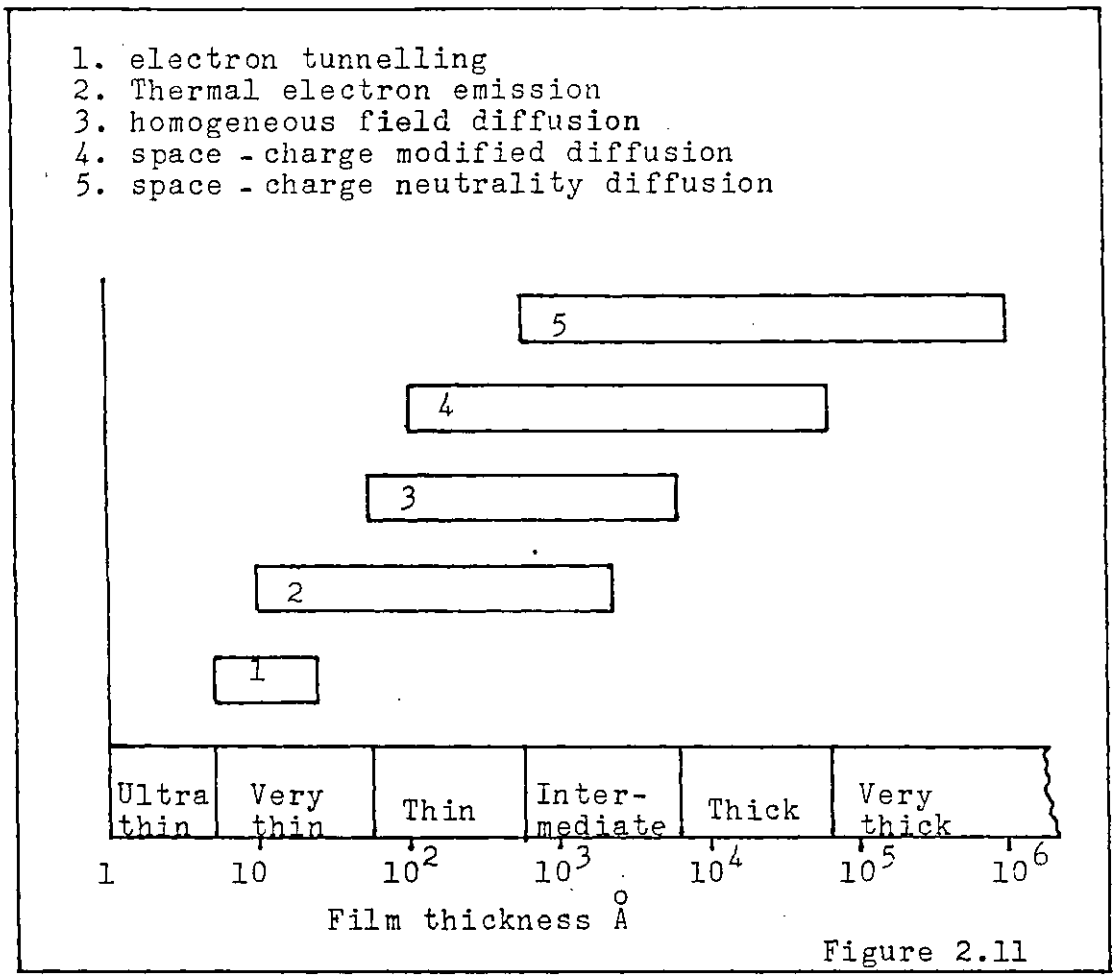

Figure 2.11

The thickness range of E.P. films is 10-1000 Å i.e. very thin to intermediate, thus electron tunnelling, thermal electron emission, homogeneous field diffusion and perhaps space-charge modified diffusion are relevant.

The Cabrena-Mott school and Fromhold have derived growth equations based at leastly partly on physical principles. There are not to be confused with the familiar 'log laws' of oxide growth which are empirical in nature. These 'laws' apply to long-term undisturbed oxidation and cannot be used for short-term oxidation or sulphidation. Some log and inverse log formulae derived however from rigorous physical reasoning are further presented.

Instead of empirical constants, precise physical quantities are present in the equations. One of the most recent derivations of oxidation growth rates has been developed by Fromhold (119). Fromhold presents this derivation as a precursor to more sophisticated treatments, thus it is chosen as a starting point for further discussion of growth equations.

2.3.6.1 Fromhold's simplified equation

Movement of ions through the oxide film is the cause of further film growth. Thus Equation (2.3) is applicable

$$dL/dt = \bar{R}\, Jo \qquad (2.3)$$

where L = oxide film thickness

t = time

$\bar{R}$ = proportionality constant between ion flux and rate of film thickness increase

and Jo = ion flux.

Ions move along concentration gradients according to Fick's law and are also driven by electric fields. The total ion flux may be split into two components, the Fickian flux and the flux due to the electric field created by the electron affinity of the adsorbed oxidant. These two fluxes are described by Equations (2.4) and (2.5) respectively:

$$J_D = - D \frac{dC}{dx} \qquad (2.4)$$

where

J_D = Fickian flux

D is the ionic diffusivity

x is the film ordinate (shown in Fig. 2.12)

and

C is the concentration of mobile ions at any point in the film.

$$J_E = \mu F_o C \tag{2.5}$$

where

J_E = flux due to the electric field

μ = ionic mobility coefficient

F_o = electric field set up within the film.

The total flux is the sum of J_D and J_E.

$$J_o = J_D + J_E \tag{2.6}$$

$$= - \bar{D} \frac{dC}{dx} + \mu F_o C \tag{2.7}$$

Equation (2.7) was solved by Fromhold to give an explicit expression for J_o.

$$J_o = \mu_o \left[\frac{C_L - C_O \exp (\mu F_o L/\bar{D})}{1 - \exp (\mu F_o L/\bar{D}} \right] \tag{2.8}$$

where C_L = concentration of ions at x = L

C_o = concentration of ions at x = O

To find L (the film thickness), Equation (2.3) is applied

$$\bar{R} J_o = dL/dt \tag{2.3}$$

An approximate solution (Fromhold) to this differential equation is in the form

$$1 + \beta t = \exp (\alpha L) - \alpha L \tag{2.9}$$

where $\alpha = \mu F_o/D$ (2.10)

and $\beta = \alpha \bar{R} F_o C_{max}$ (2.11)

C_{max} is the concentration of mobile ions at x = L or x = O, whichever is the greatest. Since if the anions are mobile then C_{max} is at x = L, if the cations (from sulphur or oxygen) are mobile then C_{max} is at x = 0 (Figure 2.12).

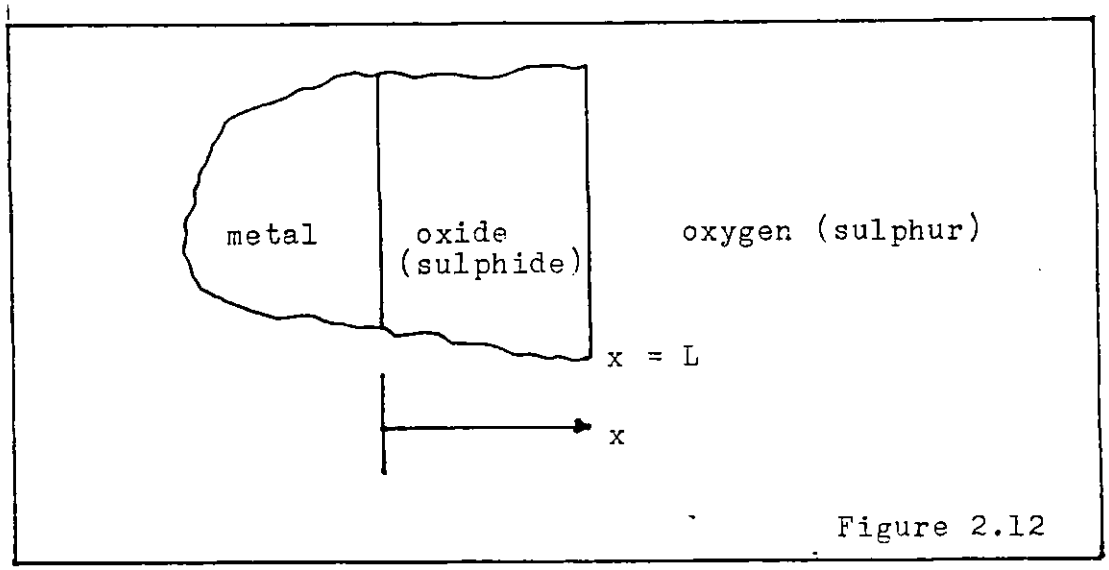

Figure 2.12

By a judiciious choice of values for D, $\dot{\mu}$ and E_o etc., Fromhold obtained quite a good fit of his equation to the published data for the oxidation of copper at 50° and 130°C (143) (144). Both the experimental and the theoretical plots tend to a limiting thickness. Figure 2.13 gives the approximate form of the growth law at 130°C for both experimental and theoretical values (there is little divergence between them (143).

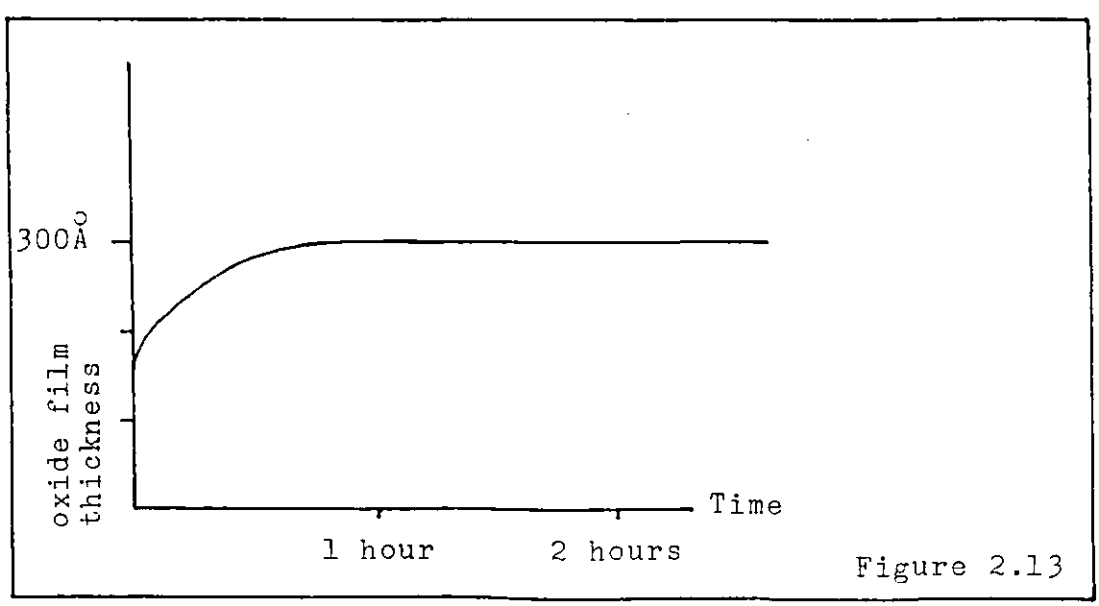

Figure 2.13

It is evident from Figure 2.13 that the parabolic law could not be employed in this case.

The assumption of a constant electric field is arbitrary. Fromhold continues in his work with more complex arguments which avoid such assumptions. For reasons of brevity, this later material is not discussed here.

The transition from low-temperature limited thickness oxidation to high-temperature parabolic oxidation can be at least partly explained by the above equations. Firstly, the relationship between ion mobility and diffusivity is sensitive to temperature. The Einstein relationship gives $D/\mu \alpha T$ (absolute temperature) (119) so that diffusion caused by electric fields is less significant at high temperatures than at low temperatures. Secondly, as L tends to a large value, F_o must decrease. Thus J_D outgrows J_E and film growth is a function of Fickian diffusion. This can be shown by the following series of equations:

$$\text{If } J_E << J_D \qquad (2.12)$$

$$\text{then} \quad J_o = -D\frac{dC}{dx} = \frac{1}{R}\frac{dL}{dt} \qquad (2.13)$$

$$\text{where} \quad \frac{dC}{dx} = \left(\frac{C_L - C_o}{L}\right) \qquad (2.14)$$

$$\therefore \quad \frac{1}{R}\frac{dL}{dt} = D\left(\frac{C_o - C_L}{L}\right) \qquad (2.15)$$

$$\rightarrow \quad L\frac{dL}{dt} = \text{constant} = B$$

$$L^2 = \tfrac{1}{2}Bt + A \qquad (2.16)$$

The constant B is proportional to D, the ionic diffusivity, which obeys the Arrhennius law. Thus one returns to the Wagner parabolic law for reaction product film growth.

Two more derivations are described; the Fehlner and Mott inverse log.law equation and Ely and Wilkinsons's direct log-law equation (127).

2.3.6.2 Fehner and Mott's equation

Fehlner and Mott summarise their theory with four cannons.

1. Oxide film growth is caused by cation migration through the film.
2. Oxygen molecules dissociate on the oxide surface causing traps with an energy eV below the Fermi level of the metal where e is the elementary unit of charge and V is the voltage difference caused by the electro-negativity of oxygen relative to iron.
3. The density of traps is sufficient to generate a potential drop across the film. Thus a field F, such that $F = V/L$, is generated across the film.
4. The activation energy E for the movement of a cation drops to $E - \frac{1}{2} q a F$, where q is the charge on the ion and a is the jump distance.

The growth rate is given as:

$$dL/dt = Na^4\nu \exp - (E - \tfrac{1}{2}q\ a\ V/L)(RT) \qquad (2.17)$$

where N is the number of mobile ions per unit volume in the oxide, ν is the jump frequency of the ions, R is the universal gas constant and L is the film thickness. This leads to the inverse logarithmic law.

$$1/L = C_1 - C_2 \ln t \qquad (2.18)$$

where C_1, C_2 are constants stemming from Equ.(2.17).

2.3.63 Ely and Wilkinson's equation

These two co-workers have used a different equation for the effective activation energy. They postulate that $E_A = E_o + cL$ where c is a constant dependent on film structure. The growth rate equation is then:

$$dL/dt = C_1 \exp - (E_o + cL)/RT \qquad (2.19)$$

which integrates to give a direct log law.

$$L = A \ln (1 + Bt) \qquad (2.20)$$

This theory is considered more appropriate to amorphous oxides where the concept of the movement of charged defects (ions or vacancies) within the crystal lattice is not really applicable. Instead 'place exchange' where adjacent atoms 'exchange places' is invoked to explain the transfer of ions. As with Fromholds work the inverse and direct log laws mentioned above can partly explain the transition from a limiting thickness oxidation to parabolic oxidation with increasing temperature. In both cases the minimum oxidation rate for a given thickness rises with temperature. Thus the limiting thickness is also raised. Fromhold's treatment though gives a clearer explanation of the transition. Fehlner and Mott's and Ely and Wilkinson's equations are more strictly limited to thin low temperature oxide films.

The logarithmic-parabolic transition however, depends on many other factors, in particular the crystalline state of the oxide (or sulphide) as is discussed below.

2.3.7 Restrictions of the oxide-growth theory

The theory of thin oxide films can now explain quite reasonably the growth of films on carefully prepared surfaces. However the behaviour of 'real' surfaces remains unresolved.

Surface oxidation and sulphidation is strongly dependent on surface conditions (128). The modifying factors can conveniently be divided into six different categories:

(a) Epitaxy;

(b) Crystalline state of the oxide;

(c) Crystalline state of the substrate metal;

(d) Mechanical activation;

(e) Oxidation under a liquid;

(f) Reactivity of sulphur and oxygen as elements or compounds.

2.3.7.1 Epitaxy

According to Fromhold, epitaxy is the preferential crystal orientation of a deposited or chemically formed layer on a given exposed crystal plane of a parent substrate of a different material. This concept is often invoked to explain the experimental fact that the rate of surface oxidation depends on which crystal face is exposed at the metal surface. The metal crystal faces which give the poorest fit with the oxide lattice tend to oxidize fastest. It is believed that the cause is due to a strain-induced increase in diffusivity. Fromhold(119) has suggested a relationship between strain and diffusivity.

$$E_A = E_o \left(a_o / a(x) \right)^n \qquad (2.21)$$

where

E_a = effective activation energy of diffusion from the strained oxide at position x

E_o = unstrained diffusion activation energy

a_o = unstrained lattice parameter

a(x) = strained lattice parameter at x

n = exponent derived from theories not described here, value as large as 10.

Strains in oxide films can be large so a strong effect on diffusivity is virtually certain.

The work function or minimum input of energy for metal to oxide cation transfer is known to vary with surface crystal orientation. Ease of cation release can exert a strong effect on oxidation. This kind of effect is usually more important for copper than for iron. Despite the uncertainty over the causes of epitaxial variation of oxide film growth rates the heterogeneous model of oxidation of Lacombe and Beaujard is almost certainly true. This model is shown below in Figure 2.14.

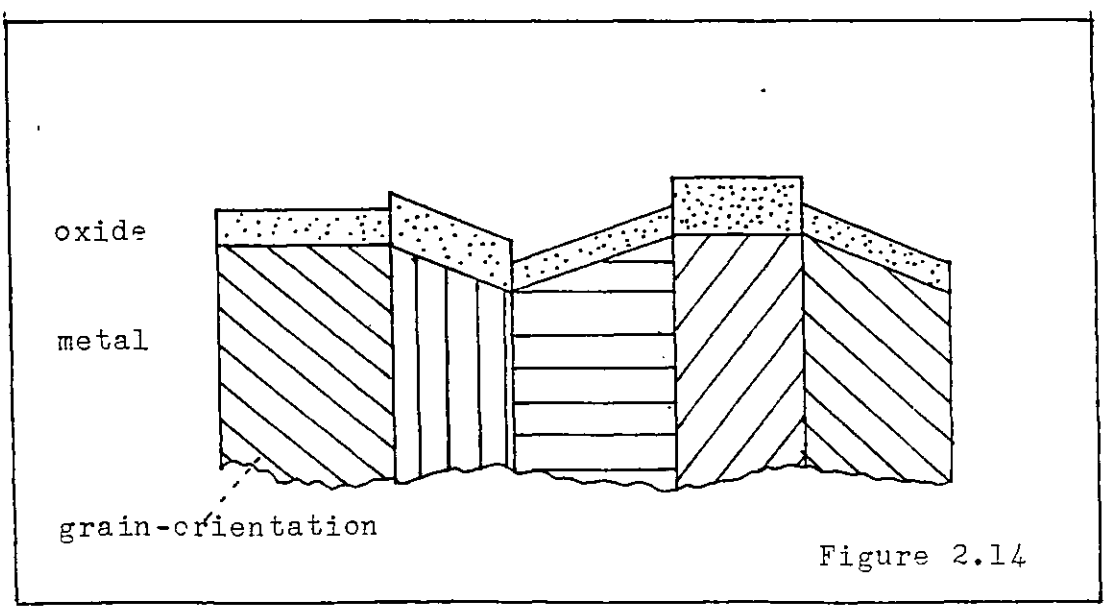

Figure 2.14

2.3.7.2 Crystalline state of the oxide

Fehlner and Mott were among the first to discuss at length the importance of the crystalline state of the oxide (124). More recently Revesz and Fehlner (129) have investigated this subject further. They divided surface oxides into three groups; single crystal (rarely found), vitreous (amorphous) and polycrystalline. In general poly-crystalline films have numerous grain boundaries which allow easy permeation and diffusion by cations and anions. Amorphous oxide films which lack grain boundaries are believed to be the cause of passivity in stainless steels. The crystalline state of the oxide or sulphide can therefore have a strong effect on kinetics.

Where a metal forms several oxides, the differences in crystalline structure between the oxides has a strong effect on the transport of ions. During the oxidation of iron, the low temperature oxide film which contains α-Fe_2O_3 grows by the passage of oxygen anions (122). The diffusion of oxygen anions in α-Fe_2O_3 is quite slow and when the oxide changes to γ-Fe_2O_3 (and later Fe_3O_4) a more rapid diffusion of ferrous cations is believed to occur.

From the available literature it appears that no parallel investigation has beenpursued with iron sulphides.

2.3.7.3 Crystalline state of the substrate metal

Revesz and Fehlner (129) have reviewed the work on amorphous metal reactivity. Polycrystalline metal is far more reactive than amorphous metal. Two causes are attributed to

this effect: the lack of grain-boundary defects on amorphous metal and the tendency for the oxide film to be also amorphous because of epitaxial forces.

Grain-boundary defects are believed to be sites for easy incorporation of cations in the oxide. A lack of grain boundaries can slow down significantly the supply of cations to the growing oxide film thus reducing the film growth rate.

2.3.7.4 Mechanical activation of surfaces

The phenomenon of 'mechanical activation' by plastic deformation of the metal has been observed by many workers. Heidermeyer gives for instance numerous examples of its effect on chemical reactions in a recent paper (92). Knowledge of the phenomen however, is virtually limited to the fact that it exerts a strong influence on chemical reaction rates and equilibria. Meyer (130) discusses the thermodynamics of raised enthalpy due to mechanical activation but there is little means of estimating the enthalpy rise and the reasoning does not seem applicable yet. Heidermeyer (92) discusses attempts to explain mechanical activation by increased surface dislocation density; but a direct application of this theory to tribological problems does not appear to be possible.

Caplan and Cohen (131) described the accelerating effect of work hardening on the oxidation of iron. Presumably mechanical activation is involved because work hardening is attained by plastic deformation of the iron. Quinn applied Caplan and Cohen's findings to his theory of oxidative wear (15) thus providing a classic demonstration of the need to consider factors relating to mechanical activation.

2.3.7.5 Oxidation under a liquid

Oxidation or sulphidation under a liquid has so far been scarcely mentioned. The main reason for this is the limited amount of literature in this field. This paucity stems from the difficulty of investigating oxide and sulphide films under liquids. Constable (147) measured the formation of copper sulphide by aqueous ammonium poly-sulphide, using optical interferommetry, but hardly any other workers have used this technique to study oxidation and sulphidation.

Infra-red spectroscopy appears to be a more popular technique: Poling (132) has reviewed the use of infra-red to monitor reactions on metal surfaces. Some useful results from in-situ analysis of oxidation under liquids have been obtained by reflectance spectroscopy but this is a difficult technique still in its initial stage.

Excluding electrolytes one may reasonably assume that the liquid state by itself does not have a strong influence on surface oxidation(121). Only a weakly polarized double layer will be formed by the metal's electric field, so that oxygen will not be barred from the surface. Reaction temperatures are high enough for 'residence times' to be short thus other adsorbed species should not block reaction sites and prevent free access of oxygen and sulphur to the metal.

2.3.7.6 Reactivity of sulphur and oxygen as elements

The question of the reactivity of sulphur and oxygen compounds compared to the elements themselves is a complex matter that is not yet well understood. The film growth equations described previously all relate to the

electron-affinity of elemental oxygen or sulphur. Extension of the electron-affinity principle to compounds does not appear to have been investigated thoroughly. To provide some indications as to the rates of film growth with sulphur and oxygen compounds the following discussion is presented.

A convenient starting point to the discussion is a general consideration of the chemistry of film growth. The envisaged reaction scheme is illustrated below in Figure 2.15.

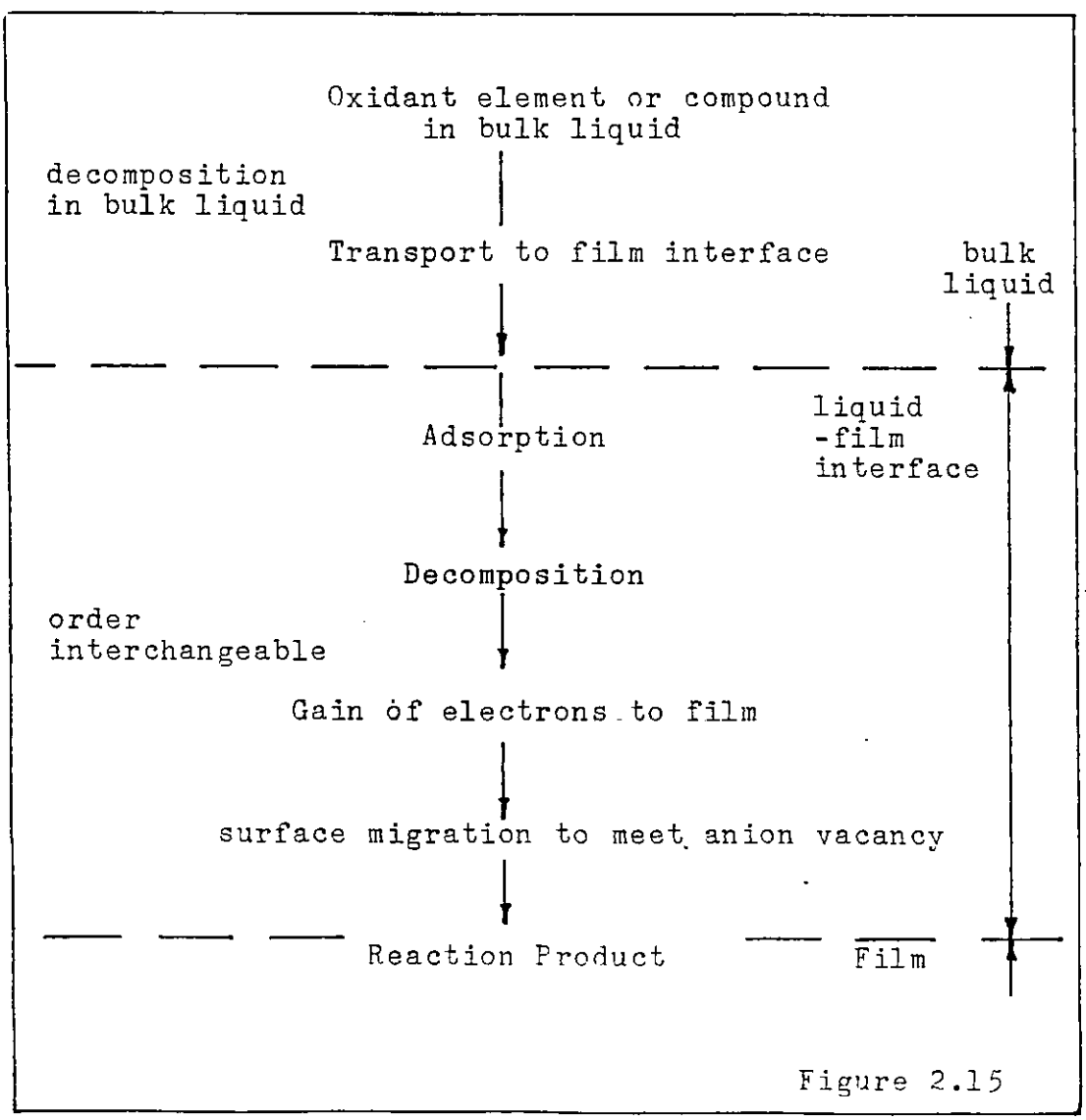

Figure 2.15

With oxidant elements the stages of adsorption, decomposition and ionization are generally assumed to be quick, low activation energy processes. The liquid-film interface is generally believed to be in a state of quasi-equilibrium. These reactions only dictate reaction rate insofar as they determine the free anion surface concentration. Most of the film growth equations already described or referred to depend on this assumption. Thus the concentration of elemental oxygen or sulphur usually exerts a weak effect on the film growth rate. For Wagner parabolic oxidation a concentration law in the form shown below has been found (115)

$$\log \text{reaction rate} = f \log (\text{oxident concentration}) + Co \qquad (2.22)$$

where f is a fraction less than 1 and Co is a constant.

With oxidant compounds the situation is most probably different. One might expect decomposition to be a limiting factor. If this is so then the film transport mechanism will not be working at the 'saturation' value and instead film kinetics will be of the form (119)

$$\frac{dL}{dt} = K \quad \text{Surface limited film growth} \qquad (2.23)$$

L = film thickness

t = time

The 'K' value by decomposition must always be much less than the saturation rate constant.

$$K_{de} << K_{sat} \qquad (2.24)$$

As film thickness increases so the saturation rate, K_{sat}, declines since

$$\frac{d^2L}{dt^2} < 0 \tag{2.25}$$

and

$$K_{sat} = \frac{dL}{dt} \longrightarrow_{sat} \text{smaller value} \tag{2.26}$$

$$\therefore \quad \frac{K_{de}}{K_{sat}} \longrightarrow \geq 1 \text{ with increase in L} \tag{2.27}$$

Thus when the film is thin, decomposition of the oxidant compound limits growth, but on reaching a transition thickness ion transport kinetics takes over, as the limiting process. There will also be a grey 'area' in between the two stages where both processes are limiting. Moreover temperature will also influence the transition point since the temperature dependence of ion diffusion and oxidant decomposition are unlikely to be identical.

2.4 Application of Surface Science to E.P. Action

Two cases are considered:

1. E.P. action by oxygen alone.
2. E.P. action with oxygen and sulphur.

The analysis for the first case contains some material common to the second, that is the principles of asperity collision and diffusion of solutes.

2.4.1 E.P. action by oxygen alone, a hypothesis

Oxygen is known to be crucial for protection against scuffing but a full understanding of its action has not yet been found. A hypothesis arising from the suggestions of Vinogradov (6) and Begelinger and DeGee (63) is now presented. The work

started from the realization that the diffusion of oxygen in oils is much slower than in air and it is from these that the presentation of the hypothesis of E.P. action by oxygen begins.

Two cases were compared: the diffusion of oxygen through the air to an oxidizing surface and the diffusion of oxygen through air and a layer of oil to the same surface.

(a) Air alone, as shown in Figure (2.16).

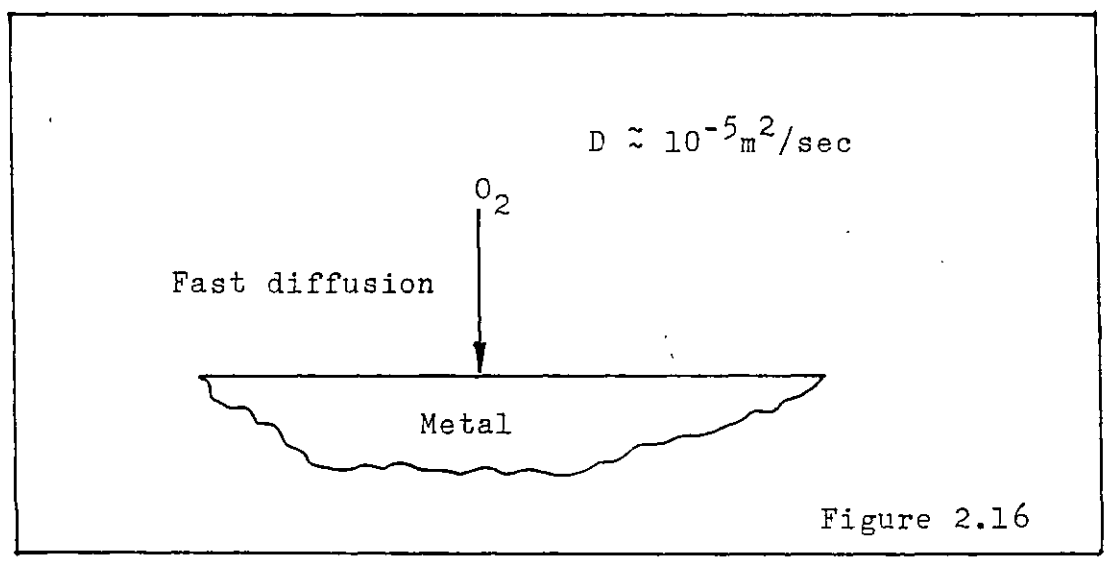

Figure 2.16

(b) Air and a layer of oil as shown in Figure (2.17).

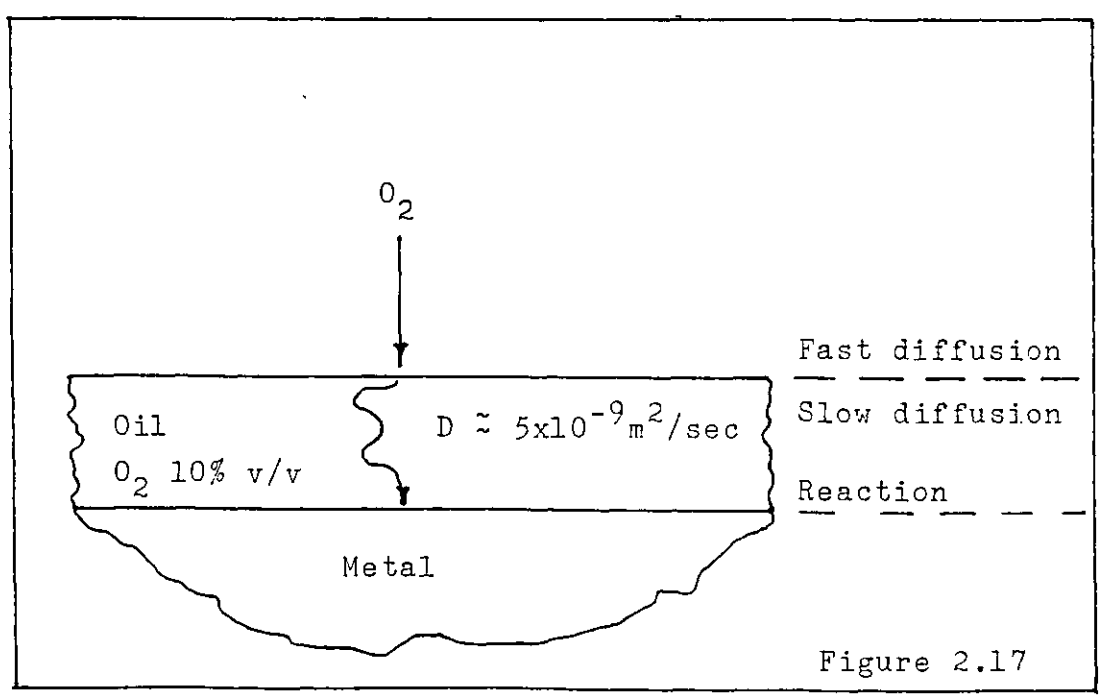

Figure 2.17

Within the oil (Figure 2.17) the concentration of oxygen is about 1/10 of its value in airand its diffusivity is about $1/10^3$ of its value in air. Thus assuming that the concentration of oxygen at the metal surface in both cases is negligible and that diffusion occurs over similar distances then oxygen transport in oil will be 1/10,000 times as slow as in air.

Transport is relevant because in the initial stages of oxidation it can control the growth rate. As mentioned in the Section 2.3.4, iron and steel oxidize very rapidly for the first 5 atom layers of 20 Å of nominal oxide thickness. Very slow logarithmic growth occurs after temperatures less than 200-300°C. Thus one can usefully divide the process of oxidation into two periods; one of fast growth the other of slow growth as shown in Figure (2.18).

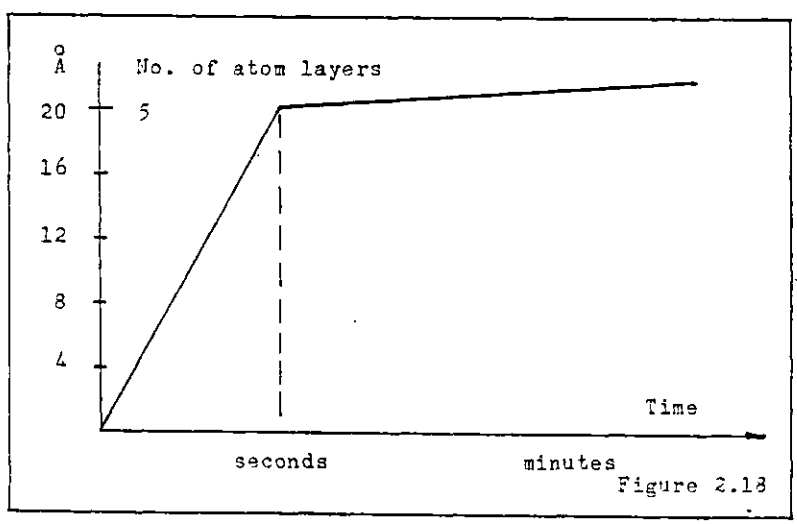

Figure 2.18

Some rudimentary calculations of reaction times to complete fast growth for iron under a layer of oil were performed. The calculations were based on the Carslaw and Jaeger solutions to one-dimensional unsteady diffusion (133).

Examples of reaction times are given below:

Under	1 micron layer of oil	50 ms
Under	10 micron layer of oil	500 ms
Under	100 micron layer of oil	3,600 ms

The calculations are based on the following assumptions. estimates:

Solvent hexadecane. Oxygen diffusivity = 5×10^{-9} m^2/sec

Concentration of oxygen in hexadecane = 100 ppm

= 3×10^{-4} kg moles/m^3

Operating equation $D \frac{\partial^2 c}{\partial x^2} = -\frac{\partial c}{\partial t}$

where c = concentration of oxygen in hexadecane

t = time

x = oil layer ordinate (i.e. dimension perpendicular to plane of layer)

Boundary conditions

$c = c_{max}$ for $t \leq 0$

At oil-metal interface and

$c = 0$ for $t > 0$

At air-oil interface

$c = c_{max}$ for all t

2.4.1.1 Minimum effective oxide thickness

It is well known that clean steel surfaces stick together and oxide-covered surfaces do not, the question is what is the minimum amount of oxide needed to be effective. Tingle (105) provided some answers to this question. He stated that for copper beyond 40 Å thickness the oxide had virtually reached the minimum value of adhesivity. A copper oxide thickness of 40 Å is just beyond the 'fast growth period for copper (maximum 30 Å). Tingle did not discuss iron in

details but it seems reasonable to assume that at the end of fast growth for iron not much more protection against adhesion is to be obtained. This can be summarised graphically by a plot of adhesivity versus oxide thickness as shown in Figure (2.19).

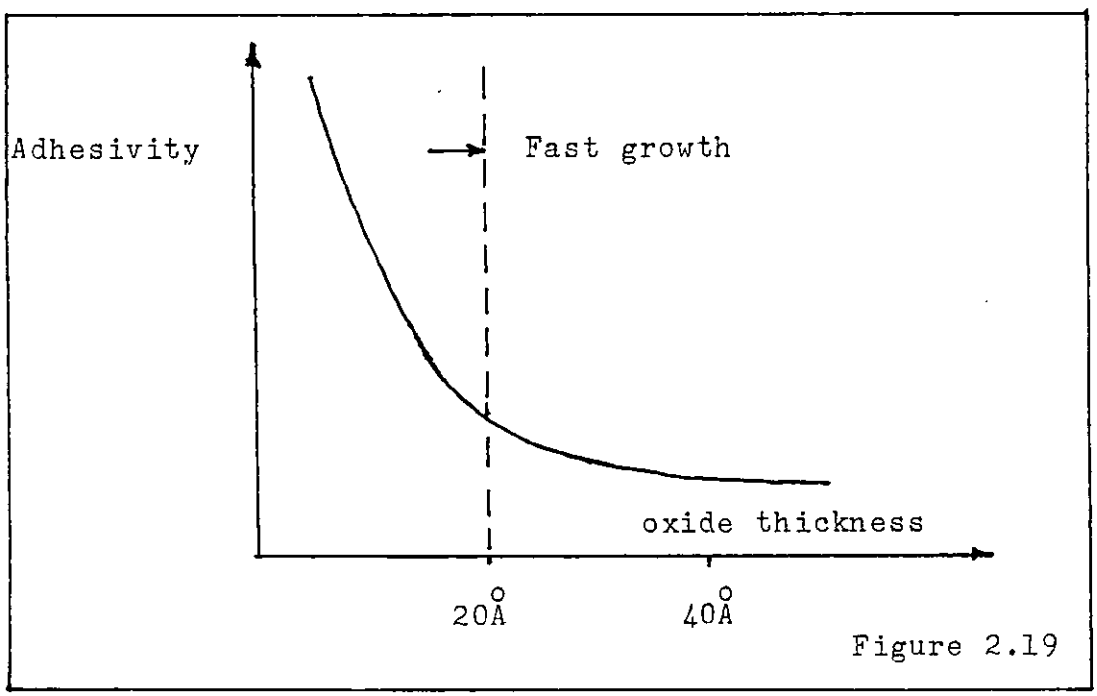

Figure 2.19

Up to 20 Å oxide thickness the surface can be regarded as 'virtually clean' and liable to adhesive contact. That fast growth also ceases at an oxide thickness of 20 Å is unlikely to be a coincidence for during 'fast growth' the iron surface is not covered by true oxide. The fast growth film consists of loosely bonded oxygen and iron undergoing rapid place exchange. Thus on contact with a surface in a similar state, rapid place exchange between surfaces or interfacial bonding would promote adhesion.

An important conclusion is that the 'fast growth' stage represents a vulnerable period for an oxidizing asperity peak.

2.4.1.2 Diffusion-determined scuffing criterion in partial EHL

Partial EHL between two steel discs rotating at slightly different speeds was chosen as a convenient example for the introduction of diffusion criteria. Shown below in Figure (2.20) is a side-view and plan view of an asperity collision in the EHL contact.

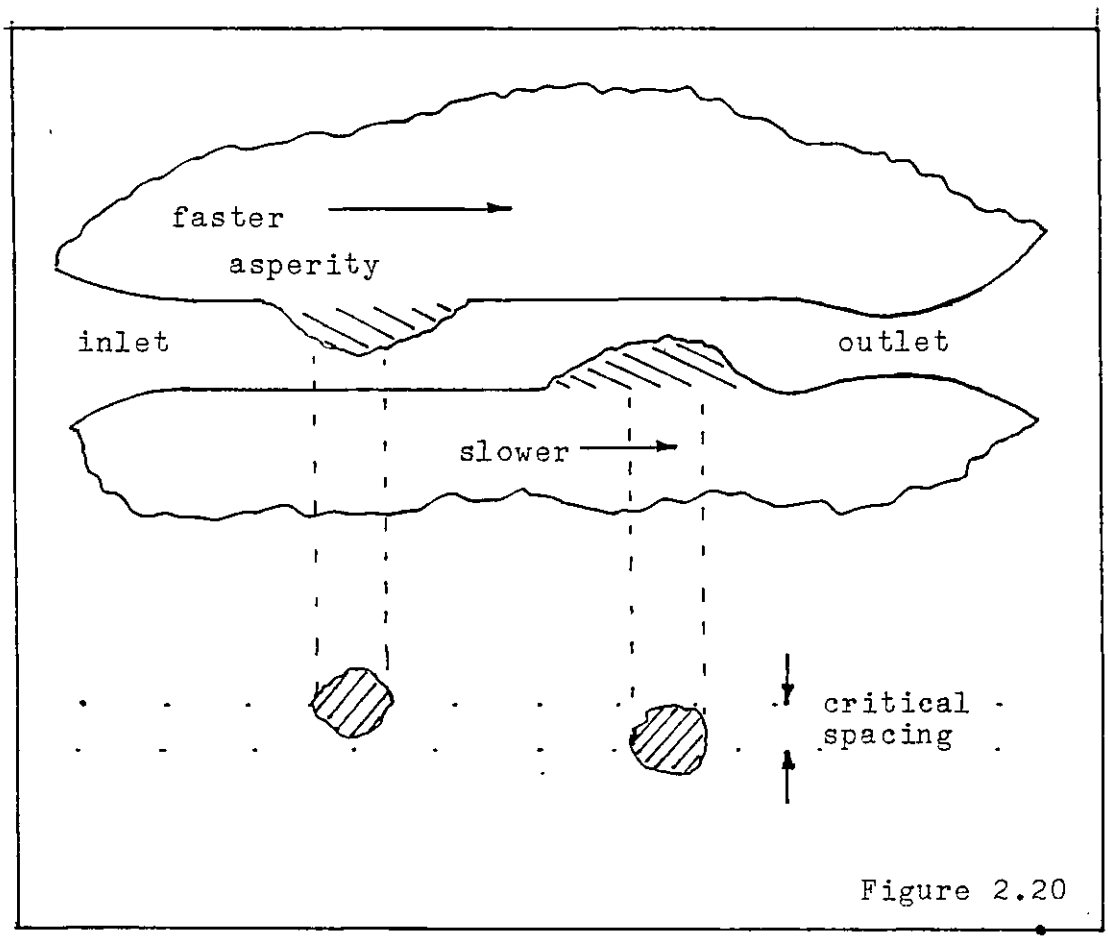

Figure 2.20

If P_c = probability of collision,

L_c = total contact length (inlet to outlet distance)

and $\bar{r}$ = average asperity collision area radius (Fig.2.21)

σ = ratio of total possible asperity collision area to EHL contact area

L_c = length of EHL contact

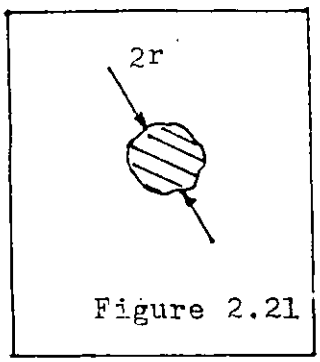

Figure 2.21

then $P_c = \frac{2}{\pi} \frac{L_c}{\bar{\gamma}} \sigma$ (2.28)

If t_r = time for any point on the rotating surface between contacts (one contact = rotation time)

then

t_c = average time between collisions for any asperity

$$t_{\bar{c}} = \frac{t_r}{Pc} \quad (2.29)$$

The collisions may be divided into 3 types:

Type I	Oxide covered to oxide covered	Safe
Type II	Oxide covered to virtually clean	Marginal
Type III	Virtually clean to virtually clean	Fatal

Each type of collision has its own probability. Let a proportion 'n' of the asperities be 'virtually clean', the rest are oxide covered, hence the expressions for the 3 probabilities are:

Type I	$(1 - n)^2 Pc$
Type II	$2n(1 - n)Pc$
Type III	$n^2 Pc$

The average time between the very undesirable Type III collisions is of particular interest and is given by the expression below

$$(\bar{t}_c)_{III} = \bar{t}_c/n^2 = t_r/Pcn^2 \quad (2.30)$$

The conditions for persistence of a 'virtually clean surface' on the rotating discs is of vital importance. If the time for completion of fast growth is longer than the average time between Type III collisions then 'virtually clean' surface will persist. The loosely bonded oxygen layers will be swept off and surface damage due to adhesive contact will result in the creation of more clean surface in addition to that swept clean. An ever-accelerating spread of clean surface will lead to the eventual scuff.

For the moment, the consequences of Type I and Type II collisions will be ignored since the purpose of this analysis is to deduce a prototype scuffing criterion. The former issue is discussed in the conclusion of the analysis and in the final section of this chapter.

So implicit in the above discussion is a ratio R_a such that:

$$R_a = \frac{t_{ox}}{t_{critical}} \qquad (2.31)$$

with a stability condition

$$\text{Scuffing } 1 \lesssim R_a << 1 \quad \text{Stable operation} \qquad (2.32)$$

Let us now estimate a value of 'n' on the borderline between scuffing and stable running i.e. when $R_a = 1$. To do this one must calculate the following quantities;

(a) Value of P_c, the probability of asperity collision per contact.

Let $L_c = 0.25$ mm

$\bar{\gamma} = 4\ \mu m \quad \therefore \quad \frac{L_c}{\bar{\gamma}} = 63$

if $\sigma = 1/100$

then $Pc = 2/\pi \; L_c/\bar{\gamma} \; \sigma = 2/\pi \times 63 \times 1/100$

$= 0.4$

(b) Value of n for $R_a = 1$

$$R_a = \frac{t_{ox}}{t_{critical}} \quad \text{and} \quad t_{critical} = \frac{t_r}{Pcn^2} \qquad (2.30)$$

Substitution $t_{critical}$ to

$$R_a = \frac{t_{ox}}{t_r} \; Pc \; n^2 \qquad (2.33)$$

For (3,000 rpm) rate of disc rotation, $t_r = 1/50$ sec.

With an average value for oxidation; $t_{ox} = 1\frac{1}{2}$ sec

Hence $t_{ox}/t_r = 1\frac{1}{2} \times 50 = 75$

So for $R_a = 1$ $\quad 1 = \frac{t_{ox}}{t_r} \; Pc \; n^2 = 75 \times 0.4 \times n^2$

$= \underline{30 \; n^2}$

$\underline{n = 1/5.5}$

Thus if 1/5 of the asperity collision area is 'virtually clean' 'virtually clean' surface will persist and propagate to cause scuffing if they occur in critical regions of the contact area.

An important corollary of this analysis is that the Type II collisions must be quite 'safe' otherwise the 'R' value will be critical for relatively small values of n.

If type II collisions are fatal then $R_a = t_{ox}/t_r \; Pc \; 2n(1-n)$ which gives $60 \; n(1-n) = 1$. The solution to this equation is $n \approx 1/60$; one-twelfth the value for the previous case. Intuitively one might expect the adsorption of fatty acids and the like to be instrumental in minimising the harmful

effects of Type II collisions. Thus when the flash temperature is exceeded it is quite likely that the effective R_a value changes from a safe value to a critical value with all the attendant consequences.

2.4.2 Elemental sulphur with atmospheric oxygen

Since oxygen is always present in a frictional contact unless precautions are taken to exclude it, the case of sulphur with oxygen instead of sulphur alone is considered despite the greater complexity. Indeed the theory of E.P. mechanism would not be complete without a consideration of oxygen's role.

As mentioned in Section 2.3.5 the fast growth mechanism is limited to a half monolayer for sulphur, so an analysis analagous to that described for oxygen cannot be directly applied.

Before moving on to an analysis however, some further background material from the literature is discussed. The value of solid-state diffusivity is essential to any discussion of film kinetics, and is used as the starting point here. Condit, Hobbins and Birchenall (134) measured the diffusivity of ferrous and sulphide ions in non-stoichiometric iron sulphide, $Fe_{1-\delta}S$. They reached three important conclusions:

1. In the temperature range measured the sulphide ion has a much smaller diffusivity than the ferrous ion.
2. The diffusivity of the ferrous ion is a function of the exact composition of iron sulphide.
3. At around 300^{o}C (570 k) the diffusivity of the ferrous ion declines sharply with lessening temperature.

Conclusion 3 is summarised graphically below in Figure 2.22

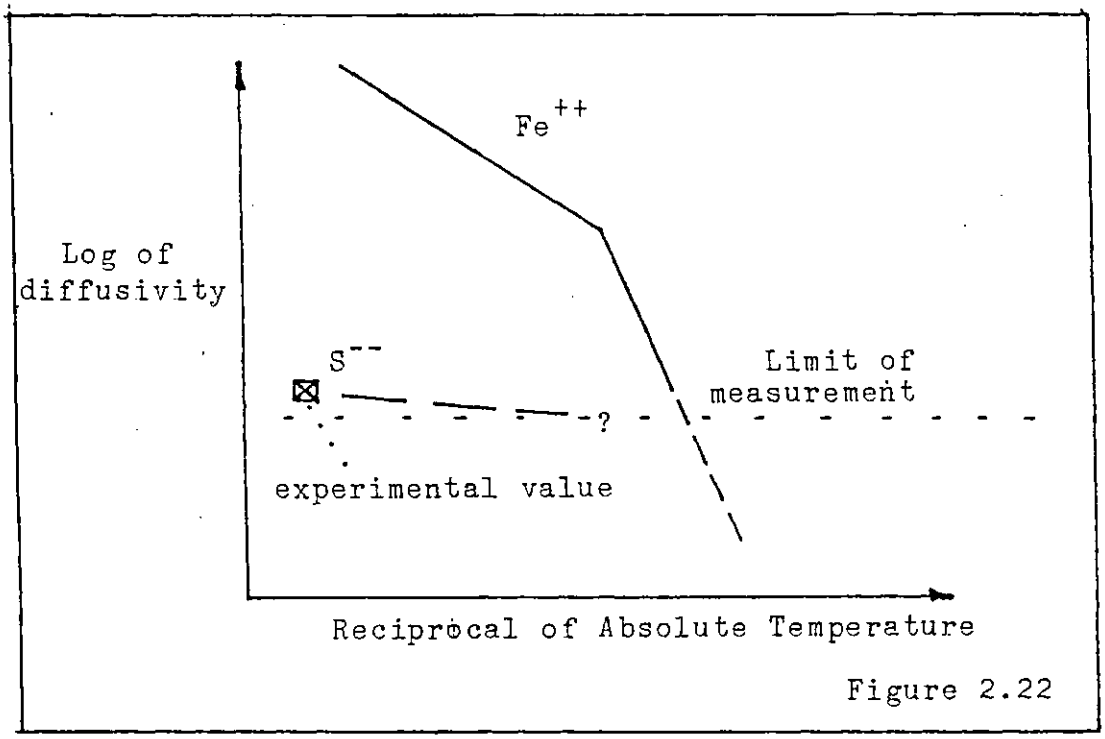

Figure 2.22

This work reinforces some profound doubts about the conventional understanding of the mechanism of sulphidation. Whilst it is generally understood that the ferrous ion is more mobile at temperatures beyond 300-400°C and thus dictates the reaction rate, Pfeiffer and Ilschner (135) found that the sulphide is the more mobile at lower temperatures. Kubaschewski and Hopkins (122) suggested that the sulphide ion could have a much lower activation energy and therefore overtake the ferrous diffusivity at low temperatures (i.e. less than 300°C). If one refers back to Figure (2.1), it is evident that Llopis's results (118) fall in line with other workers, which would not be so if a proportionality between ferrous (other factors such as sulphur adsorption are almost constant with respect to temperature) diffusivity and reaction rate was valid for all temperatures.

In any analysis of film growth, one must know which is the more mobile ion, the value of activation energy for its diffusivity and most difficult of all the pre-exponential constant.

2.4.2.1 Attempt at prediction

From the first moment that a clean surface is created in a contact, it is under attack by any available oxidant. Sulphur is much more soluble in oils than oxygen and concentrations as high as 5,000 ppm can be reached compared to 100 ppm for oxygen. Notwithstanding any differences in liquid-state diffusivity, sulphur should precede oxygen in reaction because of its greater concentration. In the previous section (2.4.1) it was shown that oxygen can form a monolayer of oxide in 10 to 800 msecs. Values for the diffusivity of sulphur in hexadecane are hard to find, but at a rough estimate the time for sulphur to deposit a half-monolayer would be around 0.2ms to 10 ms. Driscoll (136) has recently shown that once the half-monolayer of sulphur is established then any future oxidation is inhibited. Thus a 'first come-first served' principle may operate; if in the chemisorption stage mostly sulphur is adsorbed, then it is sulphidation and not oxidation that subsequently occurs. On a rough surface more than half a monolayer of sulphur may be adsorbed but the principle is the same.

2.4.2.2 Minimum effective sulphide film thickness

Buckley (146) investigated the adhesivity of steel covered with very thin layers of 'oxide' and 'sulphide'. At ½-monolayer levels sulphur gives adhesion values similar to sub-20 Å oxide films so that this small quantity of sulphide still leaves the surface 'virtually clean'. It appears that the sulphide film must thickne to provide satisfactory protection.

2.4.2.3 Film growth of sulphide beyond half-monolayer stage

There has been very little work done on low-temperature thin sulphide-film growth. All one can be sure of is that the Wagner equation (119) is not appropriate to thin films by Fickian diffusion. Film growth will probably be by electric-field forced diffusion (Section 2.3.6). Fromhold's work (119) gives some insight to the process, and a 'hopping' model of charged defect movement* is described. The principle is shown in Figure (2.23).

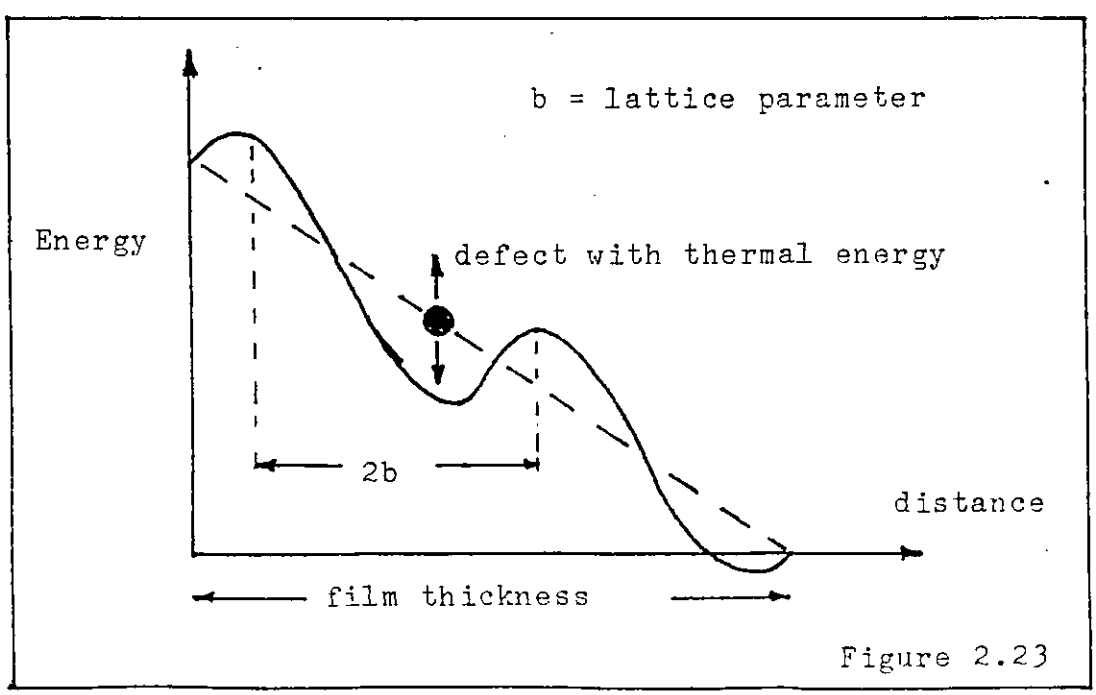

Figure 2.23

*(Charged defect = free ion or electron or a vacancy.)

The distribution of thermal energy amongst a population of defects causes a certain proportion of them to 'hop' down the energy slope i.e. jump from one stable position in the lattice to another. The energy slope (dashed line in Figure 2.23) is a function of the charge of the defect, the voltage drop across the film and the thickness of the film. From intuition, it is evident that the value of the activation energy determines the minimum energy slope at which any defect can 'roll down' the slope as shown in Figure (2.24).

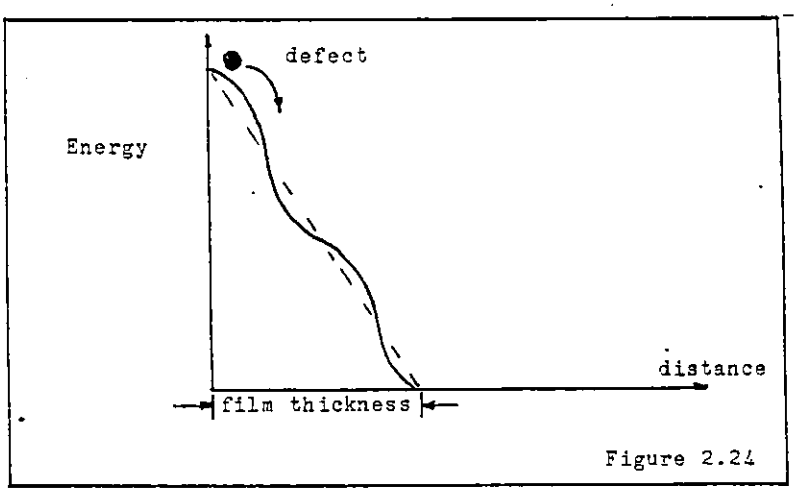

Figure 2.24

At low temperatures in particular, a dramatic rise in defect flux occurs at the transition to 'roll down'. It is evident therefore from the discussion of Condit Birchenall and Singh's (134) work that there is still not sufficient information to derive a theoretical growth rate. A crude estimate however can be made if one assumes that the parameters for sulphidation are similar to those of oxidation.

Typically, a field of around 10^7 volts/m is needed for 'roll down' and 0.1 V is the order of the voltage drop across the film. This gives a critical thickness of:

$$\frac{0.1\ V}{10^7\ V/m} = 10^{-8} m = 100\ \text{Å} \qquad (2.34)$$

If one lets the estimate span a factor of 10, a 30 to 300 Å film could form quite quickly. Thereafter Fickian diffusion takes over as the main cause of ion flux; but little can be said as to how fast is this latter mode of growth. The corrosion data of Section 2.1 gives some clues. Assuming that once a layer of sulphide say 50 Å thick is established then further growth rates are not so very dependent on whether there is or is not a thin 30 Å oxide film beneath the sulphide. This means that the corrosion data reviewed involved steel exposed to the atmosphere and can be used as an estimate. The data gives a parabolic rate of around 1 $Å^2$/sec for 200°C (2.1); so in the time scale for E.P. conditions - 1 msec to 0.2 sec the rate must be so small as to be negligible (Figure 2.25). Thus a condition of effective limiting thickness can be deduced (sulphidation at 200°C is parabolic not logarithmic). There must also be a 'critical temperature' for even 'rapid growth' to occur which is still undiscovered.

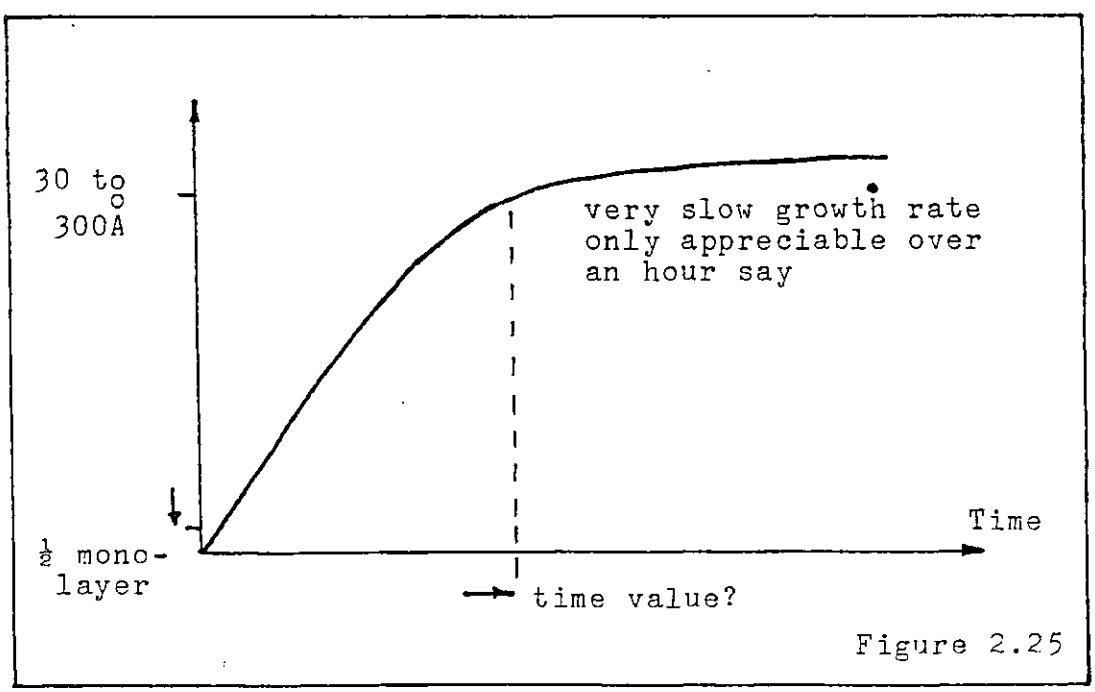

Figure 2.25

In the rapid stage of film growth the question arises what determines the rate of film growth? Control of rate growth could lie with liquid state diffusivity, at least in the early stages. Temperature is quite high, about 200°C, and the liquid state diffusivity of sulphur is high enough to give growth rates of perhaps a few monolayers ($\sim$ 20 Å) per m sec. Thus a film thickness of 300 Å could be reached in approximately 15 msecs. This film thickness must be sufficient to reduce adhesion to an acceptable value; herein may lie the explanation of E.P. action.

Comparing sulphidation with oxidation, it should be noted that non-stoichiometric ferrous sulphide ($Fe_{1-\delta}S$) is a much more defective substance than α-Fe_2O_3 which is commonly found in Low-Temperature Oxidation of spinel-type defective structure. The iron-sulphides in general offers a much faster path for solid state diffusion than most iron oxides; at low-temperatures thick, quick forming films may be possible for this reason.

Returning to the question of film growth by anion (i.e. sulphide) movement it is evident that the concentration of sulphur may exert quite a strong effect on growth rate. Instead of the quarter and seventh power laws found at high temperatures, as shown in the work of Foroulis (115) a direct proportionality between growth rate and sulphur concentration may occur.

$$K \propto \text{conc}_S \text{ not } k \propto (\text{conc}_S)^{1/7} \qquad (2.35)$$

It is apparent that the process of thin film sulphidation and its relevance to the E.P. mechanism is still a matter for future investigation. The high solubility of sulphur in most oils and the defective crystallinity of iron sulphide appear

to be crucial properties in the superiority of sulphur over oxygen as an E.P. additive.

2.5 Application of the Oxidation-Sulphidation Theory to Sulphur Compounds and Oxygen

All sulphur compounds must decompose to some extent before they can react with the metal to form sulphide. As mentioned previously in 2.3.7.5 a multi-stage process of transport, adsorption and decomposition is involved. Catalysis by the nascent steel surface may be critical. Whatever the mechanics of this process are, a half-monolayer of sulphur must be virtually completed before the oxygen-fast growth period is over. Otherwise suppression of oxidation does not occur (136). If even a thin film of oxide is established first, then the extent of sulphidation is about 0.2 secs (maximum time before film destruction) is very small, according to the results of Hopis et. al. (118).

The degree of adsorption seems to be important in determining the relative corrosivity of various sulphur compounds. Husen (137) described an adsorption mechanism to explain the aggressivity of mercaptides; some of the reaction schemes listed in her paper are shown below in Figure 2.26 and 2.27.

Reaction on nascent steel surface

R = radical

2.26)

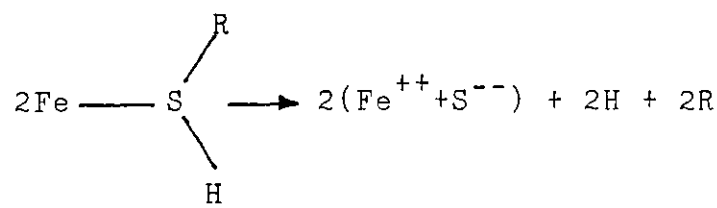

Figure 2.26

II. Reaction on sulphide surface. Defective surface with vacancies

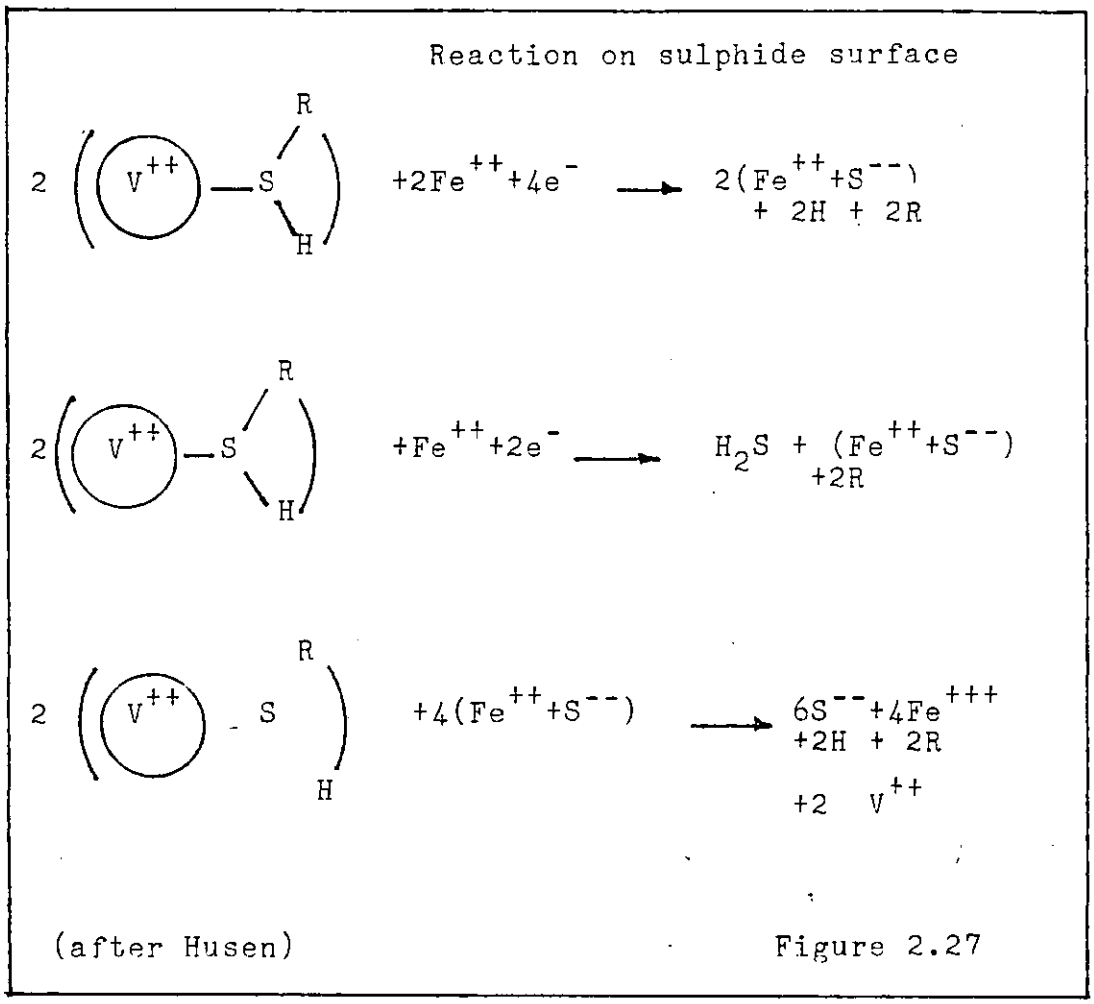

The heat of adsorption, the area density of vacancies and the size of the sulphur compound molecule are critical factors for growth rate (137)

Meyer et al (93) have shown that the degree of mechanical activation also determines the speed of reaction, particularly in the initial stages of reaction.

This is however a complex subject and few definite conclusions can as yet be reached.

2.6 Other Matters Relating to the Out of Contact Theory

In this section some additional speculations relating to the Out of Contact theory but not conforming with the discussion on film kinetics are presented.

2.6.1 Stresses caused by growth rates and their role as a cause of sacrificiality in a fast growing E.P. film

According to Fromhold (119) the major cause of stress in a fast growing oxide-film is that due to the growth rate itself. For an oxide film to grow there must be a flux of ions through the film. These ions, on moving forward through the film dispose of a considerable amount of momentum. The cumulative effect of this is a large force on the film in the direction of the ion flux. If the film grows by an outward flux of cations, then there is a net force on the film tending to pull it away from the metal. By Poisson's ratio a tensile stress must also occur in the plane of the film as shown in Figure (2.28).

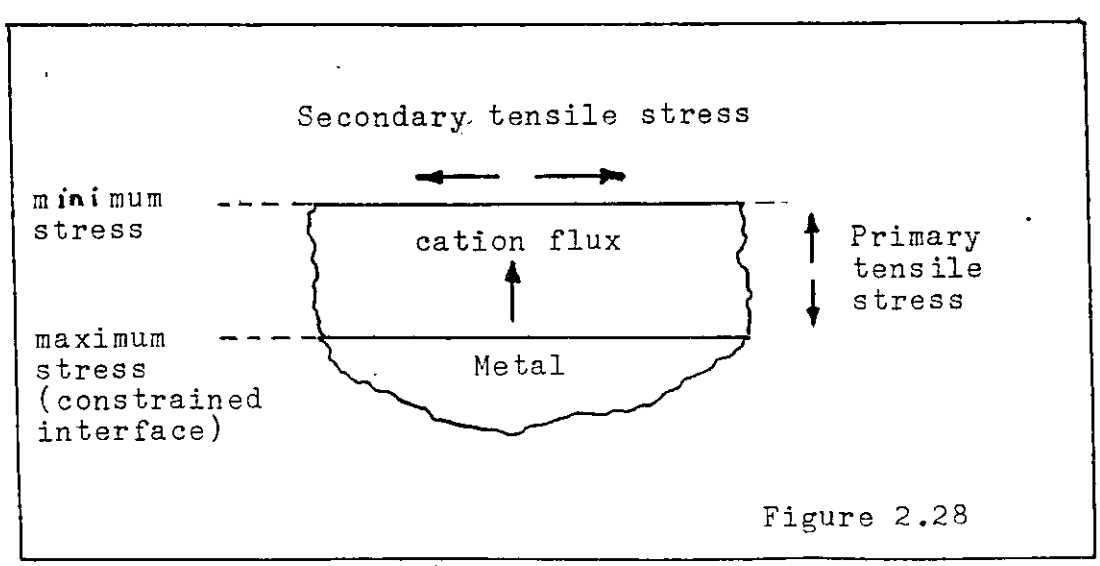

Figure 2.28

The Metal to Oxide interface (Figure 2.28) is the most highly stressed area, stress declines towards the oxide-interface in a roughly linear fashion. If the anions are mobile then the stresses become compressive (Figure 2.29).

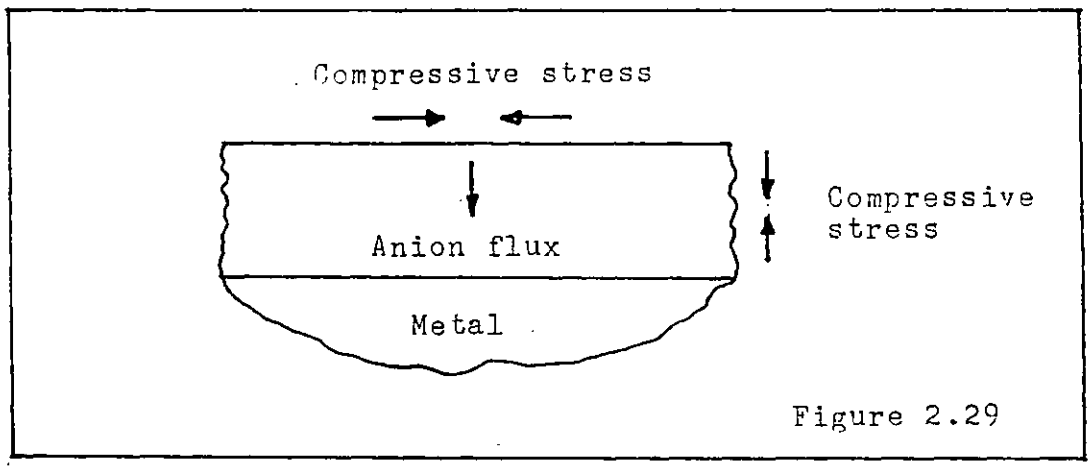

Figure 2.29

Fromhold analysed Borie, Sparks and Cathcart's (138) work on copper oxidation and obtained a satisfactory fit between his stress prediction and their results for distortion of the copper-oxide lattice parameter. Borie et al (138) studied copper oxide films 100 to 500 Å thick formed at temperatures around 250°C at reaction times up to 90 minutes. Making a comparison with E.P. films of approximately 100 Å thickness and formed in one second one can imagine that the stresses and strains in the E.P. film must be very large. How large are the stresses in E.P. films? Borie et al found strains as high as 2% in the oxide at the copper to oxide interface.

Presumably there must be compensating mechanisms or else the strains in the E.P. films would be of the order of several hundred %! Yet even so, the metal to E.P. film interface should be highly stressed and therefore a source of weakness.

Perhaps this goes some way to explain why E.P. films should be removed by even a moderately adhesive contact with another asperity. Adsorbed species on the oxide or sulphide surface may also be crucial for the reduction of asperity to asperity shear stress, so that the probability of film destruction be kept sufficiently small.

2.6.2 The relevance of the loss of diffusivity at high pressures to the Out of Contact theory

The analysis of oxygen's role in scuffing emphasised the criticality of liquid state diffusion in the E.P. mechanism. It is well known that liquid state diffusivity is inversely proportional to pressure in organic liquids (139). In an EHL contact; one may infer by the Barus law (10) that diffusivity could decrease by a factor of 10^5. Whatever the flash temperature and asperity collision temperature, oxidants are immobilised and substantial film growth cannot occur. For high temperature reactions such as fast sulphidation, reaction should occur just outside the inlet and outlet of the EHL contact where both temperature and diffusivity are high as shown in Figure 2.30.

This is why the Out of Contact zone is important for reaction, despite its lower reaction temperature than the EHL contact.

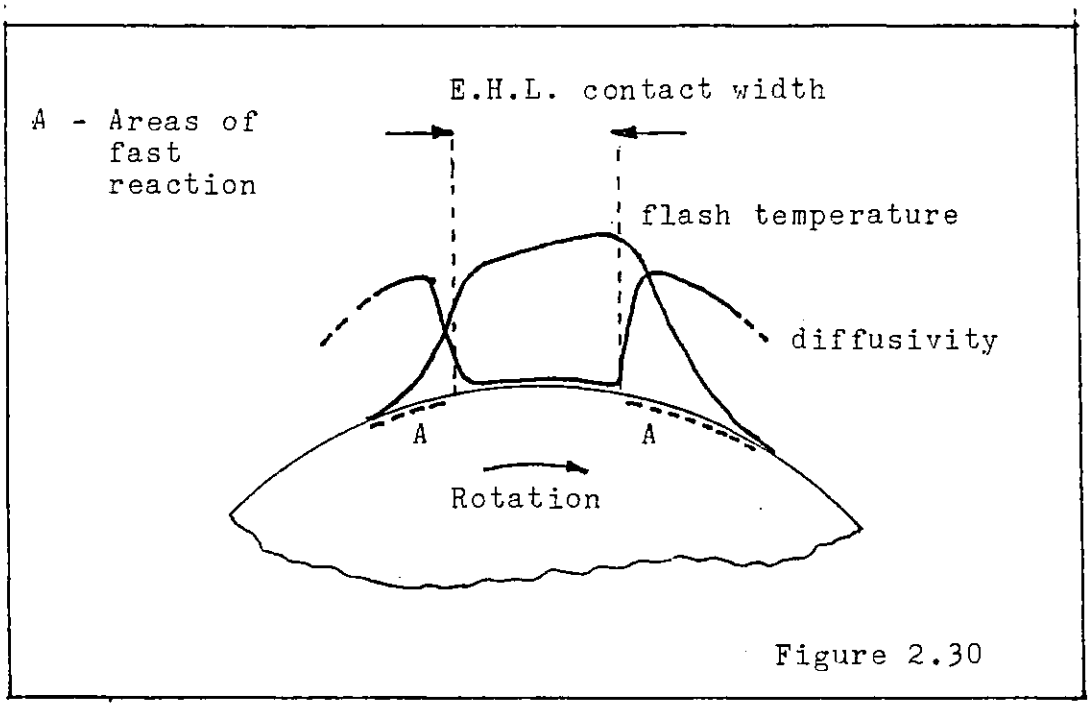

Figure 2.30

2.7 Conclusions

From the theory presented the following conclusions have been drawn.

2.7.1 By applying relevant material from corrosion science and surface science, reasons for believing that E.P. films are much smaller than is normally supposed have been deduced.

2.7.2 The influence of the low diffusivity of oxygen in oil has been used to explain the observation by Vinogradov that too much oil around an EHL contact can be deleterious.

2.7.3 The probability of very large stresses in E.P. films has been invoked as a reason for their sacrificiality.

2.7.4 Negligible diffusivity due to high pressure in an EHL contact is attributed as the reason for the Out of Contact period being critical for E.P. reactions despite the lower temperature.

CHAPTER 3

THE DESIGN OF A TEST-RIG TO INVESTIGATE THE GROWTH RATES OF EXTREME-PRESSURE FILMS

3.1 Introduction

The objective of the experimental work was to test Bailey and Cameron's Out of Contact theory which states that in a frictional contact the E.P. action of sulphur is due to the rapid formation of sacrificial sulphide films between consecutive rubbing contacts.

It was realised that direct analysis of sacrificial E.P. films in a frictional contact was impossible because of technical difficulties and a different experimental principle would have to be used. Thus it was decided to simulate the conditions found in the E.P. regime by a method which would also permit analysis of the film formed.

Very short reaction times and a nascent surface are involved; to meet these two conditions a specialised device has to be used.

Test-rigs suitable for long reaction periods have been constructed by e.g. Hathwar and Smith (144) to study the chemistry of nascent steel but nothing capable of short reaction times appears to have been developed. Thus a new test-rig had to be developed.

In this chapter is presented a discussion of the design of a short reaction period test-rig and a description of the appearance and functioning of the test-rig developed.

The chapter starts with a discussion of the purpose of the test-rig and the basic principles involved. The question of how to produce the nascent surface is then discussed followed by an outline of the design constraints. To complete the chapter there is the description of the completed test-rig and an assessment of how well the test-rig meets the design objectives.

3.2 The Need for a New Test-Rig and its Overall Purpose

Introduction. The need to design a new test-rig arose from the near-impossibility of adapting existing apparatus to the task of meeting the experimental objective. In this section (3.2) the discussion starts with a description of the difficulties involved in adopting methods which do not require a new purpose designed test-rig. The purpose of the test-rig is then described.

3.2.1 Use of existing equipment; difficulties of

Concerning the use of existing equipment, three options were considered: the measurement of E.P. films in a frictional contact, the use of previously devised test-rigs to study nascent metal chemistry and the use of bench-chemistry to reproduce the mechanism of E.P. film formation. These are discussed in the respective order below.

The oil, air and heat present in a lubricated frictional contact prevent in-situ measurement of E.P. films on the worn surfaces by currently available surface analysis techniques. E.D.A.X. for example requires a moderate vacuum during use. It is thus impossible with the limitations of current analytical techniques to monitor the formation and removal of E.P.

films in a lubricated frictional contact. Specimens of worn surfaces would therefore have to be extracted and evidence of film growth deduced from subsequent analysis of the specimens. It would not be sufficient to perform a large-area analysis of the surface, load bearing areas would have to be isolated and the time available for film formation estimated. To do this requires a knowledge of conditions in the frictional contact which is probably beyond the current level of understanding of the tribology involved. Thus this approach to the experimental problem was not developed.

Accessible literature was searched for previous investigations on nascent metal chemistry and two works were found.

Hathwar and Smith (144) developed a test-rig for studying the reaction of nascent metal with organic compounds and Tingle (105) modified the Bowden-Leben machine (68) to study the frictional properties of nascent metal lubricated by organic compounds. Both devices developed had minimum reaction periods of several seconds. No reasonable modifications of these test-rigs to enable shorter reaction periods could be conceived of, thus these test-rigs were not investigated further.

The use of bench chemistry to reproduce the E.P. film mechanism under conditions more amenable to analysis is mainly hindered by the very short reaction times of interest. Reaction times of a few milliseconds are required and so simple techniques of initiating and terminating the reaction do not suffice. To give an example of the restriction imposed by the short reaction-time, an experiment involving

abrasion of an iron surface immersed in a sulphur containing lubricant is outlined. One could immerse an iron specimen in a container of sulphurised lubricant and subsequently abrade the surface to expose nascent metal. After a prescribed period of time the specimen could be removed from the lubricant and washed by a solvent to stop the surface reaction. As is evident, the type of experiment is suitable for reaction times of at least several seconds. It was therefore concluded that bench-chemistry was not suitable and that a dedicated test-rig must be devised.

3.2.2 Purpose of the test rig

As stated in the introduction 3.1, it was realised very early on in the work that the direct study of the E.P. mechanism in a frictional contact was not possible and so the principle of simulating the E.P. mechanism would have to be employed.

It is believed that the critical characteristic of the E.P. mechanism is a very fast formation of the protective film on a nascent surface where oxide has been removed by a wearing contact. Thus the simulation of the E.P. mechanism must incorporate a means to remove the surface oxide and permit reaction by a sulphur based lubricant for a short but controlled period. The nascent surface so produced must also facilitate analysis of the film formed.

3.3 Specification of the Range of Experimental Conditions to be Studied in the Test-Rig

3.3.1 Introduction

The exact values of investigated reaction time and temperature and the degree of cleanliness of the surface

studied have a direct bearing on the design of the test-rig. The values of these three variables should both be comparable to that occurring in the E.P. regime and practicable technically. In this section is discussed the specification of reaction time, reaction temperature and surface cleanliness.

3.3.2 Reaction time, range of

According to the Out-of-Contact theory, the reaction time available to a sacrificial film is a multiple of the time between wearing contacts. If the film is entirely destroyed on each contact, then the reaction time is identical to the period between contacts as is illustrated in Figure 5.1.

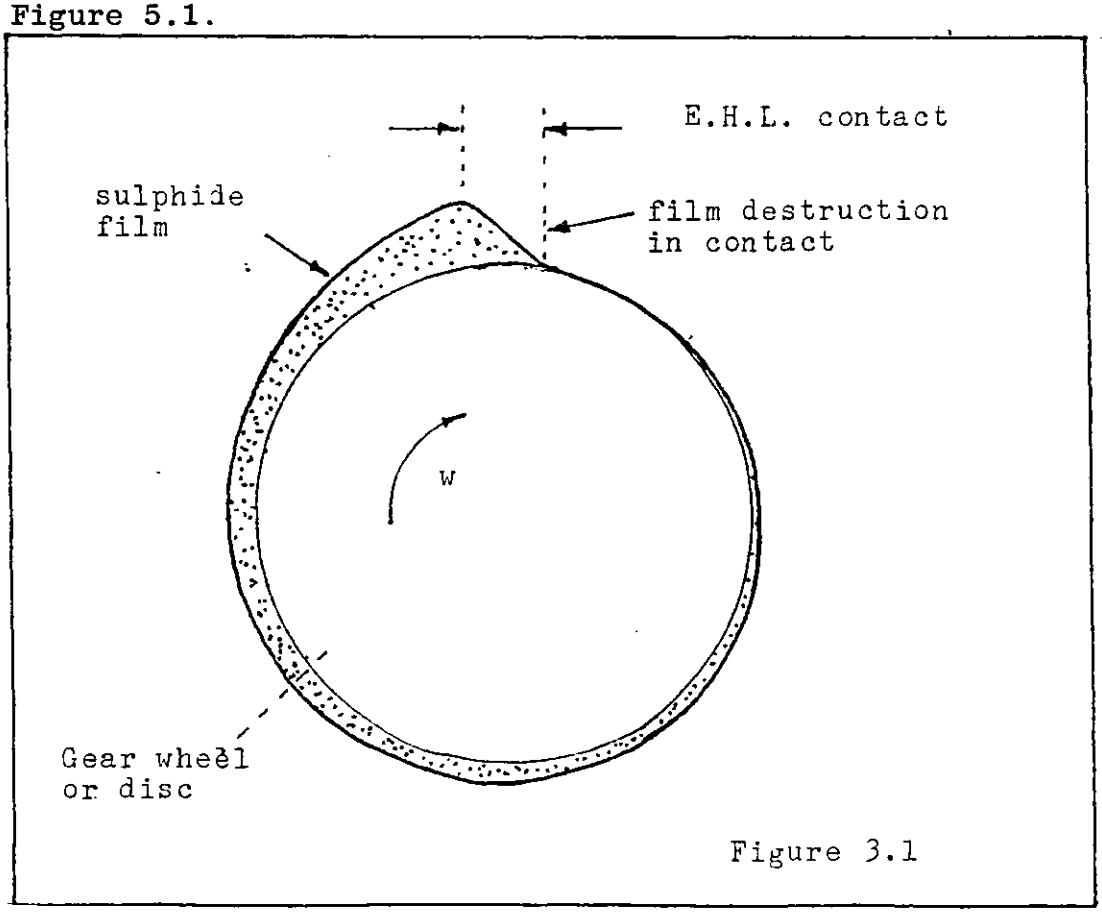

Figure 3.1

The range of reaction time studied should therefore correspond (in a reciprocal manner) to the range of contact frequencies or angular velocities commonly found in machine elements requiring E.P. lubrication. Most machine elements

do not normally rotate faster than 20,000 to 30,000 rpm thus this was chosen as the higher limit of contact frequency to be studied. Assuming one contact per revolution, the reaction time (which is equal to the time between contacts) will be 3.3 and 2.0 milliseconds for 20,000 rpm and 30,000 rpm respectively.

Reaction times as short as these create considerable difficulty in the design of a test-rig. A reaction time of 3.0 msecs is close to the minimum practicable and was therefore chosen as the lower limit of reaction time studied.

The upper limit of reaction time was not decided by such a rigorous reasoning as the lower limit. The test-rig as developed at time of writing enables maximum reaction times of between 70 and 80 milliseconds to be investigated.

As is shown by the results an approximate relationship between film thickness and reaction is observable in the 3-70 millisecond range currently attainable. Thus 70 ms was considered adequate for the upper limit of reaction time. With some modifications to the test-rig, longer reaction times could be set if desired.

3.3.3 Reaction temperature, range of

The reaction temperature for an E.P. film that develops in the Out-of-Contact period is closely related or identical to the oil film temperatures outside of the contact. E.P. action is generally thought to start at around 150^{o}C and extend to temperatures considerably higher. Experimental limitations (discussed in 4.3.1.3) restrict reaction temperatures

to not more than 185°C which was taken as the higher limit of reaction temperature. The lower limit of reaction temperature was set at ambient i.e. approximately 20°C. This causes no problems with rig design and falls short of the start-temperature for E.P. lubrications.

3.3.4 Degree of surface cleanliness; or no scenery

Some contamination of the 'nascent' surface prior to reaction with the sulphur-containing lubricant must be expected. From the material discussed in Chapter 2 it was decided that up to half a 'monolayer' of contamination on the nascent surface was acceptable.

3.4 Operating Principles of the Test-Rig

3.4.1 Preliminary considerations

From a brief consideration of the requirements of surface analysis techniques such as e.g. X.P.S. it was evident that in-situ analysis of a growing film would meet with the same difficulties as apply to the study of a frictional contact (Section 3.2.1). Most of the analysis techniques require a moderate to hard vacuum or have a long analysis time which renders them unsuitable for the contemporaneous analysis of a fast-growing film. Thus a test-rig which produces specimen surfaces suitable for analysis is the sole possibility given the current level of the technology of surface chemical analysis. The possibility of physical and chemical modification of the film (produced by the experiment) prior to analysis has to be accepted.

3.4.2 Operating principle

A four stage process was chosen as the operating principle: this is shown below.

1. Render specimen surface nascent.
2. Deposit layer of sulphur containing fluid.
3. Rinse or quench specimen surface after specified time to stop reaction.
4. Subsequent surface analysis, of extracted specimens.

The last stage, subsequent analysis involves an external facility and so is separate from the first three stages which are incorporated within the test-rig.

Implicit in the design of the process described above is the condition that the spatial ordering of the apparatus associated with the first three stages is the same as the functional ordering described above. The specimen surface moves from one stage to the next on completion of the function designated to any one stage. By moving the specimen at a high speed, the time to pass between Stage 2 and Stage 3 i.e. the reaction time can be made very short. In this manner the objective of a short reaction time is achieved.

Having found a suitable operating principle, methods to apply it were then reviewed. The next section, 3.5, discusses the question of the most suitable method.

3.5 Selection of Means of Applying the Operating Principle

3.5.1 Introduction

A short list of five methods of putting into practice the principle outlined in 3.4.2 was drawn up. All five

methods considered have a common characteristic which is thought to render them more suitable than other possible methods. In common to all five methods is that a mechanical process taking place under near-atmospheric conditions is used to produce the nascent surface. The nascent surface so produced is believed to resemble the nascent surface produced by wear more closely than for example non-mechanical methods. Thus the film kinetics of both surfaces should be similar.

This matter is not discussed further in this chapter, instead in Chapter 6 the question of similarity between the experimental and a worn nascent surface is discussed as part of an overall assessment of the results.

The discussion presented below in this section (3.5), starts with a description of the five methods considered and concludes with the reasons for the selection of a particular method.

3.5.2 Description of the methods considered

Most of the problems encountered in the design of the rig arose from the difficulties of producing a nascent surface that conformed to the specifications of reaction time, reaction temperature and surface cleanliness and avoided undesirable side-effects such as surface inhomogeneity. The principle differences between the methods considered therefore lay in the means of producing the nascent surface.

The five methods discussed involve guillotining, cutting rolling, extrusion and scraping as a means of producing the nascent surface.

3.5.2.1 Guillotine method

The method described below is illustrated in Figure 3.2. A guillotine is used to create the nascent surface by exposing a freshly cut face of a section of metal. A wick-feed to supply the sulphur containing fluid (model lubricant) and a rinse jet are mounted beneath the cut metal. As the freshly cut metal surface is forced down by the guillotine blade it is exposed in turn to the wick-feed and the rinse jet. Reaction time and temperature could be determined by blade-speed and specimen metal pre-heat respectively.

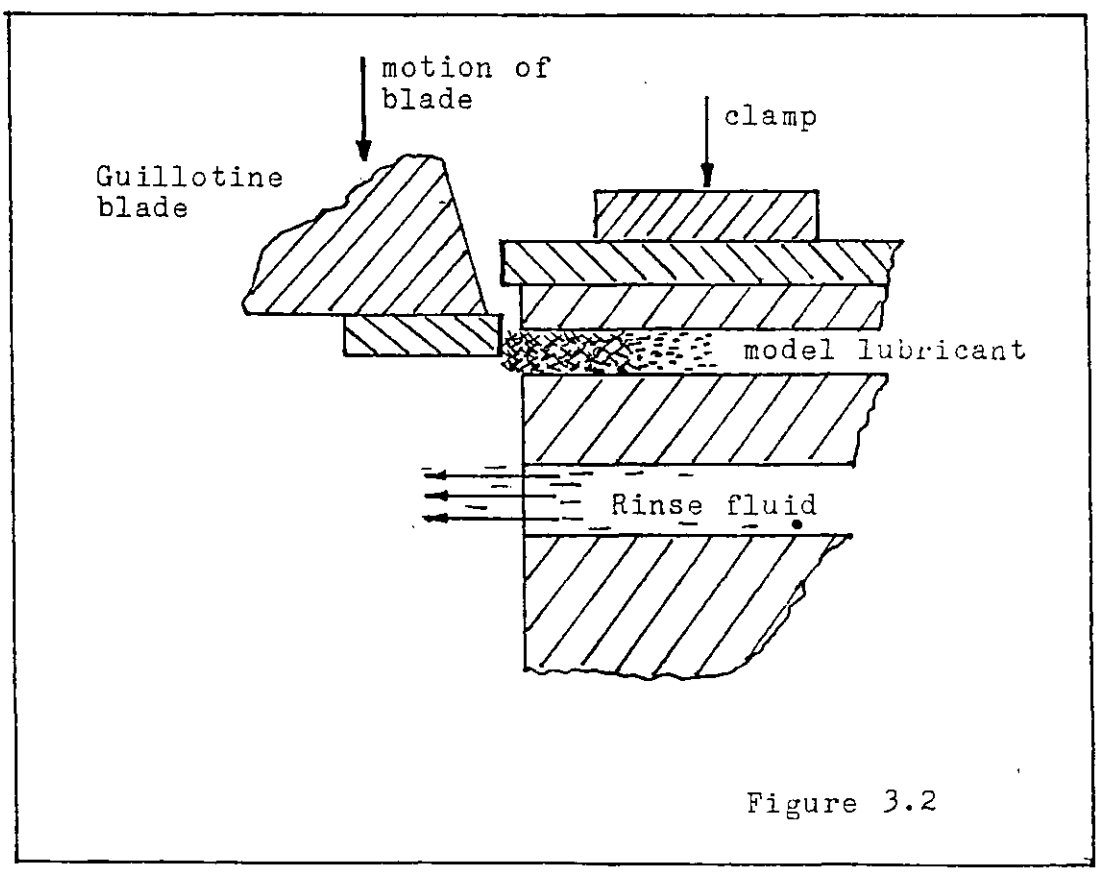

Figure 3.2

3.5.2.2 Cutting method

A moving surface of metal is cut by a tool to expose nascent metal. Behind the tool edge a model lubricant (i.e. sulphur containing fluid) is pumped onto the surface and a rinse jet is positioned at a suitable distance to terminate the reaction after the specified time. The method is illustrated below in Figure 3.3.

The metal surface could be pre-heated to the required reaction temperature and reaction time could be set by varying surface speed and rinse jet position relative to the tool.

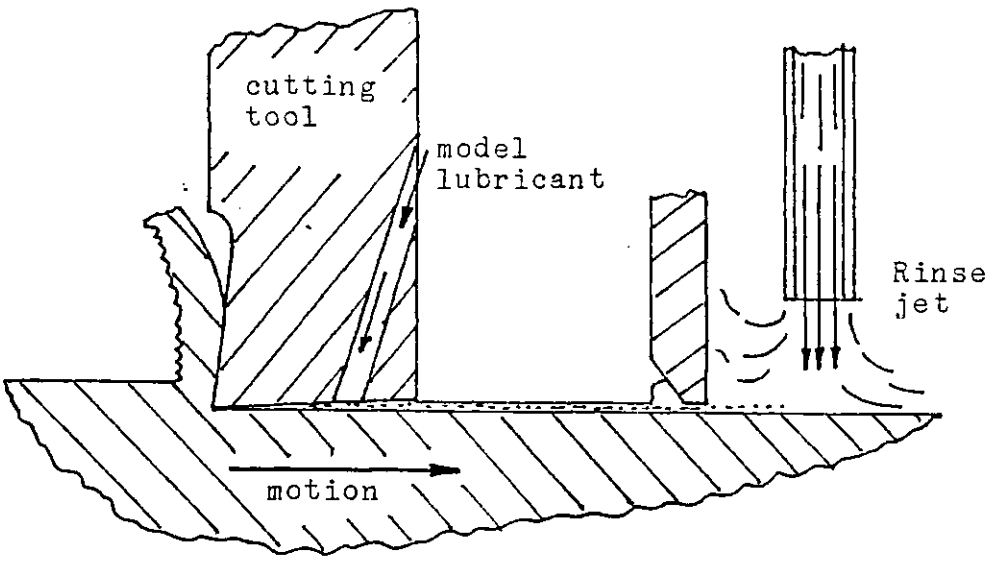

Figure 3.3

3.5.2.3 Rolling method

The increase in metal surface area by rolling causes nascent surface to appear between the fragments of oxide surface originally covering the surface. Thus a scheme involving a metal-rolling tool, a specimen sheet of metal, a wick-feed for model lubricant (in this case sulphur-containing fluid) and a rinse-jet was devised. The specimen metal passes between the rollers, model lubricant is deposited upon it and later reaction is terminated on reaching the rinse jet. The scheme is illustrated below in Figure 3. 5 Reaction time and temperature is controlled according to the same principles as stated in 3.5.2.2.

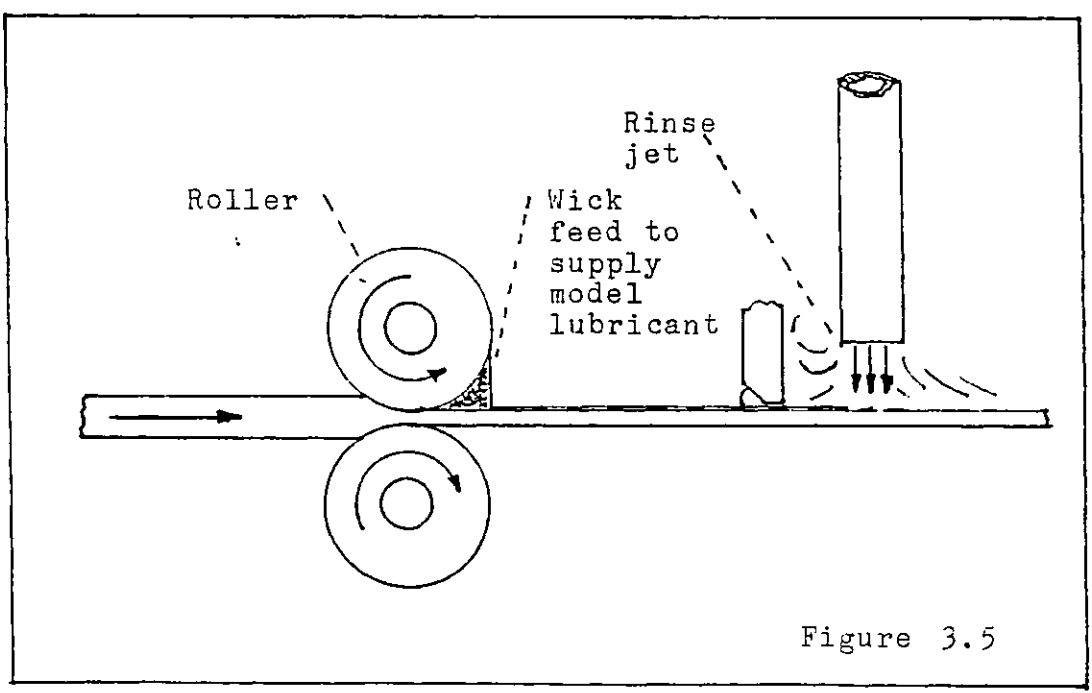

Figure 3.5

3.5.2.4 Extrusion method

As with rolling, extrusion causes an increase in the surface area of the deformed metal which breaks up the original oxide film to expose nascent metal. A process involving an extrusion press, a wick-feed for model lubricant and a rinse jet was devised. The surface of the specimen metal is stretched on extrusion to reveal nascent metal and model lubricant is deposited on the surface as it emerges from the extrusion press. The specimen surface is subsequently rinsed to terminate the reaction. The process is illustrated below in Figure (3.4).

Reaction time could be controlled by varying the rate of extrusion and the position of the rinse jet. Reaction temperature could be determined by pre-heat and heat of extrusion.

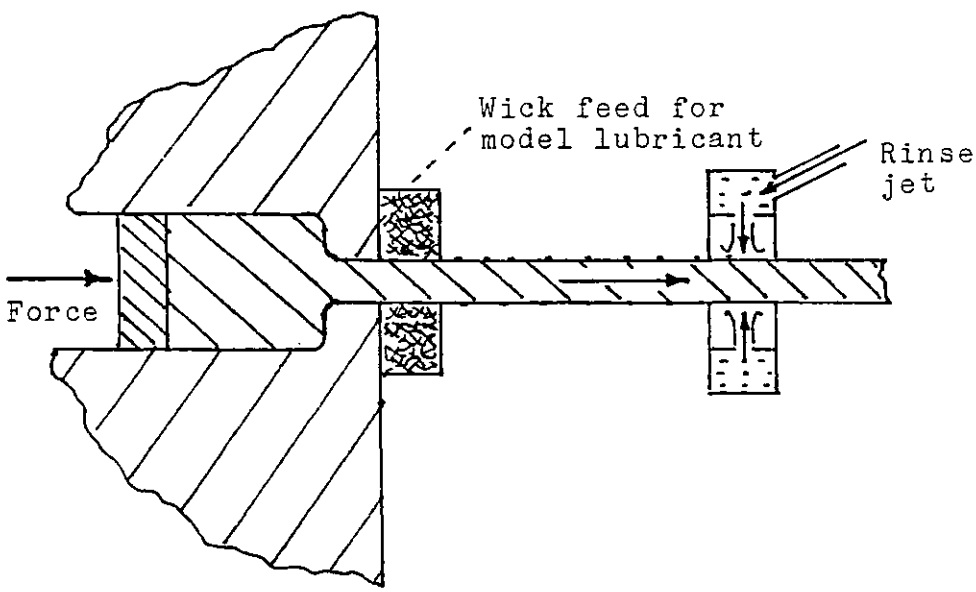

Figure 3.4

3.5.2.5 Scraping method

Scraping which results in the removal of a thin layer of metal (1 to 5 microns thick) is used to produce a nascent surface. As with the cutting method (3.5.2.2), the specimen surface passes under the tool where a cut is taken. Model lubricant is then deposited on the nascent surface which is later washed off when the scraped surface reaches the rinse jet. The principle is illustrated below in Figure (3.6).

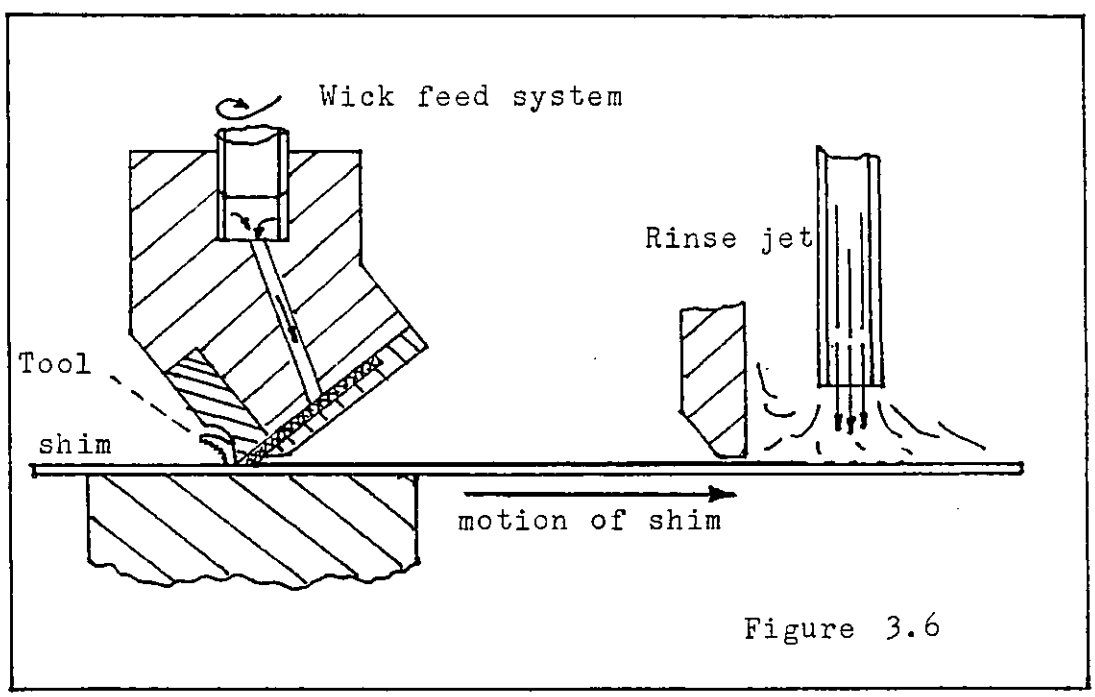

Figure 3.6

Reaction temperature is controlled by the level of pre-heating of the specimen material. Surface speed and distance between tool and rinse jet determine reaction time.

3.5.3 Selection of the method

The final choice of one of the methods described in 3.5.2 was based on five criteria. These criteria do not cover all the problems relating to the design of the test-rig but sufficed to isolate one method which on further consideration (discussed in 3.5.4) was revealed to have advantages additional to those exemplified by the criteria.

3.5.3.1 Criterion used for selection

The five criteria applied are:

1. Size of temperature fluctuation caused by the process used to create nascent surface. This fluctuation should be as small as possible since a near constant temperature during the reaction period is needed for meaningful film growth rate data to be obtained.
2. The quality and homogeneity of the nascent surface produced. The surface should be reasonably smooth and uniform in form so as to facilitate the analysis of the film and the interpretation of results with respect to surface conditions.
3. The width of the nascent surface which is the dimension parallel to the plane of the nascent surface and perpendicular to direction of specimen motion) must be wider than a certain limit so as to ensure sufficient area for surface analysis. Figure 3.7 shows the width dimension appropriate to scraping and cutting.

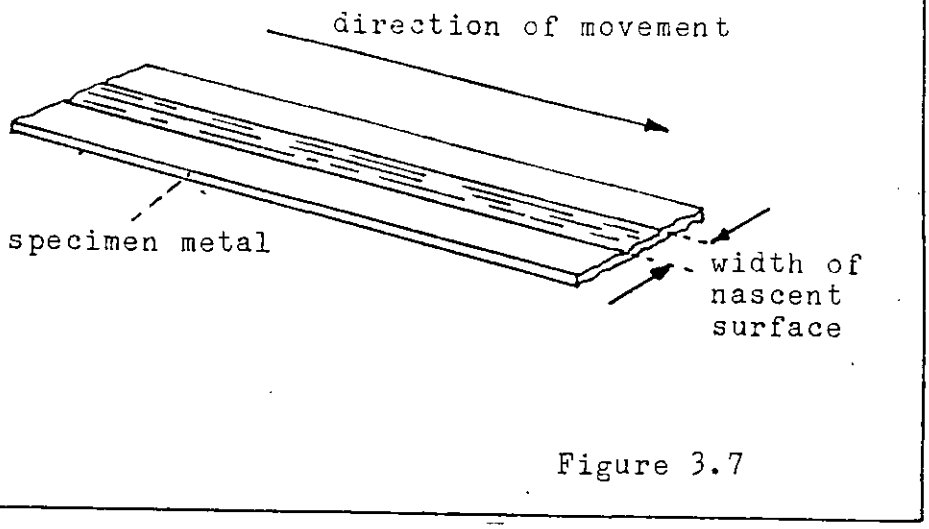

Figure 3.7

The test-rig was originally designed for surface analysis by radiochemistry involving Sulphur-35. This required a nascent surface width of at least 5 mm and the test-rig was designed accordingly. Such a width facilitates Reflectance Infra-Red spectroscopy but is not necessary for the technique of E.D.A.X. which can analyse micron size areas (as discussed in Chapter 4).

4. Pre-emption of oxygen by prompt deposition of model lubricant. A significant concentration of oxygen is present even in a high purity inert gas atmosphere. A vacuum cannot be used because of the liquid model lubricant present. The nascent surface will react with any available oxygen, very little of which is needed to oxidise the surface. Thus a special consideration must be given to the possibility of surface oxidation before the model lubricant is deposited.
5. Nascency of surface, partial or total,

Nascent surface which is mixed with oxide covered surface will be more difficult to analyse than totally nascent

surface since it is difficult to separate the nascent from the oxidised surface by large area analysis techniques. Thus total nascency is preferred.

3.5.3.2 Application of criteria

The methods described in 3.5.2 were evaluated according to the criteria presented in 3.5.3.1, the estimation of the various methods is presented in tabular form in Table 3.1. As a result of the evaluation scraping was chosen as the method with the least disadvantages.

Cutting was also rated highly as a possible method. However the small clearance angle of the tool hinders wetting of the nascent surface close to the tool edge by the model lubricant. The problem is illustrated below in Figure 3.8 for the case of rolling which has the same disadvantage. Thus oxidation of the nascent surface could occur before the model lubricant was deposited. The small quantity of energy involved in scraping compared to cutting reduces the temperature fluctuation to the minimum possible, which is another advantage particular to scraping.

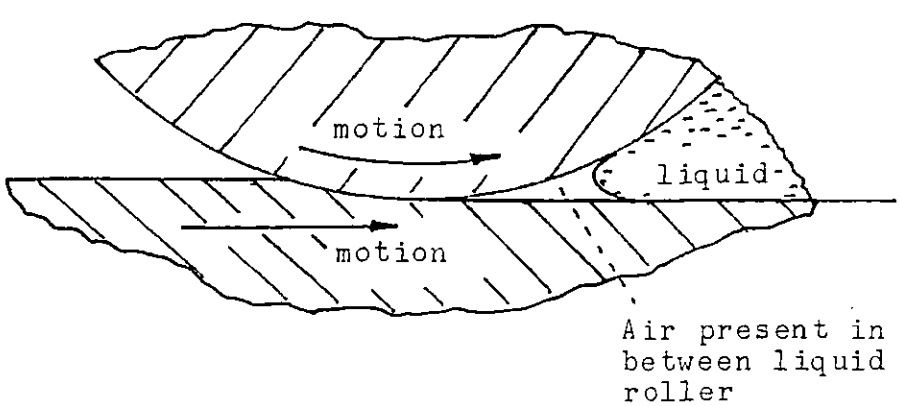

Figure 3.8

TABLE 3.1

Possible Method	Criterion				
	Temperature Fluctuation	Surface Quality	Surface Width	Pre-emption by Oxygen	Relative to Partial Nascency
Guillotining	Relatively large	Poor	Narrow	Oxygen has access before model lubricant	Total
Cutting	Relatively large	Good	Wide	Possible access by oxygen	Total
Rolling	Relatively large	Good	Wide	Possible access by oxygen	Partial
Extrusion	Relatively	?	Wide	Oxygen excluded	Partial
Scraping	Lowest possible	Good	Wide	Oxygen excluded	Total

3.6 Functioning and Appearance of the Test-Rig

3.6.1 Introduction

Having decided that scraping should be the method of producing the nascent surface (as described in 3.5.2.5), the next step was to design and construct an appropriate test-rig.

In this section, the discussion starts with an outline of the primary features of the test-rig. The mechanical aspects of the operation of the test-rig during an experiment are then described. To complete the section an illustrated description of the appearance of the rig is presented.

3.6.2 Basic functions of the test-rig

The design and functioning of the test-rig centres around the scraping tool, specimen material, wick-feed and rinse jet; or in other words the working parts directly relating to the scraping method. Subsidiary to these items are for example the mechanisms which (a) preheat the specimen material to the required temperature; (b) accelerate the specimen material to the appropriate velocity; (c) supply the pressurised solvent to the rinse jet. Figure 3.9 is used to illustrate the basic aspects of the structure and design of the test-rig and highlight some other important details. The numbers on Figure 3.9 which are referred to below mark out the principle features of the test-rig. These numbers are also used to show the functioning of the test-rig.

1. The specimen material which consists of shim with dimensions 0.5 mm x 15 mm x 2 m approximately.
2. The scraping tool, (discussed in 3.5.2.5).
3. The wick-feed system, (discussed in 3.5.2.5).
4. The rinse jet with a barrier on the side closer to the cutting tool to confine the rinse fluid.
5. A chamber which encloses the reacting specimen surface and enables the use of a blanketting gas to displace atmospheric oxygen.
6. A 'start-tube' which contains an electric heating element to enable pre-heating of the part of the specimen material that is to be scraped.
7. A 'stop-tube' which serves as a repository for the scraped specimen material.
8. A source of motive power which is needed to pull the specimen material past the scraping tool at the required speed.
9. 'Tensator' constant force springs are used to provide the pulling force mentioned in 8. Each spring consists of a coil of laminar spring steel which exerts a steady force on uncoiling.
10. A trigger which is used to release the springs described in 9. and thus cause the specimen material to move.

To set in motion the scraping process (described in 3.5.2.5), the trigger is opened and simultaneously the rinse-fluid allowed to flow. The pre-heated part of the specimen material moves from the start-tube towards the tool where it is scraped. Model lubricant (in this case sulphur-containing oil) is deposited on the scraped surface

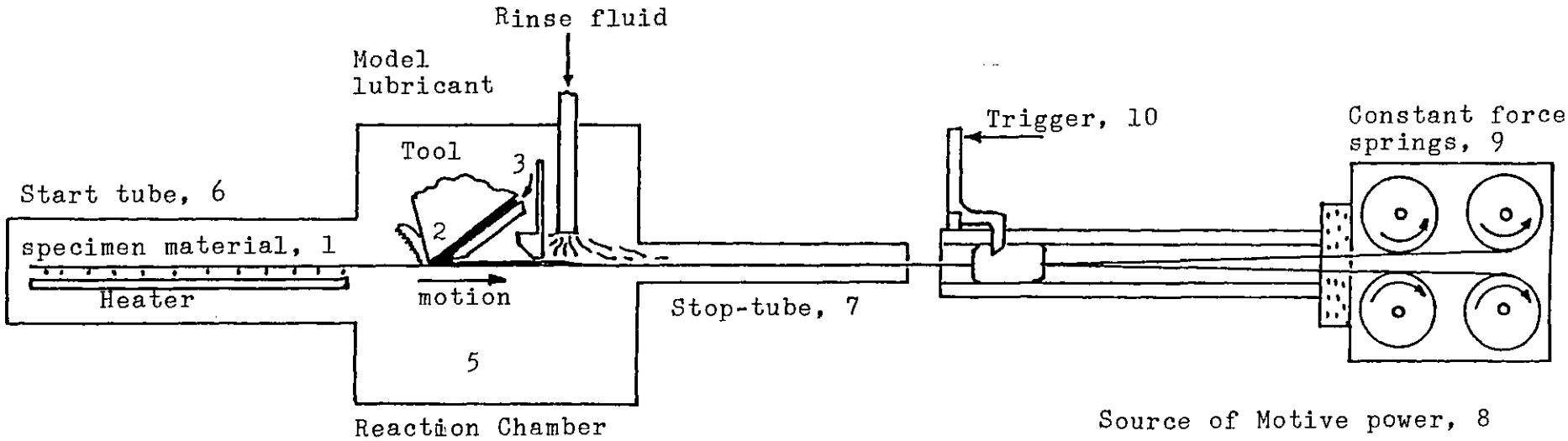

Figure 3.9 Diagram showing basic features of the test-rig.

which is subsequently rinsed. Once rinsed the scraped surface proceeds to the stop-tube. The process is completed when the springs reach the limit of permitted movement and are stopped. The specimen surface has now been scraped and allowed to react with the model lubricant and can be later extracted for analysis.

3.6.3 Use of the test-rig during an experiment

Before discussing the method by which the rig is used, the structure used to mount the scraping tool and wick-feed is described. This description is a necessary preliminary because the preparation of the tool structure or 'scraper' as it is called forms an important part of the experimental method.

3.6.3.1 The 'scraper'

The 'scraper' which is illustrated in detail in Figure provides adjustment of the scrape depth and the alignment of the tool across the scrape width (scrape width is shown in Figure 3.10). Since the scrape depth is 1-5 microns and the width of scrape 5 mm the adjustments required are very fine.

Scrape depth adjustment is achieved by sliding a tapered block beneath the tool. The amount of sliding is dictated by the number of turns on the scrape-depth adjustment screw. The change in gap thickness between tool and taper block

1 = Scrape depth adjustment
2 = Cross alignment
3 = Rinse jet
4 = Rinse barrier
5 = Wick-feed

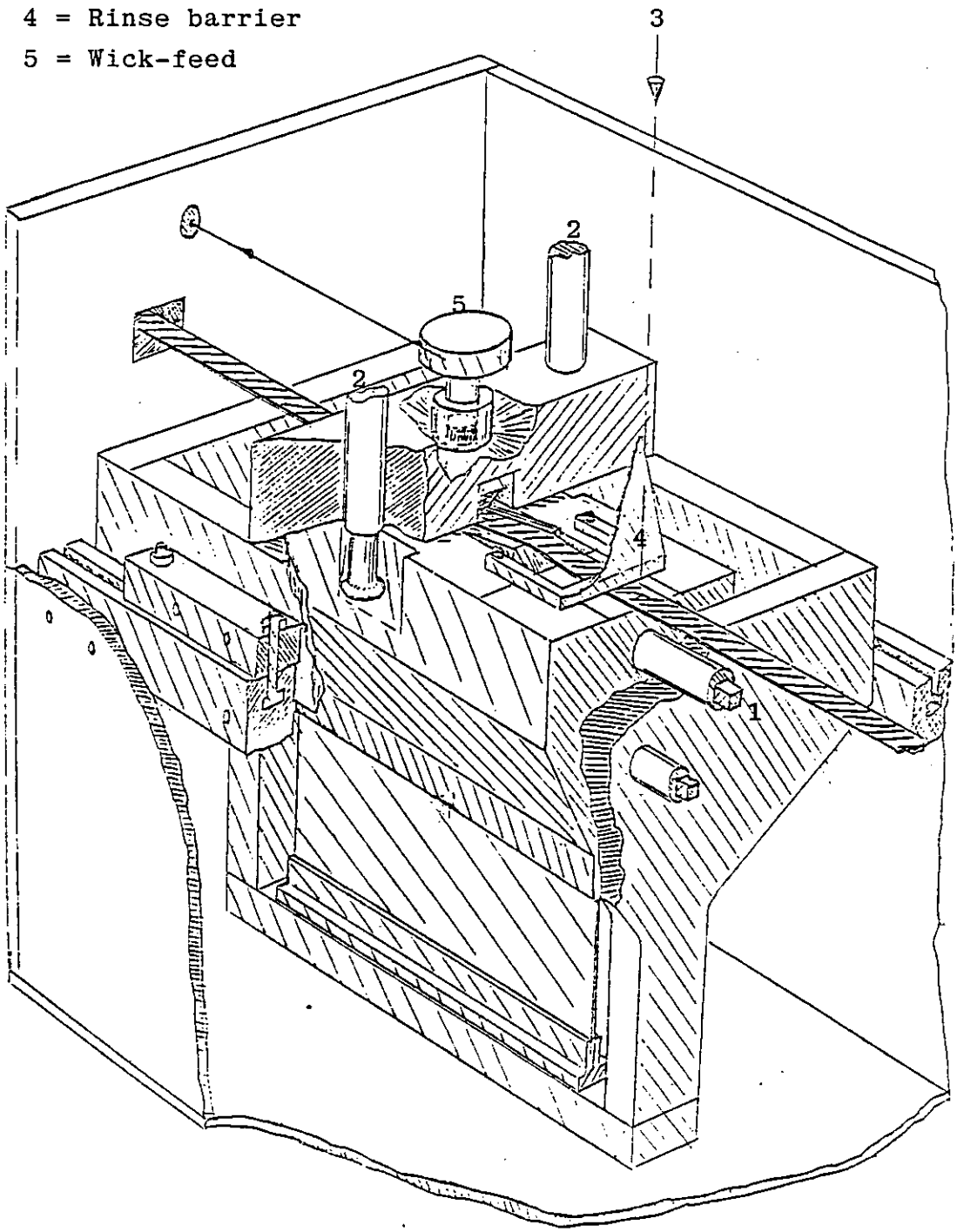

Figure 3.10 Illustration of the 'scraper'.

determines the scrape depth. With a shallow taper and fine pitch screw very small adjustments to cut depth can be made.

A similar principle is applied for adjustment of tool alignment. The structure directly beneath the tool is able to pivot by flexing its supporting plate. Two cross-alignment screws bearing on tapered slides control the degree of pivotting.

The 'scraper' is designed for maximum rigidity as scraping is prone to 'chatter'. 'The rinse barrier' which is mounted on the scraper close to the scraping tool is used to prevent the rinse fluid from flooding the tool and stopping the reaction before the set period of time. The 'scraper' can be positioned at various distances from the rinse-jet thus enabling variation of reaction distances and times.

The force-feed system to the wick is mounted directly above the tool. By rotating a threaded plunger that is seated in the receptacle containing the model lubricant, a force-feed of model lubricant to the wick is obtained. By controlling the feed rate a layer of known thickness of model lubricant is deposited on the nascent surface. This ensures that depletion of the sulphur additive does not occur because of lack of model lubricant or that rinsing fails to be effective because of excess of model lubricant.

3.6.3.2 Test procedure

In contrast to the relative simplicity of the process of 'scraping' described in 3.6.2, the test procedure itself has a certain complexity. To bring the test-rig to a state of readiness for 'scraping' several preparative tasks have to be carried out and after completion of 'scraping' a specified shut down procedure was followed before the specimen material was extracted.

To illustrate the test procedure, Figures 3,11,3.12,3.13,3.14 and 3,15 are presented. In these figures five stages of test procedure are shown, the first three stages i.e.'A' of Fig.3.11 and 'B' of Figure 3.12 and 'C' of Figure 3.13 show the preparation of the test-rig for scraping. Stage 'D' of Figure 3.14 illustrates the process of 'scraping' and Stage 'E' of the Figure 3.15 shows the extraction of specimens and shut down of the test-rig. As a means of describing the test procedure in detail the functions of each of the five stages mentioned above are outlined below.

The purpose of stage 'A' (illustrated in Figure 3.11) is to un-coil the springs from their retracted position so that they can provide the motive force required in stage 'D'. In stage 'A' a length of specimen material is attached to the Wind-out wheel and springs (No.1 of Fig.3.11). A lever (No.1 of Fig.3.11 'A') is used to turn the Wind-out wheel and draw out the springs till the trigger is reached. The distance moved is indicated by the roman numerals, I, II. On reaching the trigger the specimen material is cut (No.2 of Fig.3.11) and the start-tube is closed up (No.3 of Fig. 3.11). On completion of this stage the 'Wind-out' wheel and lever serve no further purpose in the test.

In stage 'B' (Figure 3.12) the scraper is adjusted (No.1 of Fig.3.12)) to give the appropriate depth of scrape. The wick feed is filled with model lubricant (No.2 of Fig. 3.12) and the threaded plunger (No.3 of Fig.3.12), is screwed on. Included in stage 'B' but not shown on Figure 3.12 is the task of mounting the rinse barrier in the correct position relative to the scraping tool.

In stage 'C' (Figure 3.13) the tasks preparative to 'scraping' are completed. The first task is to connect the thread plunger by a cable to the wick-feed motor (No.1 of Fig.3.13). The reaction chamber is then closed (No.2 and 3 of Fig.3.13) The supply system for rinse fluid is filled up (No.4 of Fig.3.13) and the hydro-pneumatic accumulator used to flush out the rinse fluid is pressurised with nitrogen (No.6 of Fig.3.13). Shortly before 'scraping' commences the heater (No.7 of Fig.3.13) is turned on to warm the specimen material.

In stage 'D' (Figure 3.14), the trigger (No.1 of stage 'D') is opened and 'scraping' is set in motion. Ancillary to the processes described in 3.6.2; the wick-feed motor and gate valve for rinse fluid (No.1 of stage 'D') are activated simultaneously with the trigger.

Stage 'E' (Figure 3.15) is the close-down procedure, the test-rig is allowed to cool down before opening the reaction chambers. The reacted portion of specimen is extracted and waste rinse fluid disposed of.

Figure 3.11

Figure 3.12

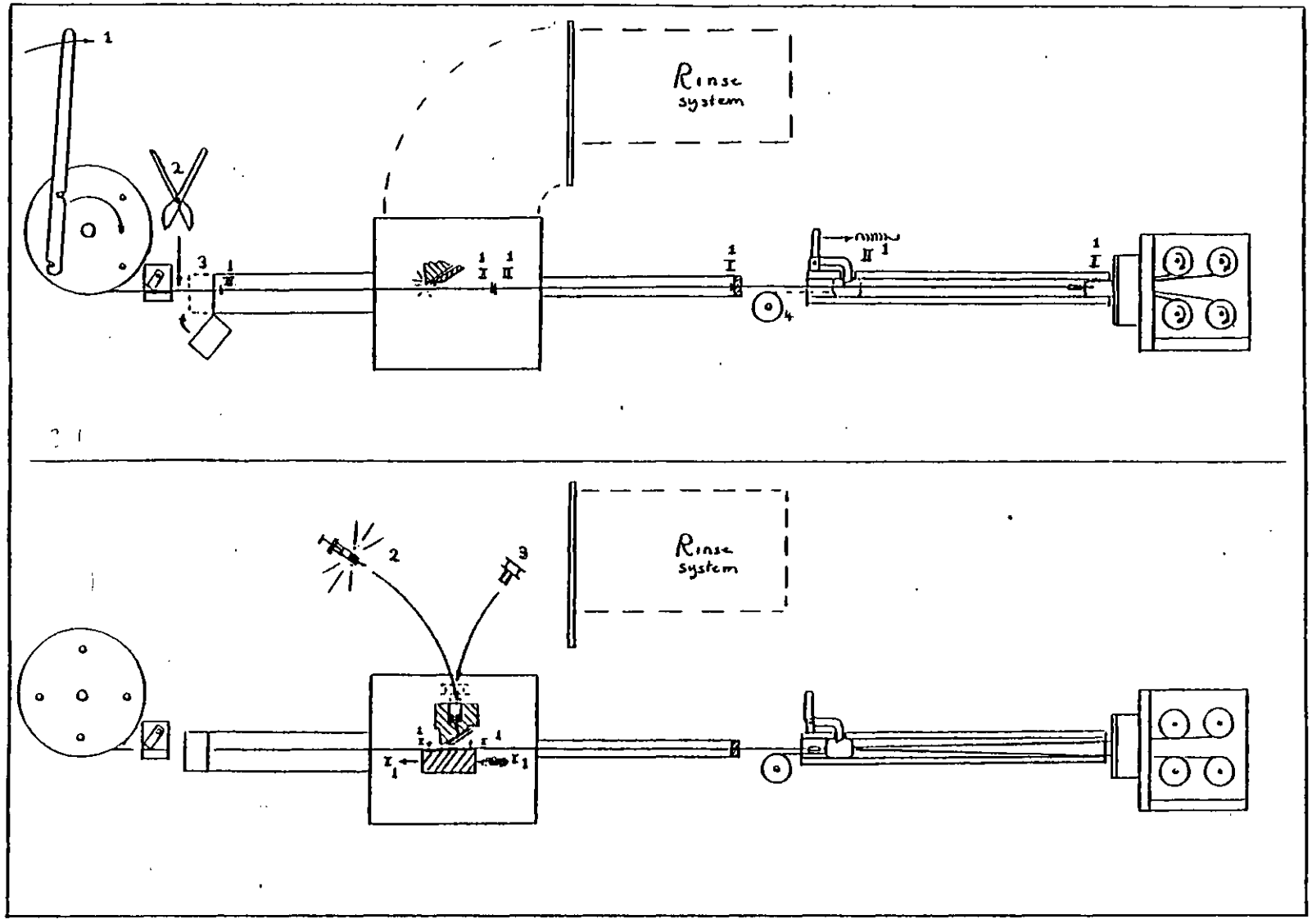

Figures 3.11 and 3.12 Stages A and B of Test procedure.

Figure 3.13

Figure 3.14

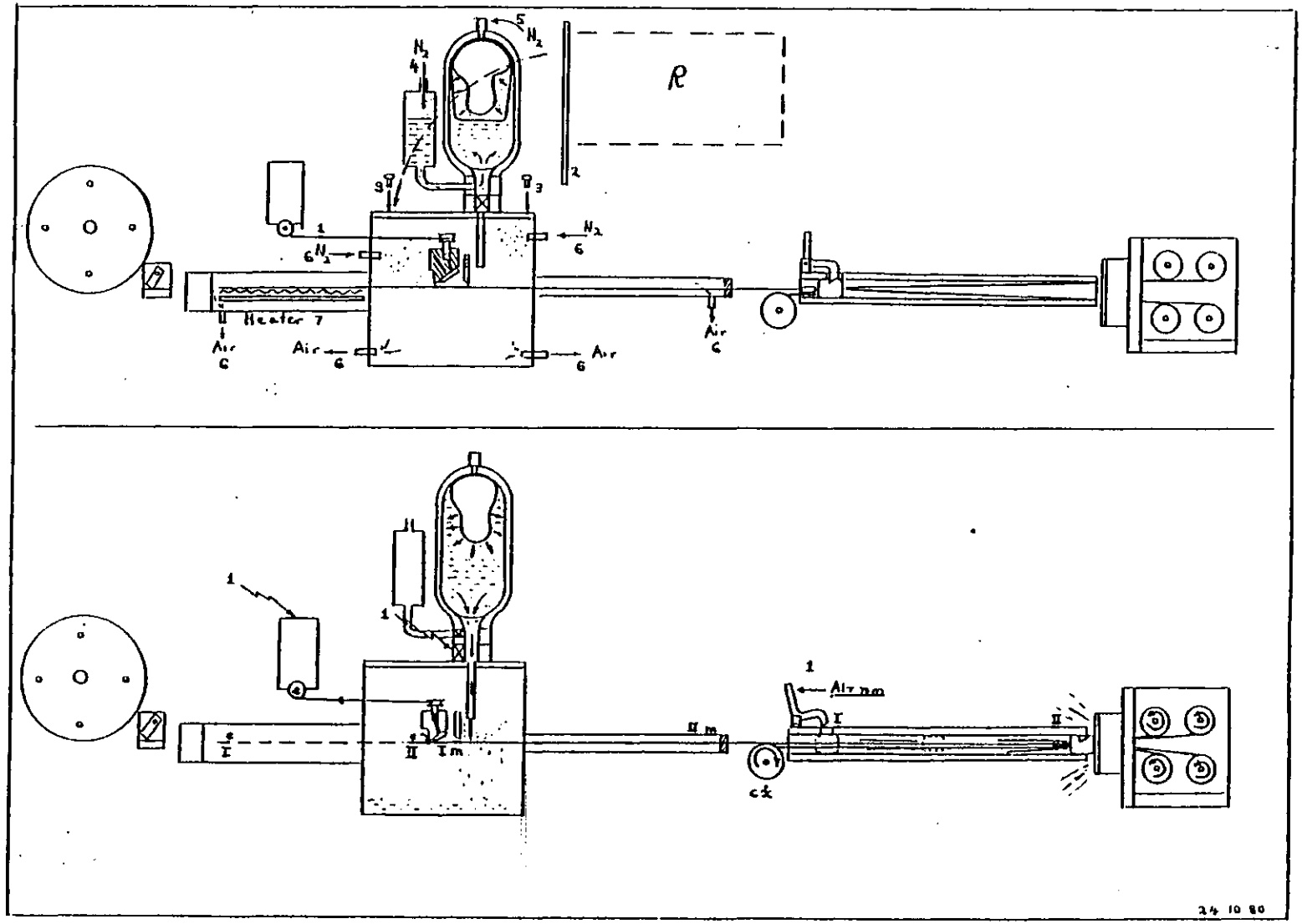

Figures 3.13 and 3.14 Stages C and D of Test procedure.

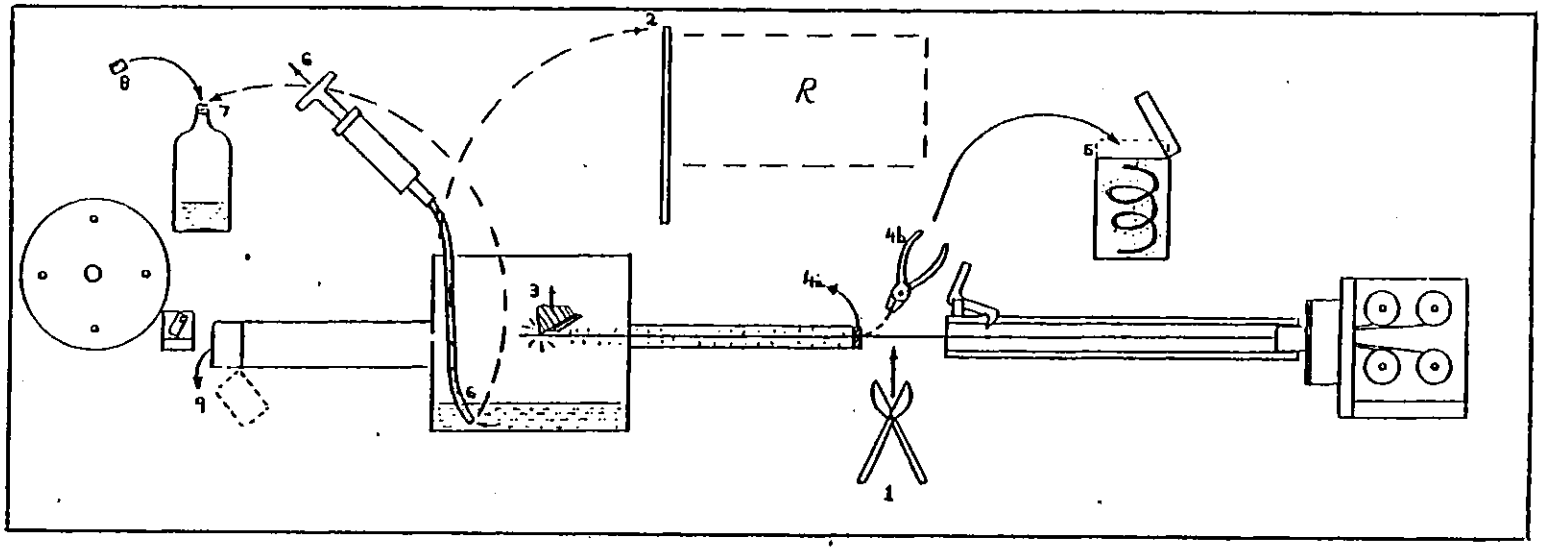

Figure 3.15 Stage 'E' of the test procedure.

Further details of the test-rig procedure such as settings of control devices are given in Appendix 2. The description above summarises the procedure of a typical test.

3.6.4 Visual appearance of the test-rig

To illustrate the test-rig in the form that it was used for the experimental work, eight photographs are presented which are enclosed in Figures 3.16-23 . The subjects of these photographs are listed below.

Figure

3.16 View of the test rig along the direction of movement of the specimen material.

3.17 View with the direction of movement of the specimen material running from left to right across the picture. The Wind-out wheel, start-tube and reaction chamber are visible.

3.18 View along the direction of movement of the specimen material showing the motive power system.

3.19 Oblique view of reaction chamber with assembled scraper present. The direction movement of the specimen material is from right to left.

3.20 Plan view of the reaction chamber with vertical axis normal to the plane of the photograph. Specimen movement from left to right.

3.21 View of the underside of the beam used to mount the scraping tool and wick-feed on the scraper.

3.22 Detail view of the tool and wick-feed.

3.23 View of the supply system for the rinse fluid.

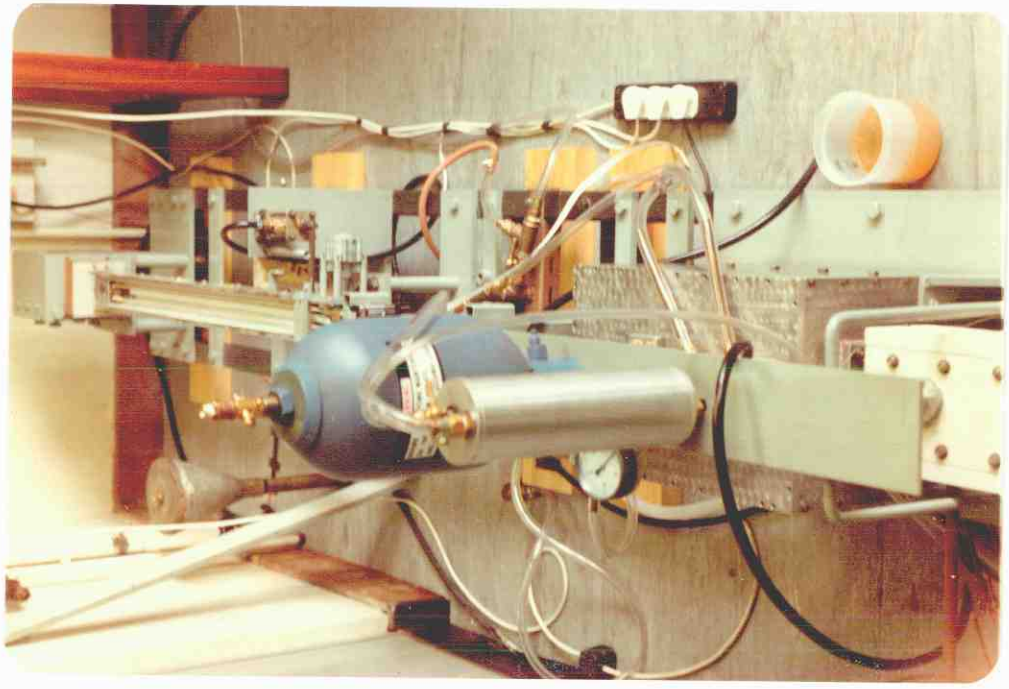

Figure 3.16 View of the test-rig along the direction of the specimen material

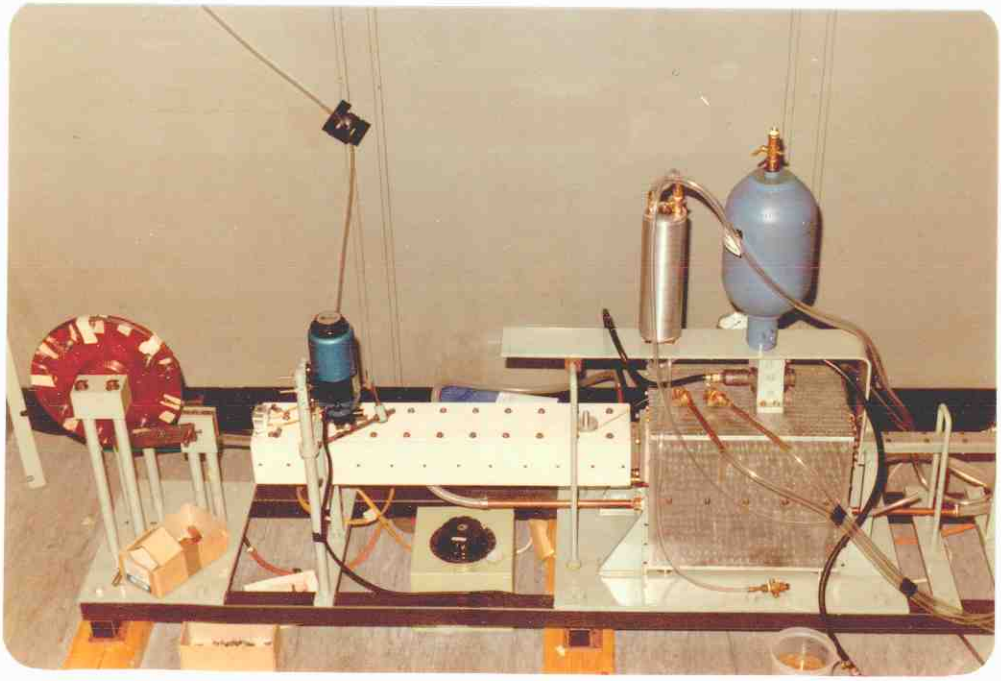

Figure 3.17 View of reaction chamber 'start-tube' and adjacent parts of the test-rig

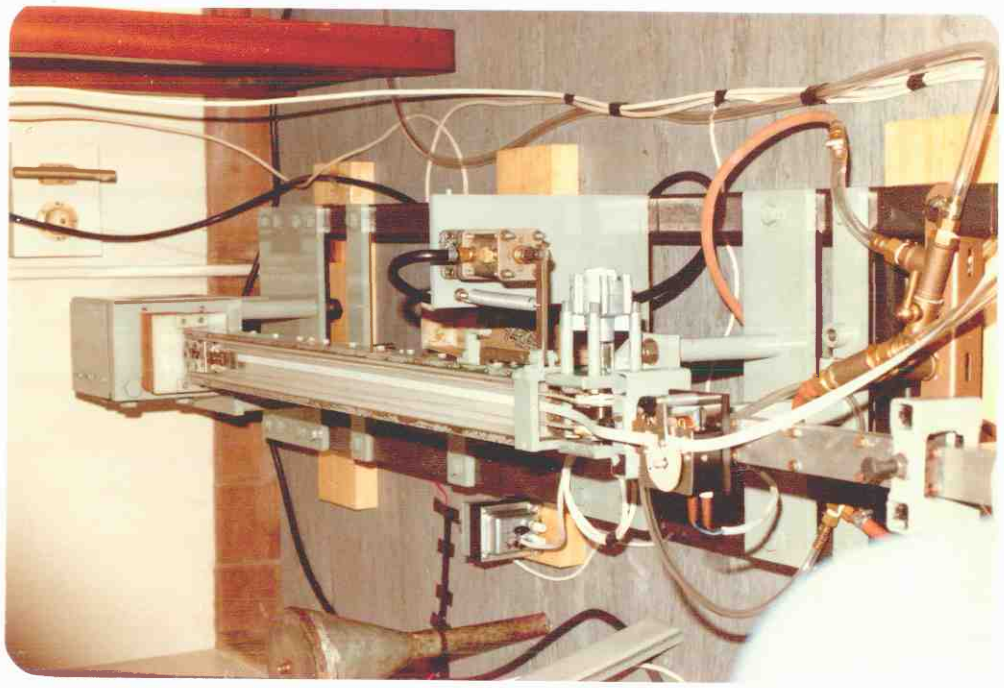

Figure 3.18 View of motive power system to test-rig

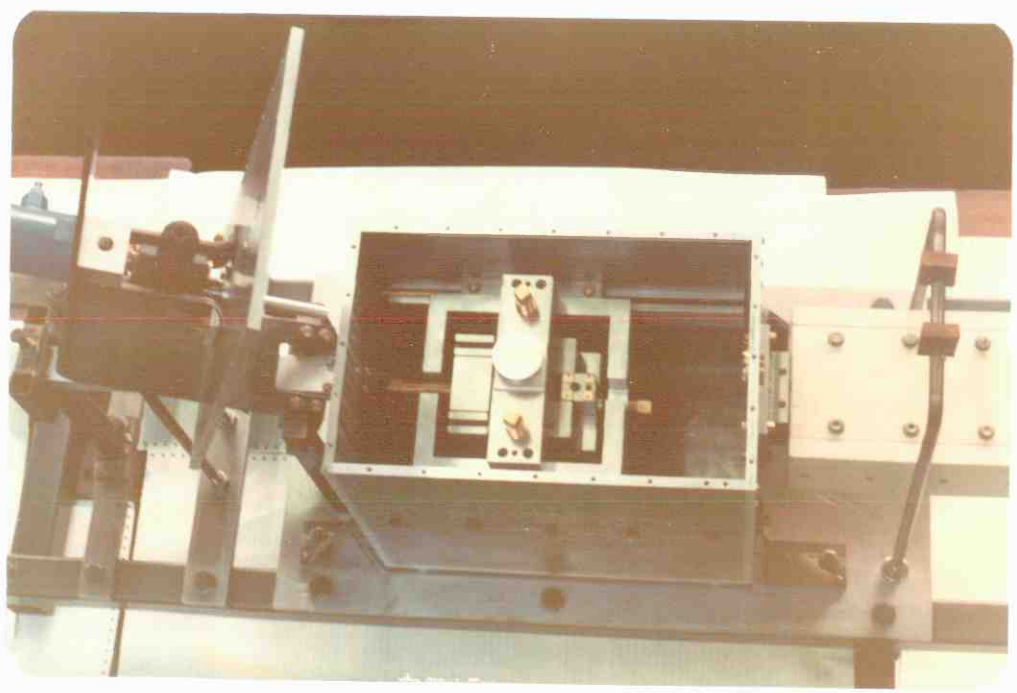

Figure 3.19 Oblique view of the reaction chamber

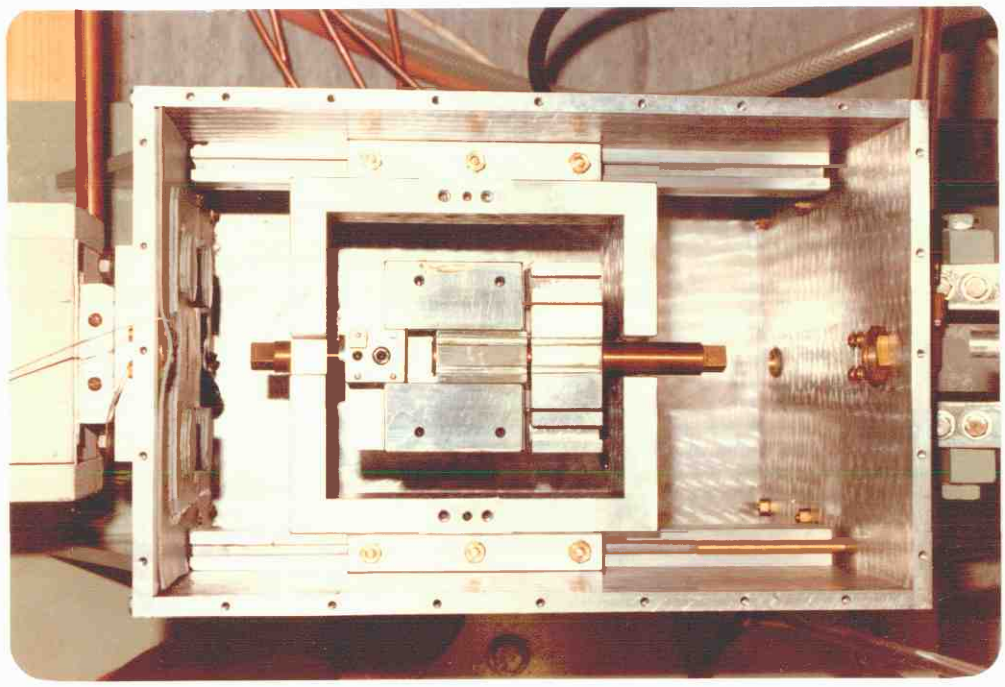

Figure 3.20 Plan view of the reaction chamber

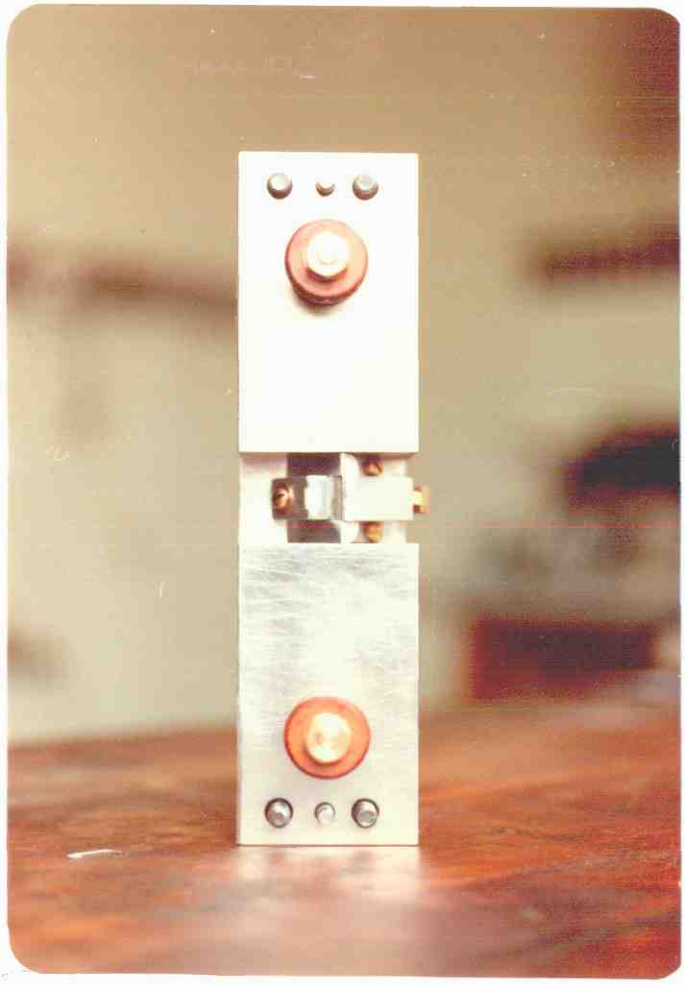

Figure 3.21 View of the 'cross beam'

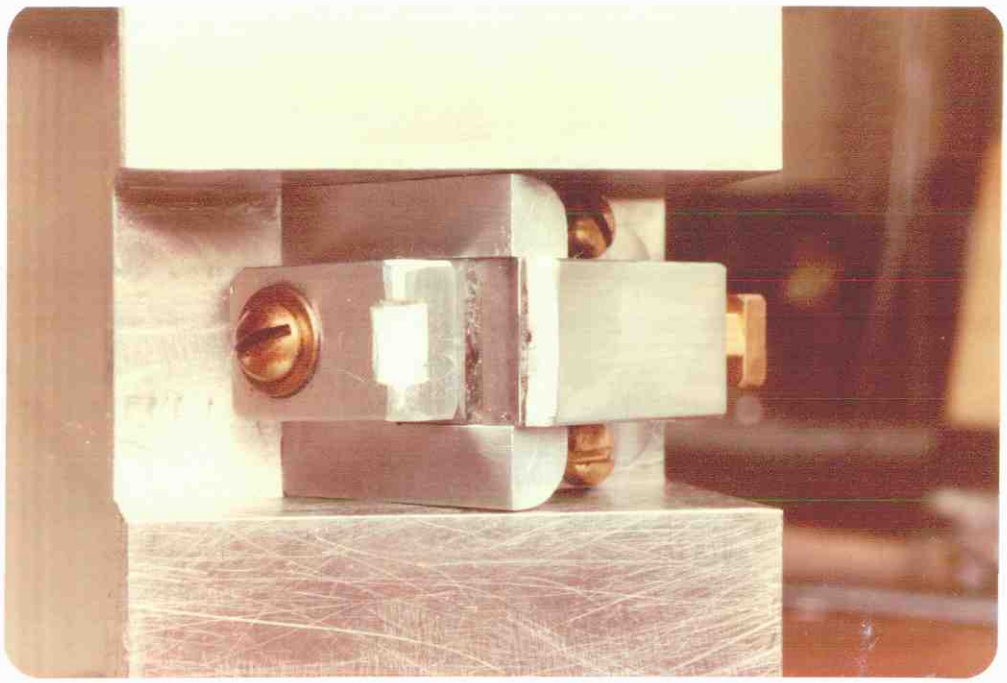

Figure 3.22 Detail of scraping tool and wick-feed

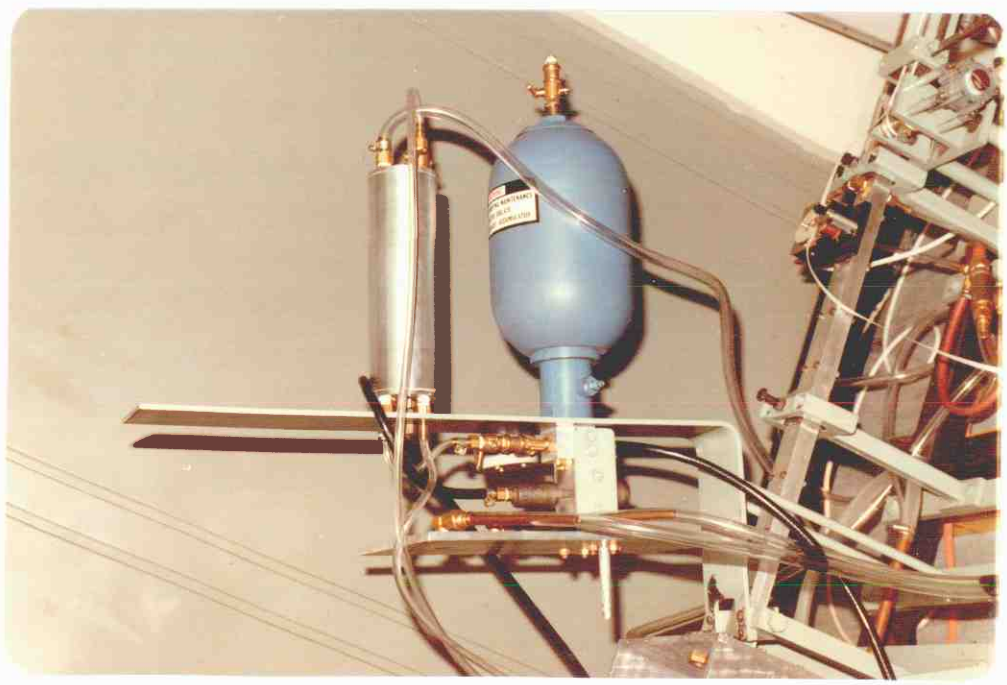

Figure 3.23 View of rinse-fluid system

Illustrated by the photographs but not discussed previously are the following working parts of the test-rig.

(a) A rotary viscous dashpot connected by nylon cables to the constant force springs and mounted close to the trigger (Figure 3.18).

(b) A Ticker-timer which is mounted on the stop-tube close to the trigger. A ticker-tape is passed through the timer and attached to the specimen material (Figure 3.18). A record of the scraping speed is thus obtained from the dots indented on the ticker tape.

(c) A variable transformer to control the power input to the start-tube heater (Figure 3.17).

Not illustrated by the photographs but adjacent to the test-rig is an electro-pneumatic control panel. Closure of the main switch of the panel activates the trigger, rinse-fluid gate-valve, wick-feed motor and ticker-timer. A cylinder of nitrogen is stored next to the control panel to supply blanketing gas and pressurise the hydro-pneumatic accumulator. A sump for waste rinse fluid is built in beneath the reaction chamber.

The overall dimensions of the test-rig are 3.7 m length x 0.4 m width x 1.1 m height.

3.6.5 Further aspects of the test-rig

Two aspects of the test-rig which do not directly relate to discussion of the basic principles and functioning of the test-rig are described in this section.

The length of the test-rig is largely determined by the distance of movement of the specimen material. This unit distance determines the minimum lengths of the start-tube, stop-tube and drive system. Thus the minimum length of the test-rig is three times the unit distance. The unit distance itself is determined by the balance between maximum practicable acceleration of the specimen material and the speed of scraping required for the shortest reaction time to be investigated. In the final design of the testing values of 0.82 m, $\sim$ 60 m/s^2 and $\sim$ 10 m/s were chosen for the unit distance maximum acceleration and top speed respectively.

The rinse fluid supply system shown in Figure is designed to provide a one second pulse of rinse fluid with a stagnation pressure of 2×10^5Pa. The purpose of this is to ensure that for the duration of 'scraping' which lasts about 0.5 seconds, the model lubricant is washed off the surface within 1 to 2 milliseconds on passing under the rinse jet. The 'wash-off time' is designed to be shorter than the minimum reaction time investigated, 3 milliseconds. The model lubricant is deposited on the reaction surface as a thin layer approximately 1 micron thick so as to facilitate a fast 'wash-off'.

The 'start-tube', reaction chamber, scraper, rinse system and 'stop-tube' are made of non-corroding materials such as stainless steel and aluminium or else coated with insoluble varnish. Corrosion of the interior surfaces by the model lubricant and rinse fluid with the attendant risk of depositing contaminants on the scraped surface is thus minimised.

3.7 Assessment of the Experimental Conditions Created by the Scraping Method

3.7.1 Introduction

During the design of the test-rig the 'scraping' method was examined for sources of experimental artefact. After consideration of the factors likely to influence experimental film growth rates four test criteria were devised and applied to the scraping method. These criteria which are listed below categorise the principle questions considered.

1. Quality of the scraped surface.
2. Temperature constancy during test reaction.
3. Access of oxygen and water to the reaction surface.
4. Depletion of the sulphur additive in the model lubricant.

Discussion of these criteria is presented below in respective order.

3.7.2 Quality of the scraped surface

A smooth uniform surface lacking pits, debris and deep grooves is ideal for quantitative surface analysis (145) To check the suitability of the 'scraping' method in this respect, samples of scraped surface were examined by Secondary Electron Microscopy (S.E.M.). Two micrographs obtained by S.E.M. which show a typical scraped surface are enclosed in Figures 3.24 and 3.25 . Figure 3.24 shows a 'plan' view of the surface and Figure 3.25 shows an oblique view of the surface. The observed surfaces consist of shallow grooves with the occasional pit which is believed to be caused by a near-surface inclusion. It was concluded that this kind of

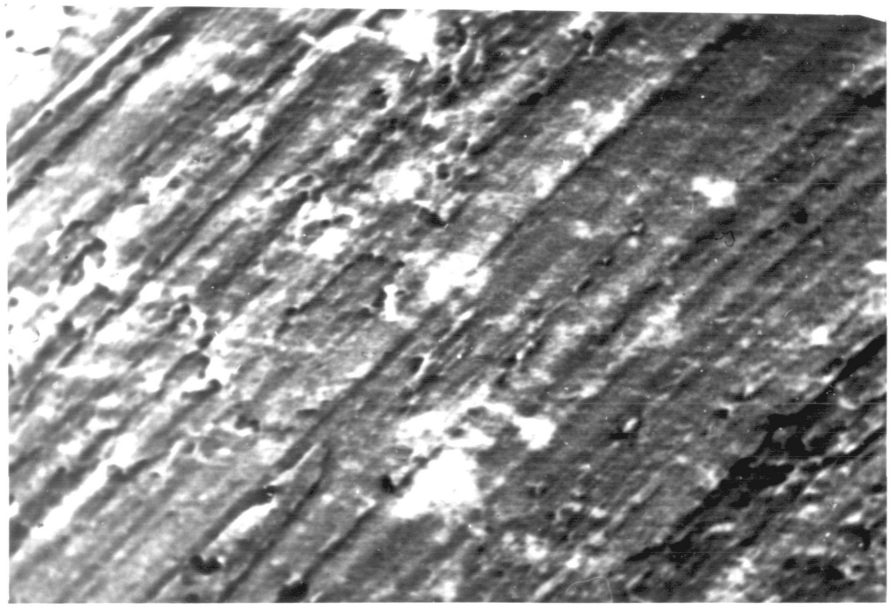

Figure 3.24 Micrograph of scraped surface

10 μm

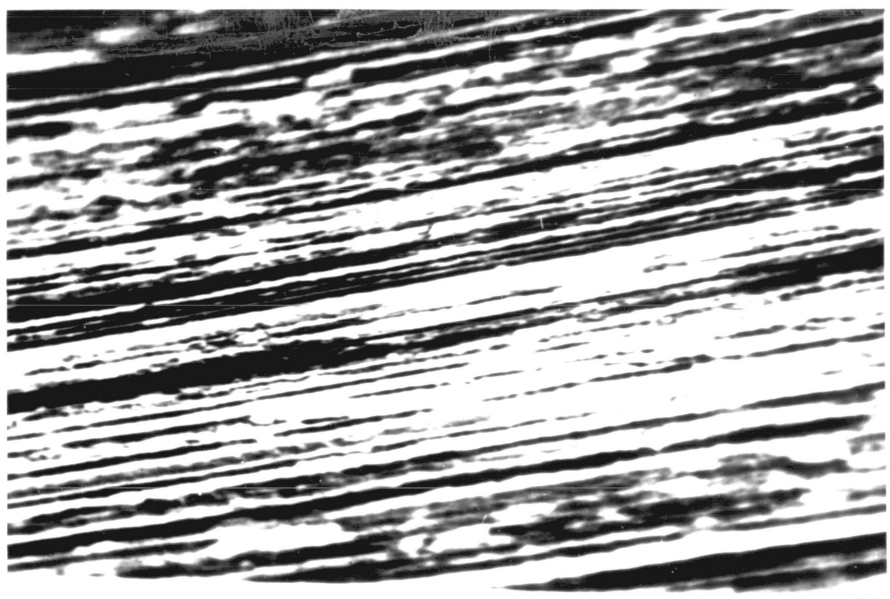

10 μm

Figure 3.25 Micrograph of scraped surface, viewed obliquely

surface was suitable for analysis by for example E.D.A.X. and infra-red spectroscopy.

3.7.3 Temperature constancy

The rate of E.P. film formation is sensitive to temperature since chemical reactions are involved. It was of great importance therefore to estimate the temperature fluctuations caused by the heat dissipated in scraping.

As a preliminary step, Boothroyd's formula (146) was used to calculate tool-tip temperatures. The calculations which are shown in Appendix 1 use experimental measurements of scraping force, scrape depth and scrape width. All other quantities in the formula are physical constants. The results of the calculations do not appear to be valid since temperatures in excess of the melting point of steel are predicted. An experimental measurement of scraping tool temperature was therefore attempted. The experiment involved a dynamic thermocouple consisting of a steel scraping tool and a copper workpiece. Details of the work are presented in Appendix 1
The thermocouple measurements which are approximate suggest a moderate temperature rise of $\sim 150^{o}C$ at the tool tip for copper scraped by steel.

The tool-tip temperatures for steel scraping steel will probably be higher than for steel scraping copper since the energy dissipated in plastic deformation of a steel chip is generally higher than with a copper chip. Tool-tip temperatures are however believed to be much smaller than the values calculated by the Boothroyd formula mentioned above.

A temperature fluctuation of the order of 150°C is however sufficient to alter the experimental film growth rate to an unacceptable extent unless there is a compensating factor. The relative shortness of the distance over which the temperature peak around the scraping tool extends, reduces the duration of the period of raised surface temperature on the scraped material. The temperature peak extends over a distance similar to the scrape depth which ranges from 1 to 5 μm. Thus, within a few millimetres distance from the clearance face of the tool surface temperature of the scraped material should not be significantly different from what it was prior to scraping.

With scraping speeds of few m/s being used in most of the experimental work, a distance of a few mm from the clearance face of the tool corresponds to a reaction time of around 1 millisecond. It was found by experiment that films of significant thickness do not occur in periods of time less than several milliseconds for most conditions investigated. Thus it was concluded that temperature fluctuations caused by scraping were not of direct significance. Figure 3.26 illustrates the points mentioned above and in Appendix 1 the question of raised surface temperature is discussed further.

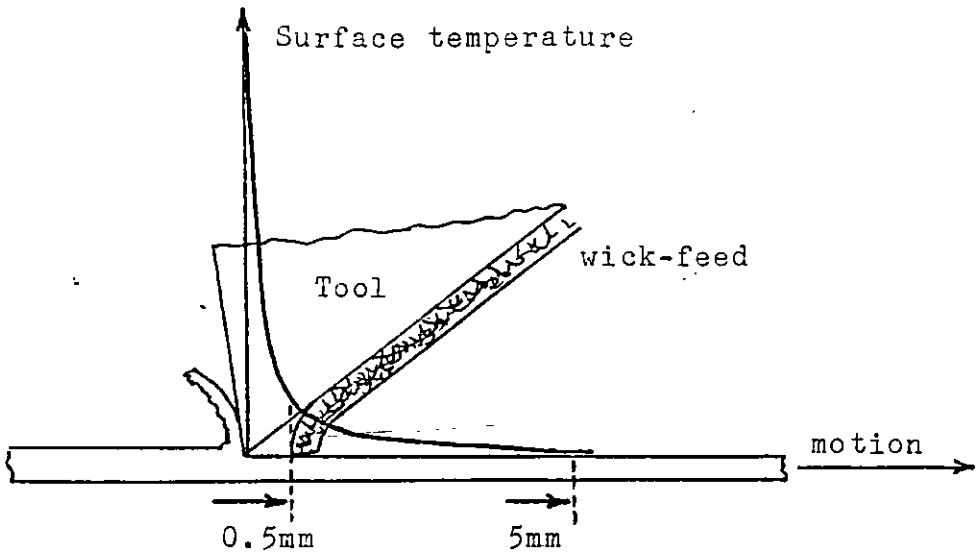

Figure 3.26

3.7.4 Access of oxygen and water to the surface

Water and oxygen are present in the model lubricant as deposited on the reaction surface and in the atmosphere of the reaction chamber. Water was not controlled as it is not believed to have a strong influence on film growth-rates provided a certain minimum humidity is present. Precautions were however taken to restrict the access of oxygen to the reaction surface since, as mentioned above (Chapters 1, 2 and 3), it can prevent the film formation reaction from occurring by oxidation of the reaction surface.

Oxidation of the reaction surface during the experiment is envisaged as taking place in two stages which are:-

1. Oxidation before the model lubricant is deposited by atmospheric oxygen in the gap between wick feed and tool.
2. Oxidation after deposition of the model lubricant by dissolved oxygen.

Oxidation in the 2nd stage constitutes part of the experiment since nascent surface is also subject to attack by oxygen dissolved in oil in a wearing contact. The direct oxidation by atmospheric oxygen in the first stage however has no parallel with the oxidation of surface lubricated by oil and should be limited to the minimum possible. An estimate was therefore made of the amount of oxidation occurring before the model lubricant is deposited.

Figure 3.27 shows the gap between the tool and the wick-feed when the specimen surface is in motion. Experimental observations with transparent models of the tool and wick-feed reveal that the gap is usally about 0.5 mm in length (Figure 3.27).

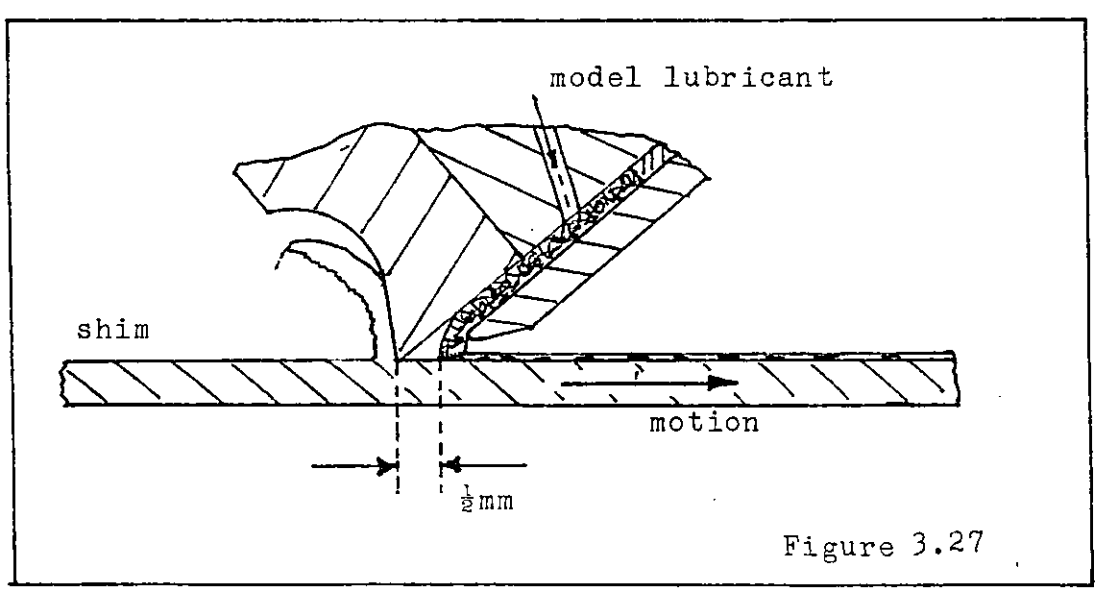

Figure 3.27

A nitrogen rich atmosphere is maintained around the tool and as little as 10 parts per million of oxygen may be present after thorough purging of the reaction chamber containing the tool. Oudar (82) quotes an empirical rule for the time to form one oxide monolayer on clean unoxidised steel surface as a function of oxygen partial pressure which is that 1 monolayer is formed in 1 second at 10^{-4} Pa oxygen, pressure, and that the oxidation rate is proportional to oxygen pressure. Thus, the partial pressure of 10 parts per million of oxygen in nitrogen at atmospheric pressure (i.e. 10^5 Pa) is 10 x 10^{-6} x 10^5 Pa = 1 Pa. The time to deposit one monolayer at 1 Pa is then 10^{-4} Pa/1 Pa x 1 second = 10^{-4} seconds.

The specimen material is designed to move past the scraping tool at speeds up to 10 m/s. The time available for oxidation is then equal to the quotient of wick feed gap length divided by the speed of the scraped specimen. At 10 m/s speed of specimen and 0.5 mm gap length the resultant time is given by the following expression:

$$\text{Time available for oxidation} = \frac{0.5 \text{ mm}}{10 \text{ m/s}} = 5 \times 10^{-5} \text{ seconds}$$

Thus about 0.5 monolayers of oxygen will be adsorbed by the steel prior to deposition of the model lubricant when the specimen material moves at 10 m/s. At lower speeds the contamination by oxygen will be correspondingly greater.

Trent (6) has observed that the oxygen around a tool is rapidly depleted by the nascent surface during the cutting of steel. A 'nitrogen cushion' builds up as cutting progresses

through which oxygen must diffuse. Elementary calculations of oxygen available in the gap between wick-feed and tool show that the 'nitrogen cushion' effect also occurs with scraping. Thus contamination of the nascent surface is expected to be much less than that stated above and so be acceptable for experimental work.

3.7.5 Depletion of the sulphur additive in the model lubricant

One of the main problems involved with 'scraping' method is depletion of the sulphur additive in the deposited layer of model lubricant. The layer of deposited model lubricant is kept very thin, approximately one micron thick, so as to enable prompt removal by rinsing of the model lubricant on completion of the reaction period. Thus only a limited quantity of sulphur additive is available to the reacting surface.

Calculations of the maximum depth of film formed before total depletion of sulphur were carried out for the typical conditions involved. For most of the experimental work a sulphur solution of approximately 1% weight is used. When this solution is present as a micron layer on the reaction surface and the film so formed is iron sulphide, then the calculated film thickness ranges from 50 to 100 Å depending on the density of the solvent. and composition of iron sulphite.

To raise the film thickness limit caused by depletion of dissolved sulphur, thicker layers of model lubricant were used in some of the tests performed where relatively long reaction times were being investigated. A greater thickness of model lubricant is possible at long reaction times

i.e. 40 milliseconds instead of 3 milliseconds, because the acceptable rinse-off time is correspondingly longer.

Depletion of sulphur was considered to be a tolerable limitation of the experimental technique since the sole method discovered of reducing the time to 'freeze' the film forming reaction was to deposit the model lubricant as a thin layer on the reaction surface.

CHAPTER 4

EXPERIMENTAL METHODOLOGY

4.1 Introduction

To obtain data of film growth rates with sulphur E.P. additives an experimental method involving the test-rig described in Chapter 3 was developed and applied. This chapter relates to aspects of experimental method external to the operation of the test-rig. The selection and preparation of experimental materials, the extraction and analysis of sample reacted surfaces, the calibration and collation of data are discussed below.

4.2 Structure of the Experimental Method

The experimental work has been divided into three stages which are described below:

Stage I. Preparation of materials

(a) Specimen steel.

(b) Model lubricants.

(c) Blanketting gas and solvent for rinsing.

Stage II. Execution of a test

(a) Adjustment of test-rig.

(b) Operation of test-rig.

(c) Extraction of samples.

Stage III. Subsequent analysis

(a) Choice of samples for analysis of film produced.

(b) Analysis of chosen samples.

(c) Compilation of test results.

(d) Collation of results of a test programme.

The experimental method is discussed below in an order corresponding to that given above.

4.3 Test Characteristics

4.3.1 Materials

The principle materials used in the experimental work were shim steel as the specimen material, formulation of model lubricant with sulphur and DBDS as the E.P. additives, rinse fluid and blanketting gas (nitrogen). These are discussed below in this order.

4.3.1.1 Specimen steel

A soft, accurately rolled shim was found to be the most suitable material for scraping. 'Roebuck' precision rolled steel shim was obtained from Buck and Hickman Ltd., Sheffield. The shim thickness is specified as 20 thousandths of an inch (0.508 mm) and its width is 4 inches (101.6 mm). The shim is usually available in metre lengths but a 30 m length was obtained for test work.

A chemical analysis of the steel was carried out by the Analytical Services of Imperial College. The results of the analysis are:

Carbon	-	0.05 wt % $\pm$ 0.01%
Sulphur	-	0.017 wt % $\pm$ 0.02%
Silicon	-	$<$ 0.05 wt %
Phosphorous	-	0.017 wt % $\pm$ 0.002%
Manganese	-	0.35 wt % $\pm$ 0.01%

Analysis by E.D.A.X. revealed no significant quantities of other elements.

The grain structure of the steel tested is shown in Figures 4.1, 4.2, 4.3. The plane of etching is parallel to the rolling direction. Sub-millimetre size grains of ferrite showing signs of deformation can be seen. It is evident that the shim consists of a moderately worked ferritic steel.

The shim is merely cut to size for a test and rubbed with tissue to remove the grease preservative. Full details of cutting technique are presented in Appendix 2 (the instructions for use of the rig). No further treatment was considered necessary since the action of scraping produces a clean surface.

4.3.1.2 Model lubricants

Hexadecane which has often been used as a carrier fluid by other workers e.g. Sakurai (117) was chosen for the experimental work. 'Puriss' grade of hexadecane was obtained from Hopkin and Williams Ltd. The level of purity of hexadecane is believed to be critical; Spikes for example (97) devoted much effort to removing trace impurities prior to frictional tests with hexadecane.

A purification procedure described by Spikes (97) was applied in this work even though the hexadecane was odourless and white on arrival from the suppliers which indicates a high degree of purity. Spikes' method is described below.

Spikes' method is begun by mixing the hexadecane with an equal volume of a 50-50 blend of alumina and activated silica. This is then left for one week. On subsequent

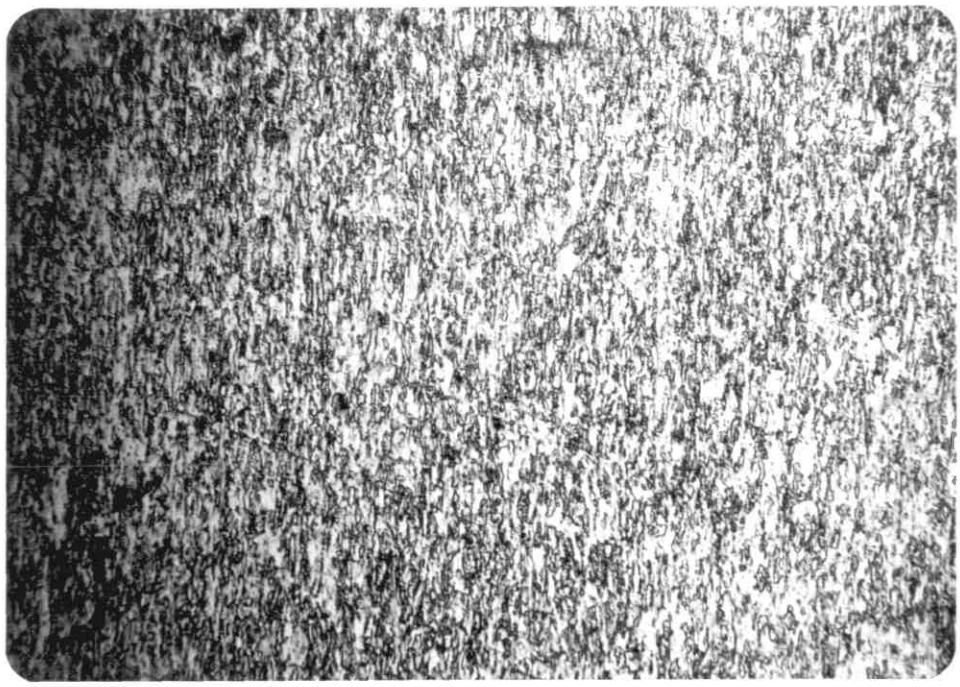

0.1 mm

Figure 4.1 Metallograph of specimen material, low magnification

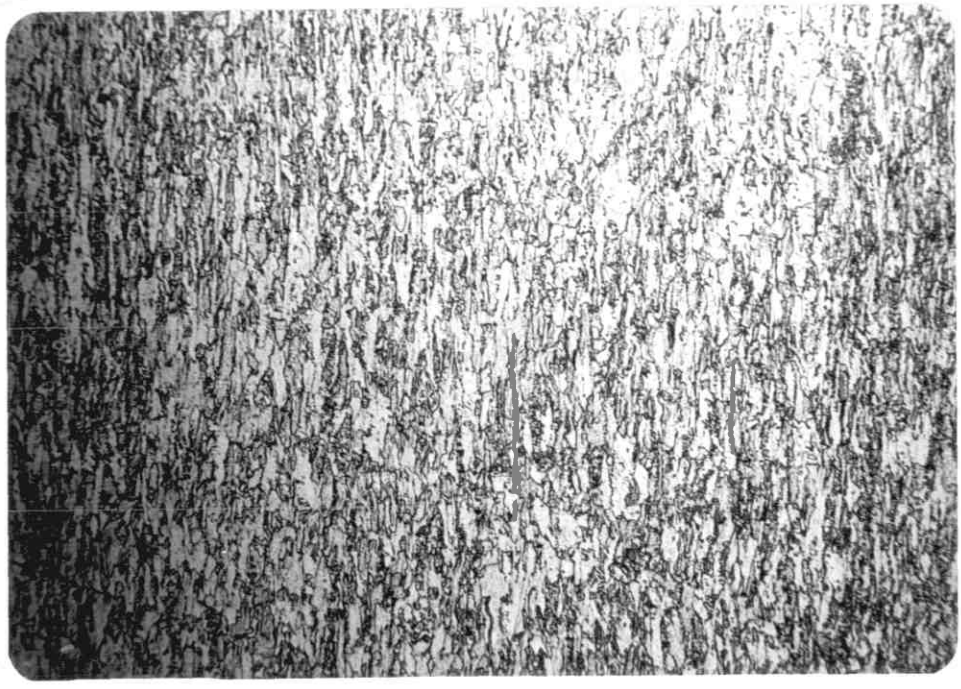

0.1 mm

Figure 4.2 Metallograph of specimen material. Medium magnification

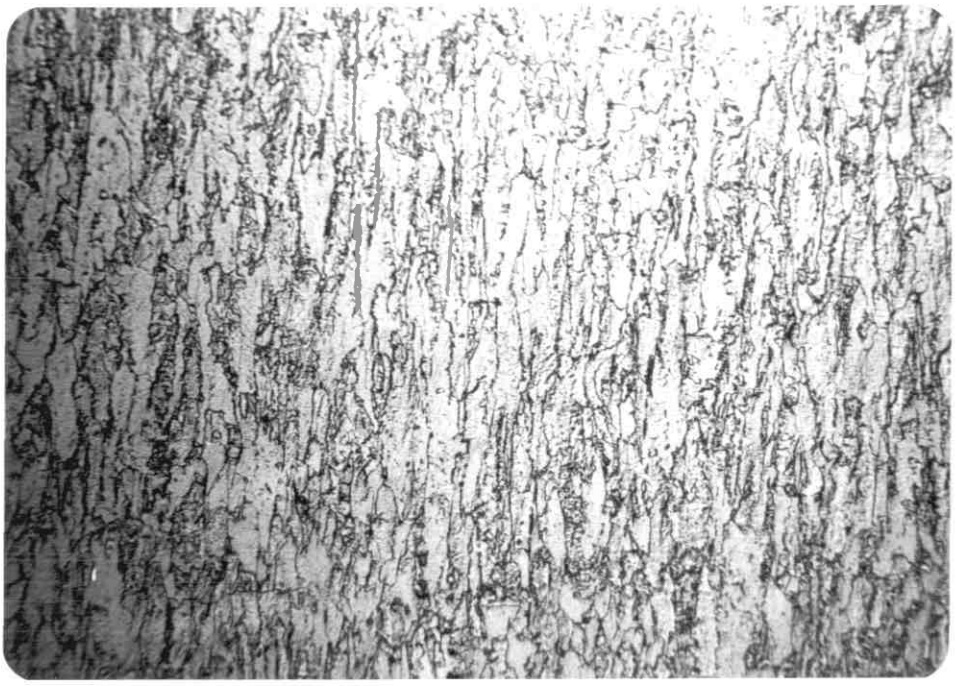

Figure 4.3 Metallograph of specimen material, high magnification

→ 0.1 mm ←

filtration, the traces of oxidation products and contaminants should be removed.

Two sulphur agents were used: elemental sulphur and dibenzyl disulphide (DBDS). British Drug Houses was the suppliers in both cases. The sulphur is described as "Sulphur, Flowers of, General Purpose Reagent". Laboratory Reagent DBDS, recrystallised by a previous member of the Lubrication Laboratory to remove possible impurities prior to friction tests, was used since it was an accessible source of reasonable pure DBDS. Since both substances are only present at concentrations of about 1% in the hexadecane their purity prior to solvation is not so critical as that of the carrier fluid itself. The method of dissolving the two E.P. additives used, sulphur and DBDS and the selection of the appropriate concentration of these additives in the hexadecane is discussed below.

To prepare a solution of sulphur, a measured quantity was dropped into the liquid hexadecane. The mixture was then heated till the sulphur melted and subsequently dissolved. The dissolution of the sulphur was quite rapid and once completed the solution was allowed to cool. Negligible oxidation of the hexadecane was believed to have occurred during this process. Sakurai et al (117) have done extensive work on the film formation rate of sulphur reacting with steel. To facilitate comparison of the results of this work with those of Sakurai et al, an 0.75 wt % concentration of sulphur (used by Sakurai et al) was chosen for this work.

A 2.5 wt % solution of DBDS was made up by the same method, this gives a sulphur equivalent that is close to the elemental solution. These are high concentrations but they are necessitated by the possibility of sulphur depletion in the layer of model lubricant deposited on the reaction surface (Chapter 3).

Both these solutions were super-saturated at room temperature but the solutes remained solved for several hours and thus did not precipitate during the course of the test.

4.3.1.3 Rinse solvent

The choice of solvent is restricted by a fairly stringent set of conditions, these are:

- The solvent must be reasonably cheap and safe since many litres are needed for a test programme and the combustion risk in the rig should be minimised.
- The sulphur concentration in the solvent must be low enough not to influence results. As it was not considered practicable to purify in-house the large quantities of rinse fluid needed for test work, the solvent had to be pure on arrival from the suppliers.
- The boiling range must be high enough to permit wetting by the solvent of the hot reactant surface.
- According to calculations derived from Fluid Mechanics the room temperature viscosity must be around 1 mPas so as to ensure a complete washing off of the model lubricant from the reacted surface.

Following the advice of Esso Petroleum Company, Esso White Spirit '100' was used since it met all the above conditions. The main difficulty in finding an appropriate solvent lay in satisfying both the requirements of high boiling point and low room temperature viscosity: this is discussed below.

Not many low viscosity hydrocarbons will wet a surface of temperature close to 200°C. The boiling range of the white spirit used is 153-195°C. The stagnation pressure rise caused by the impingement of rinse fluid on the moving specimen material is 1 to 2 x 10^5 Pa. This raises the local boiling point by 30 to 50°C. Thus the fluid should wet the hot surface. There is also present intense turbulence which should disrupt the vapour jacket otherwise formed by the solvent on the reaction surface. There may be isolated boiling with associated local vapour jacket, but not complete 'film boiling'.

The specification of the White Spirit is listed below in the form given by Esso Petroleum Co.Ltd.

Initial boiling point	153°C
5% away	163°C
10%	166°C
50%	173°C
90%	185°C
95%	188°C
Final boiling point	195°C
Dry point	193°C
S.G. at 15.6°C (60°F)	0.778

Flash point	40.6°C (105°F)
Aniline Point	57°C
K-B value	35°C
Total aromatics (Vol %)	20
Benzen (Vol.ppm)	< 100
Bromine No.	0.1
Colour (Saybolt)	+ 30
Sulphur (ppm)	2
Comp.evaporation rate	15
Viscosity at 25°C	0.87 mPas
Refractive index at 20°C	1.434

4.3.1.4 Gas blanket

Nitrogen is used to reduce the combustion risk in the reaction chamber and ensure nascency of the scraped metal. British Oxygen Co. 'Oxygen Free Nitrogen' was used, it has an oxygen content of less than 50 ppm.

4.3.2 Execution of test - an outline of

In this section aspects of the test procedure, exclusive of the specific operation of the test rig itself, is discussed. Test-rig operation has been outlined in Chapter 3 and is described, in full in, Appendix 2.

4.3.2.1 Preparative work prior to operation of the test-rig

Having prepared all the materials described in 4.3.1, the scraping tool (supplied by in-house technical services) must be sharpened and set to provide a satisfactory 'scrape'. The method applied for preparing the scraping tool began

with grinding by hand a small relief land on the clearance face. The resultant scraping tool geometry is shown in Figure (4.4).

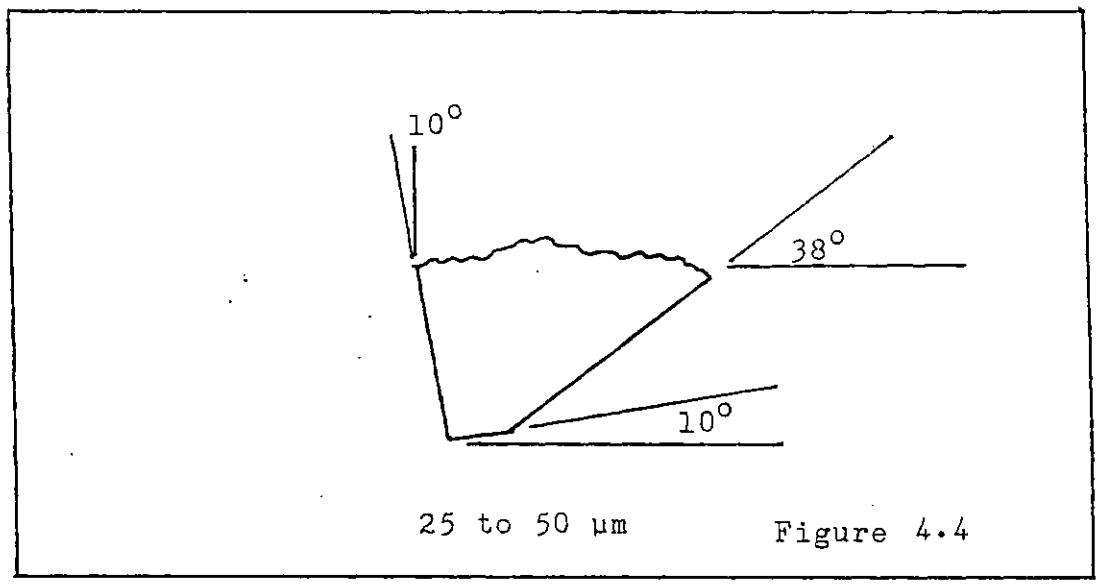

Figure 4.4

The purpose of this is to avoid tool-failure as experienced in the commissioning of the test rig. The grinding of a relief land produces a more robust edge than otherwise and enables the scraping of hot steel in a nitrogen atmosphere. Without the relief land, rapid wear of the scraping edge occurs causing tool seizure and a premature end to the 'scrape'. The method of grinding the relief land is described in full in Appendix 2.

The width of the tool edge (which is the dimension normal to the plane of Fig. (4.4)) is then reduced from 12.6 mm as

supplied by in-house technical services to a dimension ranging from 3 to 5 mm. The scraping edge width is shortened in order to reduce the scraping force to the design level. The scraping edge width is reduced by grinding away the waste to leave a section of edge at the midline of the tool. The tool is then cleaned ultra-sonically and set in the 'cross beam' of the 'scraper' (the 'scraper' as described in 3.6.3.1).

Once the scraping tool is mounted in the 'scraper', preliminary trials of scraping can begin. Trial and error 'scrapes' are carried out using waste specimen material so as to find the correct adjustment for the 'scraper'. During this stage of the work the 'scraper' is removed from the reaction chamber.

On completion of the preparation of the tool and 'scraper' (as described above), the operation of the test-rig according to the procedure discussed in Chapter 3 and Appendix 2 can be carried out.

4.3.3 Procedure at conclusion of the test

When the task of operating the test-rig is completed, the reaction chamber is opened to reveal the specimen material. The specimen material which is illustrated in Figure (4.5) is a length of the shim described in 4.3.1.1 of dimensions 0.508 mm x 15 mm x 22.1 m.

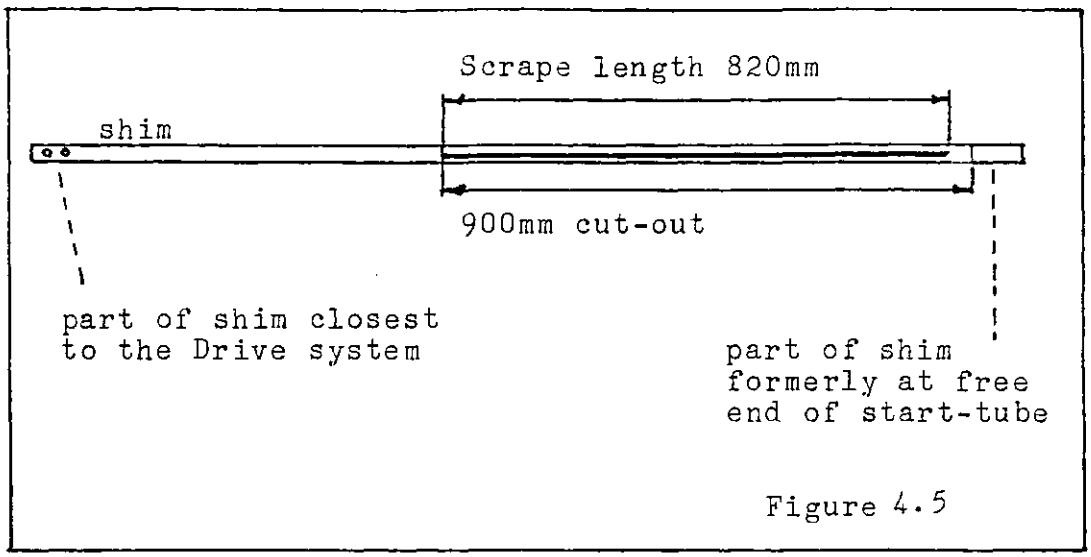

Figure 4.5

A 900 mm long section of the specimen material extending from the start of the scrape (Figure 4.5) is cut away from the remaining material. With the scraped surface still wetted by rinse solvent, the 900 mm section is cut into six lengths of 150 mm which are put into test tubes full of white spirit. The samples are protected against excessive contamination and oxidation by this method.

There is also the tickertape with a record of the speed at which the specimen material moved.

The distances between the dots left on the ticker tape are measured by a ruler and the distance from start of scrape to the dot versus dot-number (which is nominally a multiple of 20 ms) is tabulated.

A graph of the distance-time data is then plotted and the reaction time for the given reaction distance (tool to rinse-barrier distance) is deduced graphically. An example of such a graph is shown in Figure(4.6). A derivative graph of reaction distance versus scrape distance is then plotted out, an example of which is shown in Figure 4.7.

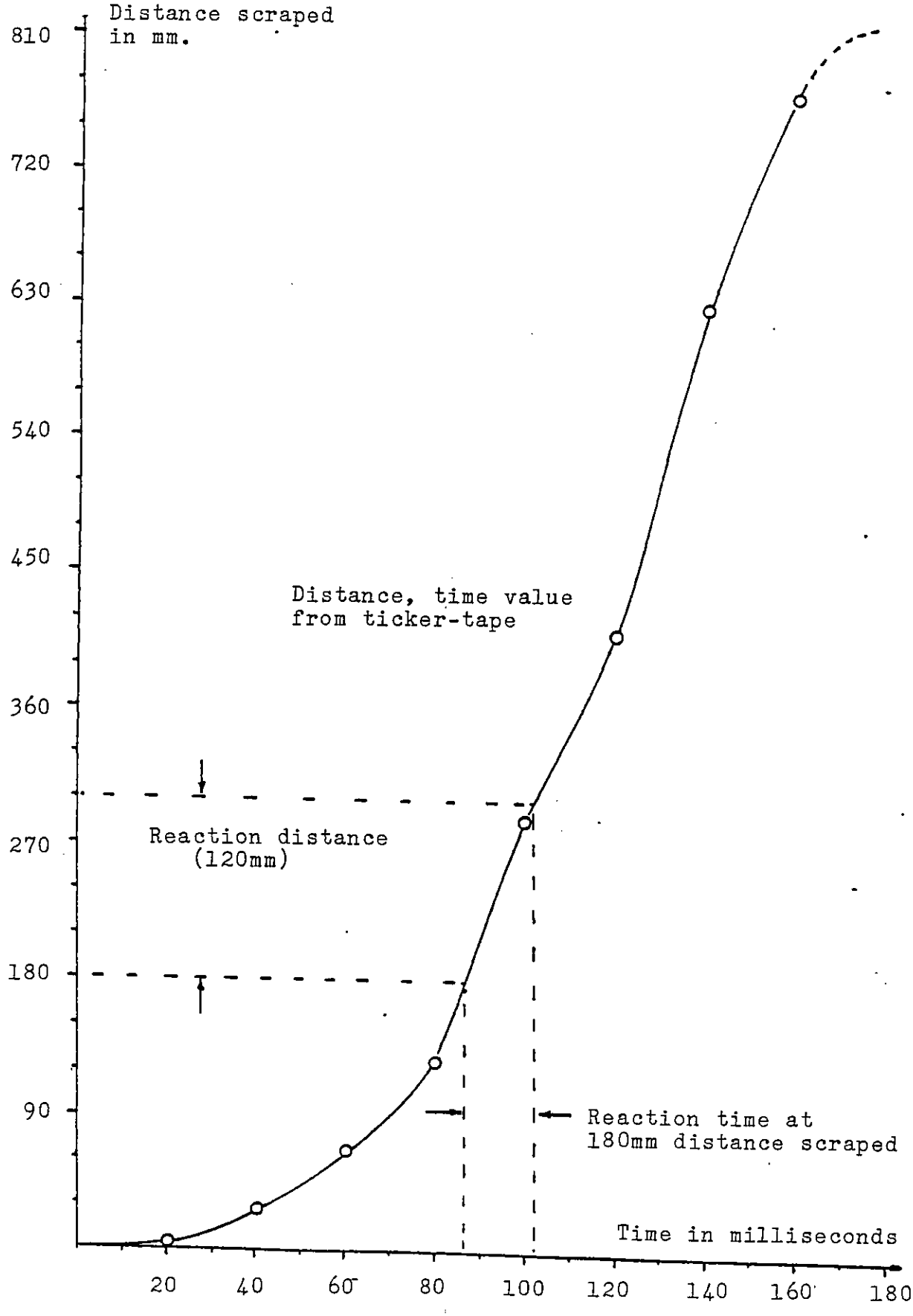

Figure 4.6 Graph of distance scraped versus time

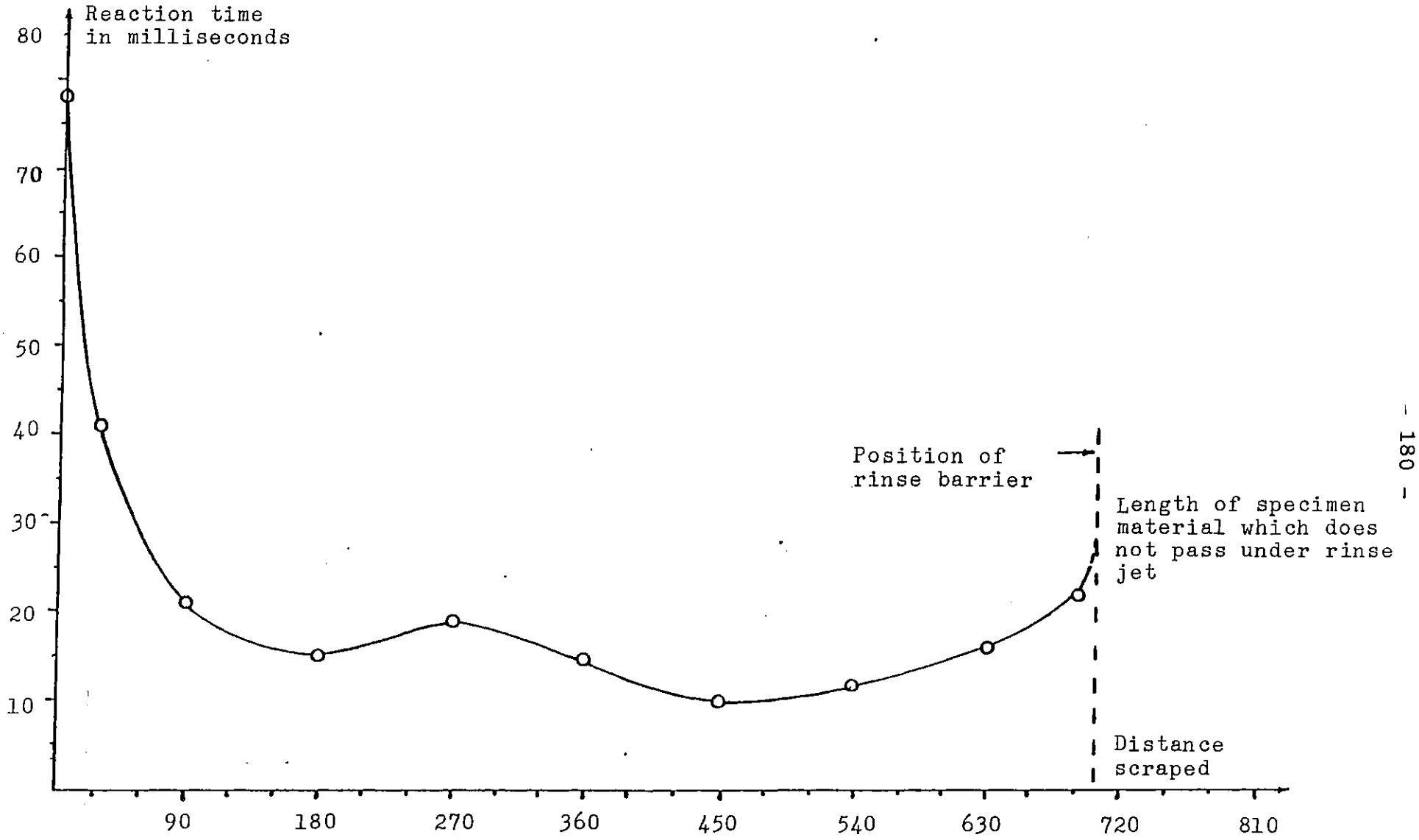

Figure 4.7 Graph of reaction time versus distance scraped

The next step is to extract a representative series of 5 or 6 samples (15 mm long) for E.D.A.X. analysis. These are approximately spaced out over the rinsed length, precise positioning depends on where the scrape is the most consistent over the sample area. It is impossible in practice to achieve a continuous uniform scrape, samples were to be extracted from the surface that is actually scraped. Areas of the surface passed over by the tool edge but not scraped were to be avoided. Imperfections in the specimen material are believed to be the cause of the irregularity in scraping.

Finally, the calibration graphs for temperature are referred to in order to establish the reaction temperature for each sample. The full details of the calibration for temperature are given in Appendix 3. The three test variables which determine the reaction temperature of the sample are heater voltage setting, distance scraped and reaction distance (which affects position of sample relative to heater).

4.4 Surface Analysis of Extracted Samples Tested

Two methods of surface analysis were used: Energy Dispersive X-ray analysis (EDAX) and Infra-Red (I-R). The former method can enable a quantitative analysis of surface sulphur, the latter can give some information on the chemical state of the sulphur present on the surface of the samples. The latter method is discussed in Chapter 5.

4.4.1 E.D.A.X. analysis

The E.D.A.X. technique has been used before in lubrication experiments e.g. by Allum and Forbes (20) or Coy and Quinn (21). The technique itself is described in detail

by Goldstein and Yakowitz (145). The E.D.A.X. measurements which were obtained in conjunction with observation of the surface by scanning electron microscopy involved the use of the following two devices:
A 'JEOL' Ltd. (Japan) JSM-T200 Scanning Electron Microscope with a Link Systems (U.K.) '860' X-ray analyser.

4.4.2 E.D.A.X. system characteristics

Four principal aspects of E.D.A.X. which have a strong influence on the nature and quality of the surface analysis data obtained were examined in order to obtain the best possible data of film growth. These four aspects of the use of E.D.A.X., beam voltage, counting time, area or spot analysis and magnification are discussed below.
I. Beam Voltage. Beam voltage determines the depth of penetration of the scanned surface by the electron beam and the range of elements identifiable. 'Penetration' is proportional to voltage; thus at 25 kV electrons reach as far as 0.5 μm into steel and at 10 kV they only reach 0.1 μm (1,000 Å). The sulphur films produced by the test rig have a thickness around 100 Å, hence 10 kV was used so as to enhance the detectability of the surface film. At higher voltages the sub-surface X-rays overwhelm the surface X-rays.

The disadvantage of voltage reduction is that it reduces the range of elements identifiable. Every element needs a beam voltage at least twice its quantum-energy voltage for it to emit a significant output of characteristic X-rays

Fortunately sulphur is a low atomic weight non-metal so its X-rays are at low electron voltages; 2.3 and 2.46 keV.

Thus a beam voltage of 10 kV is quite adequate. No other elements except iron, which is merely the balance element, were of direct relevance to the experiment.

II. Counting time. A long counting time is needed to reduce the error in signal measurement. A counting time of around 10 minutes was arrived at; counting was stopped when 5,000 counts were present in the channel for the sulphur peak (2.3 keV). This gives a nominal standard error in relative signal of $\sqrt{1/5,000}$ = 1.4%. Goldstein and Yakowitz (145) state that the minimum detectable signal is around three times the nominal error, thus ± 5% is considered as the minimum detectable relative signal (equivalent to 5/100 x 5,000 counts). It was found that this level of 'counts' results in satisfactory accuracy and reasonable counting time. 5% relative signal corresponds to about 10-20 Å of 'sulphide' film.

III. Magnification and coverage of sample area. A high magnification was needed (5,000 X) to detect the small flaws in the scraped surface. These flaws were avoided since they usually contained a manganese sulphide inclusion which would give a sulphur signal independent of the surface film. The roughness of the flaw would also influence the magnitude of the signal received.

High magnficiation does reduce surface area analysed, in this case to 200 μm x 200 μm. Thus one needs several analyses from different parts of the sample investigated in order to obtain a representative value of surface sulphur.

IV. Comparison of spot analysis and area analysis. If one suppresses the raster and fixes the electron beam on a

specified point a 'spot analysis' on some point of the surface in view (with a roster) is obtained. When the area analysis gives a significant sulphur signal then a 'spot analysis' can be applied to check whether the sulphur is due to an un-noticed inclusion or due to a surface film. (Figure 4.8)

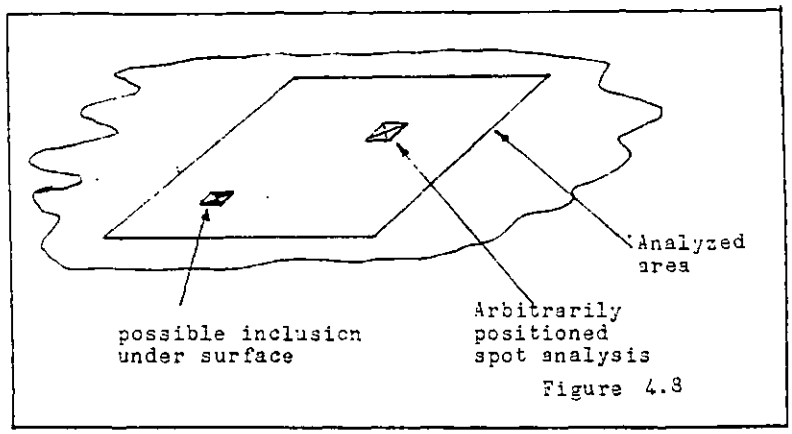

Figure 4.8

Because both the inclusion and the spot are small in size and area compared to the scanned surface, the probability of co-positioning is very low. (Figure 4.8)

When performing several area analyses on one sample it was found that if the majority of the spot analyses were 'similar' to the corresponding area analyses then the sulphur was due to a film and not a series of inclusions. 'Similarity' in signal was taken to be a difference in signal magnitude of less than 25%. The sub-surface sulphur present in the steel but not bound in inclusions was not found to generate a significant sulphur signal (i.e. greater than 5%).

4.4.3 E.D.A.X. Measurements - experimental procedure

The final specifications of the analysis procedure used in the experimental work are described below. The specifications have been divided into six subsections for the purposes of the discussion.

I. Setting of Scanning Electron Microscope.

10 kV beam voltage, 30 degrees specimen inclination

5,000 magnification.

Spot size, only restricted by stability of electron beam.

II. Analyser.

31 mm detector distance

1200 to 1800 counts per second typical

Count to 5,000-5,020 counts at 2.30 keV.

III. Usual Number of Area Analyses. (Figure 4.9)

4 (sometimes 3 or 5 areas) analysed

Positioning: datum area at one end of the specimen

2nd area 0.25 mm away axially

3rd area 2 mm away from the 2nd

4th area 5 mm away from the 3rd

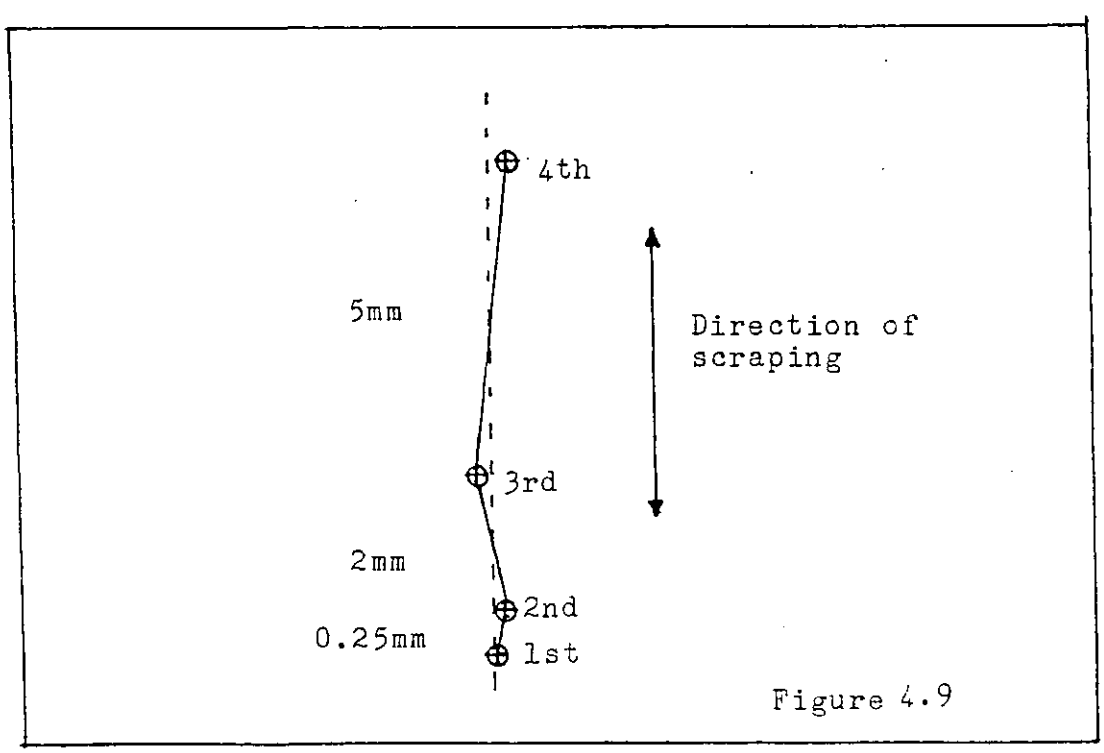

Figure 4.9

IV. Choice of surface to be analysed.

The best surface is smooth but shallow grooves and small pits were tolerated (i.e. sub-micron size pits).

V. Definition of signal.

The X-ray energy levels used to illustrate signal are shown in Figure 4.10.

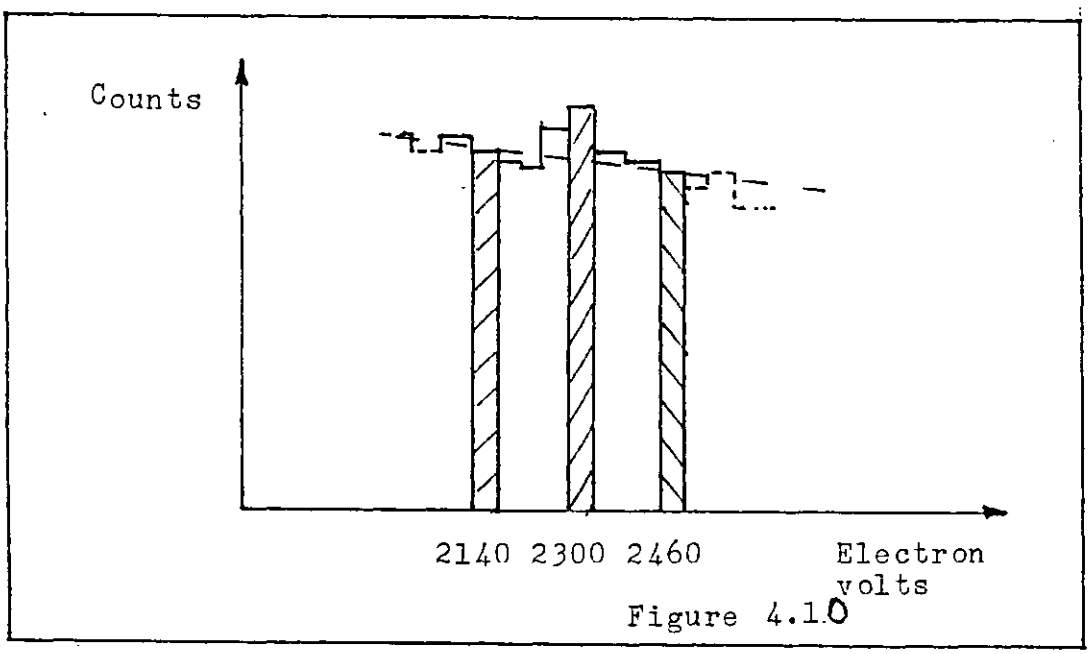

Figure 4.10

The following relation is used to define signal.

$$\text{Signal} = 100\% \times \frac{C_{2300} - C_{av}}{C_{av}}$$

where $C_{av} = (C_{2140} + C_{2460})/2$

$C_{2300}, C_{2140}, C_{2460}, C_{av}$ = counts for 2300 eV, 2140 eV, 2460 eV and average respectively.

VI. Additional spot analysis.

All signals greater than 10% were confirmed by subsequent spot analysis.

EDAX plots for a 'strong' and a 'borderline' signal are shown in Figures 4.11, 4.12.

Additional details about the method used.

All samples were cleaned ultra-sonically in pure acetone before analysis by EDAX. A purpose-built specimen holder was used to mount the specimens.

4.4.4 Gravimetric calibration of EDAX signals

The EDAX only gives a signal proportional to surface sulphur, to derive absolute values of surface sulphur external calibration is required.

A gravimetric method was used based on the weight increase when iron reacts to form iron sulphide.

A 1% wt solution of sulphur in hexadecane,(prepared in the manner described in 4.3.2)and 25 micron steel foil were the materials used. Two 10 cm x 10 cm squares of foil were prepared. These were ultra-sonically cleaned and weighed (approx. weight 2 grammes). They were then cut into 2 cm x 10 cm strips and re-weighed, negligible weight change resulted.

Sulphidation took place within a test-tube immersed in a thermostatic bath. Oxygen-free nitrogen was used to displace the oxygen in the hexadecane, and the test-tube neck was filled with glass-wool to reduce evaporation and ingress

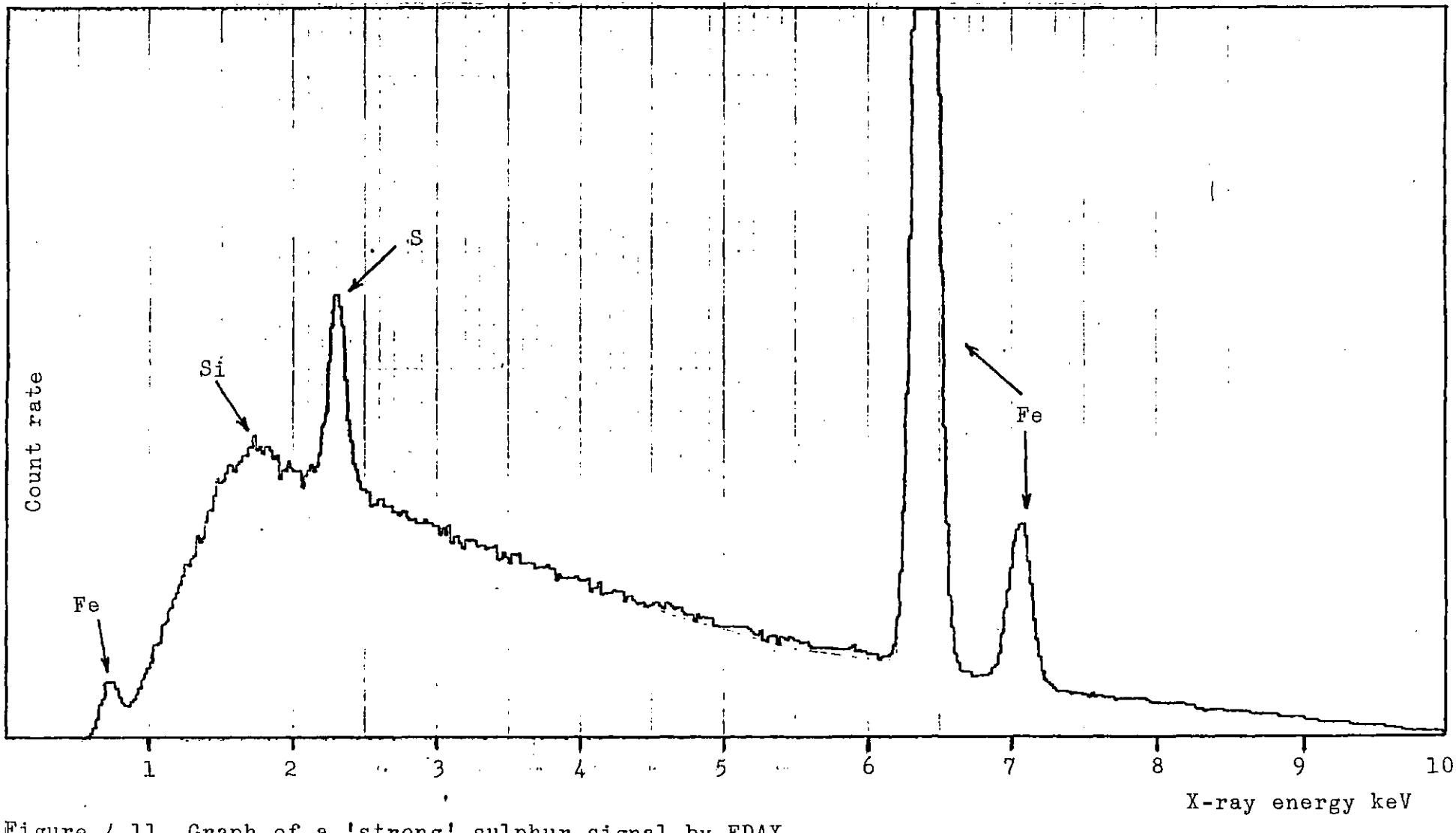

Figure 4.11 Graph of a 'strong' sulphur signal by EDAX

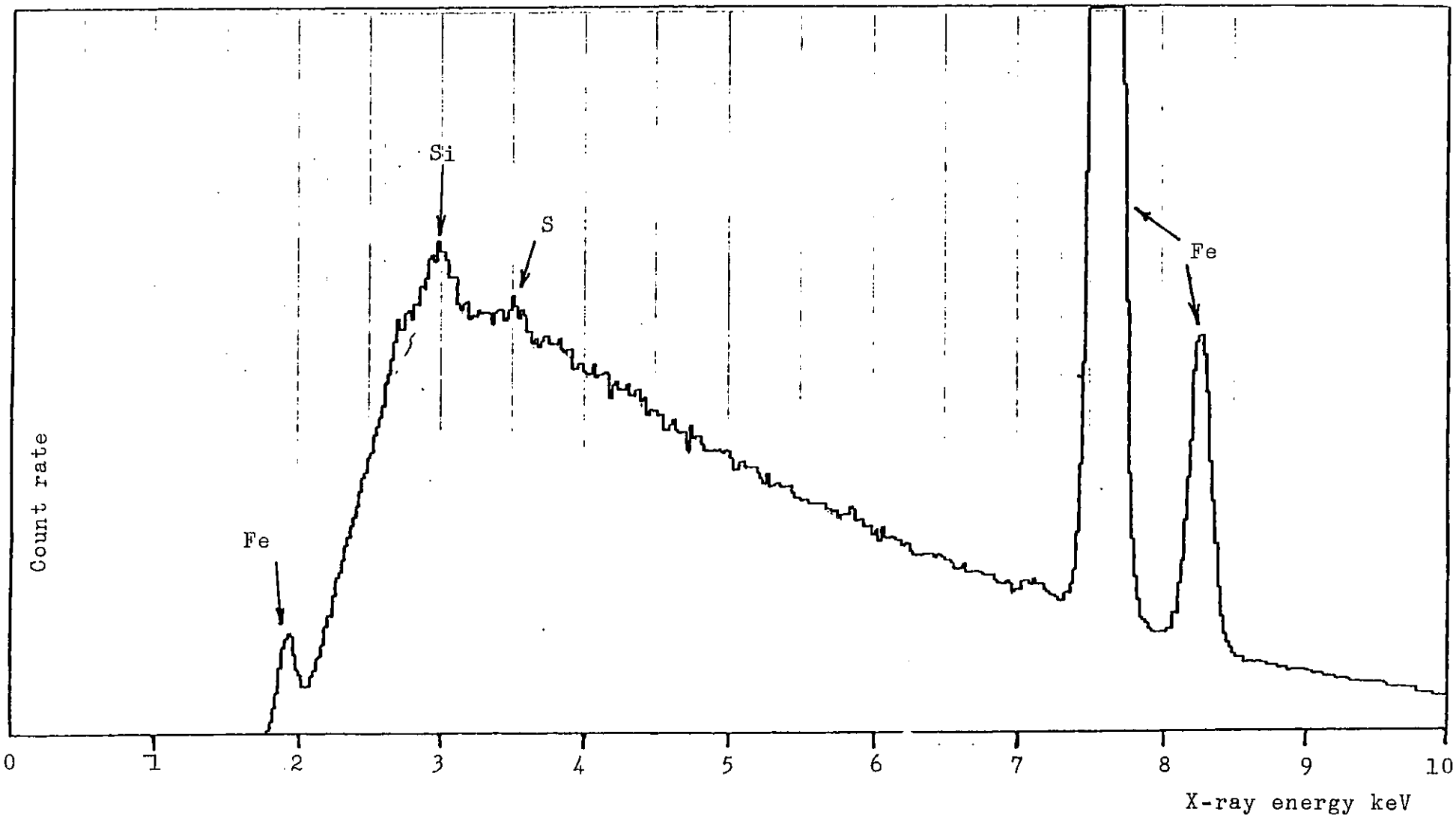

Figure 4.12 Graph of a 'border line' sulphur signal by EDAX

of air. The bath was set at 200°C to ensure speedy reaction despite the ensueing rapid evaporation of hexadecane which necessitated replenishment of the fluid during the test. Figure 4.13 shows the experimental arrangement.

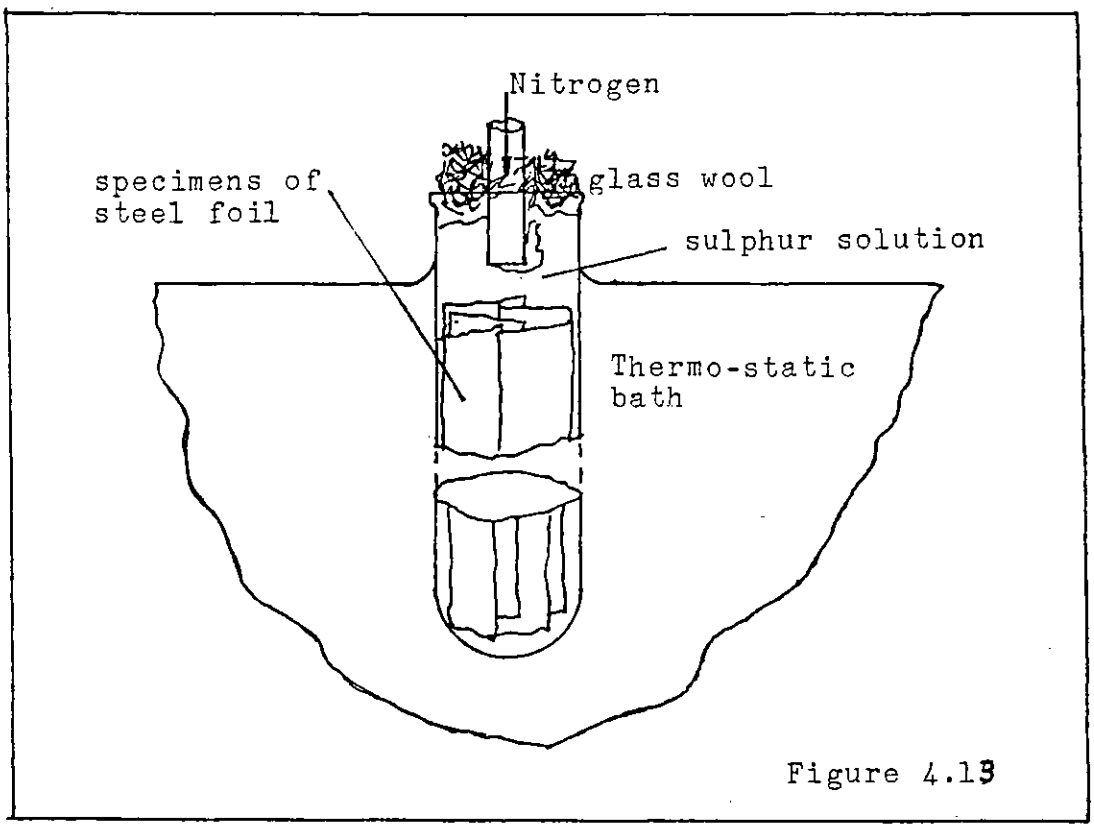

Figure 4.13

The reaction time to produce a useful thickness was estimated from the literature data discussed in 2.2. The foil was placed in the bath which was then brought to the set temperature. On completion of the set time the foil was removed, cleaned and weighed. Later the foil was cut into 15 mm x 20 mm strips for EDAX analysis. Since it was impracticable to analyse all these small squares of foil, four out of the total were randomly chosen. Each square was then analysed by the same procedure as for the scraped samples. Two tests were performed, the results of which are shown in Table 4.1.

TABLE 4.1

WEIGHT GAIN DATA

Test 'A' (i.e. 100 cm^2)	Original weight of the specimen	2.0794 ± 0.003 g
	Reacted weight	2.0820 ± 0.002 g
	Weight gain	+ 0.0026 ± 0.004 g
Test 'B'	Original weight of the specimen	2.0835 ± 0.0003 g
	Reacted weight	2.0804 ± 0.0003 g
	Weight gain	0.0069 ± 0.0005 g

Weight gains per unit area. 200 cm^2 reaction area in each case (reaction on both sides of the foil).

Test A Weight gain per unit area $= \frac{2.6 \times 10^{-3} \text{ g}}{200 \text{ cm}^2}$

$= 1.3 \times 10^{-4} \text{ kg/m}^2$

Test B Weight gain per unit area $= \frac{6.9 \times 10^{-3} \text{ g}}{200 \text{ cm}^2}$

Estimation of sulphide film thicknesses. On the evidence from the corrosion literature (Chapter 2) it is assumed that the reaction product is largely FeS. The calculation presented in Table 4.2 to derive the calibration

constant of film thickness are based on this assumption.

TABLE 4.2

CALCULATION OF SULPHIDE FILM THICKNESS

FOR A UNIT WEIGHT GAIN

Atomic weight of iron (to the nearest mass unit) --- 56

Atomic weight of sulphure --- 32

Ratio of FeS produced to sulphur uptake = $\frac{56 + 32}{32}$

Density of FeS 4.8×10^3 kg/m^3

Film thickness corresponding to a film of L kg/m^2 =

$$(\frac{88}{32} \times /4.8 \times 10^3)\ m = (5.7 \times 10^{-4} \times L)\ m$$

Film thickness for 10^{-4} kg/m^2 weight gain = 5.2×10^{-8} m

= 570 Å

The next stage is the calculation of the constant of proportionality between film thickness and E.D.A.X. signal was to find the average signal of the individual analyses performed in each test.

The E.D.A.X. results and averages are shown in Table 4.3 Figure 4.14 is also enclosed to show a typical E.D.A.X. signal observed during the analysis of the gravimetric specimens.

The gradient of the graph in Figure 4.15 represents the ratio of E.D.A.X. signal to film thickness (or weight gain) and its value is given in the expression below where 'k' denotes the proportionality constant.

$$k = \frac{3.11 \text{ units of signal}}{1.3 \times 570 \text{ Å}} = 0.00435 \text{ Å}^{-1} \qquad (4.1)$$

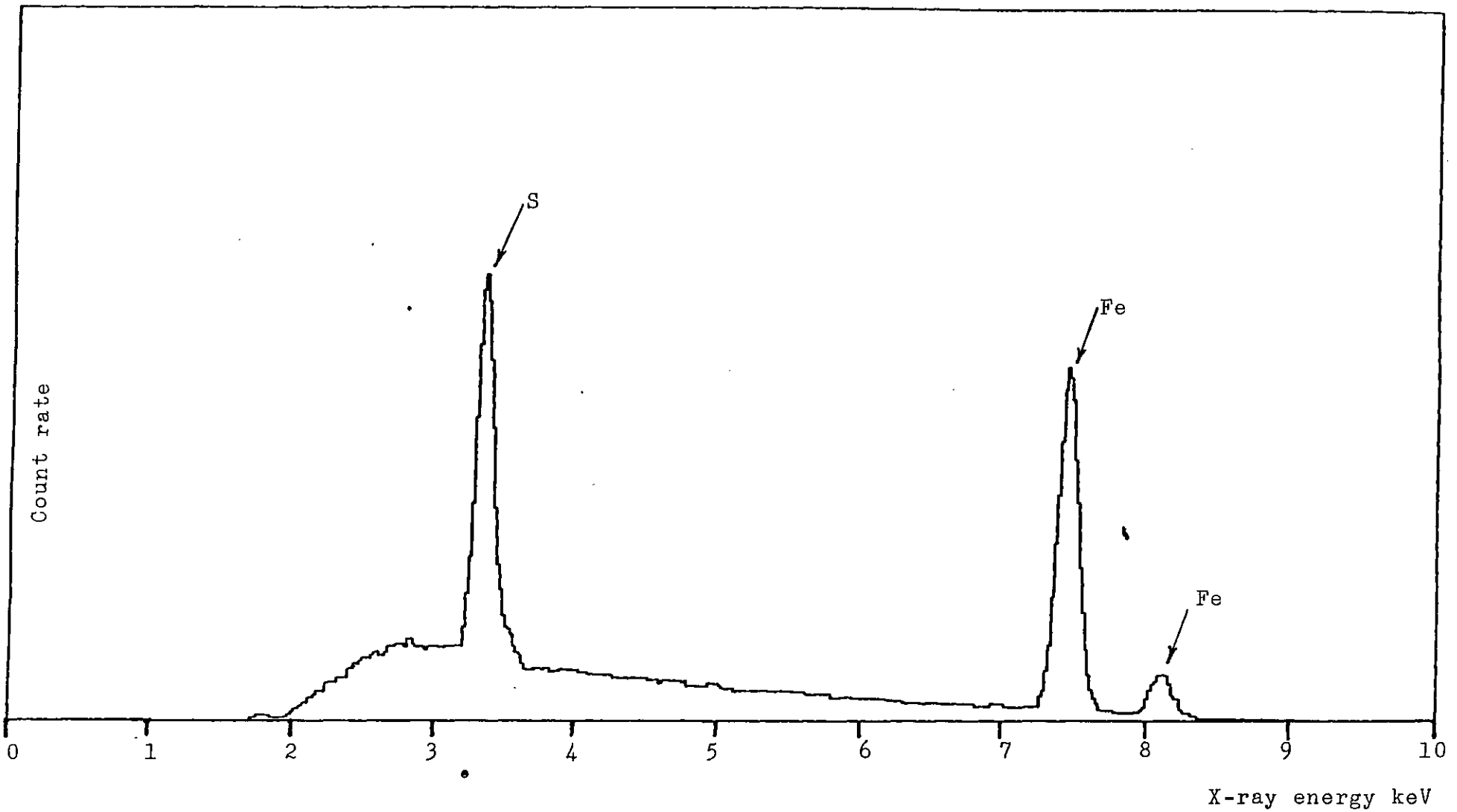

Figure 4.14 Graph of typical EDAX sulphur signal obtained during gravimetric calibration

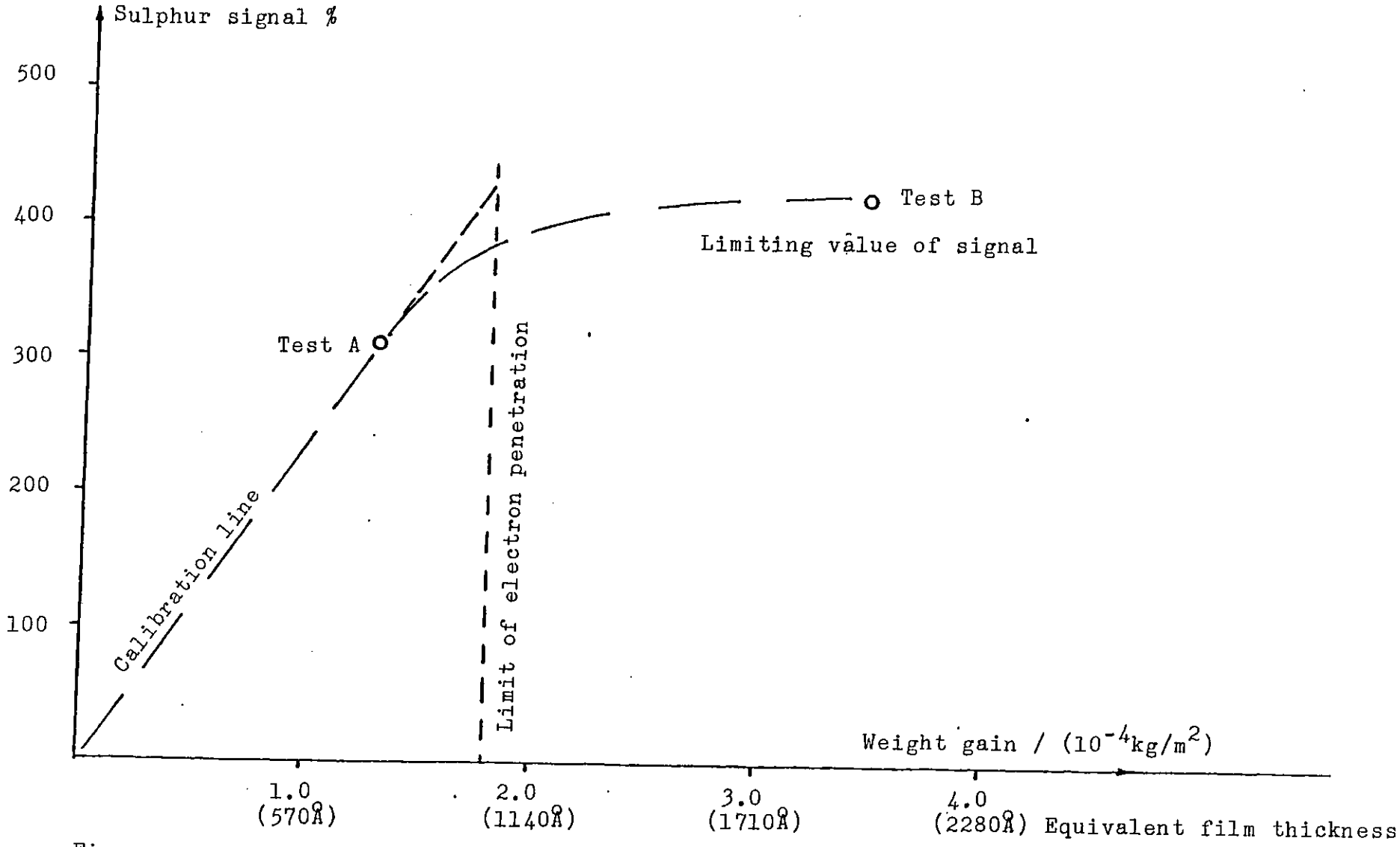

Figure 4.15 Sulphur signal by EDAX versus specific weight gain of specimen

TABLE 4.3

E.D.A.X. DATA FROM GRAVIMETRIC SPECIMENS

Test A

1st Sample	2nd Sample	3rd Sample	4th Sample	
3.4790	3.2561	3.3893	3.1983	
3.6120	3.3164	3.2872	3.2161	
3.1397	3.0764	3.2275	0.5112	
3.3046	2.9958	3.2647	3.4577	
3.3838	3.1612	3.2922	2.5958	Averages
Grand average 3.1083				

Test B

1st Sample	2nd Sample	3rd Sample	4th Sample	
5.3092	4.6933	3.35343	3.1874	
5.2677	4.6652	4.4338	3.0608	
4.6230	4.4034	2.4480	3.0514	
5.2774	4.6973	5.0048	3.6863	
5.1193	4.6148	3.8552	3.2465	Averages
Grand average 4.2090				

A more useful quantity is $\frac{100}{k}$ or the depth of film corresponding to 1% 'signal'. The value of this quantity is given below:

$$\frac{100}{k} = \frac{100}{0.00435\ \text{Å}^{-1}} = 2.3\ \text{Å} \text{ (per 1\% signal)}$$

4.5 Presentation of Results

From each sample of the scraped surface analysed by E.D.A.X. a series of signal values for a given combination of reaction time and temperature is obtained; this form of results is illustrated in Figure 4.16.

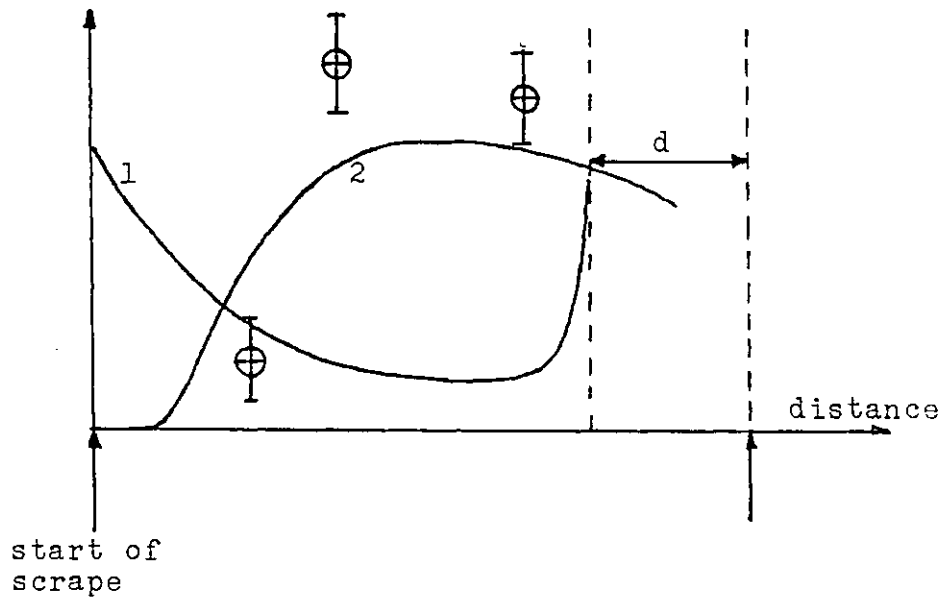

d = distance between scraping tool and rinse barrier

⊕ = Average value of analysed signals plus scatter bar

1 ~ Reaction time

2 ~ Reaction temperature

Figure 4.16

Reaction time (Figure 4.16) slowly declines from a high start value till the part of the specimen material that did not pass under the rinse-barrier is reached. There is the characteristic 'hump' (Figure 4.16) for reaction temperature as the section of the specimen material that lay over the heater is scraped. There is usually a large scatter in the signal values so it is only possible to discern general tendency for the signal to be proportional to temperature.

To obtain a general relationship for sulphur agent reactivity versus time it is necessary to collate the results of many tests under varying conditions e.g. a 'hot' test with short reaction time and 'cold' test with long reaction time. Working on the assumption that the signal is merely a function of temperature, time and random factors, the results of a series of tests are plotted on a three dimensional graph of reaction time, reaction temperature and signal (Figure 4.17).

A step-wise multiple regression was also applied in order to eliminate statistically insignificant variables from a group of possible controlling variables. This group was extended to include not only reaction time and temperature, but also 'artefact variable' such as distance scraped and time from start of scrape. Equations for E.D.A.X. signal as a function of controlling variables were also derived by this process.

4.6 Experimental Errors

The data is comprised of the values of four independent parameters and one dependent parameter, E.D.A.X., signal. The four independent parameters are the reaction time and

temperature mentioned above and two other parameters chosen as indicators of experimental artefact. These latter two parameters are distance scraped at location of sample and time from start of scrape. The errors on these parameters are discussed below in an order corresponding to that stated above.

4.6.1 Reaction temperature

The experimental error of reaction temperature is generally estimated at $\pm$ 3°C (discussed further in Appendix 3 except on parts of the specimen material where the surface temperature varies steeply with distance, the error is then $\pm$ 5°C.

4.6.2 Reaction time

The error in the reaction time largely lies in time needed to rinse off the model lubricant or otherwise stop the film forming reaction. However, for the purpose of making an initial comparison of results, the rinse-off time which was assumed to be a constant was neglected as a cause of error. Errors in the measurement of scraping speed (by ticker-tape) give an uncertainty in measured nominal rinse distance of $\pm$ 1 millisecond.

4.6.3 Distance scraped

The distance scraped is an average value for the sample analysed as it was not practicable to isolate a specific value of scrape distance for each area analysis on the sample. Other causes of uncertainty in the measurement one believed negligible so the error in the distance scraped is

approximately one half of the length of the sample (15 mm) and is therefore estimated as ± 7.5 mm.

4.6.4 Time from start of scrape

As with the distance scraped this is an average value for the sample analysed. With a scraping speed ranging from 2 m/s to 10 m/s, the maximum error in a 15 mm sample is ± 4 milliseconds.

4.6.5 Value of E.D.A.X. signal

With the uncertainties involved in analysis by E.D.A.X. an appreciable error is to be expected. Based on the scatter in the results the following estimate of error was drawn up. Error in the signal is of the order of one tenth of the value of the signal, or ± 3% of percentage signal, whichever is the least. Thus for a 50% measured value of signal, the 'time' value of signal is estimated as lying between 45 and 55%. For a 10% signal however, the time value should lie between 7 and 13%.

4.6.6 Importance of error, consideration of

The scatter in the results is much greater than would be expected were measurement error the sole cause. Thus imperfections of measurement are not considered to be as serious a problem as the difficulties caused by incomplete identification of process variables such as e.g. those that control mechanical activation of the reaction surface.

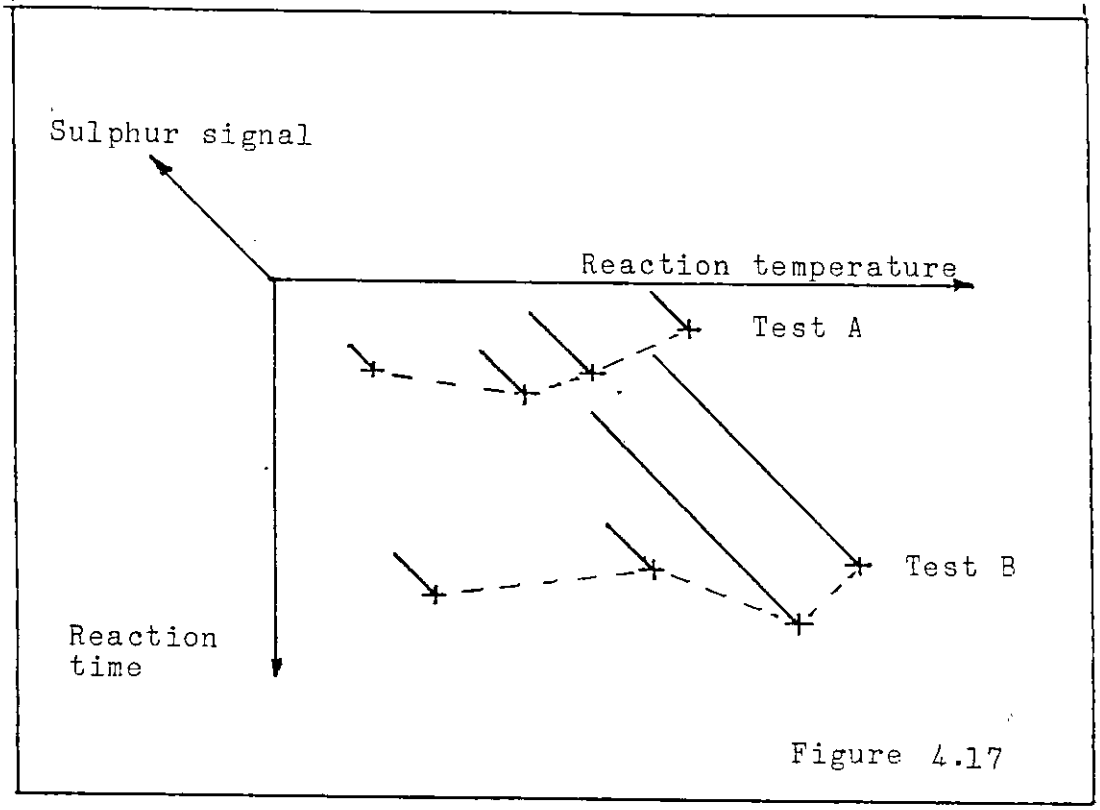
Sulphur signal
Reaction temperature
Test A
Test B
Reaction time

Figure 4.17

CHAPTER 5

EXPERIMENTAL RESULTS

5.1 Introduction

The surface analysis data produced according to the experimental method described in Chapter 4, is presented in this chapter. The investigated ranges of reaction time and temperature are discussed and the statistical tests performed on the data are described in detail. Further treatment of the data to reveal more detailed information of the controlling influence of time and temperature on film growth is then presented. The chapter is concluded with a discussion of the observations directly arising from the experimental results, deductions of a more speculative nature are left to Chapter 6.

5.2 Experiment Designs

5.2.1 Requirements of the experimental programme

The main objective of the research programme was to demonstrate a time dependence of the extent of film formation by an E.P. additive on nascent steel. If this objective were achieved then the results could be used to supply experimental values of film growth rate for Bailey and Cameron's Out-of-Contact theory (as discussed in Chapters 1 and 2).

An important objective further to that described above was to provide experimental evidence against the possibility of significant artefact in the results.

5.2.2 Experimental programme

The experiments were designed for four combinations of reaction distance and scraping speed. The mode in which reaction time is determined is very important. Very short and very long reaction times (3 to 5 ms and 30-50 ms respectively) can be only achieved by one setting of the exposure distance and scraping speed. The intermediate reaction time (10-15 ms) can however be achieved by two means: short reaction distance with a low scraping speed and long reaction distance with a high scraping speed. The modes of reaction time are shown in Table 5.1.

TABLE 5.1

Mode of Setting Reaction Time	Intended timing
Long reaction distance, low scraping speed (long, slow)	30-50 ms
Long reaction distance, high scraping speed (long, quick)	10-15 ms
Short reaction distance, low scraping speed (short, slow)	10-15 ms
Short reaction distance, high scraping speed (short, quick)	3-5 ms

A comparison of film growth at intermediate reaction times (10-15 ms) achieved by the two modes described above is considered to be useful indicator of experimental artifact.

Three kinds of test-fluids which were prepared according to the methods described in Chapter 4, were used in the experiments. The test fluids are: control fluid of pure

hexadecane and two model lubricants, 0.75 wt % sulphur in hexadecane as the strong E.P. lubricant and 2.5% wt % DBDS in nexadecane as a more mild E.P. lubricant.

The temperature to which most of the samples analysed in a given test were heated, was used as a characteristic temperature for dictating the levels of temperature used in the test programme. This temperature which is referred to as the 'plateau temperature' was set at four levels, 140°C, 155°C, 170°C and 185°C respectively. The upper level, 185°C is the maximum temperature at which the rinse fluid can be expected to function (discussion in Chapter 4). The lowest level, 140°C, was found to be an adequately low limit of plateau temperature to give a measure of the controlling influence of temperature on the film growth rate.

There were 21 tests performed in all, the first four were trial tests and two tests were failures leaving 15 tests as valid data. The latter 15 tests are listed in Table 5.2.

TABLE 5.2

Test Settings used in the Experimental Work

Test No.	Reagent	Plateau Temp.	Reaction Time	Mode
1	Control (Pure hexa-decane)	170°C	40-50 msecs	Long, slow
2	Sulphur	155°C	30-50 msecs	Long, slow
3	Sulphur	155°C	6-15 msecs	Short, quick
4	Sulphur	155°C	10-20 msecs	Long, quick
5	Sulphur	155°C	13-16 msecs	Short, slow
6	Sulphur	155°C	30-40 msecs	Long, slow
7	Sulphur	170°C	3-7 msecs	Short, quick
8	Sulphur	185°C	5-10 msecs	Short, quick
9	Sulphur	170°C	15-25 msecs	Long, quick
10	Sulphur	185°C	15-25 msecs	Long, quick
11	Sulphur	170°C	15-25 msecs	Long, quick
12	Sulphur	140°C	30-45 msecs	Long, slow
13	DBDS	155°C	50-85 msecs	Long, slow
14	DBDS	185°C	40-65 msecs	Long, slow
15	Sulphur	170°C	25-35 msecs	Long, slow

The design of the test programme resulted in a concentration of test data in the reaction temperature range 140-185°C where relatively large sulphur signals were found to occur. The performance of tests at temperatures where the sulphur signal would be immeasurably small was thereby avoided.

5.3 Experimental Data

The data was divided according to test fluid i.e. control, DBDS solution and sulphur solution as the composition of test-fluid used was found to delineate the most important differences in the data.

5.3.1 Control test

A control test with a plateau temperature setting of 170^{o}C was carried out. The probability of sulphidation by any extraneous cause would be relatively high at this temperature. The reaction time was set at the longest value and ranged from 40 to 49 ms. The data from the test is presented in Table 5.3. The average sulphur signal for all the area analyses performed on the samples is equal to 2.47% and is beneath the level of signal considered significant which is 5% (as discussed in Chapter 4). The average value of signal from the control test was therefore not subtracted from the other test results in order to refine the estimate of film growth.

Since the rinse fluid is believed to be the main source of extraneous sulphur a copper corrosion test was also carried out. Copper strips were exposed to 0.75% wt % sulphur in hexadecane and to rinse fluid. After 18 hours at 60^{o}C the copper strip in the sulphur solution was heavily corroded whilst the copper strip in the rinse fluid remained with no visible tarnish.

TABLE 5.3

CONTROL TEST IN PURE HEXADECANE

Specimens	Reaction Time	Reaction Temp.	Average Signal
1	44 ms	105°C	5.24%
2	41 ms	163°C	2.29%
3	48 ms	170°C	2.40%
4	45 ms	170°C	2.52%
5	49 ms	169°C	1.08%
		Average for total	2.47%

All specimen averages based on 4 area analyses.

5.3.2 Data from tests on DBDS

Some tests were run to investigate whether the reactivity of DBDS was comparable to sulphur. Plateau temperatures were 155 and 185°C with reaction times in the range 40-80 msecs. In both cases a null result was obtained as is shown in Table 5.4 which presents the data. Notwithstanding the doubts inherent in a null test, it is concluded that DBDS is significantly less reactive than sulphur which produced quite thick films under similar conditions. Unlike the results for sulphur, the results for DBDS were not subjected to further treatment as it was felt that little more could be deduced from them.

5.3.3 Data from tests on sulphur

The bulk of the tests involved sulphur (as shown in Table 5.1). Most of the samples extracted were analysed by

EDAX but one test was devoted to Infra-Red. The EDAX results were further subjected to step-wise multiple regression to eliminate the insignificant variables and find an equation defining the growth rate of the sulphur film. The Infra-Red analysis was used to try and deduce the composition of the sulphur film formed on the scraped surface.

TABLE 5.4

RESULTS FOR DBDS

Test No.	Specimen No.	Reaction Temperature	Reaction Time	Average Signal
1	1	142°C	57 ms	5.2 %
1	2	155°C	72 ms	3.59%
1	3	155°C	69 ms	2.29%
1	4	155°C	82 ms	2.77%
1	5	152°C	78 ms	2,67%
2	1	91°C	58 ms	2.35%
2	2	178°C	61 ms	4.93%
2	3	185°C	41 ms	3.12%
2	4	185°C	55 ms	2.61%
2	5	178°C	65 ms	2.56%

5.4 Multiple Regression Analysis

5.4.1 Outline of the analysis

Multiple regression equations (148,149) were developed based o the E.D.A.X. experimental data for sulphur. The reasons for applying the regression analysis were twofold. The first

reason was to obtain a description of the relationship between the variables (150,151) and to indicate the conditions for possible sulphur film formation. The second reason was to predict the value of an independent variable from the set of values of other independent variables. In other words separate the dependent variables from the independent variables for a certain assumed level of significance, α. Four different forms of linear regression were applied which are listed below:

1. Multiple linear regression with a constant

$$Y = C_o + C_1 X_1 + . - . \ C_n X_n$$

2. Multiple linear regression with no constant

$$Y = C_1 X_1 + C_2 X_2 + --- \ C_n X_n$$

3. Non linear regression (in the exponential form)

$$Y = C_o X_1^{C_1} X_2^{C_2} --- X_n^{C_n}$$

4. Non-linear regression (in the exponential form) with no constant

$$Y = X_1^{C_1} X_2^{C_2} -- X_n^{C_n}$$

The best fitting regression equations for each form of equation tested were selected for graphical presentation together with the experimental results. The experimental results and regressional equations are shown 3-dimensional plots, temperature versus time versus EDAX signal. As well as the expected variables of reaction time and temperature, two other variables were included in the regression analysis. These latter two variables were chosen as indicators of possible artefact in the results; they are discussed in detail below.

From the 11 tests performed for sulphur, 65 specimens were analysed to give about 200 individual E.D.A.X. area analyses.

5,4,2 Details of the analysis

As has already been mentioned the regression analysis was performed in order to eliminate the insignificant variables from the model of film growth and determine the appropriate equations for film growth (152).

The following set of variables were initially used:

Independent variables:

X_1 - Distance scraped at location of sample, expressed in mm, (variable to indicate experimental artefact).

X_2 - Time from start of scrape to the moment when the sample was scraped, expressed in ms (variable to indicate experimental artefact).

X_3 - Reaction temperature of sample in degrees Kelvin.

X_4 - Reaction time of sample in milliseconds.

Dependent variables:

Y_i - Decimal fraction of normalised E.D.A.X. signal. The subscript 'i' refers to whether the 1st, 2nd, 3rd, 4th, or average signal of each sample analysis is being regressed.

A level of significance $\alpha = 0.05$ has been assumed.

Regression equations were produced for each set of E.D.A.X. signals Y_1, Y_2, Y_3, Y_4 and for the sample average of the signals $\bar{Y}$. Such an approach was necessary as a check for possible bias in the method of performing E.D.A.X.

No comparable method of quantitative analysis by E.D.A.X. of tribological material could be found in the available literature. Thus the method described above which may not be the ideal for the purpose intended was chosen according to the then understanding of the problem.

5.4.3 Equations derived from the regression analysis

The equations produced by the regression analysis are enclosed in a series of Tables 5.5 to 5.9. The first four tables give the results of regressions with all four originally chosen independent variables, the last Table 5.9, gives the results of the regressions with X_1 and X_2 absent. In the first four tables the regression coefficients for all signals tested, Y_1, Y_2, Y_3, Y_4 and $\bar{Y}$ are present, and the regression with the highest determination coefficient is underlined. The last table gives the coefficients for $\bar{Y}$ only, which was found to give the highest coefficients of determination. The standard errors of estimate, multiple correlation coefficients, coefficients of determination and corrected coefficients of determination are also listed.

TABLE 5.5

MULTIPLE LINEAR REGRESSION WITH A CONSTANT AND FOUR PREDICTOR VARIABLES

Y	$\bar{Y}$	Y_1	Y_2	Y_3	Y_4
C	-0.1083	-0.0840	-0.1274	-0.0308	-0.0467
C_1	-0.0002	-0.0002	-0.0002	-0.0001	-0.0002
C_2	0.0004	0.0006	0.0004	0.0009	0.0002
C_3	0.0016	0.0017	0.0020	0.0007	0.0016
C_4	0.0021	0.0009	0.0021	-0.0009	-0.0002
Standard error of estimated	0.1026	0.1292	0.1339	0.0925	0.1336
Multiple correlation R	0.5247	0.4271	0.4706	0.4325	0.3496
Coefficient of determination R^2	0.2753	0.1824	0.2215	0.1871	0.1222
Corrected coefficient of determination R^2	0.2270	0.1279	0.1696	0.1329	0.0637

Regression equation in the form

$$Y_i = C + C_1X_1 + C_2X_2 + C_3X_3 + C_4X_4$$

TABLE 5.6

MULTIPLE LINEAR REGRESSION WITH

FOUR PREDICTOR VARIABLES AND NO CONSTANT

Y	$\bar{Y}$	Y_1	Y_2	Y_3	Y_4
C_1	-0.0001	-0.0002	-0.0002	-0.0001	-0.0002
C_2	0.0003	0.0005	0.0002	0.0008	0.0002
C_3	0.0011	0.0013	0.0014	0.0006	0.0013
C_4	0.0012	0.0002	0.0010	-0.0012	-0.0006
Standard error of estimate	0.1048	0.1296	0.1360	0.0920	0.1329
Multiple correlation R	0.8482	0.7989	0.7901	0.8201	0.6827
Coefficient of determination R^2	0.7195	0.6382	0.6243	0.6726	0.4661
Corrected coefficient of determination $\overline{R^2}$	0.7011	0.6145	0.5996	0.6512	0.4311

Regression equation in the form

$$Y = C_1X_1 + C_2X_2 + C_3X_3 + C_4X_4$$

TABLE 5.7

MULTIPLE REGRESSION IN THE EXPONENTIAL FORM

WITH A CONSTANT AND FOUR PREDICTOR VARIABLES

Y	$\bar{Y}$	Y_1	Y_2	Y_3	Y_4
C	0.0004	0.0001	0.00002	0.0020	0.0001
C_1	0.1582	-1.3344	-0.7612	-0.6841	0.7323
C_2	0.2153	1.3215	0.5141	0.4759	-1.9750
C_3	1.0053	1.8418	2.0749	1.2999	2.1520
C_4	0.2521	-0.2431	0.1820	-0.4823	0.1530
Standard error of estimate	0.7276	1.0352	1.3187	2.0412	2.9364
Multiple correlation R	0.5903	0.5725	0.5507	0.2891	0.3622
Coefficient of determination R^2	0.3484	0.3278	0.3033	0.0836	0.1312
Corrected coefficient of determination $\overline{R^2}$	0.3050	0.2830	0.2568	0.0225	0.0732

Regression equation in the form

$$Y = C\, X_1^{C_1}\, X_2^{C_2}\, X_3^{C_3}\, X_4^{C_4}$$

TABLE 5.8

MULTIPLE REGRESSION IN THE EXPONENTIAL FORM

WITH FOUR PREDICTOR VARIABLES AND NO CONSTANT

Y	$\bar{Y}$	Y_1	Y_2	Y_3	Y_4
C_1	0.0775	-1.4290	-0.8763	-0.7489	0.6296
C_2	-1.2214	0.1405	-0.9224	-0.3323	-3.2564
C_3	0.6221	1.3920	1.5279	0.9921	1.6640
C_4	0.0838	-0.4406	-0.0583	-0.6175	-0.0613
Standard error of estimate	0.9097	1.2152	1.5282	2.0727	2.9964
Multiple correlation R	0.9273	0.8897	0.8540	0.8270	0.8170
Coefficient of determination R^2	0.8599	0.7915	0.7293	0.6840	0.6676
Corrected coefficient of determination $\overline{R^2}$	0.8507	0.7779	0.7115	0.6633	0.6458

Regression equation in the form

$$Y = X_1^{C_1} X_2^{C_2} X_3^{C_3} X_4^{C_4}$$

TABLE 5.9

REGRESSION EQUATION OF THE AVERAGE SIGNAL

AFTER ELIMINATION OF INSIGNIFICANT VARIABLES

	$\bar{Y}*$	$\bar{Y}^{+}$	$\bar{Y}^{\dagger}$	$\bar{Y}^{\phi}$
C	-0.1030		0.0004	
C_1	0.0014	0.0009	1.0446	-0.2561
C_2	0.0028	0.0017	0.2044	-0.3236
Standard error of estimate	0.1019	0.1038	0.7167	0.9893
Multiple correlation R	0.5121	0.8461	0.5888	0.9104
Coefficient of determination R^2	0.2622	0.7159	0.3467	0.8289
Corrected coefficient of determination $\overline{R^2}$	0.2384	0.7069	0.3256	0.8234

$*\bar{Y} = C + C_1X_3 + C_2X_4$

$+\bar{Y} = C_1X_3 + C_2X_4$

$\dagger\bar{Y} = C\ X_3^{C_1}\ X_4^{C_2}$

$\phi\bar{Y} = X_3^{C_1}X_4^{C_2}$

5.4.4 Discussion of the results of the regression analysis

Comparing the determination coefficients of each form of regression applied, it is evident that the average of signals for each sample analysed gives the most consistent results. Individual signals are subject to a much higher scatter.

The artefact variables, scraping time and distance were eliminated from the regression equations as the changes in the coefficients of determination on removal of these two variables was negligible. The differences in coefficients of determination between the regressions with the four original predictor variables and those with only reaction time and temperature are listed below in Table

TABLE 5.10

CHANGES IN DETERMINATION COEFFICIENT

ON REMOVAL OF ARTEFACT VARIABLES

Form of Multiple Regression	Change in Determination Coefficient on removal of artefact Variables
Linear with a constant	- 1.31%
Linear with no constant	- 0.36%
Exponential form with constant	- 0.17%
Exponential form with no constant	- 3.10%

Two hypothesized causes of experimental artefact have not been supported by results of the regression. It was

previously feared that the rinse jet would be delayed in reaching the scraped surface and only the latter part of the scraped surface would be rinsed. Progressive tool blunting during the scrape was also believed to be a possible factor to influence film growth rates.

Four of the best fitting regression equations were selected for graphical presentation with the experimental data. Three-dimensional graphing technique is used as three variables are involved, sulphur signal, reaction time and temperature. All the regression equations presented graphically apply to the average signal $\bar{Y}$. The coefficients of the regression equations are listed below and the graphs are enclosed in Figures 5.1, 5.2, 5.3, 5.4.

Linear with four variables, determination coefficient = 0.7195

$$\bar{Y} = C_1\bar{X}_1 + X_2\,\bar{X}_2 + C_3\,X_3 + C_4\,X_4$$

where

$C_1 = -0.0001$

$C_2 = 0.0003$

$C_3 = 0.0011$

$C_4 = 0.0012$

$\bar{X}_1$ = Average scrape distance for all results = 424.1769 (mm) | Held constant

$\bar{X}_2$ = Average scraping time = 130.2615 (msecs) | Held constant

Linear with two variables (temperature, time) determination coefficient = 0.7159

$$\bar{Y} = C_1 \times X_3 + C_2 \times X_4$$

where

$C_1 = 0.0009$

$C_2 = 0.0017$

Exponential regression with four variables determination coefficient = 0.8599

$$\bar{Y} = \bar{X}_1^{C_1}\,X_2^{C_2}\,X_3^{C_3}\,X_4^{C_4}$$

$\bar{X}_1$, $\bar{X}_2$ as in the linear 4 variable case

$C_1 = 0.0775$

$C_2 = -1.2214$

$C_3 = 0.6221$

$C_4 = 0.0838$

Exponential with two variables (reaction time and temperature) determination coefficient = 0.8289 (Average signal)

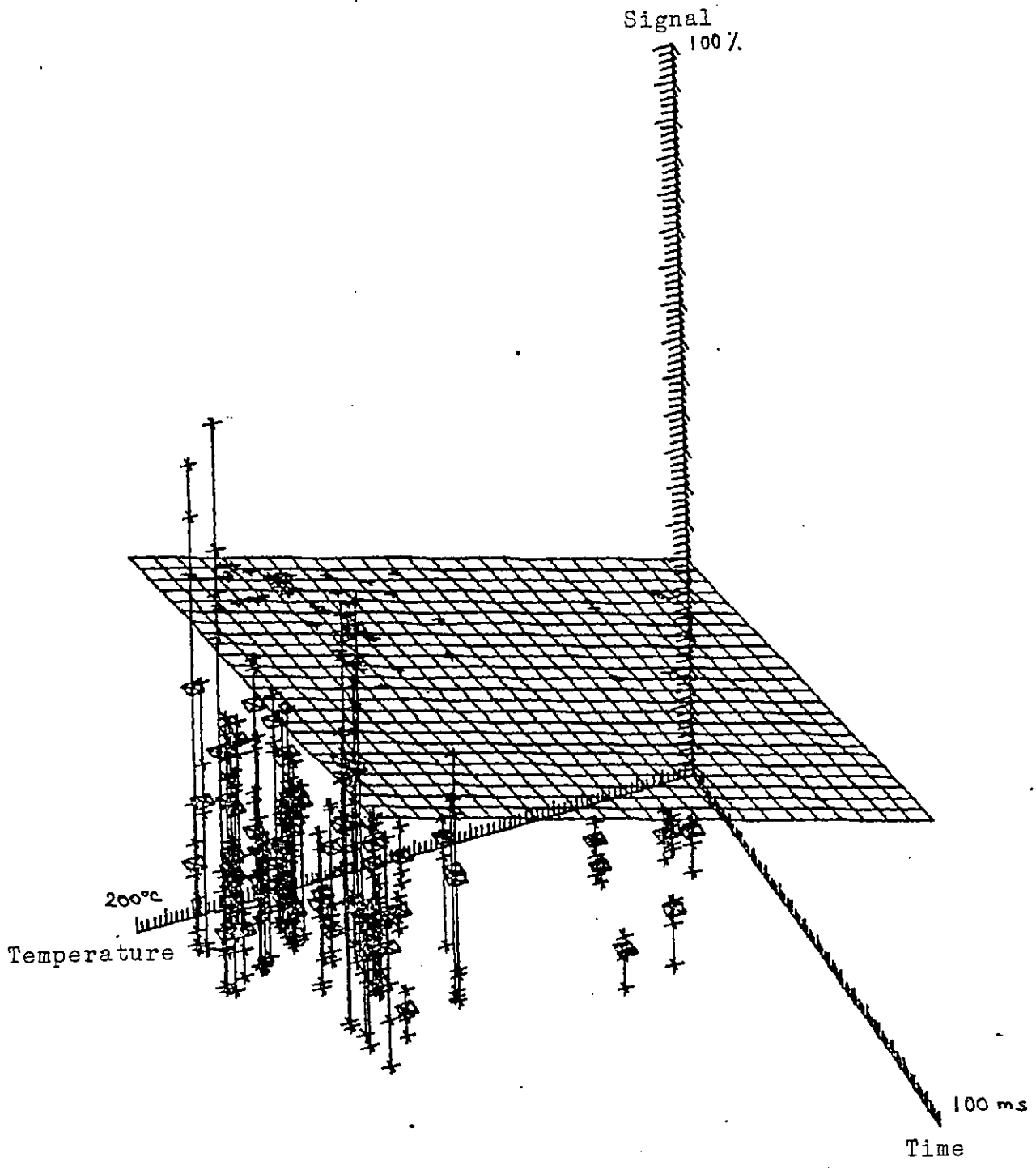

Figure 5.1 Linear regression, 4 independent variables

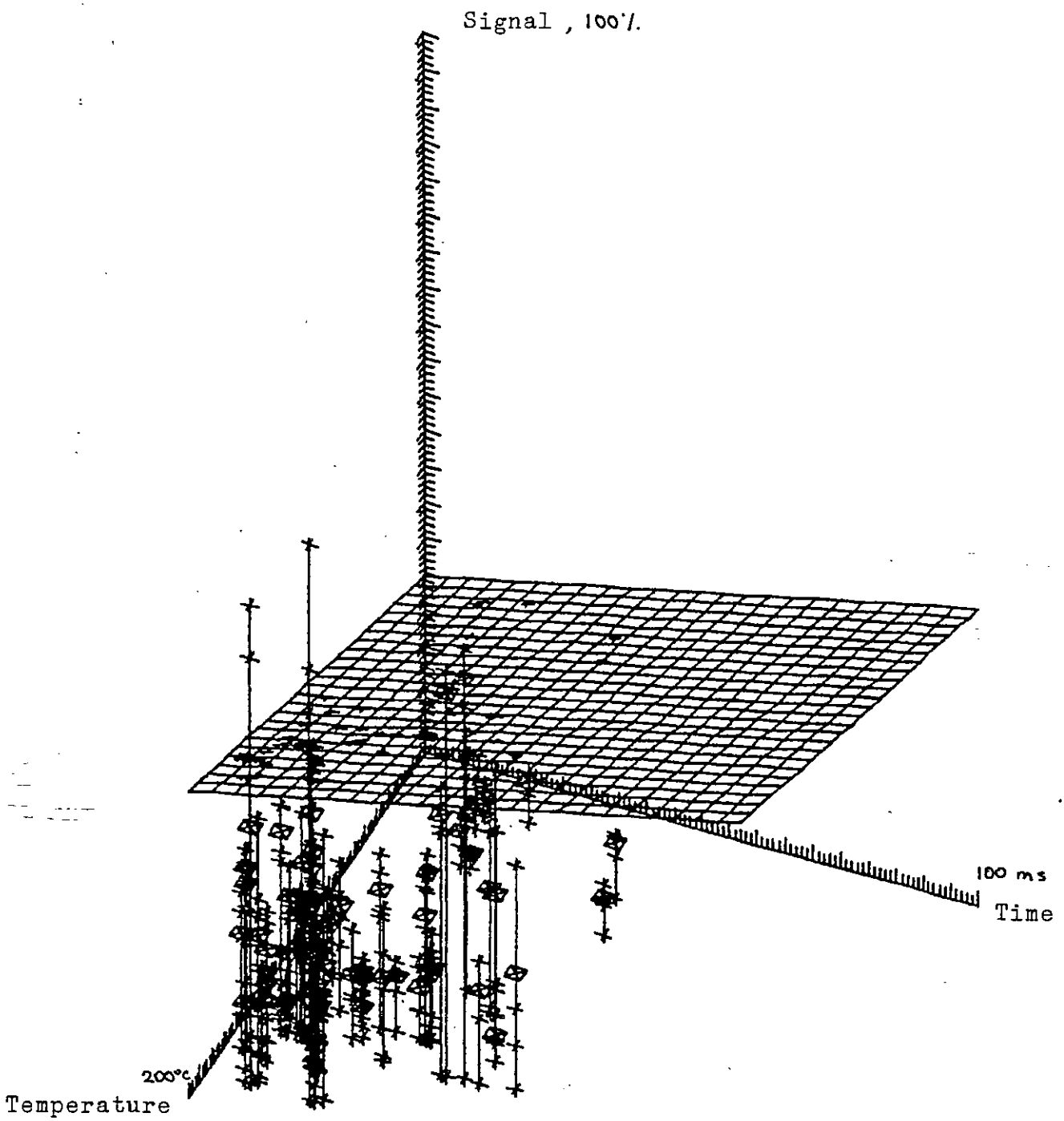

Figure 5.2 Linear regression, 2 independent variables

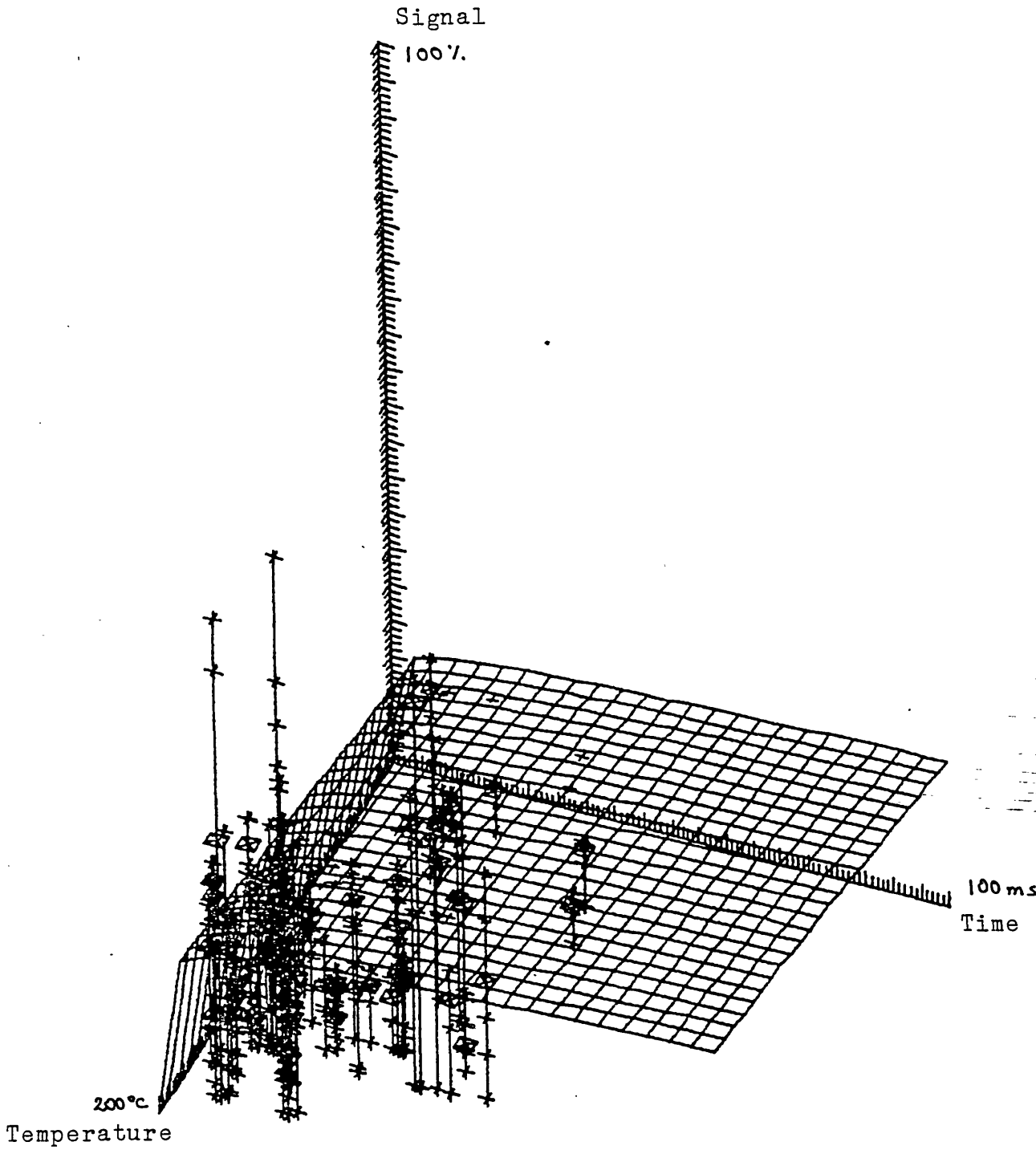

Figure 5.3 Exponential regression, 4 independent variables

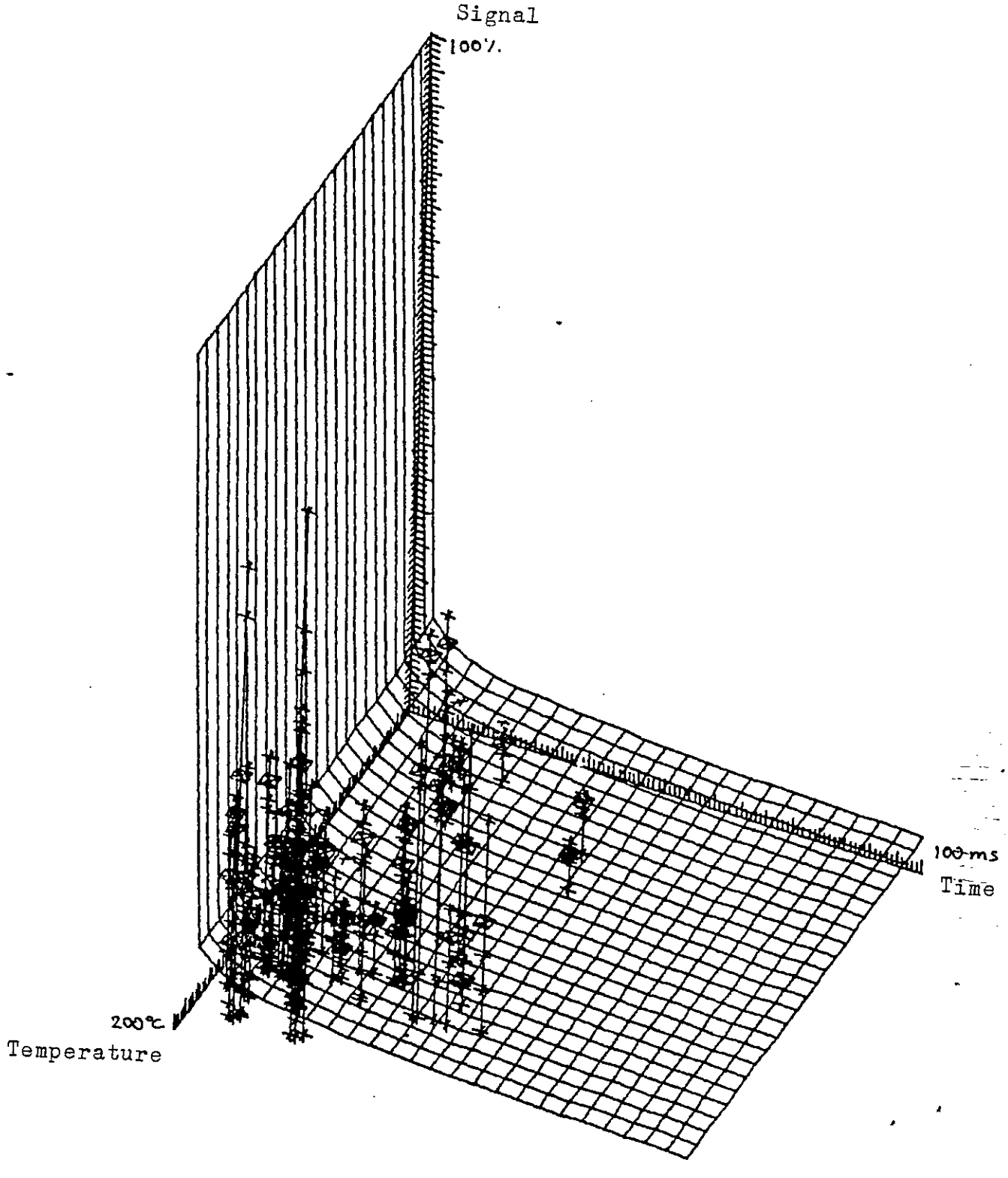

Figure 5.4 Exponential regression, 2 indepndent variables

$$\bar{Y} = X_3^{C_1} X_4^{C_2}$$

$$C_1 = -0.2561$$

$$C_2 = -0.3236$$

As can be seen from Figures 5.1-5.4 the scatter in the experimental data is very large and so prevents the regression approximations from being accurate. The main value in the regression analysis was found to lie in providing conclusive evidence against experimental artefact and in indicating the need for a much larger data set, should a more detailed investigation of film growth rates be required.

5.5 Temperature and Time Trends in the Data

Since the multiple regression analysis did not provide equations agreeing with the observed trends of reaction time and temperature in the data, a more qualitative treatment of the data was carried out in order to elucidate the trends of time and temperature.

Two different methods of transforming the data, both of which are described below, were carried out, The first being to extract the 'temperature trend', the second to extract the 'time trend'.

5.5.1 Temperature trend in the data

From the material discussed in Chapter 2 it was considered that a fractional power law (of unknown exponent) would be a reasonable approximation to the time-dependence of the data. In other words it was assumed that the data conformed to the relation:

$$\bar{Y} \propto t^{1/m} \qquad (5.1)$$

where t = reaction time

$\bar{Y}$ = average sulphur signal

If the above Equation (5.1) held true the quantity $Y\ t^{-1/m}$ would be independent of reaction time and merely a function of the other controlling variable, reaction temperature.

A series of graphs of $Y\ t^{-1/m}$ versus temperature were plotted for values of m ranging from 1 to 1000 and are presented in Figures (5.5 to 5.10).

It is evident from the graphs mentioned above that whatever the value of the exponent 'm', the reaction temperature exerts a decisive influence on the rate of film growth. Film growth rate is quite slow below 120 to 140^{o}C, but thereafter increases rapidly. The scatter present in all the graphs indicates the presence of other controlling variables and suggests that there is no universal time law for all the data.

It was of interest to check whether the Arrhenius law (as mentioned in Chapters 1 and 2) applies to the observed film growth rates. Graphs of $\log (\bar{Y}\ t^{-1/m})$ versus $1/T$ (where T is the reaction temperature in degrees Kelvin) were therefore plotted to check the applicability of this law to the data. For all values of 'm' tried there was a large scatter and no discernible trend. It was concluded that the Arrhenius law may in general be applicable,but for the range of time and temperature investigated no agreement with experimental data was apparent.

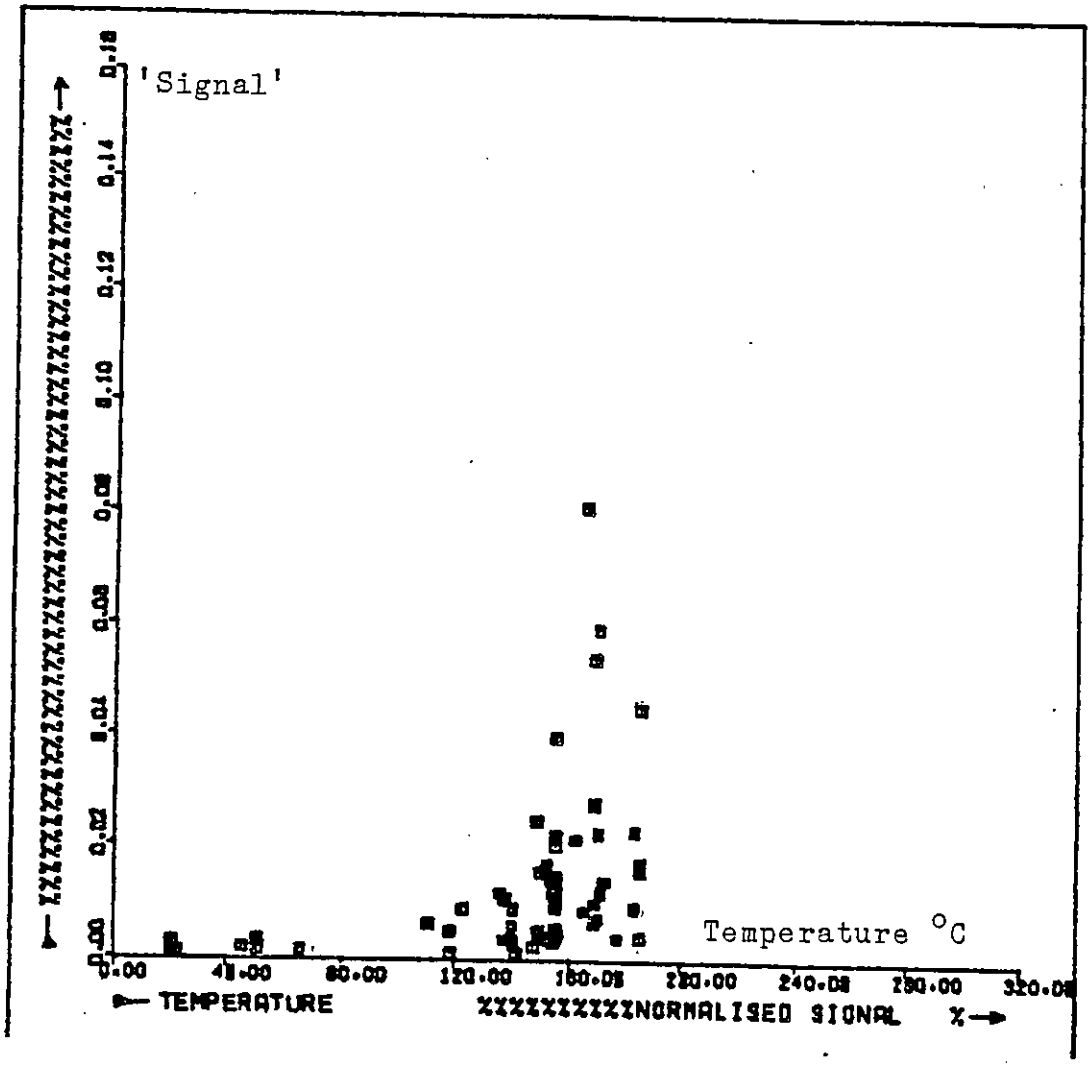

Figure 5.5 Graph of time-compensated 'signal' versus temperature 'm' = 1

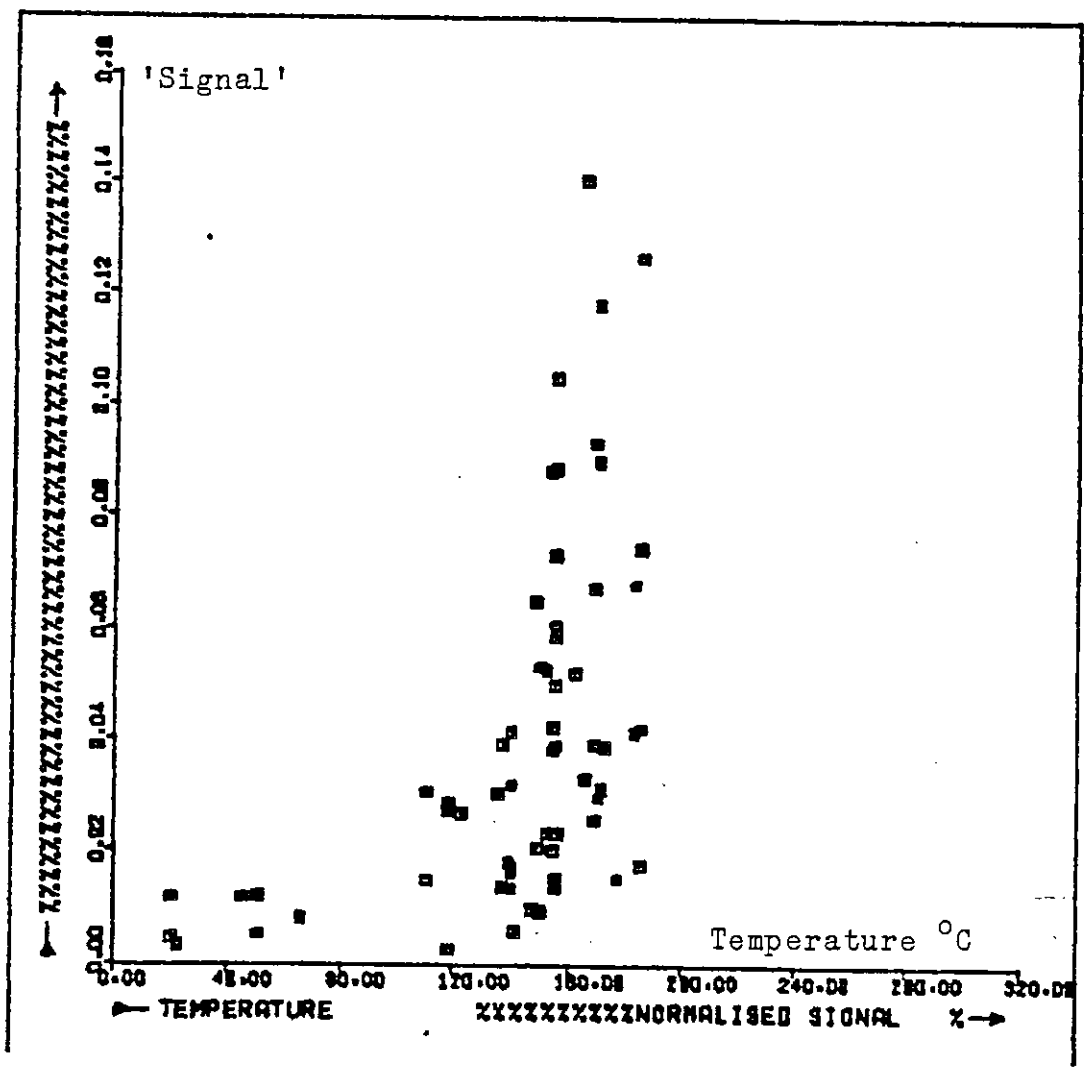

Figure 5.6 Graph of time compensated 'signal' versus temperature 'm' = 2

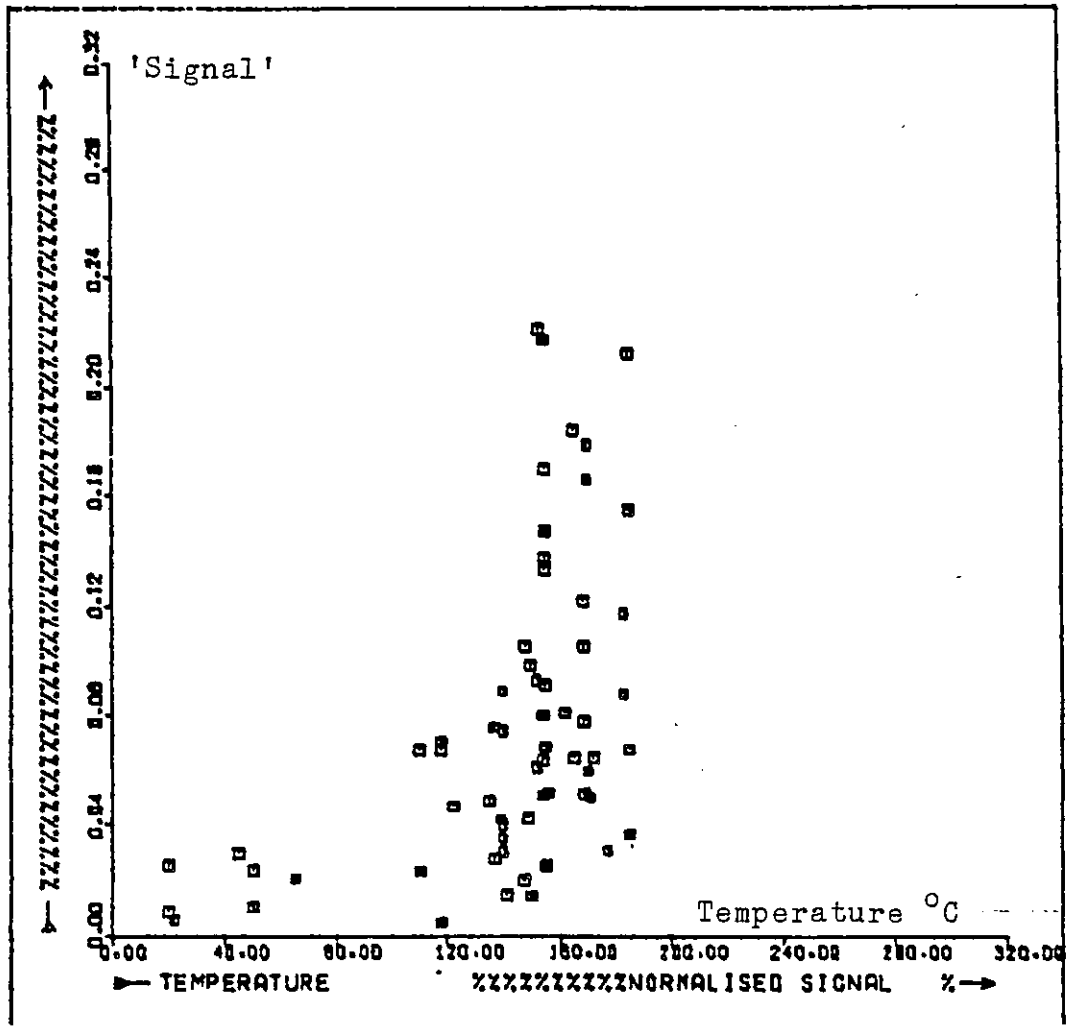

Figure 5.7 Graph of time-compensated 'signal' versus temperature 'm' = 4

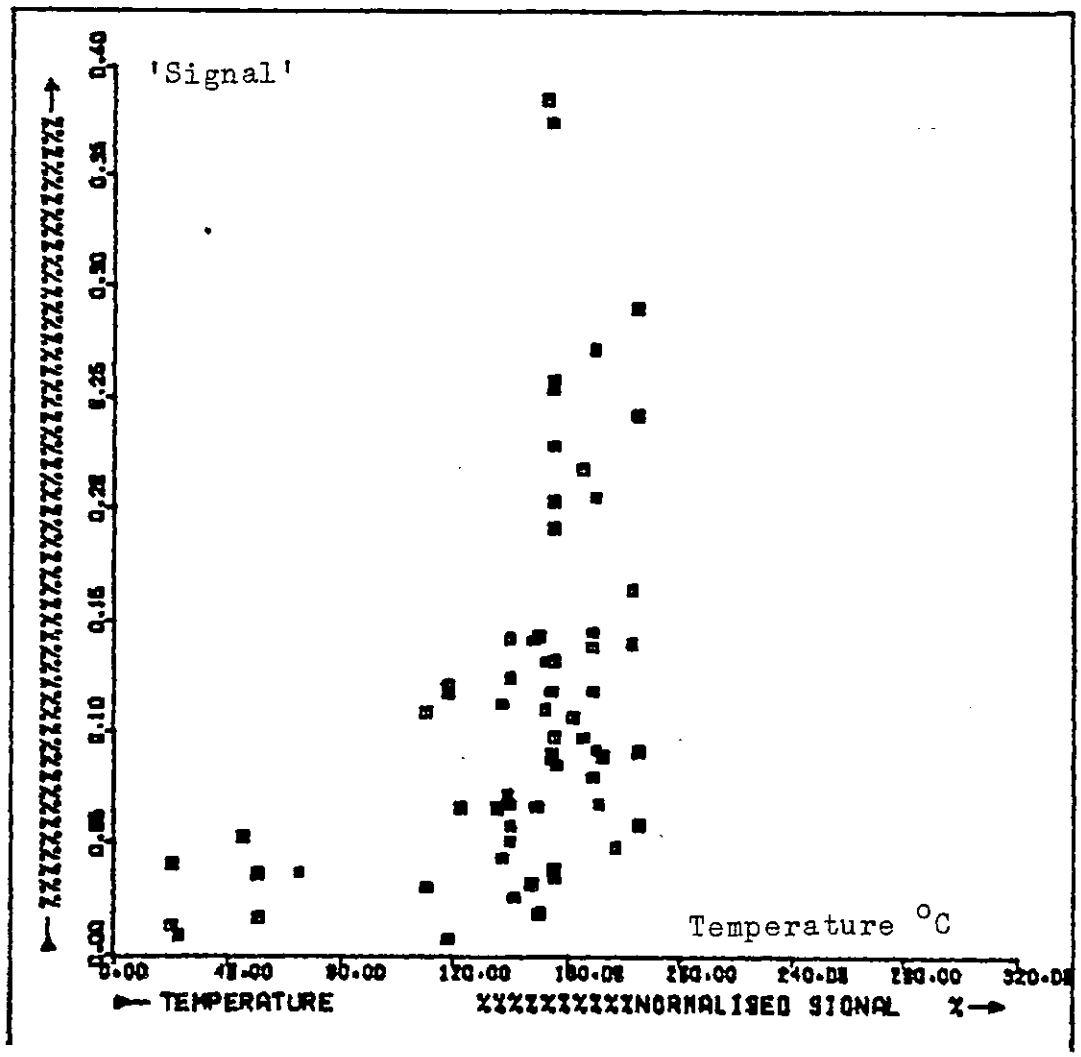

Figure 5.8 Graph of time-compensated 'signal' versus temperature 'm' = 10

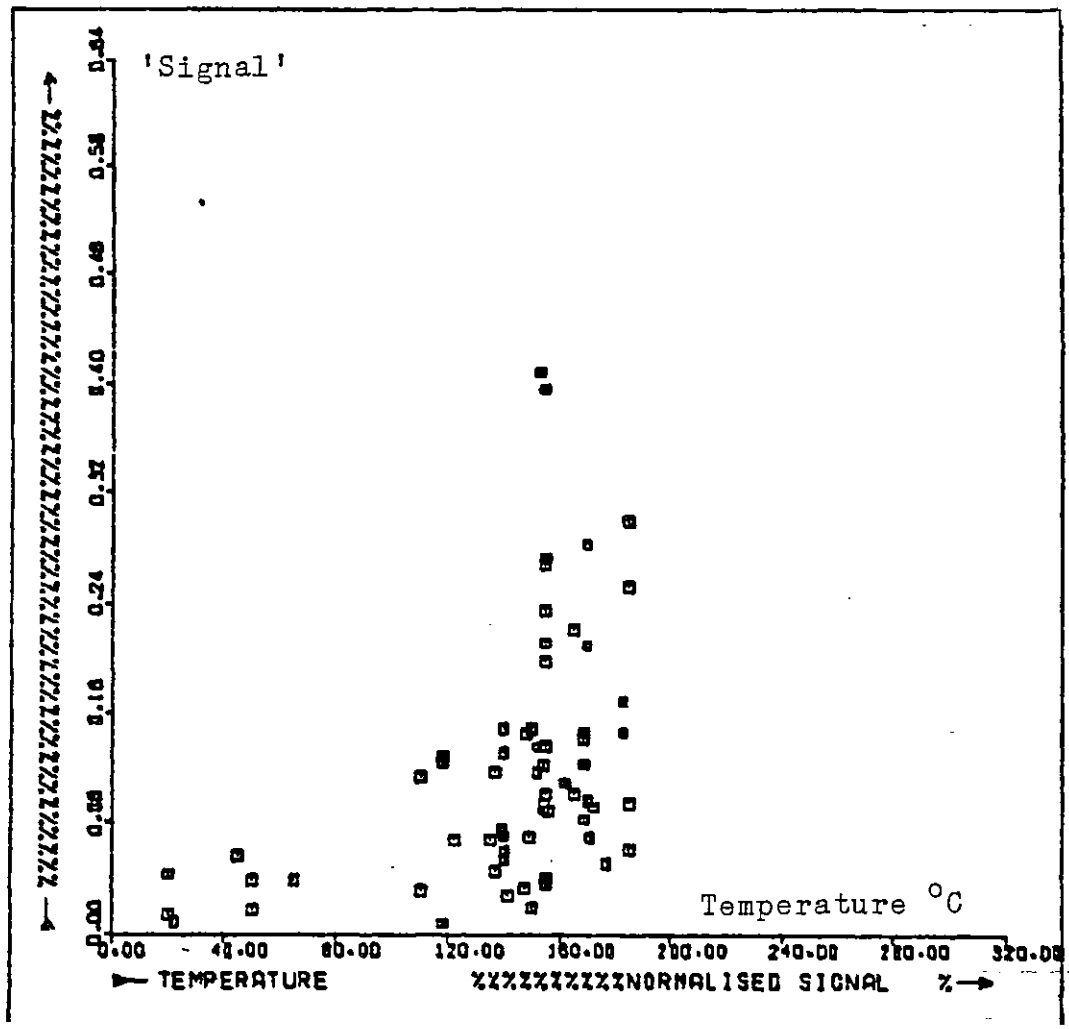

Figure 5.9 Graph of time-compensated 'signal' versus temperature 'm' = 12

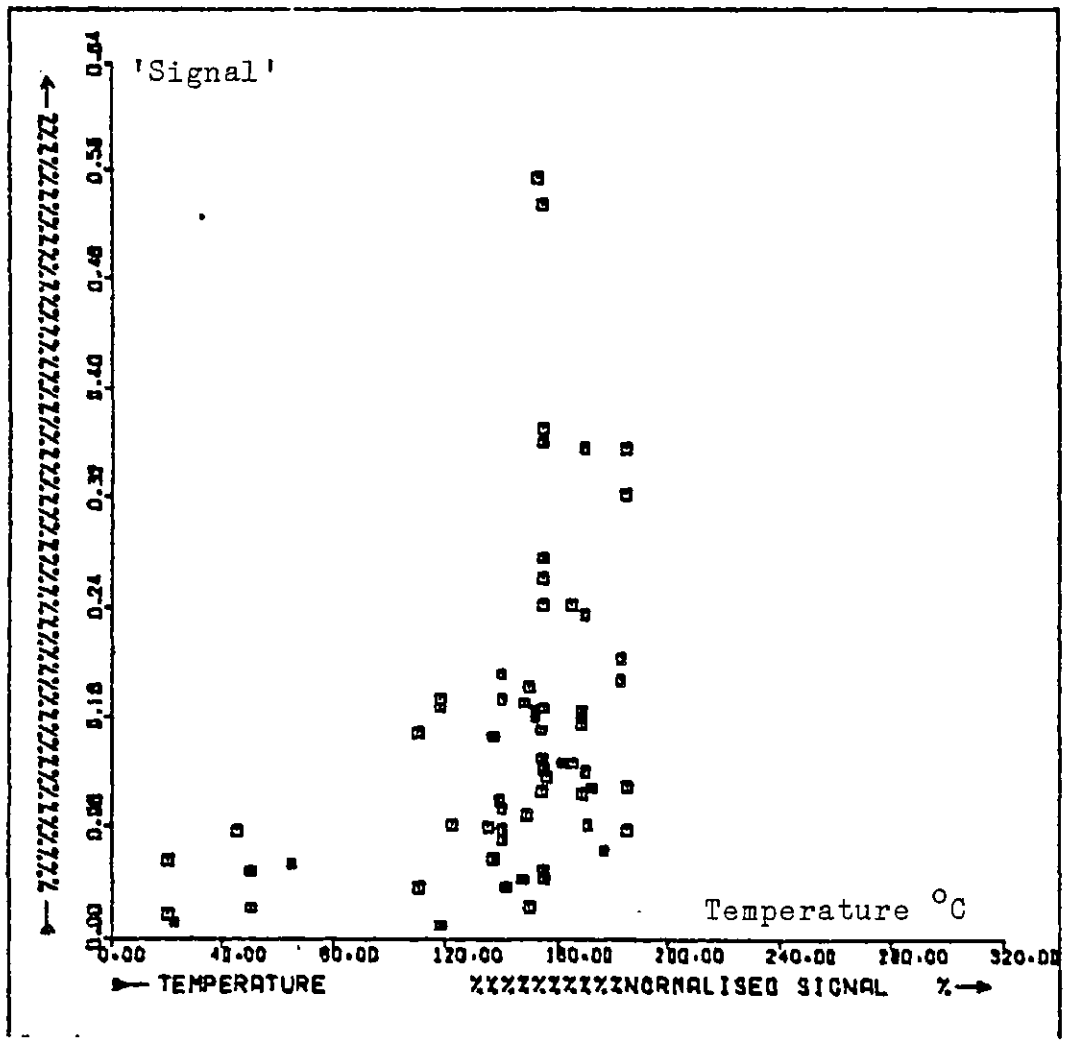

Figure 5.10 Graph of time-compensated 'signal' versus temperature m = 1000

5.5.2 Time trend in the data

The irregularity in temperature values e.g. one result may have 153°C reaction temperature, another has 150°C, prevents the use of isotherms for showing the time trend. A 'narrow section' approach was used instead where all results with temperatures lying within a common 4°C width band were grouped together for plotting on a graph. The method is illustrated in Figure 5.11. A band-width of 4°C was found to be a good compromise between having too many data groups each with a small number of results and on the other hand permitting an excessive temperature influence within the data group.

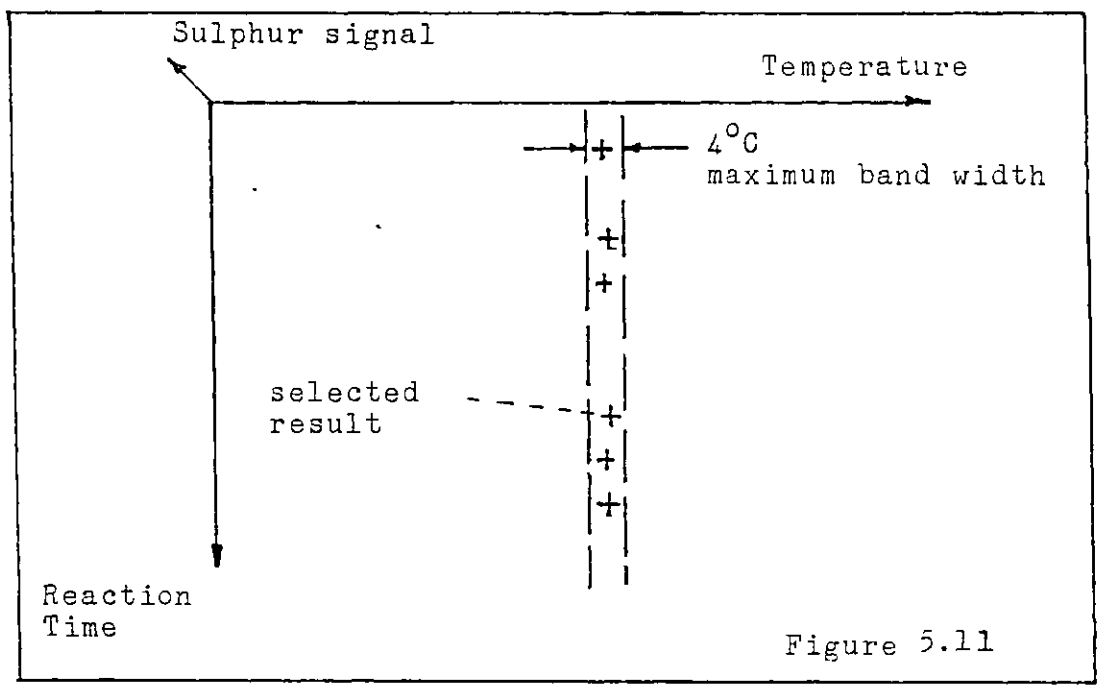

Figure 5.11

Average signals i.e. $\bar{Y}$ only are plotted as the individual analysis data Y_1, Y_2, Y_3, Y_4 are large in number and subject to a very high degree of scatter.

Ten graphs produced by the process described above are shown in Figures 5.12 to 5.21 . These cover the following temperatures: 110°C, 118°C, 135-137°C, 139-140°C, 147-150°C, 150-154°C, 154-156°C, 162-165°C, 169-172°C, 183-185°C, respectively. Below 100°C the extent of reaction is immeasurably small and therefore is not plotted by this method. In five of the graphs namely, 100°C, 118°C, 150-154°C, 154-156°C and 169-172°C, time-trends of some kind are evident. In the rest of the graphs, the scatter in the data is too large for any trends to be observable. The results of the graphical analysis is summarised below:

100°C	Time-signal proportionality evident
118°C	Time-signal proportionality evident
135-137°C	Trend questionable
139-140°C	Weak contrary trend
147-150°C	No trend
150-154°C	Trend evident
154-156°C	Trend evident
162-165°C	No trend
169-172°C	Weak trend
183-185°C	Very weak trend

The experimental calibration for film thickness (Chapter 4) gives a proportionality constant of approximately 2.3 Å film thickness per 1% signal, so a 20% and 40% signal indicate a 46 Å and 92 Å film thickness respectively. This scale of film thickness leads to the following conclusions:

I. If the temperature lies between 100 and 130°C, then a predictable and relatively slow growth of film with

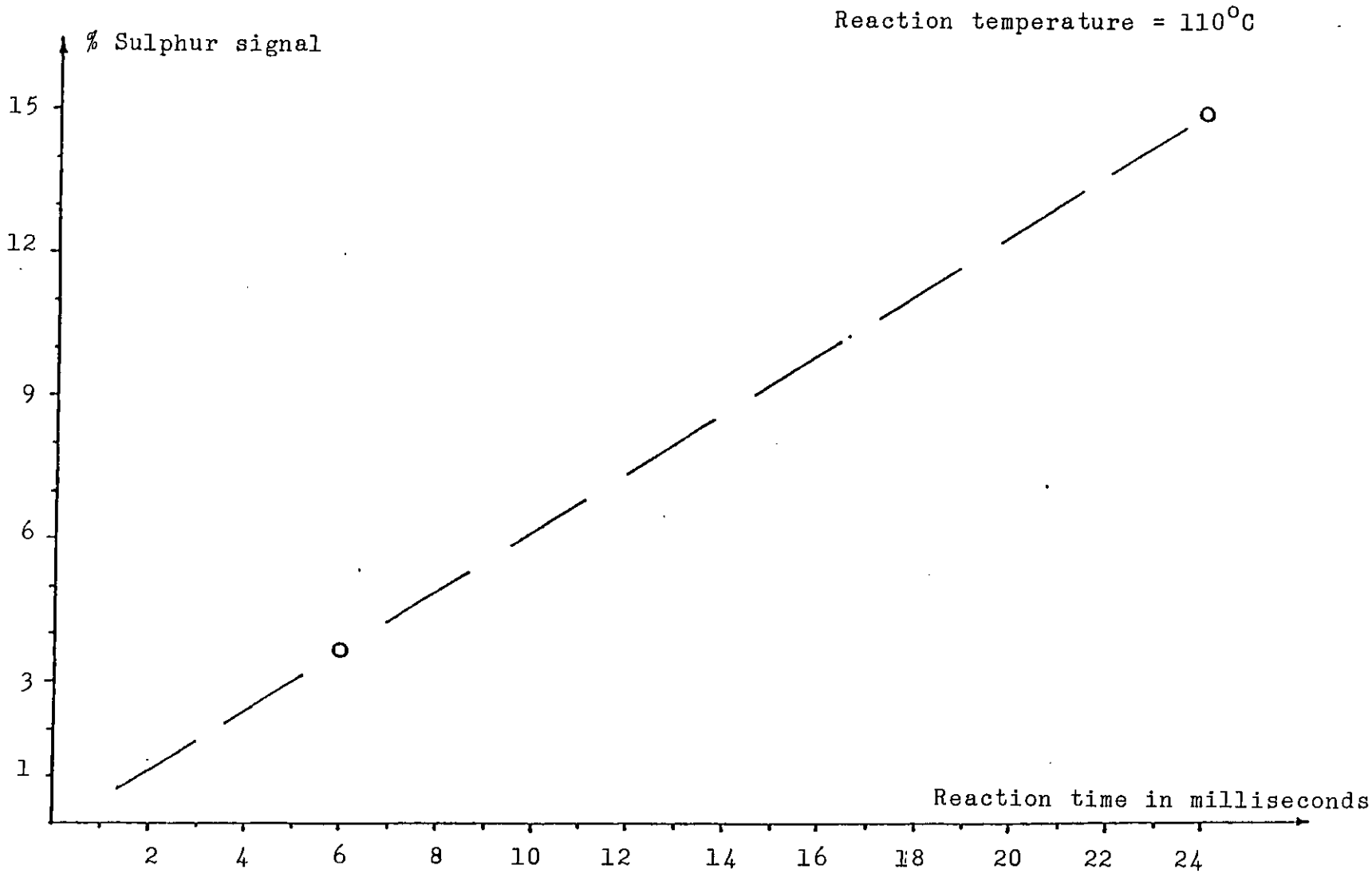

Figure 5.12 Graph of average signal versus reaction time at 110°C

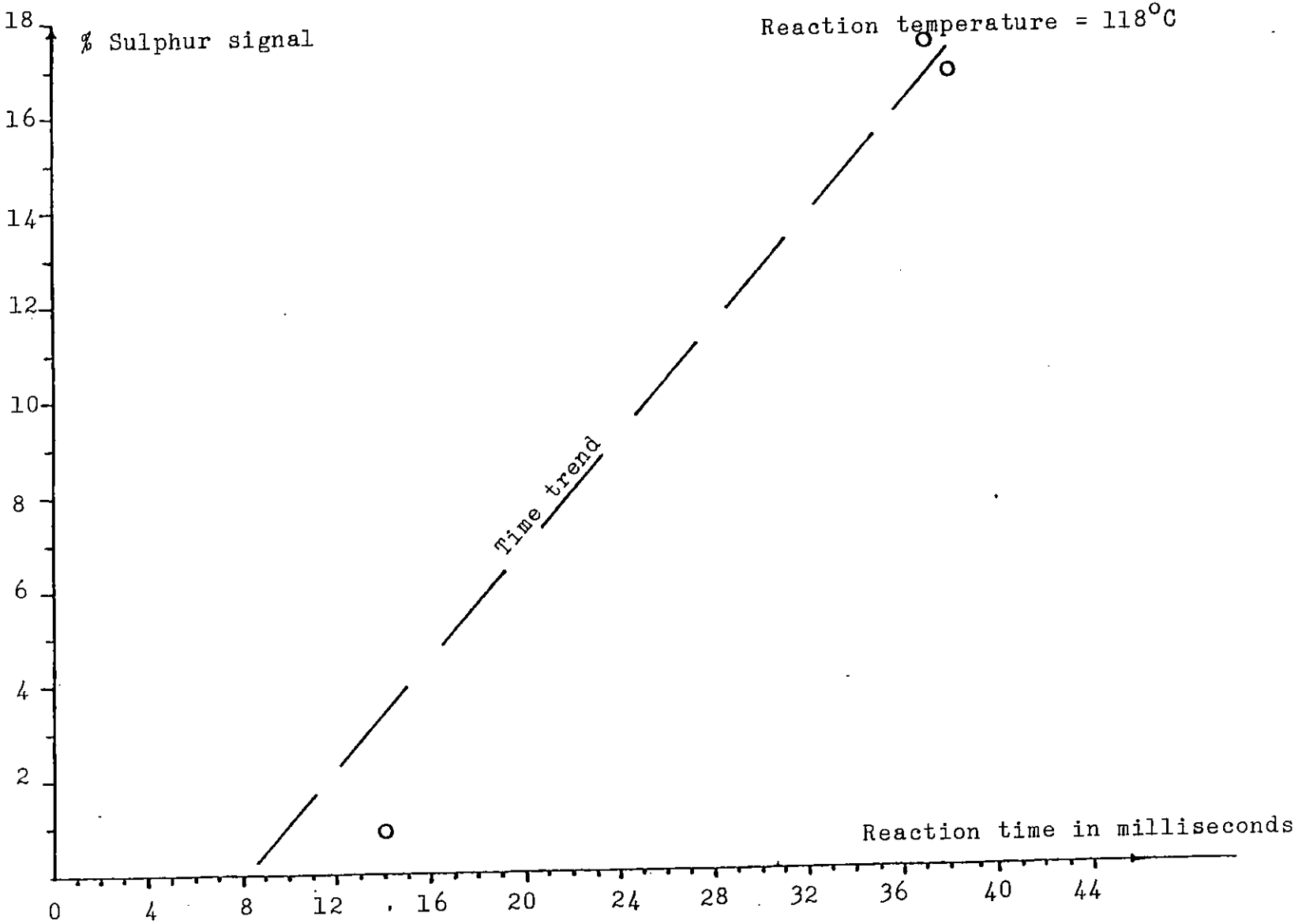

Figure 5.13 Graph of average signal versus reaction time at 118°C

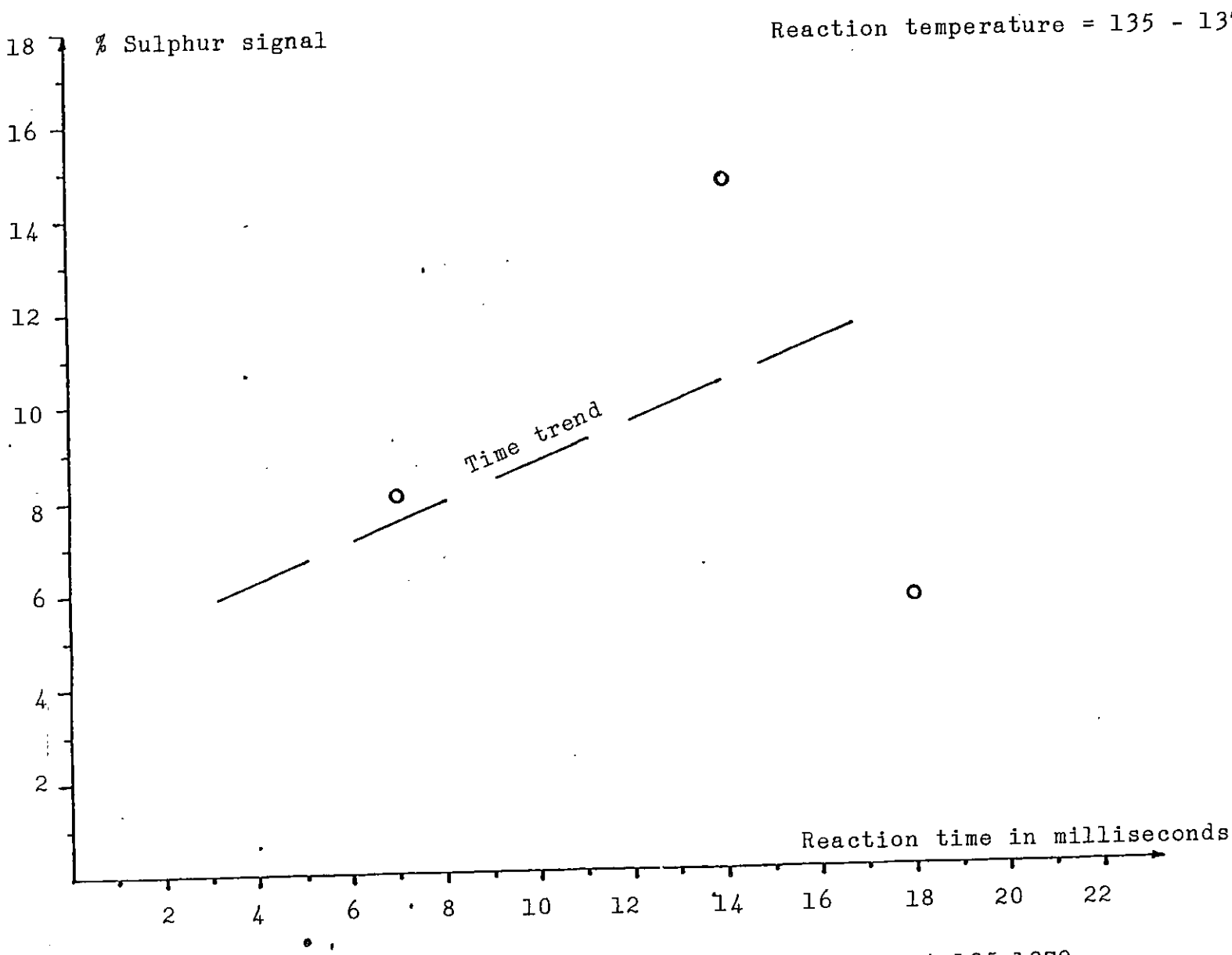

Figure 5.14 Graph of average signal versus reaction time at 135-137°C

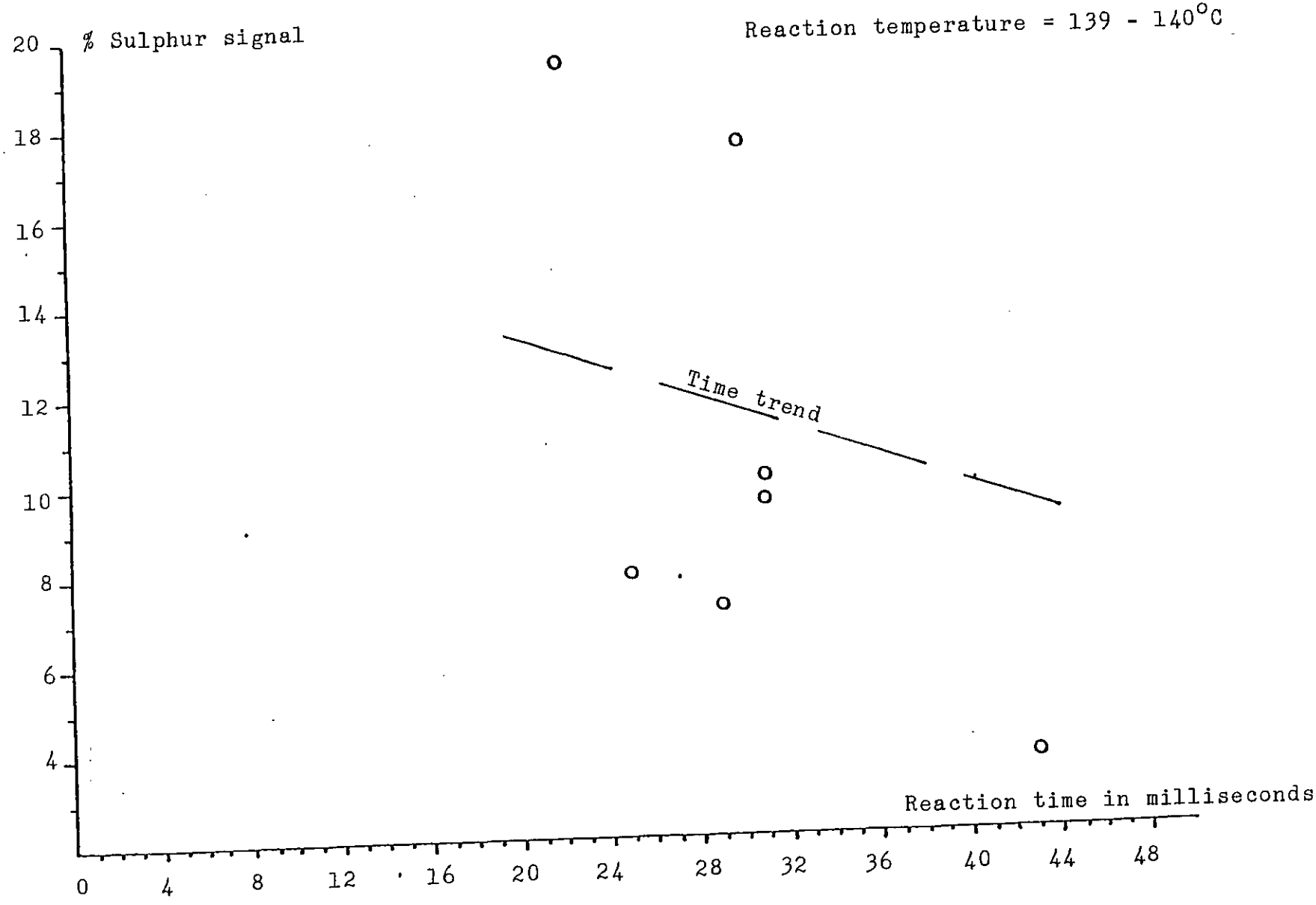

Figure 5.15 Graph of average signal versus reaction time at 139-140°C

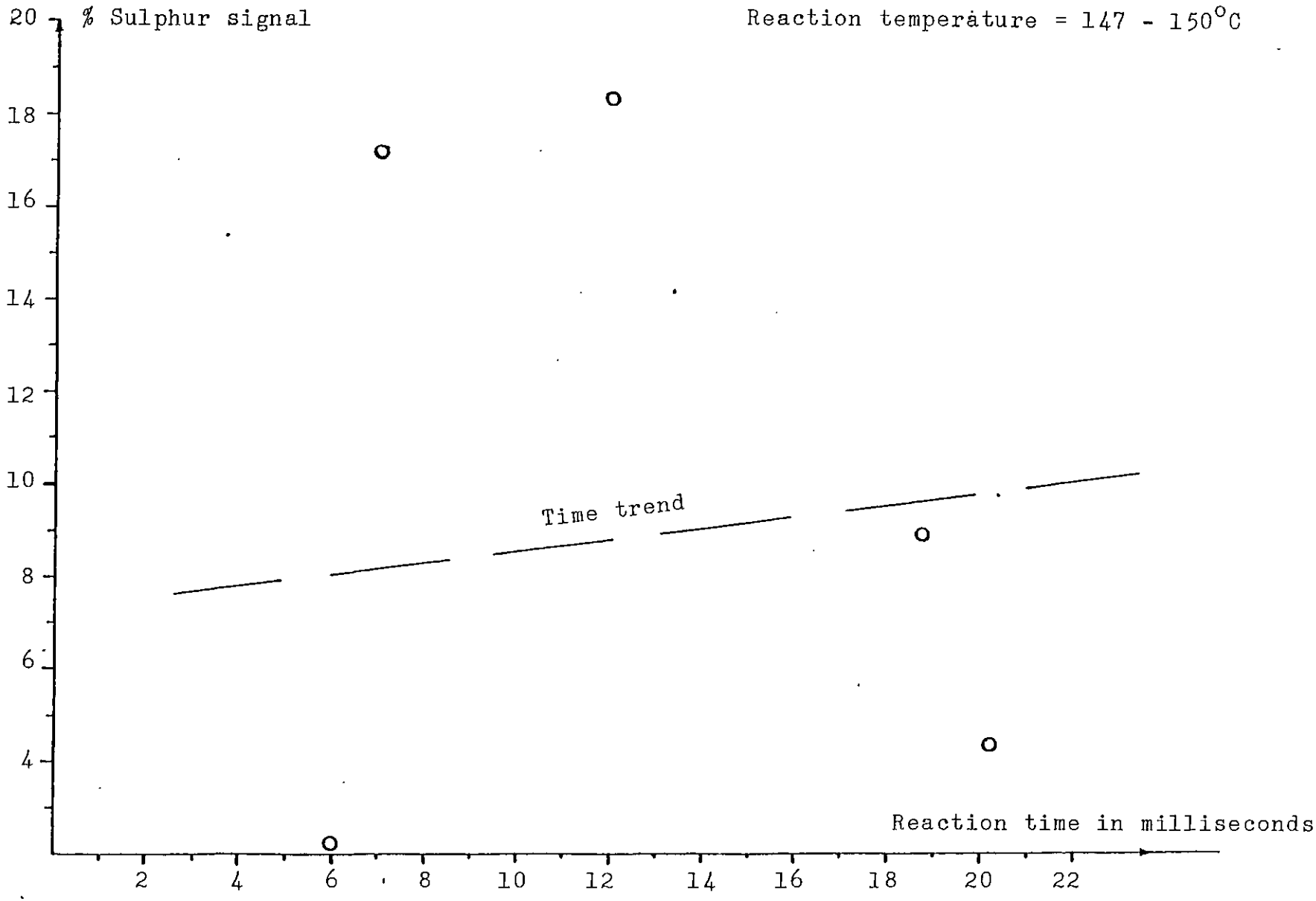

Figure 5.16 Graph of average signal versus reaction time at 147-150°C

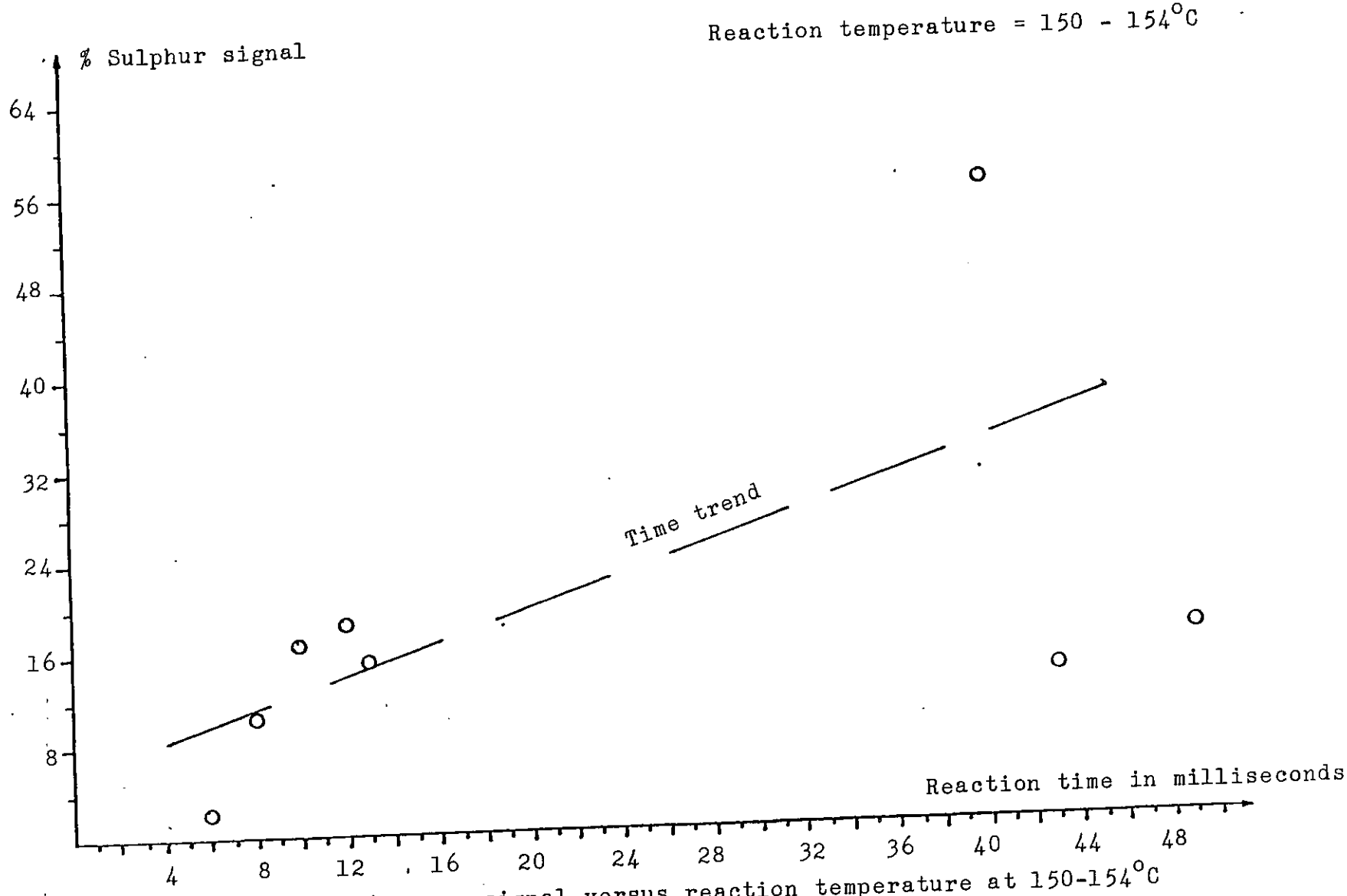

Figure 5.17 Graph of Average signal versus reaction temperature at 150-154°C

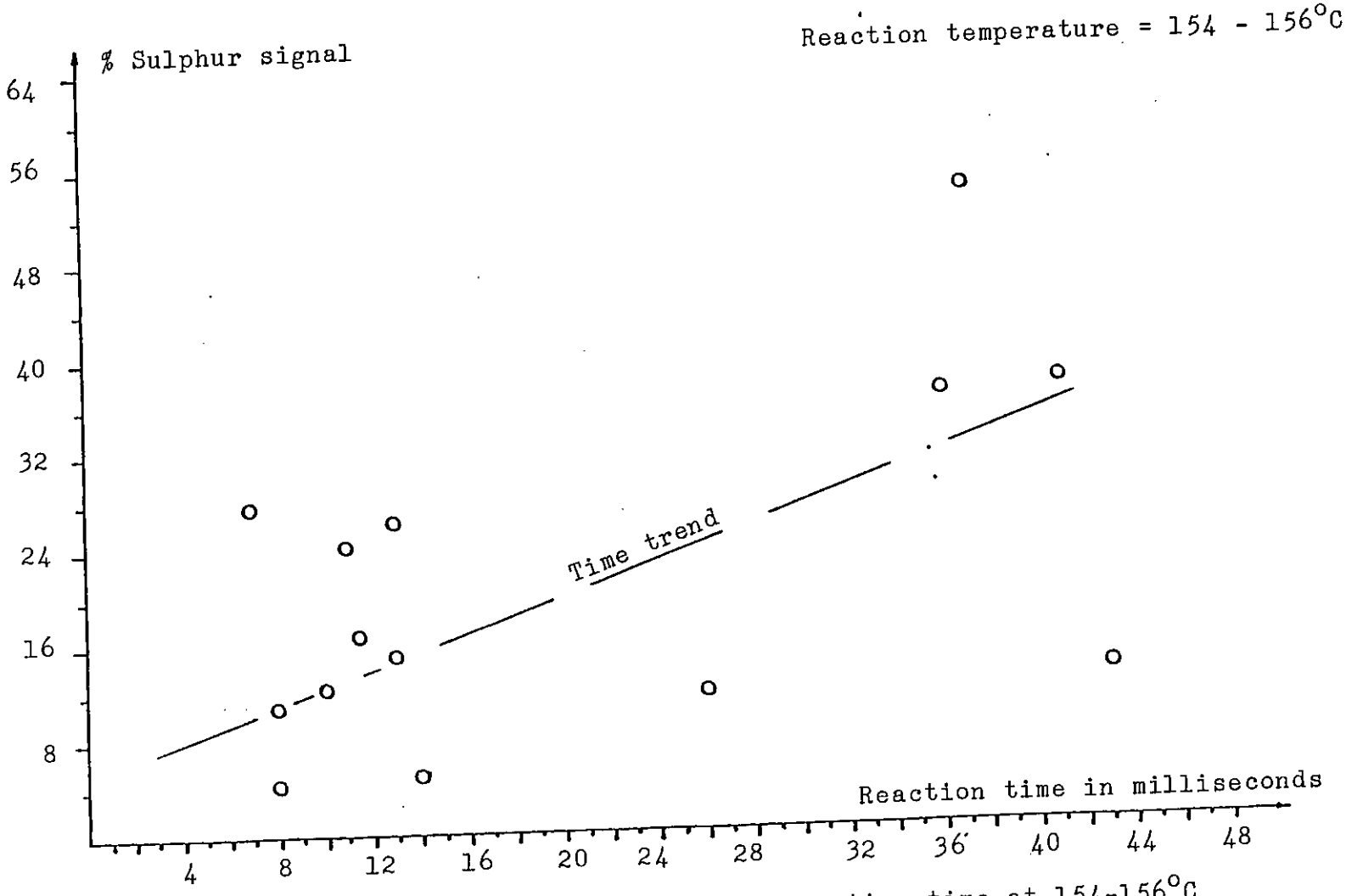

Figure 5.18 Graph of average signal versus reaction time at 154-156°C

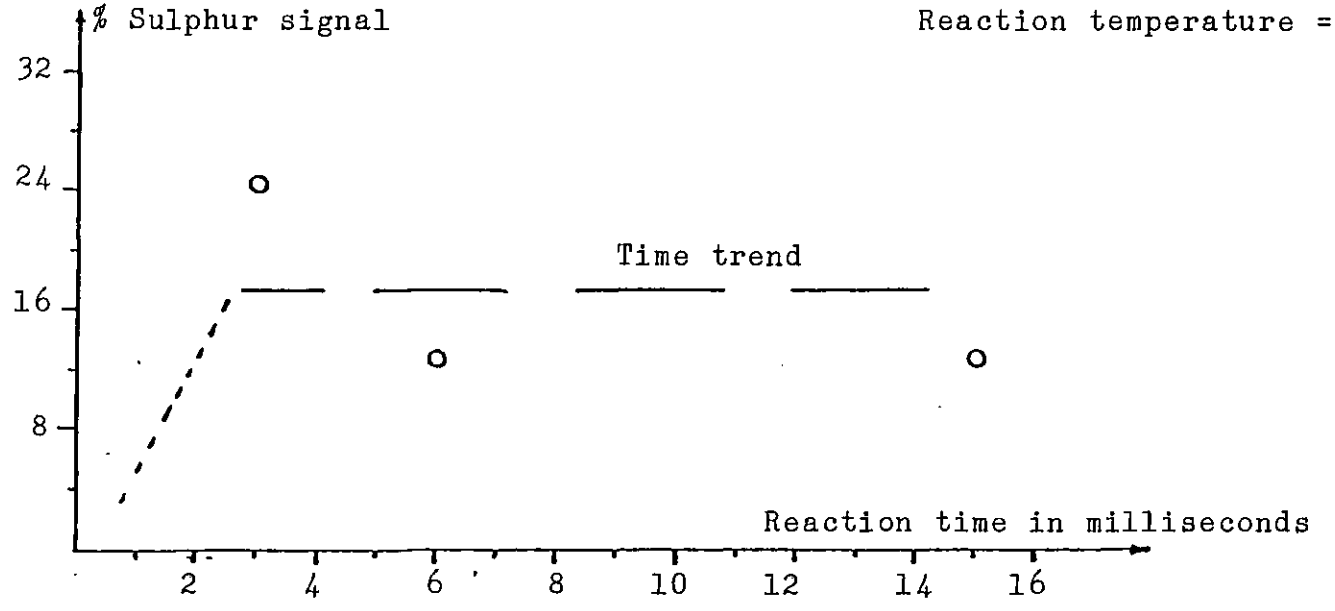

Figure 5.19 Graph of average signal versus reaction time at 162-165°C

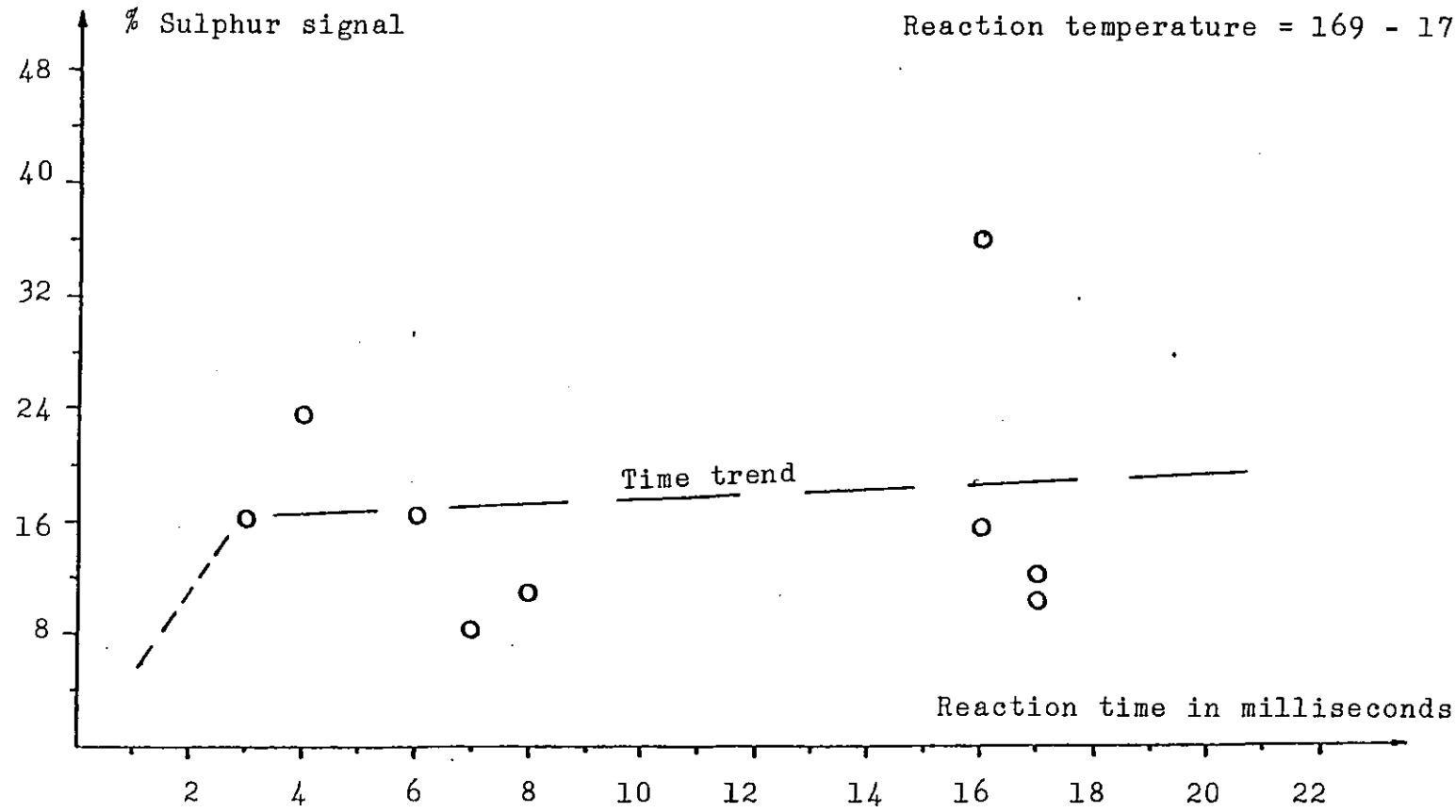

Figure 5.20 Graph of average signal versus reaction time at 169-172°C

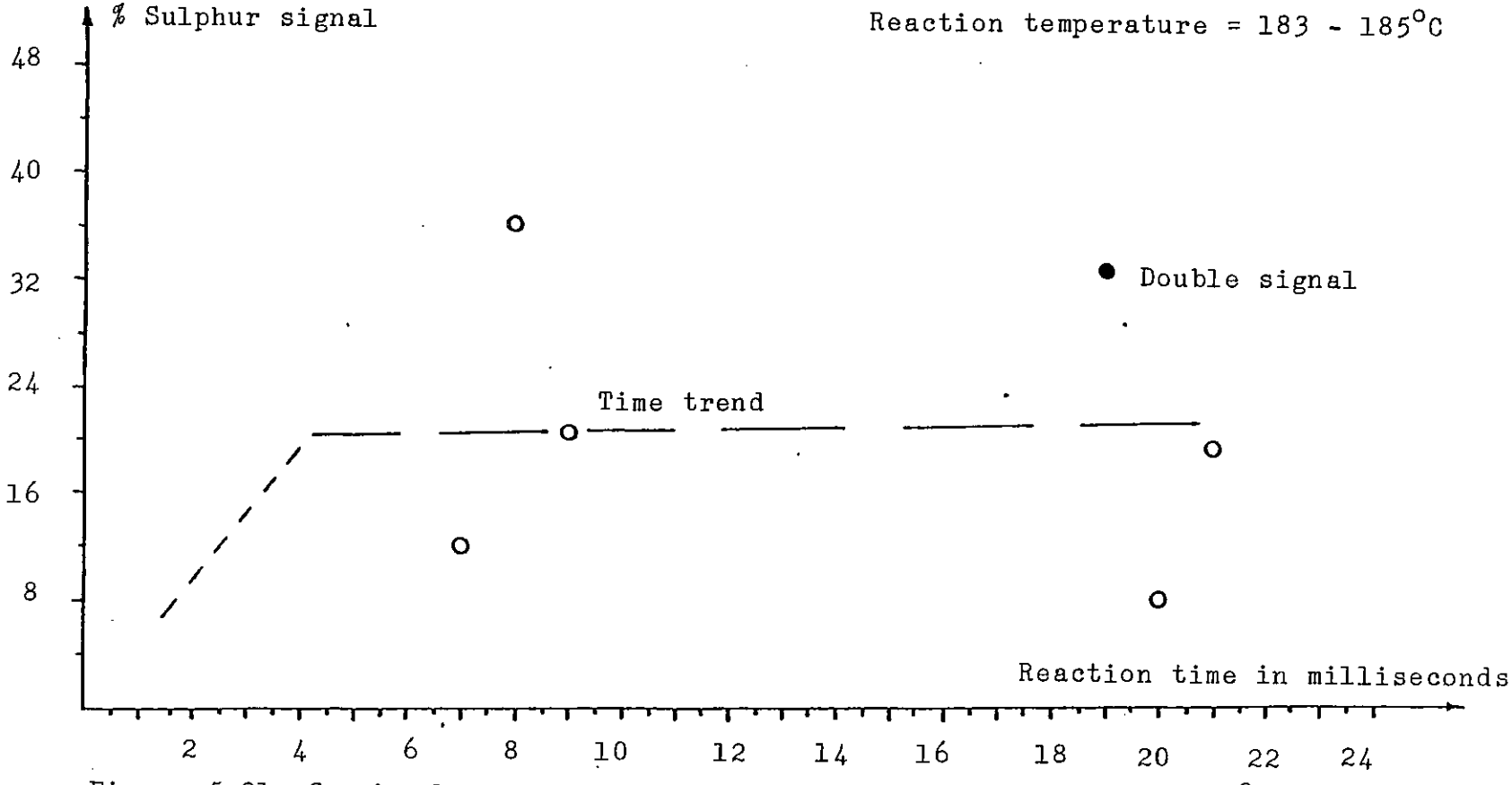

Figure 5.21 Graph of average signal versus reaction time at 182-185°C

a rate of approximately 1 Å/ms and upper limit of 30 Å can be observed.

II. If the temperature is between 130 and 150°C then the film growth rate lies in a transition between slow and fast growth. Small variations in 'surface reactivity' can make a large difference to growth rate thus a growth trend based on data from different specimens is not easily obtained. The effect is illustrated below in Figure 5.22.

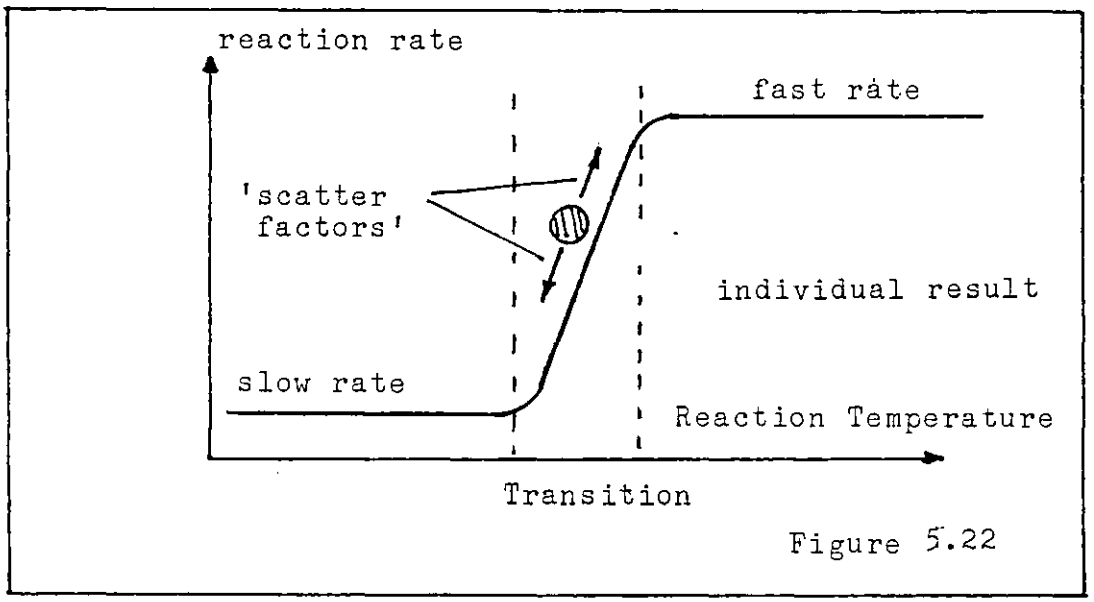

Figure 5.22

III. If the temperature lies between 150°C and 160°C, then fast unpredictable growth occurs with an approximate proportionality observable between time and film thickness.

IV. If the temperature lies between 160°C and 185°C then increasing scatter obscures any time-film thickness proportionality. A limiting thickness of ∿ 70 Å is evident. Sulphur may be reacting with the surface to form the film in a time less than 3 ms which is

shorter than the minimum reaction period which can be investigated using the test-rig in its current form.

5.6 Infra-Red Analysis

One test was devoted to the Infra-Red analysis of the film formed by sulphur. Two specimens from the test were subjected to Infra-Red reflectance spectroscopy. The instrument used was a Perkin-Elmer 580B with a 3500 data station. Radiation was scanned over the range of wave numbers 1800 to 600 cm^{-1}. Mode 2B, low noise and high energy was used. The Infra-Red beam was polarised parallel to the plane of incidence to enhance the spectra. Scanning area was 3 mm x 2 mm and a conventional beam condenser with specular reflection unit was used. Net spectra, i.e. scraped spectra - unscraped spectra, are presented with a x10 magnification. The spectra of two specimens studied are shown in Figures 5.22 and 5.24 , reaction conditions are respectively 40 ms, 105°C, and 26 ms, 170°C.

A broad iron sulphate peak at 1000 cm^{-1} is present on the specimen at 105°C but not on the specimen at 170°C. The iron sulphate would be presumably, sulphide that oxidised during the delay of several days between the test and the analysis. The lack of sulphur product on the high temperature specimen analysed provides further evidence of the unpredictability of sulphide film formation. The Infra-Red analysis does however provide evidence that a film of an iron-sulphur compound does form during the test and that only a small part of the surface sulphur could be present in elemental form.

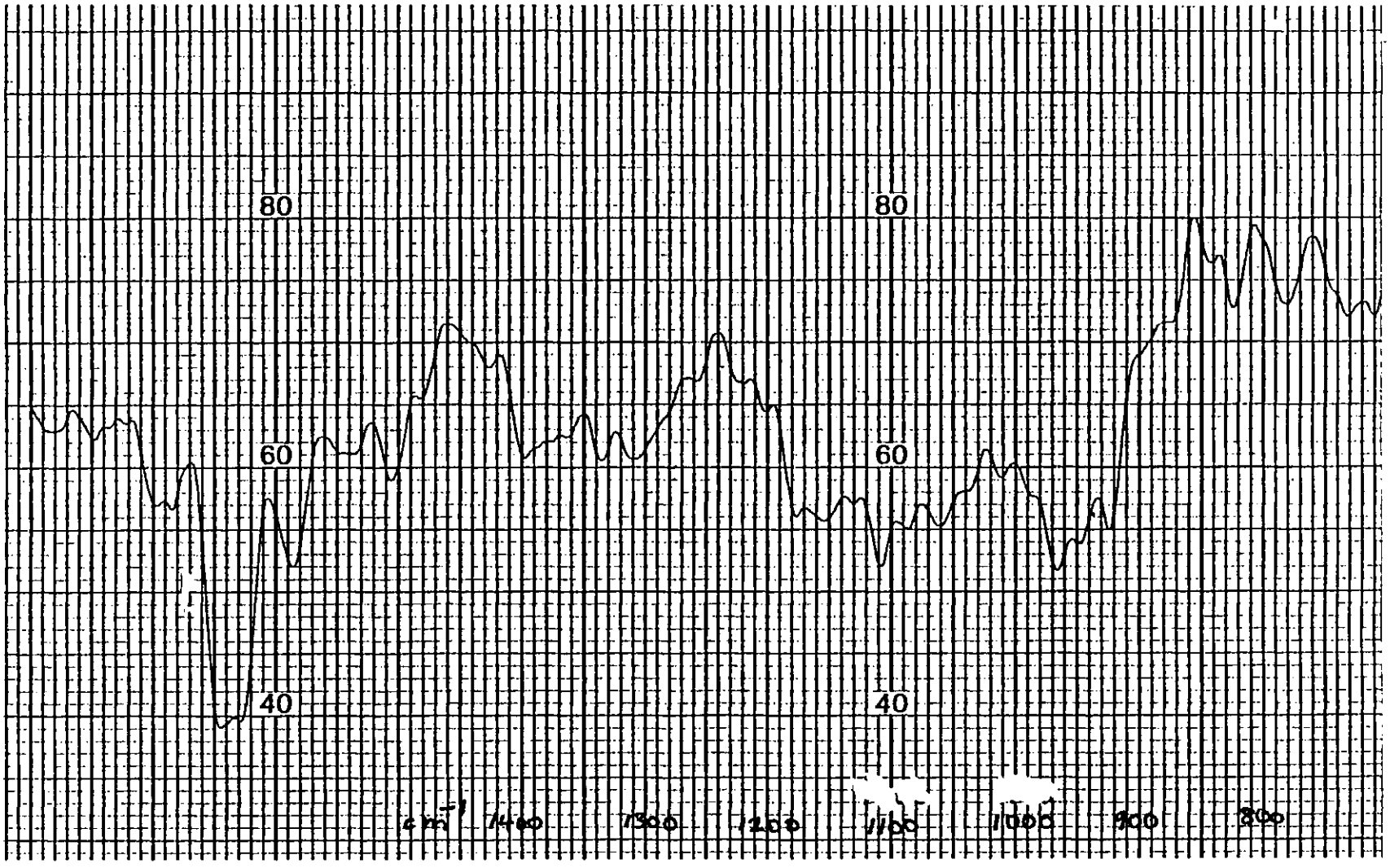

Figure 5.23 Infra-red spectroscopy of scraped surface 105°C, 40ms.

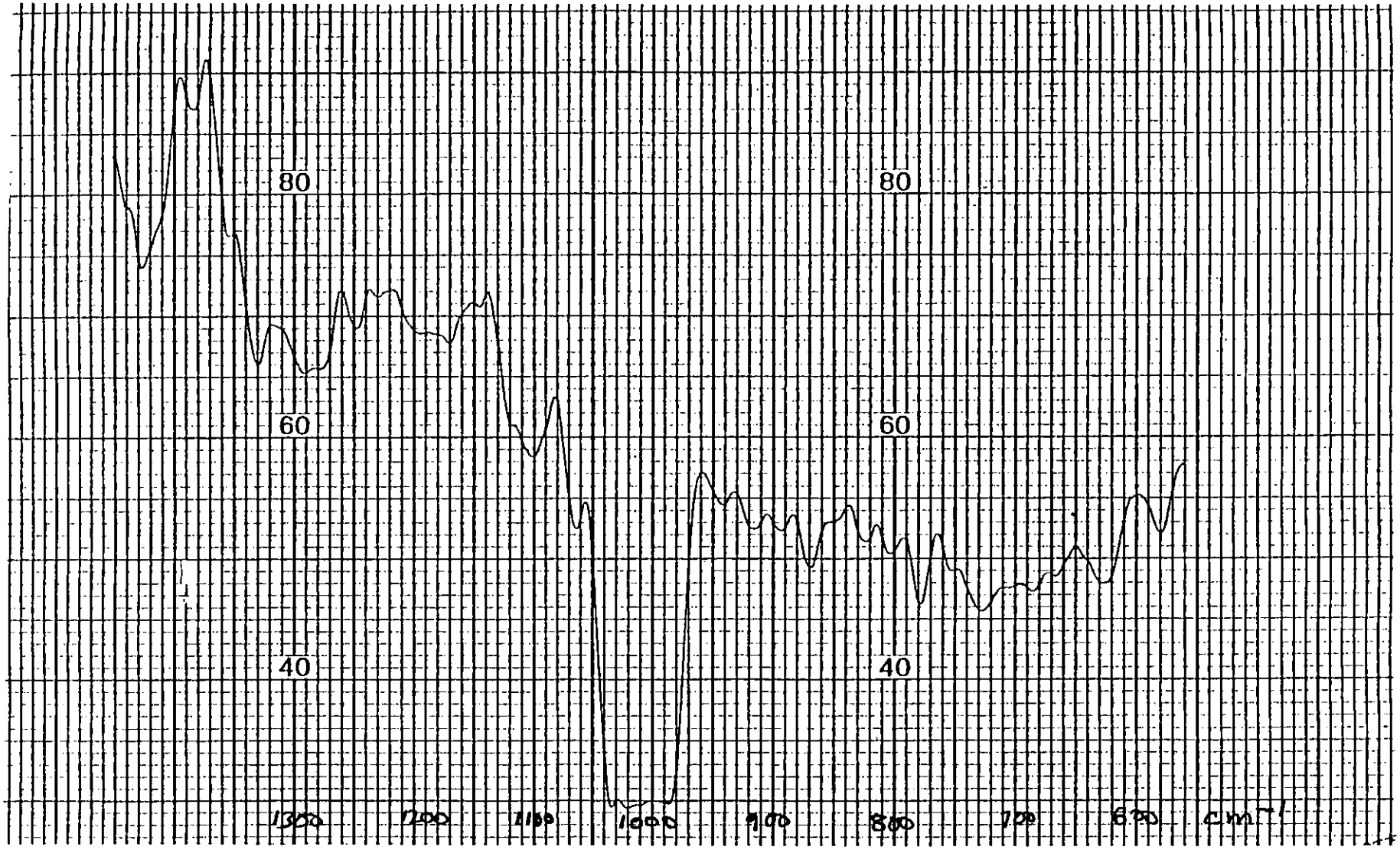

Figure 5.24 Infra-red spectroscopy of scraped surface 170°C, 26ms.

The presence of mostly elemental sulphur on the surface would be indicative of inadequate rinsing causing less soluble components of the model lubricant to be held on the surface.

CHAPTER 6

THEORETICAL IMPLICATIONS OF THE RESULTS

6.1 Introduction

Having obtained some experimental data on sulphide film growth rates, the next stage in the work was to examine the significance of the data in terms of both the theory of thin film sulphidation and the Bailey-Cameron Out-of-Contact theory. From the attempts to match the experimental results with known theory there arose several questions, of which listed below are those considered to be of principle interest.

(a) What is the mechanism of film formation by sulphur on nascent steel,

(b) Does the data support the Out-of-Contact theory,

(c) Is there a different lubrication mechanism for DBDS and other not so reactive sulphur compounds,

These questions are discussed below in this chapter.

6.2 Mechanism of the Sulphide Film Formation

The results show that a very fast form of sulphidation may occur when elemental sulphur meets nascent steel. The value of growth rate observed, 1 to 10 Å/ms, is very high for the range of temperature studied, 150-185°C.

For reasons described in Chapter 2, one would not expect that Fickian diffusion of ions through the film could achieve this order of growth rate. The very slow growth of sulphide films on oxidised steel is explained by this process (Chapter 2) but not the rapid growth observed for nascent steel. Some

form of assisted diffusion must occur in the case of nascent steel.

It is believed that the electric field in the film, caused by the electro-negativity of the sulphur with respect to the steel (as discussed in Chapter 2), is strong enough to raise the ion flux to a much higher level. The field must be strong enough to reduce significantly the outward value of activation energy. Thus a far larger proportion of the ions are mobile than would be without the field. A large ion flux will persist till the increased sulphide film thickness reduces the field to an ineffective value.

Wtih this process the Wagner parabolic equation (Chapter 2) is not applicable, instead sulphide film growth tends towards a limiting thickness as is shown in Figure 6.1.

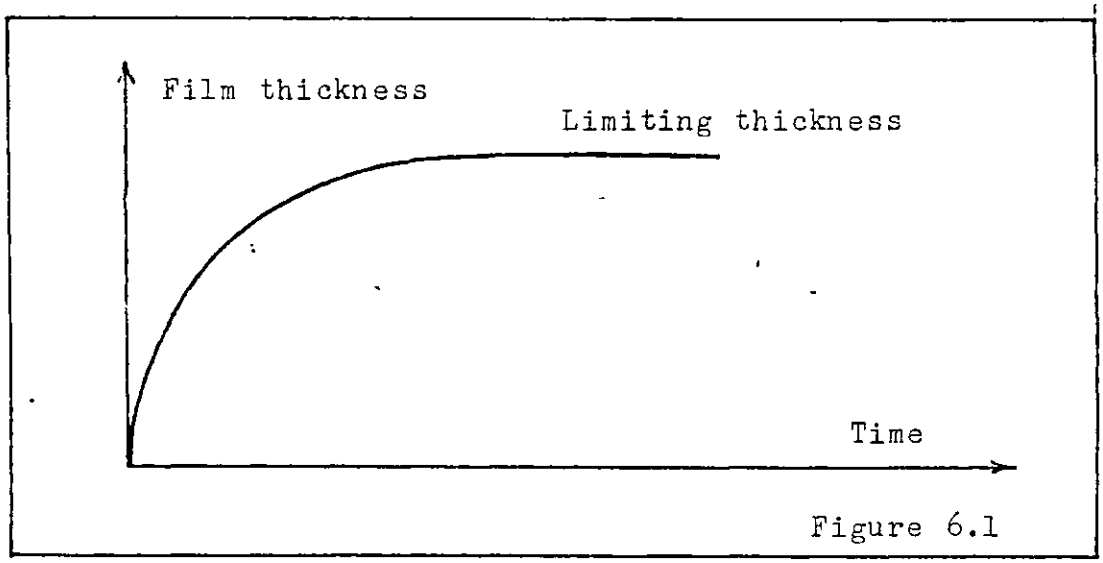

Figure 6.1

Fromhold's equation which may be more appropriate is discussed in Chapter 2.

There is no direct evidence for the theory of field assisted diffusion and values of relevant parameters,

e.g. diffusional activation energy, could not be found in the accessible literature so that it is not possible to pursue the theory further.

Mechanical activation could be highly significant, a comparison with Meyer et al's (93) work on annealed nascent iron may be of relevance. Meyer et al found a 'start-temperature' for the iron-sulphur reaction close to 200^{o}C; in the tests performed in this research work a transition temperature in the range 130-150^{o}C was observed. Mechanical activation from scraping and rolling to produce the shim, (which is the specimen material) may be the determining factor if these two transitions in reaction rate are comparable.

As discussed in Chapter 2, the low level of understanding of mechanical activation limits the discussion to merely a recognition of the effect.

6.2.1 Influence of bulk liquid on observed process of sulphidation

Compared to the diffusion limited rate for oxidation under a liquid, the observed sulphidation rate is very rapid. Sulphidation was observed to occur at something like 10 to 100 times the oxidation rates mentioned in Chapter 2. Ignoring the differences in diffusivity*, this factor of 10 to 100 approximately fits the concentration difference (sulphur 1% wt and oxygen 0.01% wt in hexadecane). Thus bulk liquid diffusion may also limit sulphidation.

---

*Literature values of sulphur diffusivity in hexadecane are not available.

Depletion of available sulphur may also have occurred during the test (as discussed in Chapter 3). The sulphur bearing lubricant is deposited as a thin layer approximately one micron thickness on the nascent steel surface (Chapter 3).

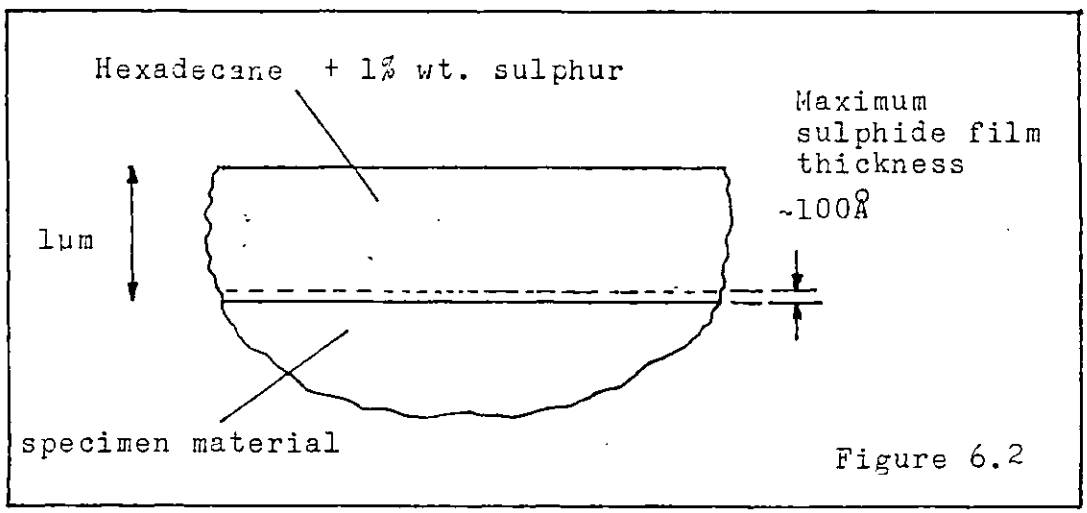

Figure 6.2

For a uniform surface reaction, sulphidation is limited to about 100 Å before depletion of sulphur occurs (Fig.6.2). So depletion proceeded by bulk-liquid diffusion limited growth may have occurred in the tests which produced ∿ 100 Å films in a few milliseconds as is shown in Figure 6.3.

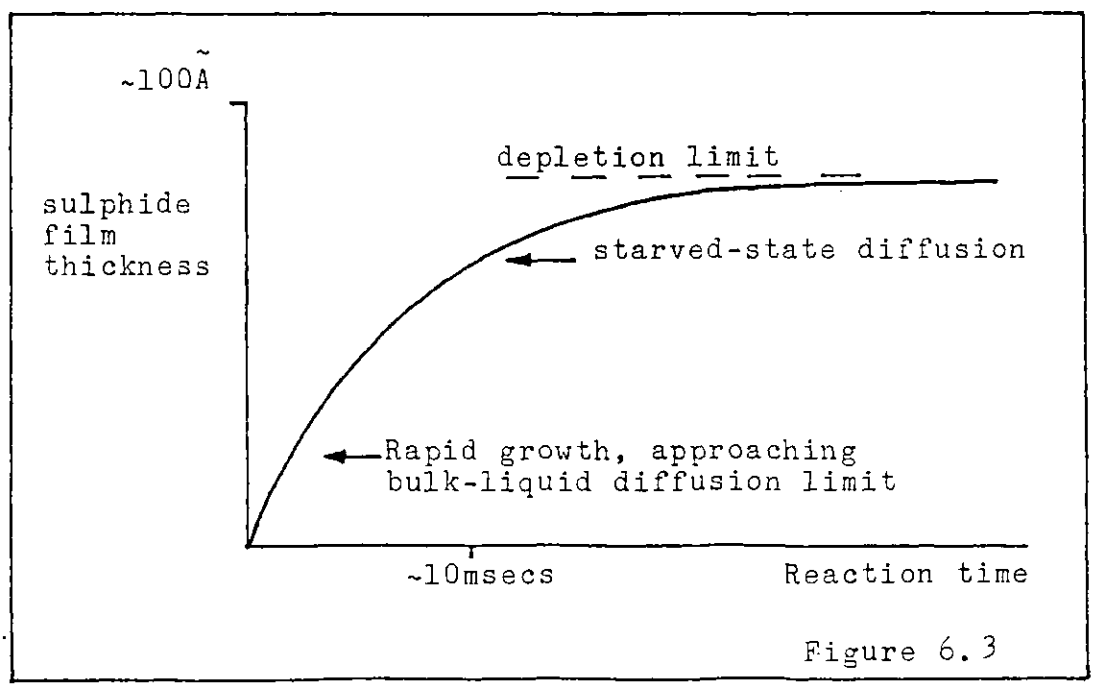

Figure 6.3

Control of sulphide film growth rate by bulk liquid diffusion agrees with the model of sulphide film growth by assisted ion diffusion. If the transport of ions through the film is rapid,then either the surface reactions at the liquid to film interface,or bulk-liquid diffusion may take over as the limiting step.

6.3 Experimental Confirmation of the Out-of-Contact Theory

The principle objective of the experimental work was to provide evidence for the Out-of-Contact theory (as discussed in Chapters 2 and 3). To test the theory, the asperity collision analysis described in Chapter 2 was applied to the experimental results of sulphide film growth rate.

Implicit in the above discussion is the assumption that the sulphide film growth rates obtained from the experimental work are similar to sulphide film growth rates on a nascent surface as produced by asperity collision. The literature discussed in Chapters 1 and 2 provide evidence that surface characteristics have a strong influence on reaction rate. For instance the extent of mechanical activation at the surface and the surface density of atomic defects and grain boundaries can have a strong influence on film growth rates. Thus it is probable that the sulphide film growth rates found by experiment and those occurring in a wearing contact will differ somewhat. No attempt is made therefore,to provide a prediction of E.P. action using the Out-of-Contact theory and experimental growth rates.

It is believed however that the change in film growth rate with varying surface characteristics is not so great as

to prevent an approximate test of the Out-of-Contact by the method described below.

6.3.1 Application of asperity contact model to test the Out-of-Contact theory

The mechanism of sulphur-based E.P. lubrication is assumed to be similar to the oxygen mechanism, except that the Cabrera-Mott theory of oxidation ( ) does not apply in this case and that the critical film thickness is different.

The following relations and quantities were defined in Chapter 2. The critical Ratio R_a such that

scuffing --- $1 \lesssim R_a << 1$ - stable operation. (2.32)

$$R_a \equiv \frac{t_{ox}}{t_{critical}} \tag{2.31}$$

where

t_{ox} = oxidation time

$t_{critical}$ = critical time or maximum time available for oxidation

The critical time available for oxidation is defined as:

$$t_{critical} = \frac{t_r}{P_c n^2} \tag{2.30}$$

where

t_r = time for one revolution

n = proportion of asperity contact surface that is virtually clean

P_c = probability of collision for any one asperity

$$= \frac{2}{\pi} \frac{L_c}{\bar{a}} \sigma \tag{2.28}$$

and L_c = inlet-outlet distance in Herz contact

$\bar{a}$ = average asperity radius

$$\sigma = \frac{\text{asperity interaction area}}{\text{Herz contact area}}$$

Assuming that instead of a 20 Å oxide film, a 50 Å to 100 Å sulphide film is needed to change a surface from 'virtually clean' to 'sulphidized'. From the experimental data, it is evident that a 50 to 100 Å sulphide film requires about 30 ms to form. Thus 't_{sulph}' the time to form the protective sulphide film is assumed to have the following value:

$$t_{sulph} = 30 \text{ ms} \qquad (6.1)$$

Comparing this value with the time, 't_{ox}' to form a protective oxide film which is 1.5 seconds, then it is evident that there is a difference of a factor of 50 in the magnitude of the two periods of time, thus for a given '$t_{critical}$'

$$\frac{R_{\text{oxygen only}}}{R_{\text{sulphur present}}} = 50 \qquad (6.2)$$

The introduction of sulphur will therefore lower the risk of scuffing by virtue of its faster growth rate. As well as considering the case of a variable 'R' and a constant '$t_{critical}$' the opposite case can also be analysed. Thus on adding sulphur to a system $t_{critical}$ may be reduced by a factor of 50 to maintain a given value of R. To vary in such a manner '$t_{critical}$', the contact frequency could be increased and so reduce 't_r', or 'σ' could be raised by increasing the load on the Herz contact.

The analysis described above refers to scuffing caused by propagation of nascent surface by collisions between 'virtually clean' surfaces on opposing asperities designated Type I collisions in Chapter 2. Type I collisions have a lower probability of occurring than collisions where one asperity surface is virtually clean and the other is covered with oxide or sulphide (designated as Type II collisions). Thus the 'R_a' value associated with Type II collisions (represented as R_{II}) is higher than the 'R_a' value due to Type I collisions (represented as R_I).

Should R_{II} reach a critical value because only oxygen is present, then the addition of sulphur will reduce R_{II} to a lower value by the same principle as discussed above for 'R_I' (or 'R_a' as it is written above).

Type II collisions are believed to be critical when there is little or no adsorbent on the oxide or sulphide surfaces. Moderately adhesive contacts between nascent metal and film covered surface could then occur, leading to removal of the film present (as discussed in Chapter 2).

Summarising then, the Out-of-Contact theory can explain some of the crucial aspects of E.P. action by sulphur, such as the ability to lubricate under much higher loads and speeds than oxygen alone and an independence of adsorbed lubricity agents.

6.4 Mechanism of E.P. Action

An illustration of the mechanism hypothesised of E.P. action is shown in Figure 6.4.. The figure incorporates the work of Bailey and Cameron (3) and Spikes (23) and others.

Four important features of the mechanism are:

(a) The 'growth stress' as described in Chapter 2 in the sulphide film which ensures sacrificiality on asperity collision.

(b) Pressure block to reaction within the EHL zone. With organic fluids lower the solute diffusivity is drastically reduced or raising pressure (Chapter 2).

(c) The tail-end of the EHL zone is the part of the wearing contact most conducive to E.P. film growth.
The solute diffusivities and temperature of the lubricant are highest at this point. A deviation from the strict out of contact theory which states that reaction rate must be directly proportional to the out-of-contact distance may thereby occur. The length of the conjunction temperature tail is proportional to the E.H.L. contact length and not to the Out-of-Contact distance.

The length of the E.H.L. contact is of the order of a millimetre which is small compared to the Out-of-Contact circumference which is of the order of 100 mm. The conjunction-temperature 'tail' which is similar in length to the E.H.L. contact length is therefore not likely to raise the temperature of the rotating surface for a time sufficient to markedly affect total film formation.

Illustration of theory of E.P. action in a twin disc rig

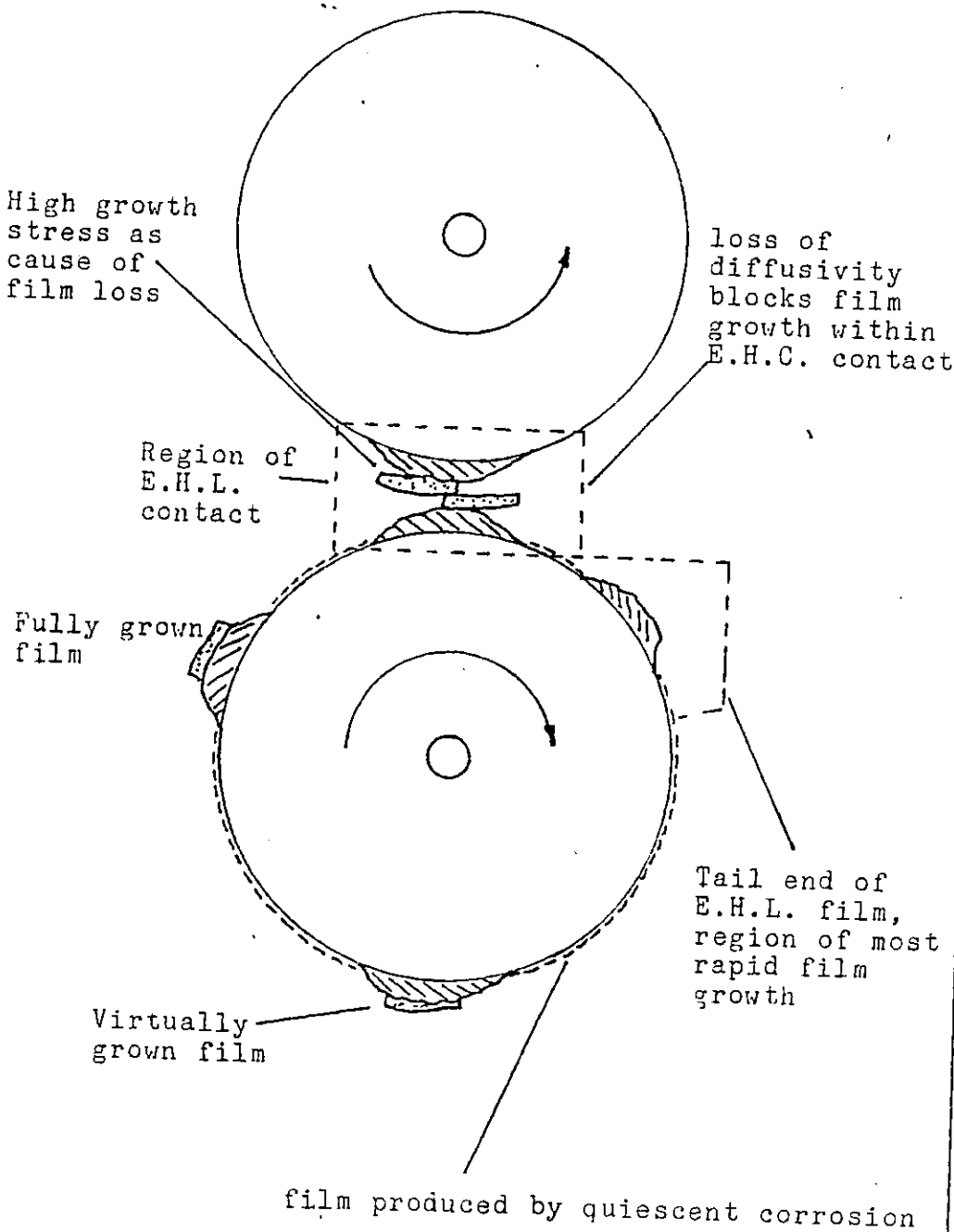

Figure 6.4

(d) Slow corrosion by oxygen or sulphur of the rotating surface not covered by asperities occurs when the overall operating temperature of the surface is high enough. The mechanism and rate of this mode of chemical attack by oxygen or sulphur is not believed to be directly related to the E.P. mechanism.

6.5 Mechanism of DBDS and Other Less Reactive Compound Action

Fast sulphidation was not observed for DBDS, thus the Out-of-Contact theory as developed for sulphur will not apply in this case and a different mechanism of E.P. action has to be proposed.

Date (34) in a recent work discovered that slightly oxidised sulphide films (i.e. sulphate covered) adsorbed stearic acid and similar surfactants very strongly. There is evidence in the literature that adsorbed species can reduce tangential forces in an asperity collision (68). It is suggested therefore that provided there is an adsorbed species on top of the load-bearing film it is unlikely that the load-bearing film is removed by a single asperity collision. There is also evidence that oxygen boosts E.P. action by organo-sulphurs (Chapter 1), thus a hypothesis invoking the combined action of oxygen and sulphur appears to be appropriate.

The hypothesis starts from the consideration of a growing sulphide film which is also subject to oxidation, and to form perhaps sulphate. There will be a mixture of sulphate and sulphide and perhaps some iron oxides (which

are not considered in this case) within the film. The question is what is the ratio of sulphide to sulphate? A control volume analysis which was used to find this result is described below.

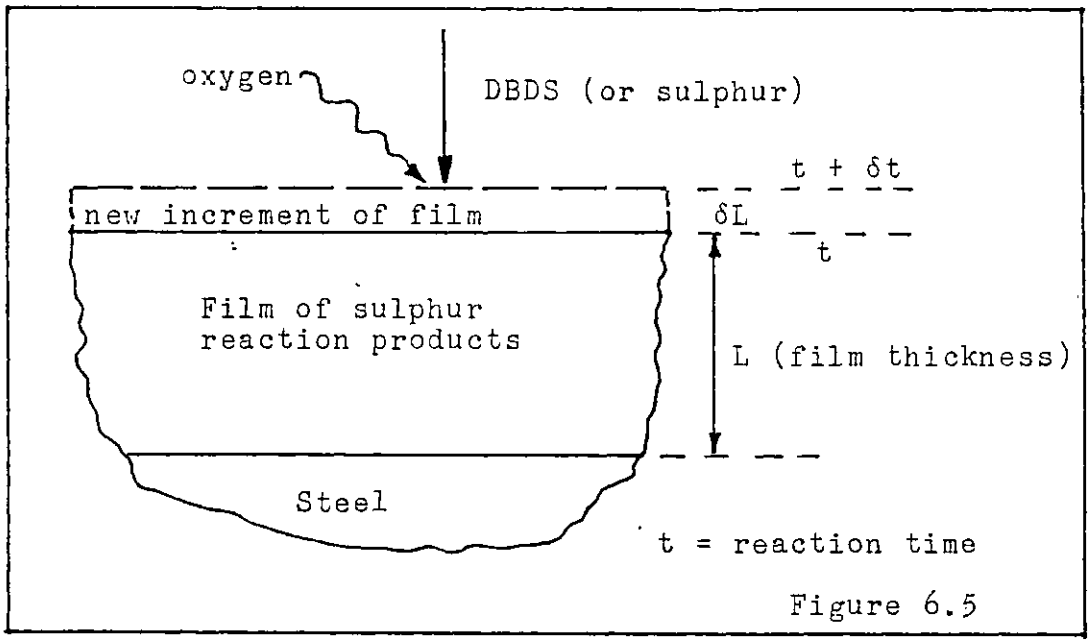

Figure 6.5

Referring to the following equations were devised within the new increment of film.

$$Fe + S \xrightarrow{V_2} Fe\,S \quad \text{I} \quad \text{Formation of sulphide} \tag{6.3}$$

$$FeS + 2O_2 \xrightarrow{V_2} FeSO_4 \quad \text{II} \quad \text{Subsequent oxidation to sulphate} \tag{6.4}$$

where k_1 k_2 are reaction velocities.

Thus

$$\frac{[FeSO_4]}{[FeS]} = \frac{V_2\,\delta t}{(V_1 - V_2)\delta t} \tag{6.5}$$

$$= \frac{V_2}{V_1 - V_2} \tag{6.6}$$

For sulphur, presumably $V_1 >> V_2$ since V_1 is very large. For DBDS however, V_1 is small thus it is possible that $V_1 \approx V_2$ and a high concentration of sulphate results. Furthermore V_1 which is proportional to film growth rate is always falling with 'sulphide' film thickness so that a critical film thickness may result where V_1 tends to V_2 or some multiple therefore.

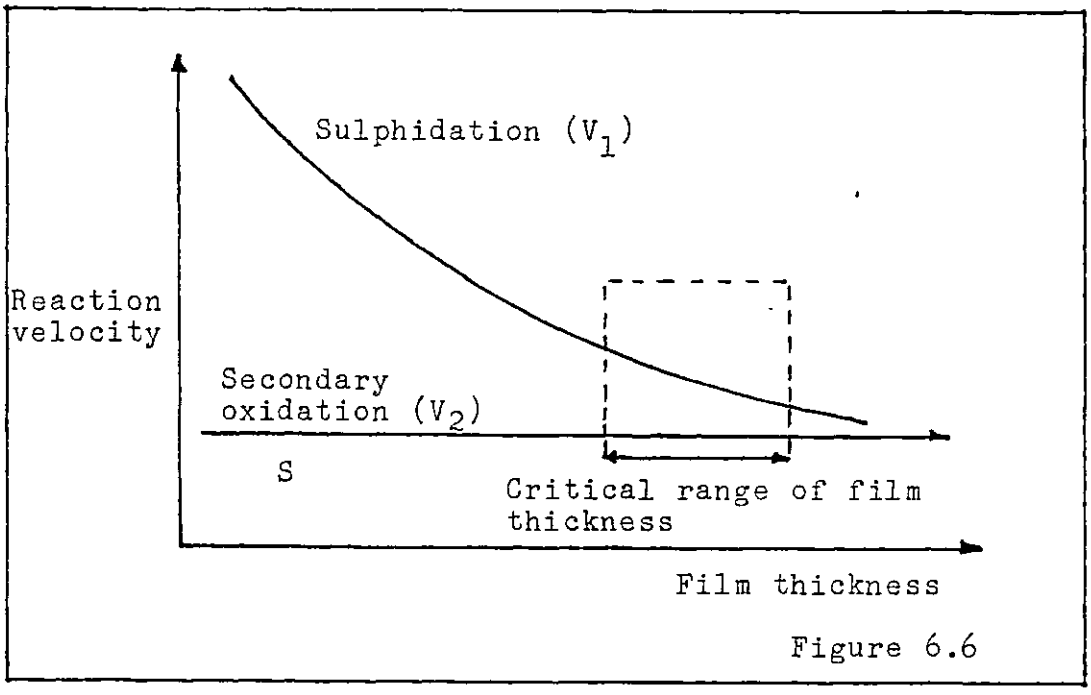

Figure 6.6

The critical film thickness for DBDS may be one where the sulphide formation rate falls to a low enough level to permit a high concentration of sulphate. The surfactants i.e. DBDS or fatty acids are then bonded to the surface with a higher heat of adsorption than for pure sulphide and the "Critical Temperature" to drive off the surfactants is thereby raised (34).

There is not the data available to support this, but at a temperature greater than 200^{o}C, DBDS should revert to the mechanism of E.P. action by fast sulphide film growth.

CHAPTER 7

SUMMARY, CONCLUSIONS AND SUGGESTIONS FOR FUTURE WORK

7.1 Summary

The work was originally divided in two stages. The first stage was to develop a test-rig enabling the measurement of the growth of sulphide films under conditions similar to those occurring in the regime of E.P. lubrication. In the second stage of the work, experiments were performed using the test-rig and data on sulphide film growth rates under E.P. conditions obtained.

The test-rig was designed to meet experimental requirements deduced from the evidence of the available literature concerning E.P. lubrication and the study of sulphide film formation. All the sub-systems of the test-rig, such as the scraping machine, the model lubricant supply and rinse-off systems were developed with the purpose of ensuring the greatest possible similarity between experimental conditions and those believed to occur in the E.P. regime. The experimental methodology relating to the use of the test-rig was developed with the objective of obtaining the widest possible information about the phenomenon of sulphide film formation under E.P. conditions.

The range and number of results obtained which were limited by experimental requirements were sufficient to prove that the test-rig functions in the desired manner. The results also sufficed to enable elucidation of some fundamental aspects of sulphide film growth under E.P. conditions and to provide evidence in support of a theory explaining

the basic mechanism of E.P. lubrication, i.e. the Bailey-Cameron Out-of-Contact theory (as mentioned in Chapter 1).

The Bailey-Cameron theory has been further refined to provide a more detailed explanation of the processes occurring in E.P. lubrication.

A hypothesis concerning E.P. action by oxygen has also been developed.

7.2 Conclusions

The conclusions drawn from the work presented are discussed below.

7.2.1 The experimental results confirm the findings of other studies of E.P. lubrication: that on a nascent steel surface an iron-sulphide film is formed far more rapidly than on an oxide covered surface. Sulphide film growth rates of the order of 10^3 to 10^4 Å/s were measured, whereas steel covered by an oxide film has been shown by other workers to form a sulphide film at a rate of $\sim$ 1 Å/sec. The thin 50 to 100 Å depth film of iron oxide commonly found on steel surfaces can exert a remarkable influence on the physico-chemistry of iron and steel.

7.2.2 Though an approximate proportionality between reaction time and iron-sulphide film thickness was observed, the scatter in the results indicates that other controlling parameters are of importance. From theoretical considerations (Chapter 2) epitaxy and the local degree of surface mechanical activation ought to be considered.

7.2.3 The strong effect of temperature in the experimental data of sulphide film growth rates is in agreement with the observed sensitivity of E.P. lubrication to operating temperature. The experimental data for elemental sulphur provides evidence of a transition in the temperature range 130-150°C separating two levels of film growth rate differing by a factor of 10. A temperature dependence of fast sulphide film growth (i.e. the 10^3-10^4 Å/s rate mentioned in 7.2.1) which is believed to be the basis of E.P. action has been demonstrated. The higher level of film growth was also found to be associated with a greater degree of variability of sulphide film thickness over the reaction surface.

7.2.4 It was found that the scatter in the experimental data of iron sulphide film growth rate necessitated the use of statistical techniques to evaluate the data. A dense coverage of the time-temperature parameter space is needed if a close estimate by multiple regression analysis of the dependence of film growth rate on these two parameters is to be obtained.

The average of several small area analyses obtained by E.D.A.X. proved to give the best (or most reliable) estimate of the amount of sulphur on a specimen.

7.2.5 The large difference in film formation rates (revealed by the data) between sulphur and DBDS indicates that for most sulphur compounds, 'rapid' sulphidation of nascent metal is limited by the rate of decomposition of the compound

to produce sulphide ions. The limiting stages of the film formation process therefore occur at the liquid-film interface and not within the film itself.

7.2.6 The rapid growth of iron sulphide films on nascent steel occurring when elemental sulphur is present may be caused by field-assisted diffusion of ferrous or sulphide ions through the sulphide film. The Wagner parabolic law of film growth is therefore unlikely to be applicable; film growth would instead tend to a limiting thickness.

7.2.7 Diffusion through the bulk liquid to the reaction surface by sulphur may be a limiting factor for sulphide film growth. Depletion of available sulphur can occur if the depth of liquid over the reaction surface is of the order of a micron. Limitation of sulphide film growth by depletion and bulk liquid diffusion is almost certain to occur for solute concentrations of sulphur less than the 0.75 wt % studied.

7.2.8 From an analysis of asperity collision rates in partial E.H.L., it is concluded that the rapidity of sulphide film growth on nascent steel surface compared to oxide film growth on nascent steel surface explains the superiority of sulphur over oxygen in E.P. lubrication. The Out-of-Contact theory is confirmed as an explanation of E.P. action and the prevention of scuffing.

The higher solubility in oils of sulphur than oxygen is also believed to be a factor promoting the E.P. action of sulphur.

7.2.9 The work shows that iron sulphide films can be formed very rapidly on nascent steel. This rate is not, however believed to be sufficient to enable the formation of sacrificial E.P. films with thicknesses ranging from 1,000 to 5,000 Å in the conditions prevailing in the E.P. regime. If the E.P. film is to be sacrificial i.e. removed on the first wearing contact, then its thickness must be less, 100 to 500 Å is believed to be the probable range of thickness.

7.2.10 Dibenzyl disulphide was found to be less reactive than elemental sulphur. The Out-of-Contact theory as applied to sulphur does not appear applicable for DBDS. A different mechanism involving secondary oxidation of iron sulphide to iron sulphate has had to be invoked. Iron sulphate is known to have a higher heat of adsorption of many lubricity agents than iron oxides. The desorption temperature of for example stearic acid, is highest on iron sulphate. DBDS could therefore act by raising the temperature limit of adsorption-based lubrication.

7.2.11 It is believed that a large reduction in solute diffusivity occurs in the E.H.L. contact resulting from the high pressure involved and that there are high stresses in the E.P. film caused by rapidity with which the film grows. These are effects confirmed by other fields of science such as high pressure liquid state chemistry and thin film physics. The former effect explains why the Out-of-Contact period should be critical for E.P. film growth and not the period of time spent in the E.H.L. contact by any one point

on the wearing surface. This is despite the higher surface temperatures occurring within the E.H.L. contact than in the Out-of-Contact region.

The latter effect explains why virtually any asperity contact should remove an E.P. film from the surface, thus causing the E.P. film to act in a sacrificial manner within the E.H.L. contact.

7.2.12 Kinetic properties appear to be critical to the performance of sulphur-based E.P. lubricants. For instance, it is believed that the crucial difference between iron sulphides and iron oxides as components of the E.P. mechanism lies not in the frictional coefficient of films composed of these substances, but in properties determining film growth rate under E.P. conditions. Iron sulphide films grow in general faster than iron oxide films, a condition which is to a large extent due to the more defective crystalline structure of iron sulphides compared to iron oxides.

As discussed in 7.2.8, the higher solubility of sulphur than oxygen in oil also ensures that sulphur-based E.P. films grow faster and are more effective than oxygen-based E.P. films.

7.3 Suggestions for Future Work

Some problems for future research that follow directly from the work presented above are discussed below.

7.3.1 Methods of examination of worn surfaces could be refined to enable discrimination of the small fraction of the

surface that is subject to frequent asperity contact from the larger fraction of the surface that is not. If this refinement of technique is achieved then it would be possible to search for the hypothesised thin load bearing films as opposed to the thicker films believed to be formed by quiescent corrosion.

7.3.2 The mechanism of E.P. lubrication is still far from being well understood. The science of thin oxide and sulphide films should be studied further as this subject could yield vital clues to the E.P. mechanism.

7.3.3 The investigation of E.P. film formation ought to be extended to cover the widest possible range of conditions. Three courses of action are suggested below.

7.3.3.1 It is important to test the applicability of the current Out-of-Contact theory to all E.P. lubricants in common use.

A large number of E.P. lubricants based on sulphur or other elements such as phosphorous and chlorine therefore await experimentation by the technique developed in this work.

7.3.3.2 A wider range of surface analysis techniques e.g. X-ray photo-electron spectroscopy could be used in future experimental work in order to obtain a more extensive knowledge of the structure and composition of the E.P. film. Such a knowledge is essential to the prediction of both E.P. film growth rates and of aspects of the E.P. mechanism as yet unknown and impossible to observe directly due to experimental difficulties.

7.3.3.3 The test-rig could be modified to extend the ranges of reaction time and temperature investigable. No severe difficulties are anticipated in raising the maximum reaction temperature and time. The reduction of the minimum reaction time however, is believed to be severely hindered by the limitations of mechanical design relating to the test-rig. The level of acceleration of scraping speed required by the shorter reaction times would be expected to cause particular difficulty.

7.3.3.4 It is of profound importance to correlate the formation of an E.P. film with its friction and wear characteristics. In other words, search for the hypothesized critical thickness, reaction time and temperature of E.P. films whereby friction is reduced from seizure values to a level where scuffing is unlikely to occur. Two approaches could be used. The first mentioned which is the simpler of the two is to test specimen surfaces (produced by the technique described in this work) in a Bowden-Leben machine (68) and relate the friction characteristics to the E.P. film present. This approach has the drawback of allowing decomposition of the film prior to testing on the Bowden-Leben machine.

The other approach which is illustrated in Figure 7.1 is to remove the rinse jet from the test-rig and replace it with a friction measuring stylus. Measurements of friction of the film as it is formed could be thereby obtained.

The worn surface could be subsequently examined for further information about the nature of wear occurring

i.e. indicative of seizure of or mild wear. Some means would however have to be found of avoiding hydro-dynamic effects or excessive conjunction temperatures, as scraping speeds are high ∿ 3 to 10 m/s .

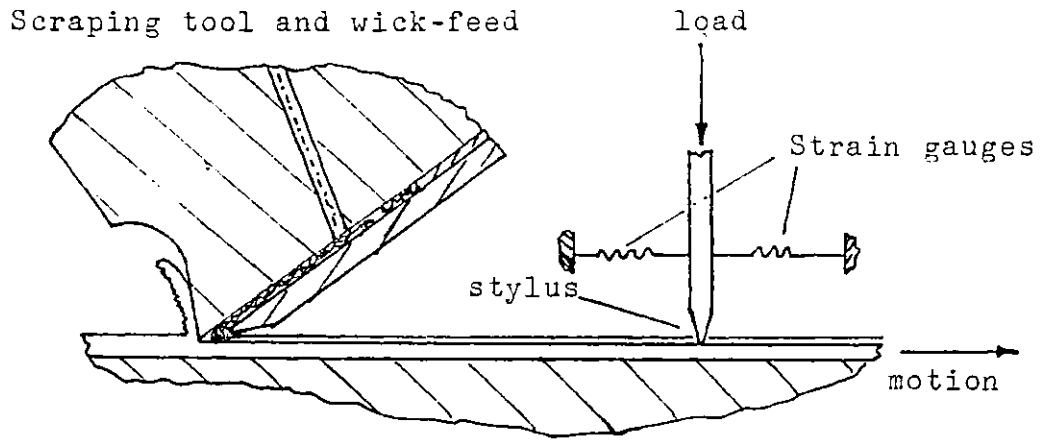

Figure 7.1

APPENDIX 1 : A THEORETICAL AND EXPERIMENTAL INVESTIGATION OF THE TEMPERATURE AT THE TIP OF THE SCRAPING TOOL.

Introduction

A knowledge of the temperatures of the scraping tool-tip and scraped surface close to the tool are of vital interest to the estimation of the influence of temperature fluctuations (caused by scraping) on the experimental E.P. film growth rates. This Appendix describes the work done to measure the tool-tip temperature and the importance of tool-temperatures is discussed in detail further to that of the main text.

Theoretical estimation of the scraping temperature

Boothroyd (146) gives an expression (which is described below) for the temperature at the tip of a cutting tool.

$$\theta_s = \frac{(1-\Gamma)P_s}{\rho c v a_c a_w} \qquad (A1.1)$$

where:

θ_s = average temperature rise of the material passing through the primary deformation zone = temperature rise of metal just beneath the cut depth.

Γ = Partition coefficient i.e. proportion of heat to the chip.

P_s = Power expended on cutting

ρ = density of the material that is being cut.

c = specific heat of the material.

a_c = depth of cut.

a_w = width of cut.

v = velocity of cutting.

A calculation of scraping tool-tip temperature based on the Boothroyd expression is described below.

Calculation

(a) It is assumed that, $\Gamma = 0$ for an estimate of maximum possible temperature rise.

(b) P_s/v = Cut force = 200N.

(c) Values not discussed above:

$\rho = \rho_{steel} \simeq 8 \times 10^3 kg/m^3$

$c = c_{steel} \simeq 4.5 \times 10^2 J/kgK$

a_c = depth of cut $\simeq 2.5 \mu m$

a_w = width of cut = 5mm.

Thus the calculated value of θ_s, the tool tip temperature is given by the following expression:

$$\theta_s = \frac{200N}{8\times10^3 kg/m^3 \times 4.5\times10^2 J/kgK \times 2.5\times10^{-6} m \times 5\times10^{-3} m} \quad \text{(Kelvins)}$$

$$= \frac{1}{225} \times \frac{10^2 \times 10^9}{10^5} \quad K$$

$$\simeq 4{,}400 \text{ K.}$$

This high calculated value of temperature implies that the tool should melt or soften, even if the partition coefficient is not equal to zero but instead reaches 0.8. Thus the formula is regarded as inapplicable and experimental results are considered more valid.

Experimental investigation of the cutting temperature

Two experiments, both of which involved an application of the dynamic thermocouple principle (43) were carried out. In the first experiment to be performed, a workshop scraping

tool was drawn over a copper plate and the change in voltage in the measuring circuit noted. The experiment is illustrated in Fig.(A1.1).

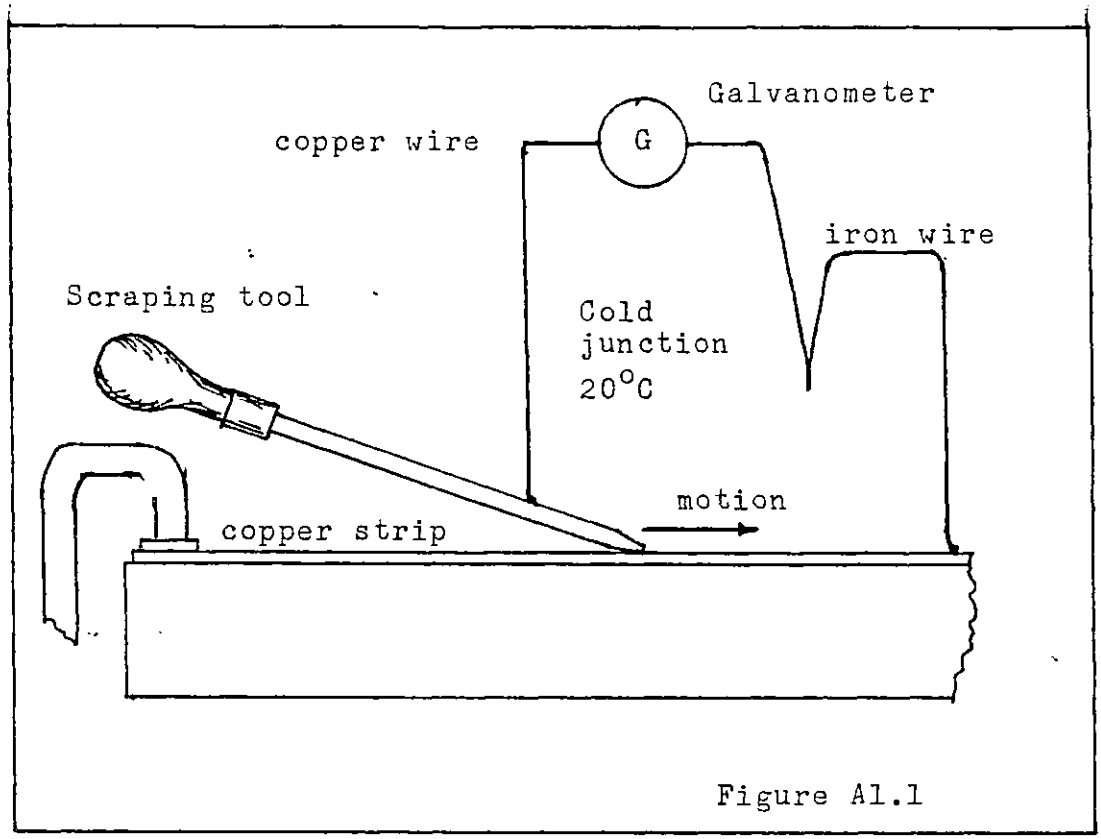

Figure A1.1

A voltage change of about 0.02 to 0.04mV was observed when the scraping tool was in motion. By comparison, if the cold junction (Figure A1.1) was heated from 20°C to 50°C a voltage rise of 0.06mV occurred with a sense oppposite that produced by the scraping tool. Assuming a direct proportionality between voltage rise measured and tool-tip temperature rise relative to the cold junction, the tool tip temperature in this case lies between 10 and 20°C.

The latter experiment which involved a scraping tool and a copper tube rotating in a centre lathe is illustrated in

Figure A1.2.

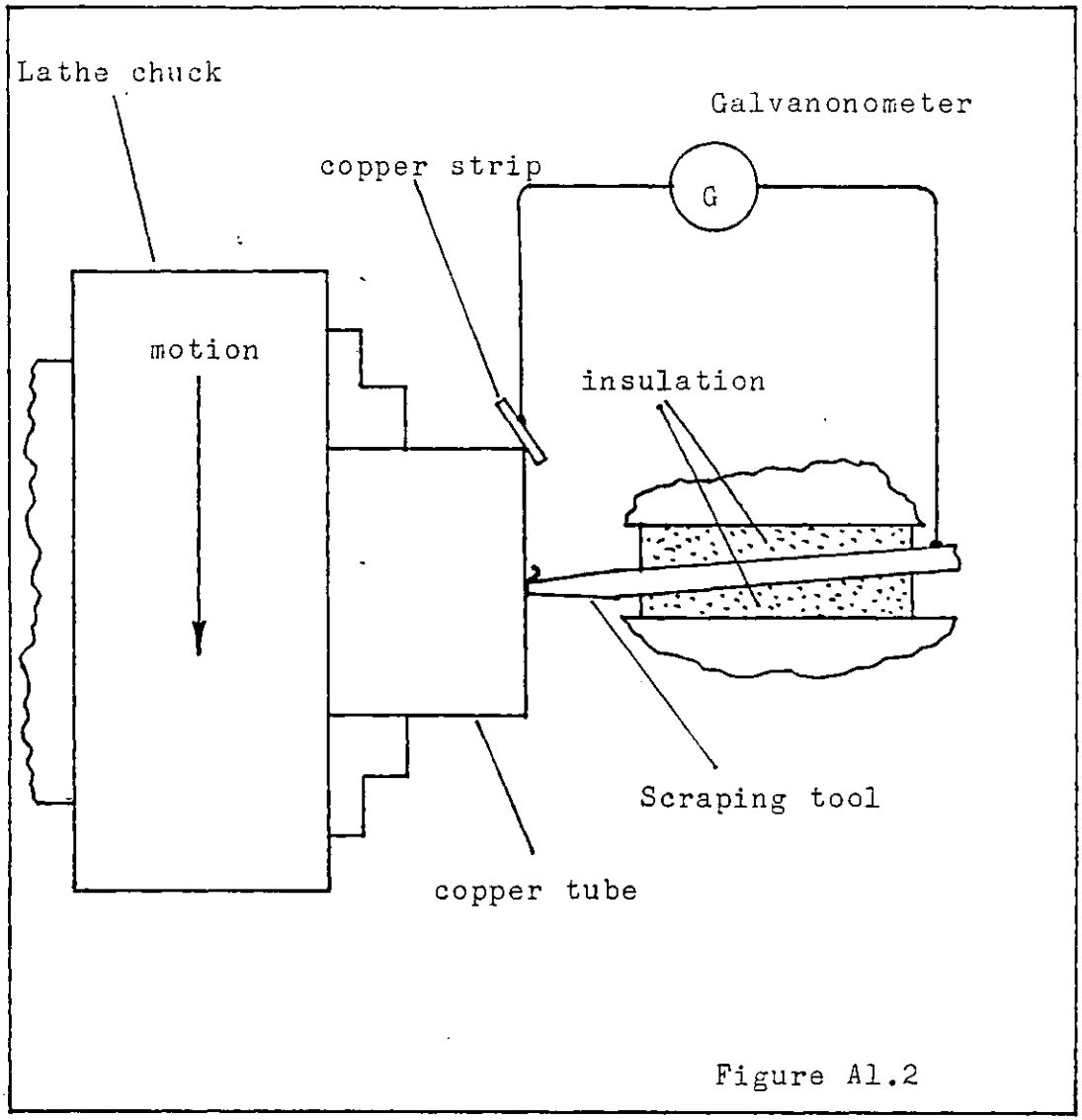

Figure A1.2

When the lathe (Figure A1.2) was rotating at 500 to 1,500 r.p.m., the scraping speed ranged from 0.6 to 1.8m/sec (25mm outside diameter of tube, 2mm wall thickness) and the measured voltage rise ranged from 0.25 to 0.35mV. Assuming that there is a constant of proportionality between voltage rise and tool-tip temperature similar to that of the first

experiment, then the tool-tip temperature is estimated to lie between 125 and 175°C.

The dynamic thermocouple technique is generally considered to give a measure of the average temperature at the tool-tip (43) and peak temperatures may be much higher. The temperature of particular interest is however, not the peak value but the temperature of the scraped surface and clearance face (or surface) of the tool at the point where the two surfaces part. It is here that the scraped surface is first accessible to an external oxidant. This temperature which is situated at a position some distance from where the generation of heat (by metal deformation and friction) is most intense, is believed to be a little less than average value. Thus the experiments described above are believed to give a reasonable measure of the temperature rise caused by scraping on the nascent surface when first accessible to chemical reagents.

Conclusion to experimental work

From the experimental work, the estimated rise in surface temperature of a copper work piece when scraped is estimated as 10°C at slow scraping speeds, (approximately 0.1m/sec), and 125-175°C at higher speeds, 0.6 to 1.8m/sec.

Decline in temperature of scraped surface with distance from tool.

The rise of surface temperature due to scraping declines with distance from the tool. As mentioned in Chapter 3, the model lubricant is deposited at about 0.5mm from the tool

edge, a distance much greater than that over which the heat of scraping is produced (as illustrated in Figure 3.26). Thus a significant decline in transient temperature before the model lubricant is deposited can be expected.

The distance over which the scraping heat is generated is similar to the cut depth, 2μm, and for the purposes of calculation assumed to be identical. Thus the heat generation distance is a fraction 4×10^{-3} of the distance from tool to the point of deposition of model lubricant. Cameron (10) gives a formula described below, which was found to be useful to estimating the decline of transient temperature with distance.

$$\frac{T}{T_{max}} < (\sqrt{x/L} - \sqrt{(x/L)-1}) \qquad \text{Eq.A1.1}$$

where

T = Temperature rise at x, i.e. away from heat source

T_{max} = Characteristic or average temerature rise of heat source.

x = distance from source of heat

L = length of heat source, $L << x$

In the case described above $x/L = 250$.

To make a more conservative calculation x/L is set at 100.

Thus

$$\frac{T}{T_{max}} < (\sqrt{100} - \sqrt{99})$$

$$< 0.05.$$

Thus it is estimated that when the model lubricant is deposited the transient temperature of the scraped surface will have declined to 0.05 of its initial value at the point of scraping if the temperature rise at the point of scraping is of the order of 200°C then the model lubricant will react with a surface which is initially about 10°C higher than the set temperature. This level of temperature fluctuation was considered acceptable given the transient temperature would be negligible within 5mm of the tool (equivalent to 1 millisecond reaction time at 5m/sec.).

APPENDIX 2 : DETAILS OF METHOD OPERATING THE TEST-RIG.

1. Preparation of materials prior to operation of a test

The work for a particular test started with the preparation of the shim (which is the 'specimen material'). A 4.5m length of shim was cut into 3 or 4 strips 14.2 to 15.2mm wide. A technique of cutting was developed to prevent the strips of shim from distorting. An electric cutter is used to slice off a strip and tin-snips are then used to cut away the distorted metal left on the shim remaining after cutting off the strip. The next strip to be sliced off does not suffer distortion if this method is used. A 2m. straight-edge was useful for marking out the line of cut with sufficient accuracy.

Two litres of rinse fluid and 10ml. of model lubricant are needed for each test.

As described in Chapter 4, the tool bits have a relief land ground on the scraping edge and the width of scraping edge is reduced. A metal bevel and a fine sharpening stone were used. Figure A2.1 illustrates the disposition of the tool during grinding of the relief land, movement of the tool is normal to the plane of the figure.

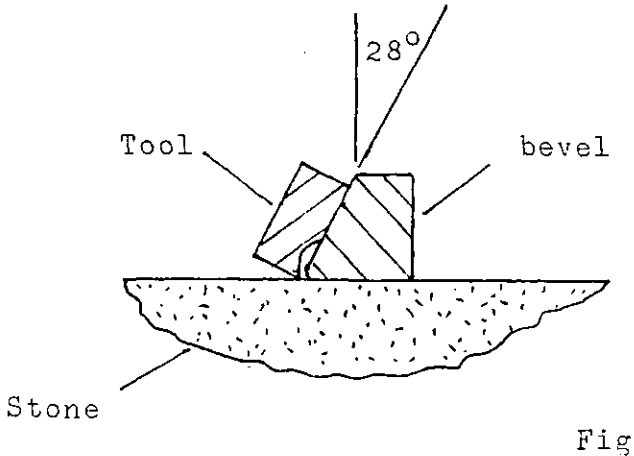

Figure A2.1

To reduce the cutting width, the edge to be prescribed is covered with masking tape and the tool rubbed along the edge of the stone. The tool is viewed under a light microscope (x40 magnification) to check for flaws in the scraping edge.

The test-rig was designed in imperial units and it was found to be convenient to have accessible the following tools: 2 'B.A.' and ¼ B.S.F. spanners, Allen key 3/16 inches across flats.

2. Preparation and adjustment of the 'scraper'.

The next stage in the work is to set the 'scraper' (as illustrated in Figure 3.10). Work is begun with the ultra-sonic cleaning in acetone of the tool bit and adjacent parts. The 'cross-beam' is also rinsed in acetone.

The tool bit is then mounted in the 'cross-beam', aluminium foil is used as packing to reduce movement of the tool during scraping. The wick (for the model lubricant) is positioned in the wick feed mechanism, Figure A2.2.shows the final position of the wick.

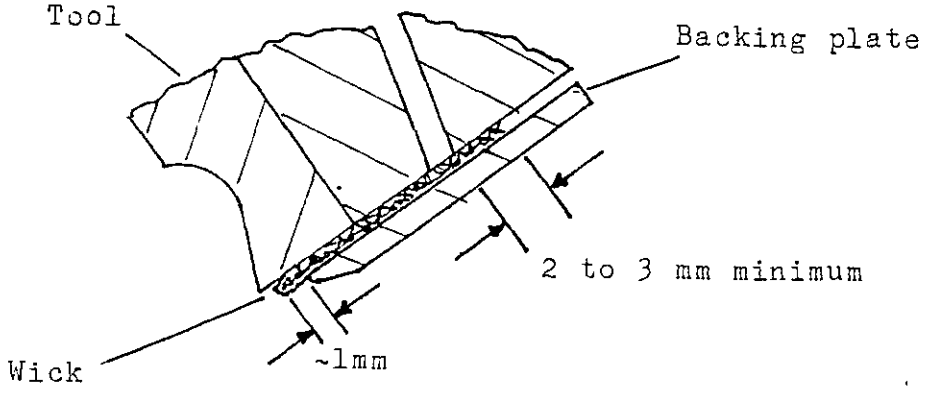

Figure A2.2

Adjustment of the 'scraper' can now begin, a strip of waste shim (i.e. shim as specified in Chapter 4) is positioned on the sub-frame of the 'scraper' and the assembled 'cross-beam' is then bolted into position. Some means was devised of pulling the waste shim. The thicknesses of the waste shim and the shim to be used in the test should be within 10 microns of each other. The position of the scraping tool relative to the scraped shim is initially set with aluminium foil packing under the cross beam as the range of scrape depth adjustment is limited to 0.07mm. One revolution of the scrape depth screw changes the nominal scrape depth by 2 microns. The screw is turned one or two revolutions and the scrape tested, a process which is repeated until a satisfactory scrape is obtained. A scraping force of approximately 250N (i.e. the strength of one hand pulling) is taken as indicative of a satisfactory scrape. Smaller rotations of the scrape depth adjustment screw than the initial 1 to 2 revolution movements may be needed to finalize the adjustments of the scraper.

There is often a problem of misalignment of the tool with the shim. The cross adjustment screwa are worked in the manner shown in Figure A2.3 until a scrape of even depth is obtained.

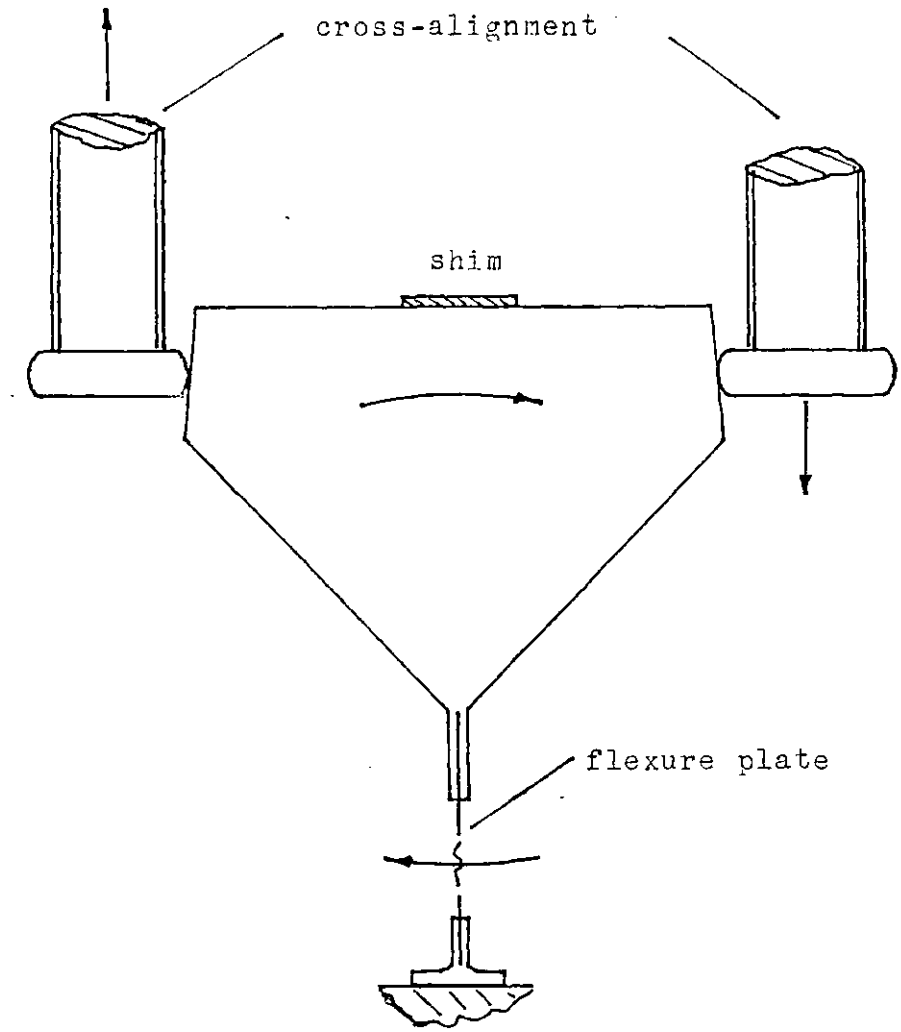

Figure A2.3

Once the scrape depth and cross alignment had been set the 'scraper' was ready for use in a test.

3. Preparation of testing prior to operation.

The 'cross beam' of the 'scraper' is removed from the sub-frame (of the 'scraper') which is then placed in the reaction chamber. The prepared strip of shim is rolled on to the 'Wind-Out Wheel', a hole drilled at one end of the shim serves as an attachment to the wheel. The shim is then unwound from the wheel and passed through the 'Start-tube', 'Reaction chamber', 'Stop-tube' and Drive System'

until the constant force springs are reached. It was found that the shim slides through the system either easily, or not at all. Ofter it was necessary to retract the shim and file off a bulge in the shim. The shim is prone to jamming at the end of the start-tube closest to the Wind-Out Wheel. The shim is then joined to the constant force springs by drilling two holes in the shim at the end closest to the springs and inserting this end of the shim into the adjacent 'connector'.

A length of ticker tape is passed through the ticker-timer and attached to the shim as close as possible to the constant-force springs. A dot is then marked on the tape to indicate the starting position. The cover panel to the slideway (down which the constant force springs retract) which was removed at the end of the previous test is now replaced.

The test-rig is now ready for 'Wind-Out'. The wind-out wheel is rotated using a lever and the shim so moved pulls out the constant force springs. The 'wind-out' was performed with a series of short movements of the shim, this enabled two cables to the speed controller to be wound back without entanglement. The speed controller is set at a high value of damping to provide the maximum possible braking force should control be lost over the constant force springs. A slight knock conveyed by the shim to one's hand on the lever indicates that the trigger has been reached and little further movement of the lever is necessary. A clip is later used to secure the trigger.

The rinse barrier is then cleaned utlrasonically in acetone and assembled on the 'subframe' of the 'scraper'. The side of rinse-barrier farthest from the tool is taken as the nominal point of rinse. Two modes of mounting, which are illustrated in Figure A2.4 are used to allow for short and long reaction distances.

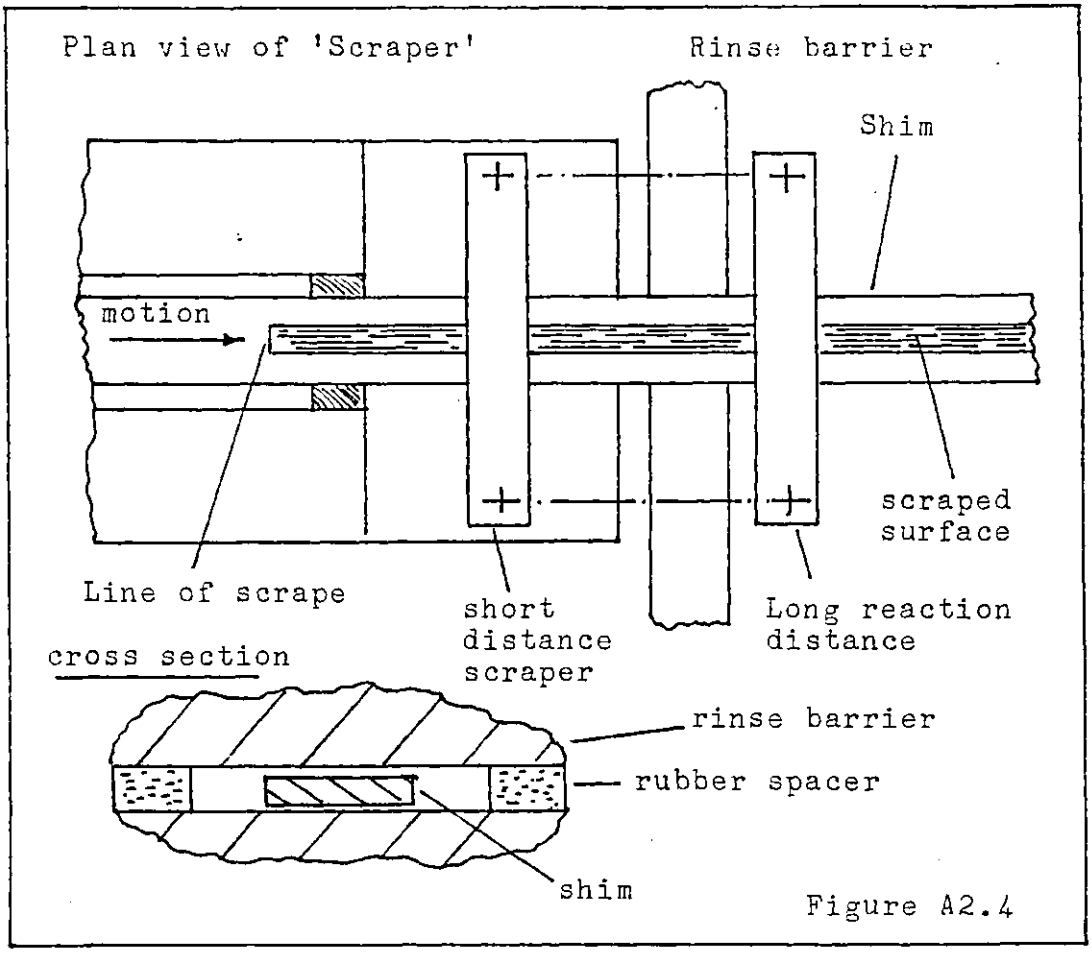

Figure A2.4

To achieve the right fit between the shim and rinse barrier, bolts bearing on rubber washers are tightened so as to close the gap available to the shim (as shown in Figure A2.4). The rinse barrier is considered set when it can be slid along the shim with moderate friction. At this setting there is a gap of approximately 10-25 microns between the upper surface of the shim and the upper half of

the rinse barrier. This gap is calculated as narrow enough to hold back the rinse fluid during scraping.

The 'subframe' is then bolted down onto its mountings in the reaction chamber in a position such that the rinse barrier is 10 ± 2mm from the edge of the rinse jet. The surface of the shim that will be directly beneath the tool at the start of the scrape is then cut away to about 30μm depth, so as to facilitate a rapid start to the scrape. The 'cross-beam' is mounted once again on the 'subframe' and model lubricant is poured into the receptacle on the 'cross-beam'. A minute is allowed for the model lubricant to saturate the wick before the screw plunger is inserted into the receptacle. The screw plunger is wound down until friction sufficient to maintain a tension in the wick-feed cable occurs.

The reaction chamber can now be closed up, thus completing the preparative stages of the test procedure.

4. Operation of the test-rig.

Shortly before purging the reaction chamber with nitrogen the system is purged and loaded with rinse fluid. A diagram of the rinse system is shown in Figure A2.5. To purge and load the rinse system the following actions are carried out. The rinse system is connected to the nitrogen supply and purged for 25 minutes to remove old rinse fluid and air. The hydropneumatic accumulator (Figure A2.4) is usually pressurized to 32KPa to ensure that the rubber balloon inside the accumulator does not deflate.

The filling vessel (as shown in Figure A2.4) is joined to the rinse system. After blowing out any air remaining in the piping, the nitrogen system is cut off to the rinse system and 'rinse fluid' is poured into the filling vessel. 1.3 litres of fluid are then forced by gravity head into the rinse system. To complete the loading procedure, the storage vessel (Figure A2.4) is pressurized and the valve on the accumulator partly opened so as to allow the volume of rinse fluid in the storage vessel to be transferred to the accumulator. Once this is done the valve between stoage vessel and accumulator is closed and apart from final pressurization of the accumulator the system is ready to deliver rinse fluid.

The test-rig is then ready for purging, a 1.5 to 2 hour purge was used. The volume of air to be purged is $0.06m^3$ and ten times that volume, i.e. $0.6m^3$ was passed through

Once the purge is completed then the electric power supply to the start tube heater is turned on. 20 minutes is the specified heating time. The 'plateau temperature' of the shim is set by the voltage supplied to the heater (as described in Appendix 3).

In the last five minutes prior to trigger release all settings on the rig are checked and the hydro-pneumatic accumulator is pressurized. The main switch of the control panel is then closed and a 'scrape' occurs.

Once the 'scrape' is completed all electric power to the test-rig is cut off and the hydro-pneumatic accumulator is de-pressurized. The nitrogen purge is continued for

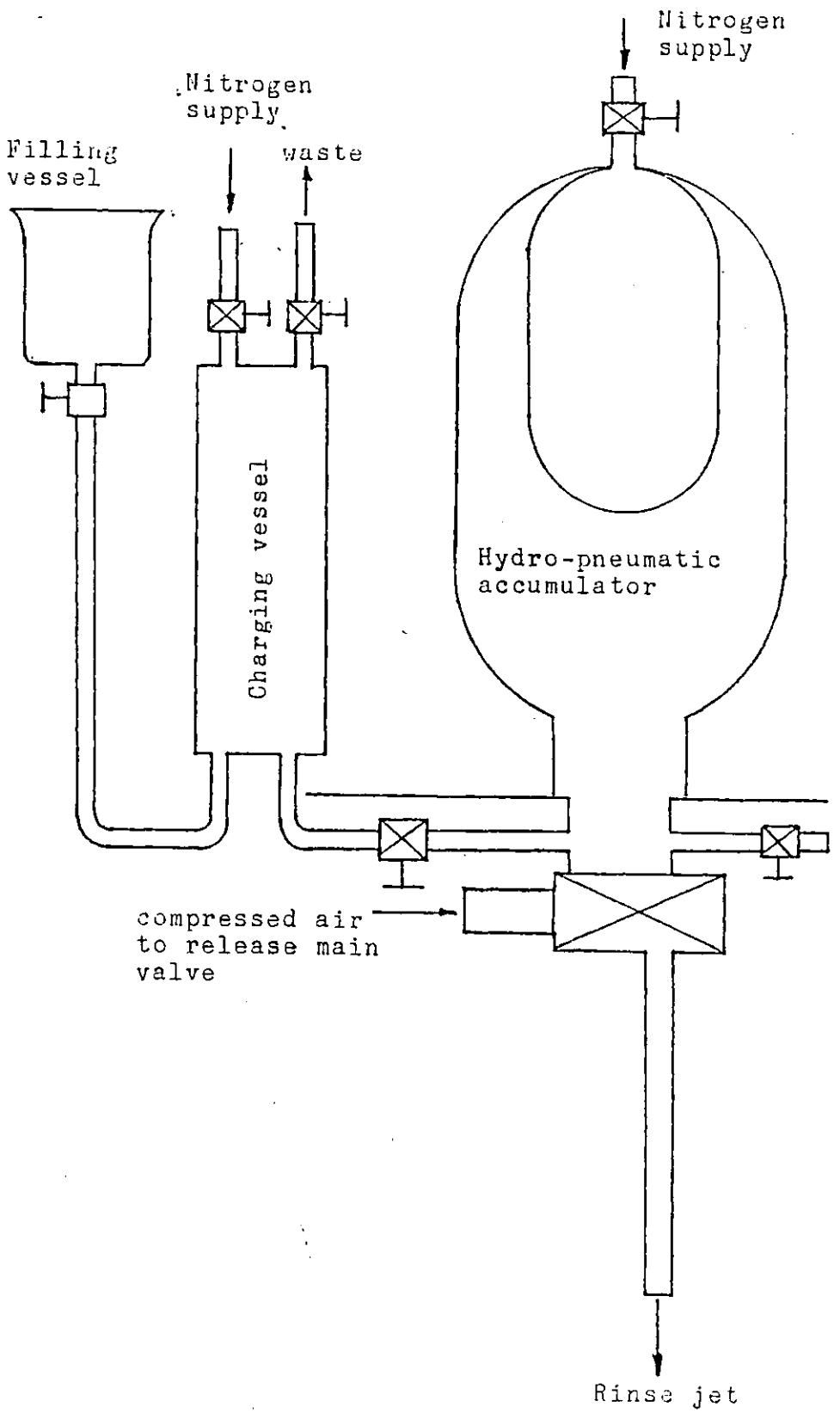
Nitrogen supply
Nitrogen supply
waste
Filling vessel
Charging vessel
Hydro-pneumatic accumulator
compressed air to release main valve
Rinse jet

Figure A2.5

another two hours until the start-tube is sufficiently ccol for the reaction chamber to be opened up. The shim and ticker tape are then extracted for further analysis and waste rinse-fluid from the sump is disposed of.

5. Settings of control devices on test-rig.

Settings relating to reaction time.

The wick feed motor, speed controller, pressure of hydro-pneumatic accumulator and reaction distances have to be set to match the reaction time selected. Table A2.1 shown below gives the details of the settings used in the experimental work.

TABLE A2.1 : TEST-RIG SETTINGS.

Intended reaction time	3-5ms	10-15ms	10-15ms	30-50ms
Speed setting on wick feed motor	8-9	2-3	8-9	2-3
Pressure in accumulator pressure	$4x10^5$Pa	$2x10^5$Pa	$4x10^5$Pa	$2x10^5$Pa
Speed control setting	'Minimum'	'Maximum'	'Minimum'	'Maximum'
Reaction distance	45mm	45mm	120mm	120mm

Settings relating to reaction temperature.

The power levels used for the start-tube heater are described in Appendix 3.

Safety aspect.

The constant force springs are very powerful and therefore are a possible hazard. It is advised that the

procedure described above for 'Wind-out' be followed and that improvised means of restraining the constant force springs, e.g. G-clamps, should be avoided. Any other moving part connected to the constant force springs, i.e. shim, Wind-out Wheel, rotors and cables to speed control system may also become a hazard should control be lost over the constant force springs.

The Nitrogen blanket is necessary for reduction of the combustion risk present in the reaction chamber where there is the combination of hot shim and volatile hydrocarbon rinse fliud. It is therefore advised that the procedure described above for purging the chamber of air should be followed unless a better procedure can be devised.

APPENDIX 3 - CALIBRATION OF SURFACE TEMPERATURE OF MATERIAL

The temperature which the specimen material is heated to before scraping was measured and calibrated in terms of heating power and position on specimen material relative to the heater. The duration of heating which also has a strong influence on the specimen material was held constant at 20 minutes. This period of time was found to be long enough to allow the specimen material to be heated to the required temperature, but short enough to prevent excessive heating of the reaction chamber. The reaction chamber is kept as cool as possible in order to minimise the combustion risk occuring on release of rinse fluid into the reaction chamber.

To measure the temperature of the upper face of the shim (which is the part of the specimen material that is scraped), 'Hermet' temperature-indicating labels were obtained from Levermore Ltd. Figure A3.1 illustrates the appearance of the label and the method of temperature measurement.

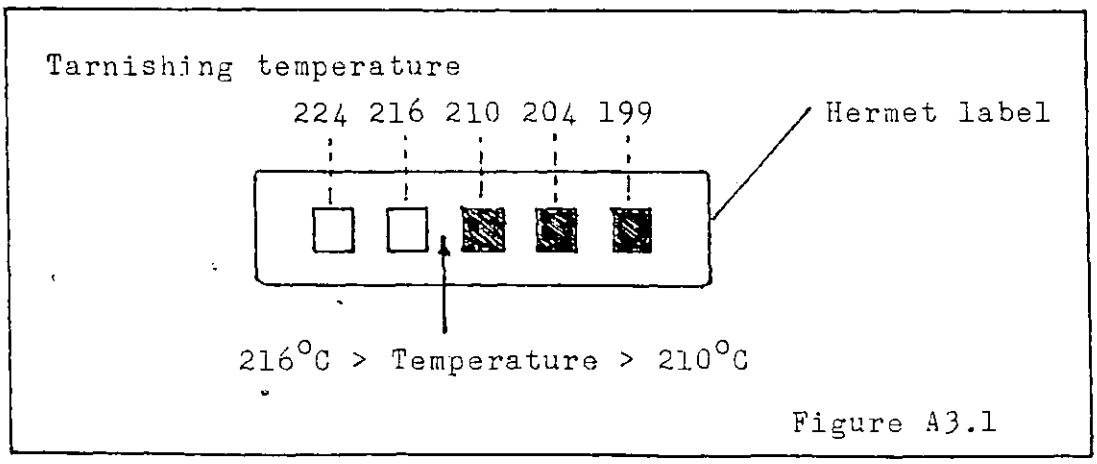

Figure A3.1

The Hermet labels were positioned on a length of shim which was then inserted in the 'Start-tube'. The 'start-tube' was then heated for 20 minutes and after it had cooled down, the shim was extracted. The temperature profile along the upper face of the shim was deduced from the changes in colour of the labels. Figure A3.2 shows the temperature profiles obtained in this manner:- The ordinate is temperature in ^{o}C and the abscissa is distance in mm. from the inner face of the reaction chamber adjacent to the start-tube. The 'plateau' temperature (illustrated in Figure A3.2) was subsequently plotted versus the square of the voltage setting to the heater, the graph of which is shown in Figure A3.3. A direct proportionality between these quantities was expected by Ohm's Law and Newton's Law of Cooling. As is evident in Figure A3.3 this assumption is approximately correct, though the derivations from strict linearity have been allowed for in drawing the calibration line.

Reference graphs for scraping temperature could then be plotted based on the data discussed above. Figures A3.4 to 3.7 show the reference graphs used. The abscissa is distance from the scraping tool and the ordination is temperature in degrees Celsius. In plotting the graphs, the plateau temperature was taken from Figure A3.3 and the temperature profile deduced by interpolation between the temperature profiles shown in Figure A3.2. The scraping tool is further from the heater than the inner face of the reaction chamber (adjacent to the start-tube) which is the datum position in A3.3 and the temperature profiles in Figures A3.4 to A3.7 are

accordingly shifted. The scraping tool is positioned at 120mm reaction distance, temperature values at other reaction distances are calculated by allowing for the shift in tool position. For example, at 45mm reaction distance the tool is 75mm (120-45mm) farther from the heater, Figures A3.4 to A3.7 show the temperature profiles for power settings 46, 49, 53 and 56 (on the (Variac) which correspond to plateau temperatures 140, 155, 170 and 185 ^{o}C respectively.

The values of reaction temperature for scraped surface presented in this work were all taken from the data discussed above.

Numbers attached to curves refer to voltage settings used.

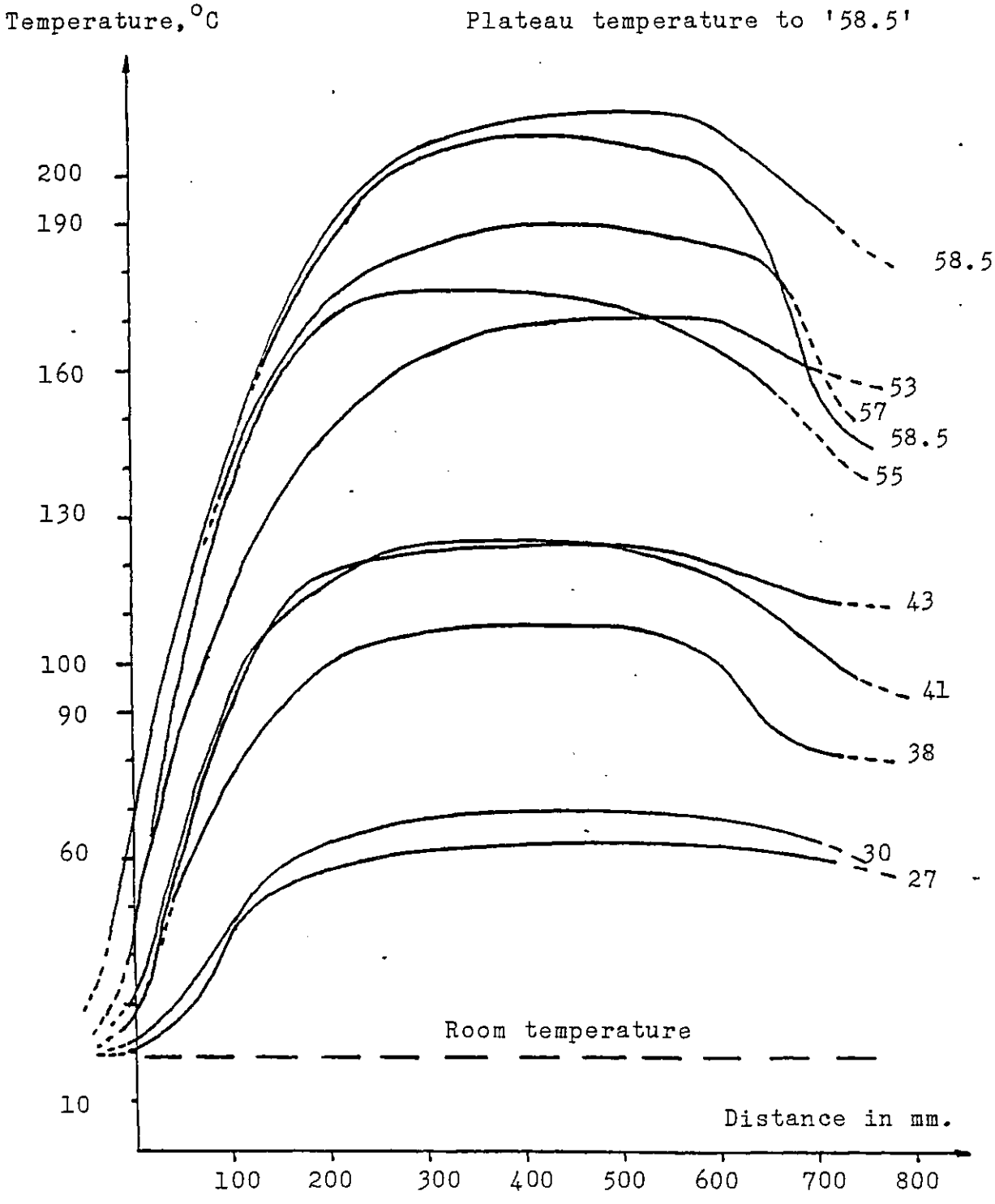

Figure A3.2 Graph of measured temperature profiles of specimen material

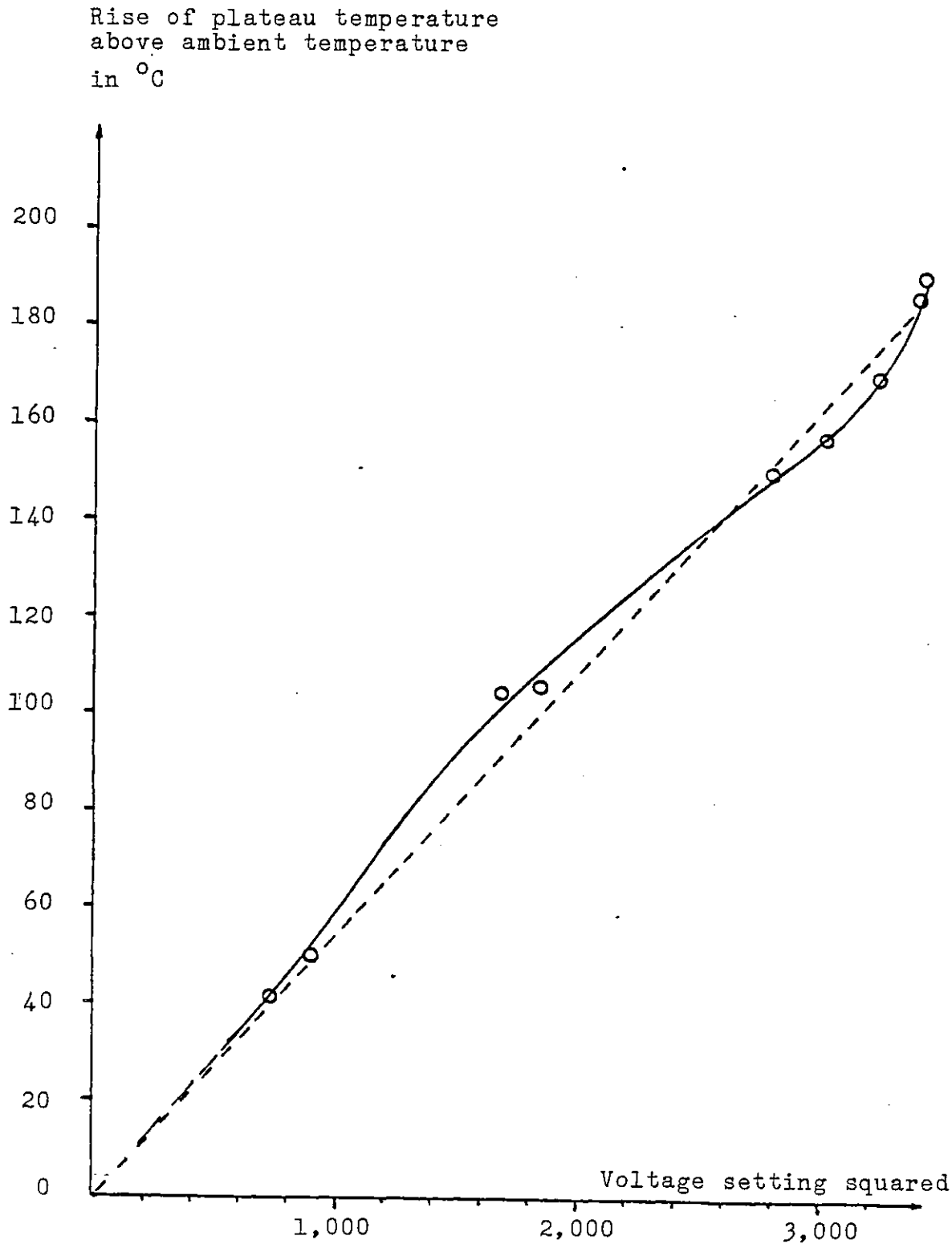

Figure A3.3 Graph of plateau temperature versus square of voltage setting.

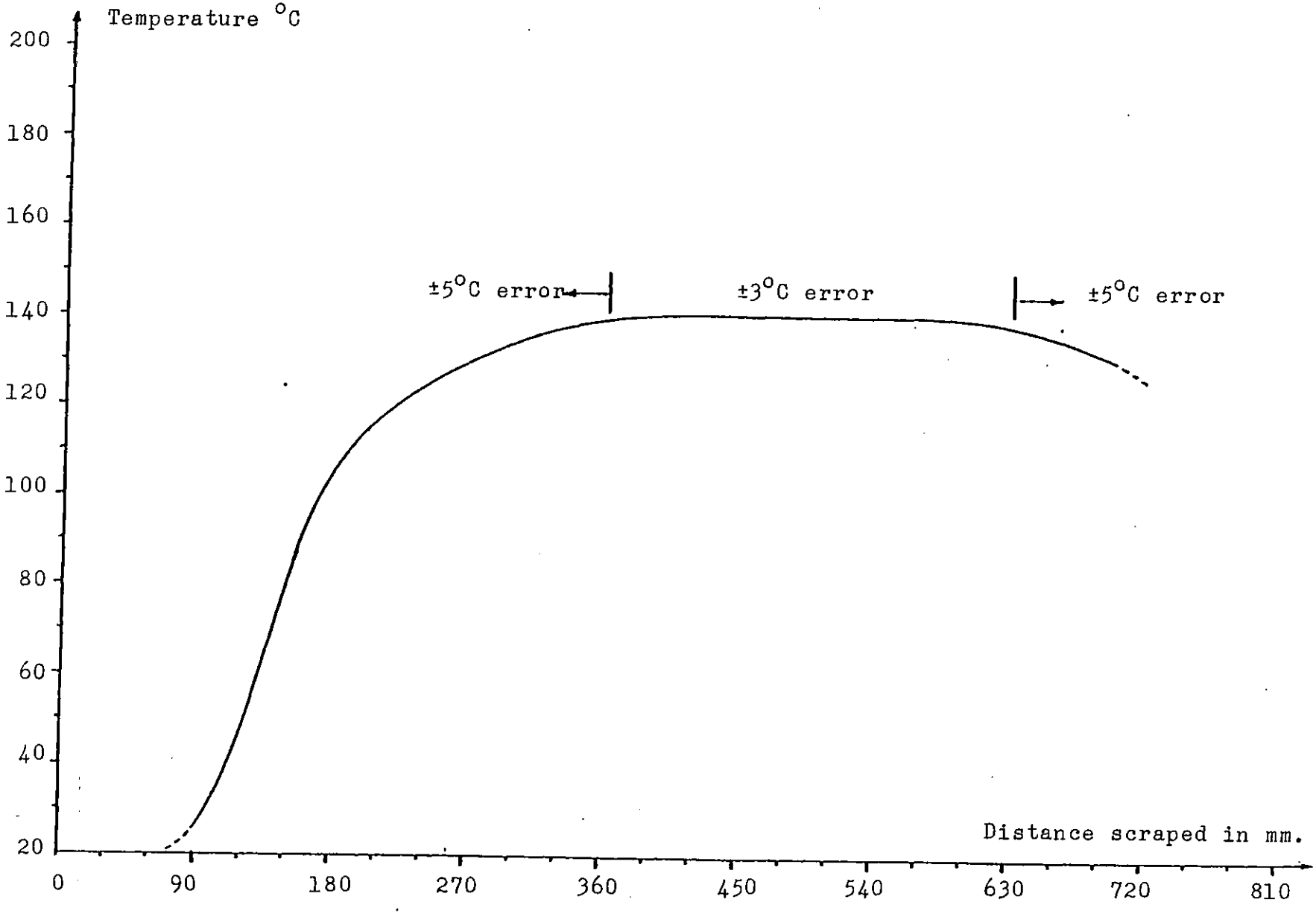

Figure A3.4 Temperature profile for 140°C 'Plateau temperature'

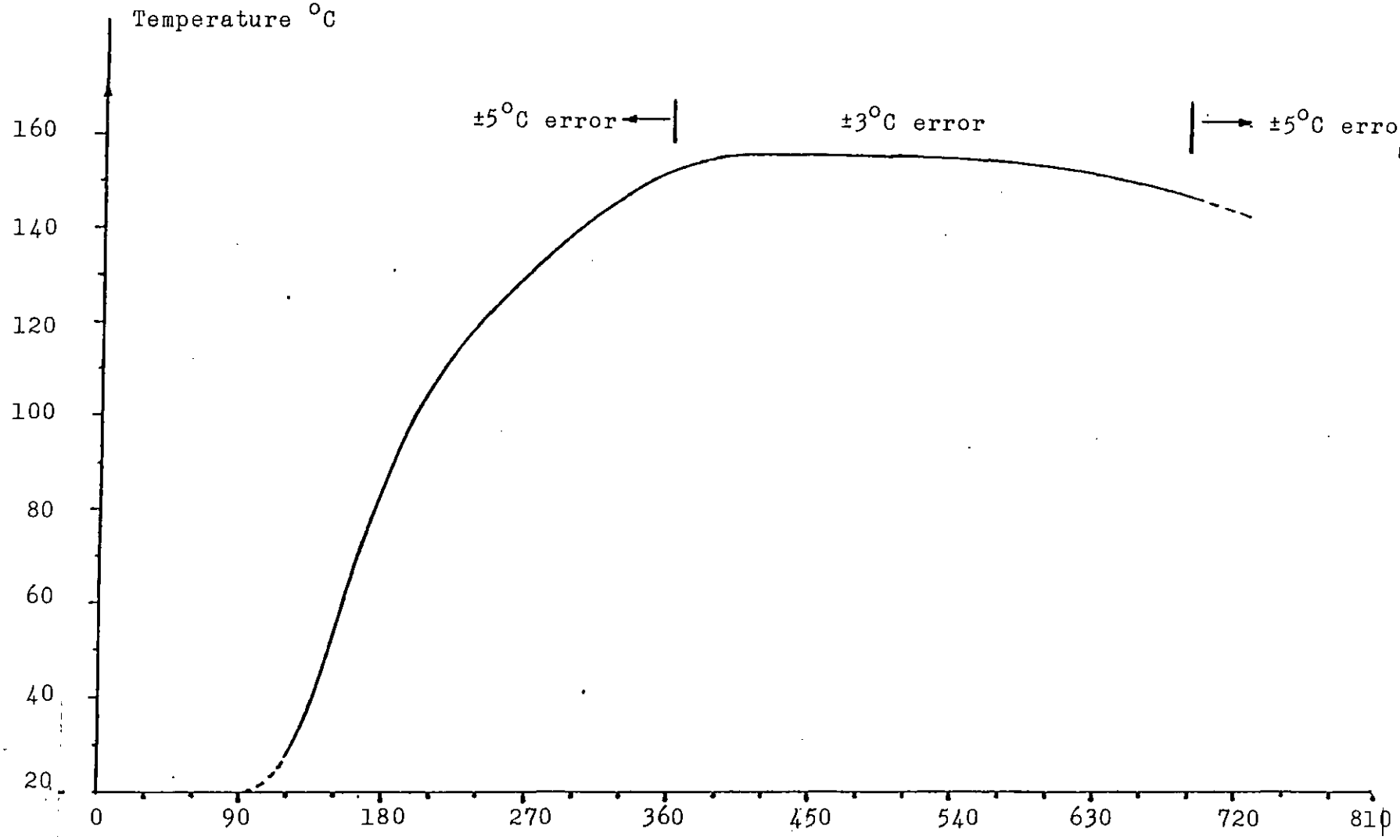

Figure A3.5 Temperature profile for 155°C 'Plateau temperature'

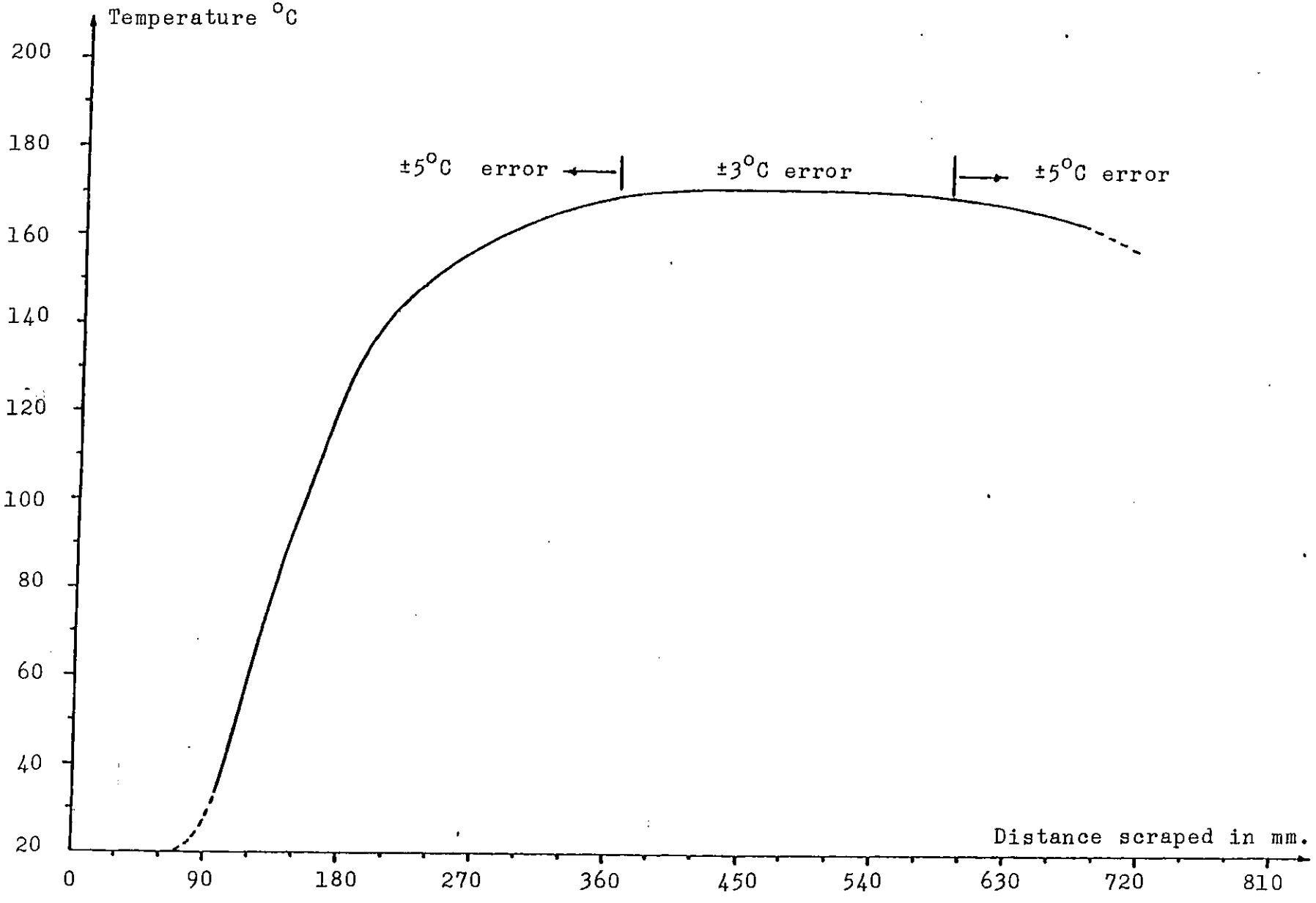

Figure A3.6 Temperature profile for 170°C 'Plateau temperature'

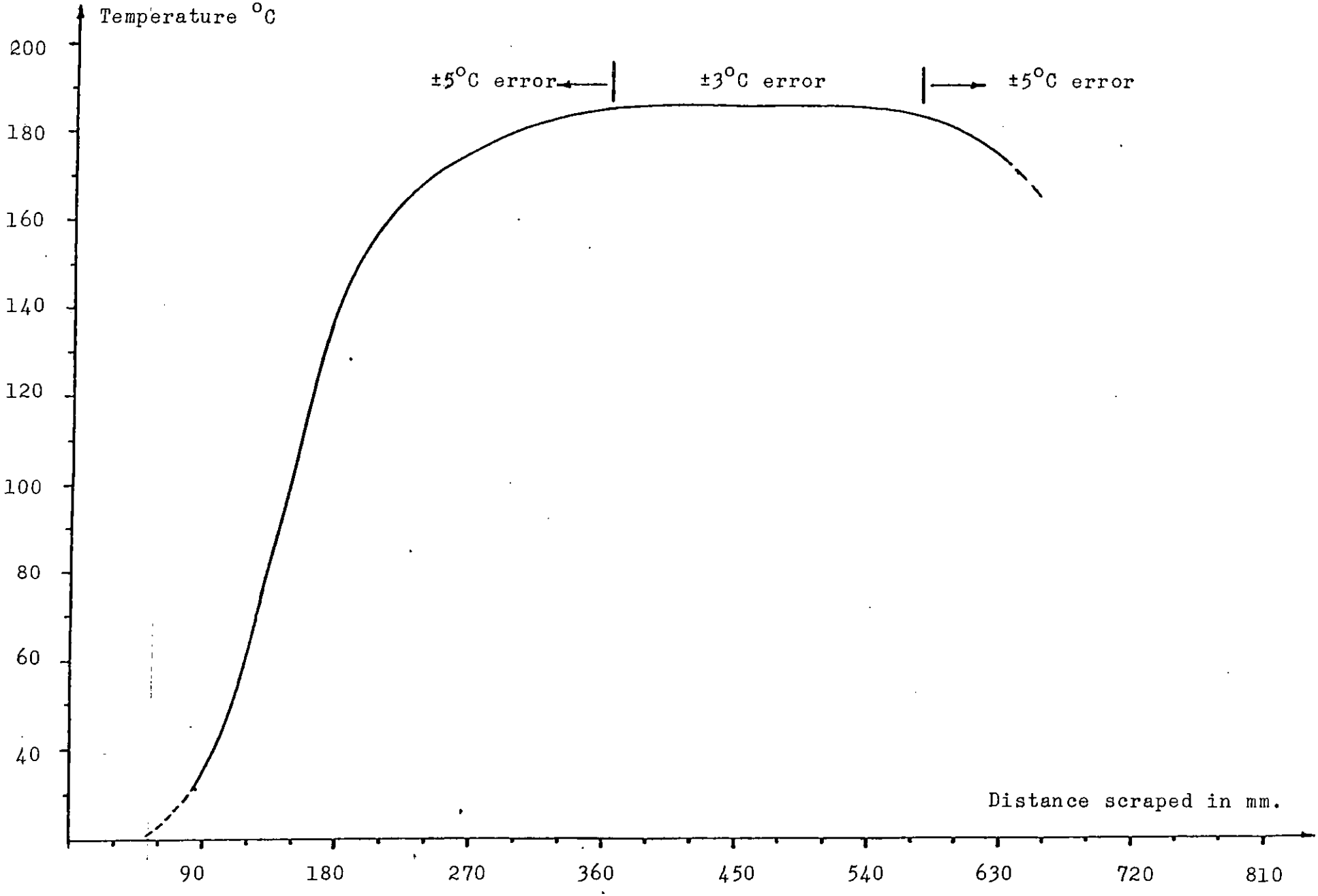

Figure A3.7 Temperature profile for plateau temperature 185°C

REFERENCES

1. Dowson,D.,History of Tribology. Longman, 1st.ed. 1979.
2. Brown,R.R., U.S.Patent 22,621 (1859). Source: Musgrove,F.F.J. J.Inst.Petroleum Vol.32 (1946) p.32.
3. Dyson,A., "Scuffing, a review" Tribology Vol.8 (1975), 2 parts - I pp.77-87; II pp.117-122.
4. M.W.Bailey and A.Cameron "The effect of Temperature and Metal Pairs on Scuffing" A.S.L.E.Trans.Vol.16 (1973) pp.121-122
5. Bowden,F.P. and Young,J.E., "Friction of Clean Metals and the influence of Adsorbed Gases, the Temperature Coefficient of Friction", Proc.Roy.Soc (London) Vol.A172 (1939) pp.263-279.
6. Trent,E.M.,Metal Cutting. Butterworths, 1st.ed. 1977.
7. Reynolds,O., "On the Theory of Lubrication and its Application to Mr.Beauchamp Towers' Experiments including an Experimental Determination of the Viscosity of Olive Oil" Phil.Trans.Roy.Soc.(London) Vol.177 (1886) p.157.
8. Grubin,A.N., "Fundamentals of the Hydrodynamic Theory of Lubrication of Heavily Loaded Cylindrical Surfaces", Symposium: Investigation of the Contact of Machine Components, Central Scientific Institute for Technology and Mechanical Engineering (TsNiiTMash). Book no.30. Moscow, (1949).
9. Hardy, Sir William Bate, "Problems of the Boundary State" Phil.Trans.Roy.Soc.(London), Vol.230 (1931) pp.1-37.
10. Cameron,A., Principles of Lubrication. Longmans Green & Co.Ltd., c.1966.
11. Campbell,W.E., "Solid Lubricants" Chapter 10 pp.197-227, Boundary Lubrication, an appraisal of World Literature. A.S.M.E. c.1969.
12. Campbell,W.E., "Boundary Lubricants" Chapter 6 pp.87-117, Boundary Lubrication, an appraisal of World Literature, A.S.M.E c.1969.

13. Archard,J.F. and Hirst,W., "The Wear of Metals under Unlubricated Conditions", Proc.Roy.Soc.(London), Vol.A236 (1959), p.397.

14. Quinn,T.F.J., "The Effect of 'Hot-Spot' Temperatures on the Unlubricated Wear of Steel", A.S.L.E.Trans, Vol.10 (1967), pp.158-168.

15. Quinn,T.F.J., "New Developments in the Oxidational Theory of the Mild Wear of Steels", A.S.M.E. International Conference on the Wear of Materials (1979), pp.1-11.

16. Quinn,T.F.J., "Dry Wear of Steel as revealed by Electron Microscopy and X-ray Diffraction", I.Mech.Eng.Proc. Vol.182 Part 3N p.201, (1968)

17. Archard,J.F., "The Temperature of Rubbing Surfaces", Wear Vol.2 (1958) p.438.

18. Wilson,J.E., Stott,F.H. and Wood,G.C. "The development of Wear Protective Oxides and their influence on Sliding Friction", Proc.Roy.Soc.(London) Vol.A369 (1980), pp.557-574.

19. Davey,W. and Edwards,D., "The Extreme Pressure Properties of some Sulphides and Di-Sulphides in Mineral Oils as assessed by the 4-ball machine", Wear, Vol.1 (1957), p.291.

20. Allum,K.G. and Forbes,E.S., "The Load Carrying Mechanism of Organic Sulphur Compounds", A.S.L.E.Trans, Vol.11 (1968), pp.162-175.

21. Coy,R.C. and Quinn,T.F.J., "The Use of Physical Methods of analysis to identify surface layers formed by Organo-sulphur compounds in wear tests", A.S.L.E.Trans, Vol 18 (1975), pp.163-174.

22. Wheeler,D.R., "X-ray Photo-electron spectroscopic study of Surface Chemistry of Dibenzyl Disulphide on Steel under Mild and Severe Wear Conditions", Wear, Vol.47, (1978), pp.243-254.

23. Spikes,H.A. and Cameron,A., "Additive Interference in Dibenzyl Disulphide Extreme-Pressure Lubrication", A.S.L.E.Trans, Vol.17 (1974), pp.283-289.

24. Bird,R.J. and Galvin,G.D., "The Application of Photo-Electron Spectroscopy to the Study of Extreme Pressure Films on Lubricated Surfaces", Wear, Vol.37 (1976), pp.143-167.

25. Godfrey, D., A comment on the Paper by I.L.Singer and J.S.Murday; "Investigation of Lubricated Bearing Surfaces by X-ray Photoelectron Spectroscopy and Auger electron spectroscopies" pp.13-81 of Fundamentals of Tribology c.1980, M.I.T.Press ed.N.P.Suh and N.Saka.

26. Loeser,E.H., Wiquist,R.C. and Twist,S.B., "Cam and Tappet Lubrication, IV, Radio-active Study of Sulphur in the E.P. film", Trans.A.S.L.E., Vol.2 (1959-60) pp.199-207.

27. Borsoff,V.N. and Wagner,C.D., "Studies of Formation and Behaviour of an Extreme Pressure Film", Lubn.Eng.Vol.13 (1957), p.91.

28. Campbell,R.B., "The Study of Hypoid-Gear Lubrication using Radio-active Tracers", Inst.Mech.Eng.Lubrication and Wear Conv. (1963), p.286.

29. Prutton,C.F., Turnbull,D. and Dlouhy,G., "Mechanism of Action of Organic Chlorine and Sulphur Compounds in Extreme-Pressure Lubrication", J.Inst.Pet. Vol.32 (1946) p.90.

30. Baldwin,B.A., "Relationship between Surface composition and Wear: an X-ray Photo-electron Spectroscopic study of Surfaces tested with Organo-sulphur compounds", A.S.L.E.Trans, Vol.19 (1976), pp.335-344.

31. Archard, J.F., "Single Contacts and Multiple Encounters", Journal of Applied Physics, Vol.32 (1961) p.1420

32. Godfrey,D.,"Chemical Changes in Steel Surfaces during Extreme-Pressure Lubrication", A.S.L.E. Trans Vol.5 (1962), pp.51-66.

33. Hironaka,S., Yahagi,Y., Sakurai,T., "The Heats of Adsorption and Anti-Wear Properties of some polar substances", Bull.Jap.Pet.Inst. Vol.17 (1975), p.201

34. Date,K., "Adsorption and Lubrication of Steel with Oiliness Additives", Ph.D. Thesis, London University, Sept.1981.

35. Greenhill,E.P., "The Lubrication of Metals by compounds containing sulphur", J.Inst Pet. Vol.34 (1948) p.659.

36. Mills,T.N., and Cameron,A., "Basic studies on Boundary, E.P. and Piston Ring Lubrication using a special apparatus", A.S.L.E. Trans. Vol.25 (1982), pp.117-124

37. McCarroll,J.J., Mould,R.W., Silver,H.B., and Sims,M.C. "Auger Electron Spectroscopy of Wear Surfaces", Nature (London), Vol.266 (1977), p.519.

38. Gaucher,A., Guilhot,G. and Amsellem,C. "Surface treatment for Iron and Steel", Tribology Vol.9 (1976), p.131.

39. Gregory,J.C. "Chemical conversion coatings of metals to resist scuffing and wear", Tribology Vol.11 (1978), pp.105-112.

40. Blok,H. "Theoretical study of Temperature Rise at Surfaces of Actual Contact under Oiliness Lubricating Conditions", Proc.Inst.Mech.Eng., General Lubrication Discussion, Group IV, (1937), pp.26-39.

41. Blok,H. "The Flash Temperature Concept", Wear Vol.6 (1963), pp.483-494.

42. Francis,H.A., "Interfacial Temperature Distribution within a Sliding Herzian Contact", A.S.L.E. Trans Vol.14 (1971), pp.41-54.

43. Furey,M.J., "Surface Temperatures in Sliding Contact" A.S.L.E. Trans. Vol.7 (1964), pp.133-146.

44. Sakurai,T., Okabe,H. and Sethuramiah,A. "Surface Temperatures in Dry Friction and Boundary Lubrication" Bull.Jap.Pet.Inst. Vol.13 (1971), p.89.

45. Hsu,S.M. and Klaus,E.E. "Estimation of the molecular junction temperature in 4-ball contacts by Chemical Reaction Rate Studies" A.S.L.E. Trans. Vol.21 (1978) pp.201-210.

46. Barcroft,F.T. and Daniel,S.G., "Extreme-Pressure Film formation on Hypoid Gears - studied with Sulphur-35" Inst.Mech.Eng. Lubrication and Wear Conv. (1965), p.265.

47. Sakurai,T., Sato,K. and Yamamoto,Y., "Reaction between Chlorine Extreme Pressure additives and Metal Surfaces at High Temerperatures", Bull.Jap.Pet.Inst. Vol.7 (1965), p.17

48. Bell,J.C., Dyson,A. and Hadley,J.W., "The effect of rolling and sliding speed on the Scuffing of Lubricated Steel Discs", A.S.L.E. Trans. Vol.18 (1975), pp.62-73

49. Carper,H.J., Ku,P.M., and Anderson,E.L. "Effect of some Material and Operating Variables on Scuffing", Mechanism and Machine Theory Vol.8 (1973), pp.209-225.

50. Borsoff,V.N. and Godet,M.R., "A Scoring Factor in Gears" A.S.L.E. Trans. Vol.6 (1963), p.157.

51. Spikes,H.A. and Cameron,A., "Scuffing as a Desorption Process - an explanation of the Borsoff Effect", A.S.L.E. Trans. Vol.17 (1974)

52. Rowe,N.C., "Some aspects of the Heat of Adsorption in the Function of a Boundary Lubricant", A.S.L.E. Trans. Vol.9 (1966), pp.100-111.

53. Bollani,G. "Failure criteria in Thin Film Lubrication with E.P. additives", Wear, Vol.36 (1976)pp.19-23

54. Bell,J.C. and Dyson,A., "The Effect of some Operating Factors on the Scuffing of hardened steel discs", 2nd.Leeds Symposium on Elastohydrodynamic Lubrication, Inst.Mech.Eng., 1972, paper C11/72.

55. Sakurai,T., Sato,K., Hamaguchi,H. and Matsuo., "Effect of Internal Stress on the Wear Behaviour of Steel during Boundary Lubrication", A.S.L.E. Trans. Vol.17 (1974), pp.213-223.

56. Ura,A. "The Relationship between Tribofailures and Surface Roughness" in to"Fundamentals of Tribology", ed.Suk,N.P. and Saka,N. MIT Press c.1980, pp.28-81.

57. Hirst,W. and Stafford,J.V. "Transition Temperatures in Boundary Lubrication", Proc.Inst.Mech.Eng. Vol.186 (1972), pp.179-190.

58. Sharma,J.P. and Cameron,A., "Surface Roughness and Load in Boundary Lubrication", A.S.L.E. Trans. Vol.16 (1973), pp.258-266

59. Rabinowicz,E., Comment on Sharma and Cameron (58).

60. Salomon,G., "Failure Criteria in ThinFilm Lubrication, the IRG program", Wear, Vol.36 (1976), pp.1-6.

61. Baldwin,R.R. and Daniel,S.G., "Solubility of Gases in Lubricating Oils and Fuels", Inst.Pet.J. Vol.39 (1953) p.105-124.

62. Vinogradov,G.V. and Arkharova,V.V., "Anti-wear and anti-frictioon Properties of Hydrocarbons under heavy loads", Wear Vol.4 (1961), pp.274-291.

63. Begelinger,A. and DeGee,A.W.J.,"Boundary Lubrication of Sliding Concentrated Steel Contacts", Wear, Vol.22 (1972), pp.337-357.

64. Klaus,E.E. and Bieber,H.E., "Effect of some physical and chemical properties of Lubricants on Boundary Lubrication", A.S.L.E. Trans Vol.7 (1964), pp.1-10.

65. Rounds,F.G., "Effect of Aromatic Hydrocarbons on Friction and Surface Coating Formulation with three Additives", A.S.L.E. Trans Vol.16 (1973), pp.141-149

66. Vere,R.A. "Lubricity of Aviation Turbine Fuels", S.A.E. Meeting, Los Angeles, Oct.1969, paper 690667.

67. Aird,R.T. and Forgham,S.L. "Lubricating Quality of Aviation Fuels", Wear, Vol.18 (1971) pp.361-380.

68. Bowden,F.P. and Tabor,D. The Friction and Lubrication of Solids Part I; Oxford University Press publ.1954

69. Sakurai,T and Sato,K. "Study of Corrosivity and Correlation between Chemical Reactivity and Load-carrying cpaacity of Oils containing Extreme-Pressure agents", A.S.L.E. Trans Vol.9 (1966) pp.77-87.

70. Housz,A.J. "Scuffing as a factor in the design of Nylon Gears", Wear, Vol.10 (1967) pp.118-126

71. Sikorski,M.E., "Correlation of the Coefficient of Adhesion with various Physical and Mechanical Properties of Metals", A.S.M.E. Journal of Basic Engineering, Vol.85, (1963), pp.279-285

72. Grew,W.J.S.and Cameron,A."Role of Austensile and Mineral Oil in Lubricant failure", Nature Vol.217 (1968) pp.481-482

73. Rounds,F.G.,"The influence of Steel composition on Additive Performance", A.S.L.E. Trans, Vol.15 (1972), pp.54-66.

74. Said Jahanmir "Wear of AiSi 4340 Steel under Boundary Lubrication", Wear, Vol.74 (1981/2), pp.51-65

75. Buckley, D.H.,"Definition and effect of Chemical Properties of Surfaces in Friction, Wear and Lubrication" Fundamentals of Tribology. MIT Press 1980, ed. Suh,N.P. and Saka,N. pp.173-199

76. Wheeler,D.R. and Buckley,D.H. "Texturing in metals as a result of Sliding", Wear Vol.33 (1975), pp.65-74

77. Kislik,V.A.,"On the nature of the White-Layers formed on Friction Surfaces", Trenie i Iznos Mashinakh Vol.15 (1962). (Friction and Wear in Machinery - Translation by A.S.M.E., Vol.15, pp.153-172).

78. Eyre,T.S. and Baxter,A.,"The formation of white layers at rubbing surfaces", Tribology Vol.5 (1972) p256.

79. Bayliss,A.A., "The Kinetics of Extreme-Pressure Additives", Ph.D., University of London, Sept.1975.

80 Ferrante,J. and Buckley,D.H.,"A Review of surface segregation, adhesion and friction studies performed on Copper-Aluminium, Copper-Tin and Iron-Aluminium Alloys" A.S.L.E. Trans Vol.15 (1972), pp.18-24.

81. Moore,A.J.W.,"Effect of Included Oxide films on the structure of the Beilby Layer", Proc.Roy.Soc. Vol.A212 (1952) pp.458-459.

82. Oudar,J. Physics and Chemistry of Surfaces. Blackie & Son 1975

83. Prutton,M. Surface Physics. Oxford Physics Series. Clarendon Press, Oxford. 1975.

84. Chowdhury,S.K.Roy, and Pollock,H.M. "Adhesion between Metal Surfaces: the effect of Surface Roughness", Wear Vol.66 (1981), pp.307-321.

85. Buckley,D.H.,"The influence of Atomic nature of Crystalline materials on Friction", A.S.L.E. Trans Vol.11 (1968) pp.89-100

86. Inman,M.C. and Tipler,H.R.,"Interfacial energy and composition in Metals and Alloys", Metals Review Vol.8 (1963), pp.105-166

87. Rabinowicz,E. "Practical uses of the Surface Energy criterion", Wear Vol.7 (1964), pp.9-22

88. Rabinowicz,E.,"Influence of Surface Energy on Friction and wear phenomena", Journal of Applied Physics Vol.32 (1961), pp.1440-1444

89. Buckley,D.H.,"The use of Analytical Surface Tools in the fundamental study of Wear", Wear Vol.46 (1978) pp.19-53.

90. Gulbransen,E.A.,"The role of Minor elements in the Oxidation of Metals", Corrosion Vol.12 (1956),pp.61-67

91. Muetterties,E.L., "The Organo-Metallic Chemistry of Metal Surfaces", Pure and Applied Chemistry Vol.54 (1982), pp.83-96.

92. Heidermeyer,J.,"Influence of the plastic deformation of Metals during Mixed Friction on their Chemical Reaction Rate", Wear Vol.66 (1981) pp.379-387.

93. Meyer,K., Berndt,H. and Essiger,B. "Interacting mechanisms of Organic sulphides with Metallic surfaces and their importance for problems of Friction and Lubrication", Applications of Surface Science Vol.4 (1980) pp.154-161.

94. Groszek,A.J.,"Activation of Iron Surfaces by Chemisorption of some E.P. and Anti-wear compounds", Wear, Vol.18 (1971) pp.279-289.

95. Bjerk,R.O.,"Oxygen - an Extreme Pressure Agent", A.S.L.E.Trans Vol.16 (1973), pp.97-106.

96. Vinograd,G.A. Discussion of ref.32.

97. Spikes,H.A., "Physical and Chemical Adsorption in Boundary Lubrication". Ph.D. Thesis, London University, (1972).

98. Buckley,D.H.,"Oxygen and Sulphur Interaction with a clean Iron Surface and the effect of rubbing contact on these interactions", A.S.L.E. Trans Vol.17 (1974) pp.206-212

99. Tomaru,M., Hironaka,S. and Sakurai,T.,"Effects of oxygen on the losd-carrying action of some additives", Wear Vol.41 (1977) pp.117-140

100. Barcroft,F.T., "A Technique for investigating reaction between E.P. additives and Metal surfaces at high temperatures", Wear Vol.3 (1966) p.440.

101. Landheer,D.,Dackus,A.J.G. and Klostermann,J.A., "Fundamental aspects and Technological implications of the solubility concept for the prediction of running properties", Wear Vol.62 (1980) pp.255-286.

102. Tomashov,N.D., Theory of Corrosion and Protection of Metals. Macmillan & Co., (New York), 1966

103. Farnsworth,H.E.,"Characterization and preparation of atomically clean surfaces for invesigation in Ultra-high vacuum" in Clean Surfaces : Their preparation and Characterization for Interfacial Studies ed. Goldfinger,G. Marcel Dekker Inc.(New York).

104. Goldman,I.B. and Appledorn,J.K.,"Scuffing as influenced by oxygen and moisture", A.S.L.E. Trans Vol.13 (1970) pp.29-38.

105. Tingle,E.D.,"The importance of Surface Oxide films in the Friction and Lubrication of Metals, Part 2 - The Formation of Lubrication films on Metal Surfaces". Trans.Far.Soc. Vol.326 (1950), pp.97-102

106. Spurr,R.T.,"The Coefficient of Friction of Metals at slip", Wear Vol.10 (1967), p.326

107. Krause,H.,"Tribochemical reactions in the friction and wearing process of iron", Wear Vol.18 (1971) pp.403-412.

108. Padmore, E.L. and Rushton,S.C., "Effects of loading procedure on surface failure in gears". Proc.Inst.Mech. Eng. Vol.179 Part 3J (1964-1965) pp.278-289.

109. Rabinowicz,E.,"Theoretical criteria for the effectiveness of a lubricant film" A.S.L.E. Trans Vol.2 (1958), pp.96-100.

110. Rowe,N.C., "Role of Additive adsorption in the mitigation of Wear", A.S.L.E. Trans Vol.13 (1970), pp.179-188.

111. Grew,W.J.S. and Cameron,A.,"Thermodynamics of Boundary Lubrication and Sliding", Proc.Roy.Soc. (London) Vol.A327, pp.47-59.

112. Finkin,E.F., "A Theory for the friction of sulphide and other films". Wear Vol.18 (1971), pp.231-241.

113. Stolarski,T.A.. "A Contribution to the theory of Lubricated Wear", Wear Vol.59 (1980) pp.309-322

114. Sakurai,T., Ikeda,S. and Okabe,H. "The mechanism of Reaction of Sulphur compounds with Steel surface during Boundary Lubrication using S-35 as a tracer". A.S.L.E. Trans Vol.5 (1962) pp.67-74.

115. Foroulis,Z.A., "Kinetics and Mechanism of the reaction of iron with sulphur vapour in the temperature range of 250 to 500°C", Werkstoff und Korrosion Vol.29 (1978) pp.385-393

116. Dravnieks,A.,"Corrosion of Steel in Molten Sulphur", Industrial and Engineering Chemistry, Vol.43 (1951) pp.2897-2900.

117. Sakurai,T., Sato,K. and Ishida,K., "Reactions between Sulphur Compounds and Metal Surfaces at high temperatures" Bull.Japan Petroleum Inst. Vol.6 (1964) p.40.

118. Lopis,J., Gamboa,J.M., Arizmendi,L., Gomez-Minana,J.A. "Surface Reactions of Iron with Hydrocarbon solutions of Organic sulphides", Corrosion Science Vol.4 (1964),

119. Fromhold,A.T.Jnr. Theory of Metal Oxidation Vol.1 - Fundamentals. North-Holland Publishing. (Amsterdam),1976.

120. Cabrera,N.and Mott,N.F., "Theory of the Oxidation of Metals", Reports Prog.Phys. Vol.12 (1948/9), p.163

121. Evans,U.R., "The Corrosion and Oxidation of Metals", Edward Arnold Ltd., London c.1960

122. Kubaschewski,O. and Hopkins,B.E. Oxidation of Metals an Alloys. Butterworths (London). 1967

123. Weissmantel,C.H., "Kinetik der Sauerstoffsorption von Metallfilmen", Werkstoffe und Korrosion Vol.11 (1962) pp.682-691.

124. Fehlner,F.P. and Mott,N.F. "Low Temperature Oxidation", Oxidation of Metals Vol.2 (1970) pp.59-99

125. Tennyson Smith and Crane,L.W., "Adsorption of Oxygen on Steel", Oxidation of Metals, Vol.10 (1976) pp.135-148.

126. Langell,M.A. and Bernasek,S.L. "Transition Metal Compound Surfaces", Progress in Surface Sci. Vol.9 (1979), pp.165-189

127. Eley,D.D. and Wilkinson,P.R.,"Adsorption and Oxide formation on Aluminium films", Proc.Roy.Soc.(London) V.254A (1960) pp.327-342

128. Graham,M.J. and Hussey,R.J.,"The growth and structure of Oxide films on Fe: I Oxidation of (001) and (112) Fe at 200 to 300°C; II Oxidation of Polycrystalline Fe at 240 to 320°C", Oxidation of Metals Vol.15 (1981) pp.407-435

129. Revesz,A.G. and Fehlner,F.P.,"The Role of non-crystalline Films in the Oxidation and Corrosion of Metals", Oxidation of Metals Vol.15 (1981) pp.297-319.

130. Meyer,K. Physikalisch-chemische Kristallographie. Copyright VEB Deutscher Verlag für Grundstoffindustrie, Leipzig, 1977. Printed in the German Republic by Gutenberg Buchdruckerei (Weimar).

131. Caplan,D. and Cohen,M.,"The effect of Cold Working on the Oxidation of Iron from 100 to 650°C", Corrosion Science V.6 (1966) p.321.

132. Poling,G.W. "Infra-red Reflection Studies of Metal Surfaces", J.Colloid and Interface Sci. Vol.34 (1970) p.365.

133. Carslaw,H.S. and Jaeger,J.C. Conduction of Heat in Solids. 2nd.ed. Oxford:Clarendon Press. 1959

134. Condit,R.H., Hobbins,R.R. and Birchenall,C.E.,"Self-diffusion of Iron and Sulphur in Ferrous Sulphide", Oxidation of Metals, Vol.8 (1974) pp.409-455

135. Pfeiffer,H. and Ilschner,B. "Material transport through Oxidation layers", Z.Elektrochem, Vol.60 (1956),p.424

136. Driscoll,T.J.,"The initial Oxidation of Iron at 200°C and 300°C and the effect of Surface Sulphur", Oxidation of Metals Vol.16 (1981), pp.107-131.

137. Husen,C.,"High temperature Corrosion by Organic Sulphur Compounds" in High Temperature Metallic Corrosion of Sulphur and its Compounds ed.Foroulis,Z.A. New York: Electrochemical Society. 1970, pp.187-207.

138. Børie,B., Sparks.J.R., and Cathcart,J.R. and J.V., "Epitaxially Induced Strains in Cu_2O films on Copper Single Crystals: I X-ray diffraction effects". Acta Metallurgica Vol.10 (1962), pp.691-703.

139. Issacs,N.S., Liquid Phase High Pressure Chemistry. John Wiley and Sons. 1981.

140. Toyoguchi,M. and Takai,M., "The E.P. Lubricating Properties of some Sulphur Compounds in Mineral Oil and the effect of dissolved oxygen". Bull Jap.Petrol. Soc., Vol.3 (1961) p.63

141. Rhodin (Jnr.),T.N., "Low Temperature Oxidation of Copper II. Reaction Rate Anisotropy". J.Am.Chem.Soc. Vol.73, pp.3143-3146,(1951)

142. Cathcart,F.W. and J.V., and Gwathmey,A.T., "The Rates of Oxidation of several faces of a single crystal of Copper as determined with elliptically polarizes light", Acta Metallurgica Vol.4, (1956), p.145

143. Buckley,D.H. source reference Y.Kimura. "Some problems in the Adhesion Theory of Friction", ed.Suh,N.P. and Saka,N. c.1980 MIT Press.

144. Hathwar,G.S. and Smith,H.A., "The adsorption of organic compounds on freshly machined surfaces". N.A.S.A. AROD-2281-41963, (1963).

145. Goldstein,J.I. and Yakowitz,H., editors and main authors, "Practical Scanning Electron Microscopy". Plenum Press, New York, c.1975.

146. Boothroyd,G., "Fundamentals of metal machining and machine tools". McGraw-Hill Book Co., c.1975.

147. F.H.Constable, "Sulphide on Metallic Copper". Proc.Roy.Soc., Vol.125A, pp.630-635.

148. N.R.Draper and H.Smith, "Applied Regression Analysis", J.Wiley & Sons, 1966.

149. Kendall, M.G. and Stuart, A., "The Advanced Theory of Statistics". Vol. 2 Interference and Relationship, (3rd ed.), Griffin, 1973.

150. Williams, E.J., "Regression Analysis". Wiley, 1959.

151. Huang, D.S., "Regression and Econometric Methods", Wiley, 1969.

152. Stachowiak, G.W., "Mathematical Models of Contact Fatigue" PhD University of London, July 1980.